TECHNISCHE UNIVERSITÄT MÜNCHEN

WISSENSCHAFTSZENTRUM WEIHENSTEPHAN FÜR ERNÄHRUNG, LANDNUTZUNG UND UMWELT

PROFESSUR FÜR BIOTHERMODYNAMIK

DEEP EUTECTIC SOLVENT- AND IONIC LIQUID-BASED BIPHASIC SYSTEMS IN CENTRIFUGAL PARTITION CHROMATOGRAPHY

Franziska Bezold

Vollständiger Abdruck der von der Fakultät Wissenschaftszentrum Weihenstephan für Ernährung, Landnutzung und Umwelt der Technischen Universität München zur Erlangung des akademischen Grades eines

Doktor-Ingenieurs (Dr.-Ing.)

genehmigten Dissertation.

Vorsitzender: Prof. Dr.-Ing. Heiko Briesen

Prüfende der Dissertation: 1. Prof. Dr.-Ing. Mirjana Minceva

2. Prof. Dr.-Ing. Harald Klein

3. Prof. Dr.-Ing. Irina Smirnova

Die Dissertation wurde am 22.01.2019 bei der Technischen Universität München eingereicht und durch die Fakultät Wissenschaftszentrum Weihenstephan für Ernährung, Landnutzung und Umwelt am 09.09.2019 angenommen.

„Once mixed, always mixed.“

Wolfgang Arlt

Acknowledgements

Die vorliegende Arbeit ist das Ergebnis meiner Forschungsarbeiten bei der Professur für Biothermodynamik am Wissenschaftszentrum Weihenstephan.

Ich möchte mich sehr herzlich bei meiner Doktormutter Prof. Dr.-Ing. Mirjana Minceva bedanken, für ihr Vertrauen und die Möglichkeit die Bearbeitung meines Themas selbstständig und frei zu gestalten. Danke, dass ich viele wissenschaftliche Konferenzen besuchen durfte und die Gelegenheit bekommen habe, meine Forschungsergebnisse vorzustellen! Außerdem gilt mein besonderer Dank meinen Gutachtern Prof. Dr.-Ing. Irina Smirnova und Prof. Dr.-Ing. Harald Klein, sowie Prof. Dr.-Ing. Heiko Briesen für die Übernahme des Prüfungsvorsitzes. Und großer Dank geht an meine Mentorin Liudmila Mokrushina, die mich immer unterstützt hat!

Vielen Dank an alle meine Kollegen in der Biothermodynamik für die schöne Zeit. Besonderer Dank geht an Simon, den besten Bürokollegen und Leidensgenossen auf dem Weg zur Promotion! Danke an Andreas Frey, der mich während meiner Arbeit mit so manchem guten Rat unterstützt und motiviert hat. Vielen Dank, Joachim und Christoph für die Zusammenarbeit auf dem Gebiet der Mikroalgen! Auf diesem Wege möchte ich mich auch noch einmal herzlich bei allen Studenten bedanken, deren Abschlussarbeiten oder Praktika ich während meiner Zeit bei der Biothermodynamik betreuen durfte: Lukas, Ramona, Melanie, Clarissa, Sandra, Maria, Franziska, Simone, Jahyun, Swati, Alex, Edgar, Jennifer, Michael, Anna, Maria, Sebastian, und Eleni. Vielen Dank für Euren Beitrag zu den verschiedenen Forschungsprojekten und für die gute Zeit!

Ich möchte mich außerdem bei den ehemaligen Nachbarn vom Lehrstuhl für Systemverfahrenstechnik bedanken, die Simon und mich zu Kaffeepausen und gemeinsamen Abenden aufgenommen haben, als wir neu in Weihenstephan waren. Vielen Dank für die lustige Zeit und die interessanten Kaffeepausen-Ideen! Danke für die unterhaltsamen Freitage im Klimperkasten, zusammen mit Michael, Tijana, Christoph, Dimitrios, Carsten, Paul, Chrissi, Steve, Moritz, und Max vom SVT! Besonderer Dank geht an Michael für die erfolgreiche Zusammenarbeit im Kaffeeprojekt und die spannenden Unterhaltungen über Kaffee. Ferner möchte ich mich bei Max, Ekaterina und Moritz für die Zusammenarbeit auf dem Gebiet Molekulardynamik bedanken! Auch hier wurde aus einer Kaffeepausenidee am Ende eine wissenschaftliche Veröffentlichung.

Und extra großer Dank geht an die Mittagessensfreunde Carsten, Christoph und Hans! Ihr habt mich während der Promotionszeit unterstützt und euch so manche Probleme angehört. Und außerdem habt ihr die Messlatte sehr hoch gelegt, was aufwändig gebastelte Geschenke angeht!

Vielen Dank an alle Freunde und Wegbegleiter für die Unterstützung!

Der größte Dank geht an meinen Ehemann Florian, der mich immer unterstützt bei allem was ich tue, und an meine Eltern und meine Schwester Elisabeth. Vielen Dank für alles!

Abstract

Centrifugal partition chromatography (CPC) is a versatile technology that is most commonly applied for the separation of natural compounds and active pharmaceutical ingredients. The method uses the two liquid phases of a biphasic solvent system as stationary and mobile phases for a chromatographic separation. Biphasic systems for the separation of medium polar target compounds are well characterized in literature. For very hydrophilic or hydrophobic substances the number of reported solvent systems is limited. Thus, the objective of this thesis is to explore alternative solvent systems for the separation of hydrophilic and hydrophobic compounds with CPC. The work focuses on biphasic systems containing ionic liquids (ILs) and deep eutectic solvents (DES). In the first part, aqueous two-phase systems (ATPSs) containing ILs are applied for protein separation. In the second part, DES-based biphasic systems are investigated.

ATPSs are applied for protein separation since organic solvents may cause them to denature. ILs can selectively tune the partition coefficients of certain proteins in ATPSs. At the same time, the effect of small amounts of ILs on other process properties of the biphasic system, such as stationary phase retention, is marginal. A mixture of two model proteins, myoglobin and lysozyme, was separated with CPC using ATPSs. It was shown that the ability of hydrophilic ILs to modify protein partition coefficients can be employed in CPC separations.

The second part of the thesis concentrates on the application of DES-based biphasic systems as stationary and mobile phases in CPC. DES can be formed by non-toxic natural compounds and have gained attention due to their beneficial properties. They can be used to form water-free biphasic systems for the separation of hydrophobic compounds, which are still sparse in CPC. Up to now, there is not much guidance on how to select suitable DES-based biphasic systems. Hence, the application of a computational solvent system screening method applying the Conductor-like Screening Model for Realistic Solvation (COSMO-RS) was evaluated. Different modelling approaches were compared and the prediction accuracy was found sufficient for screening purposes for systems with DES-constituents mainly present in one of the phases. The procedure was successfully applied to select a DES-based biphasic system for the separation of tocopherols.

Most literature data on liquid-liquid equilibria (LLE) of systems composed of organic solvents and DES originate from extraction applications. In liquid-liquid extraction, it is a prerequisite to retain the DES-constituents in one of the phases. Hence, data was only available for pseudo-ternary biphasic systems. Quaternary systems with DES-constituents distributed between both liquid phases could help understand their molecular interactions in liquid solution. Also, in CPC it is not necessary to keep the DES-constituents in only one of the phases. Thus, LLE data of three novel quaternary biphasic systems containing *n*-heptane, methanol, and DES composed of hydrophobic monocyclic terpenes and a carboxylic acid were measured. It was found that the ratio of the DES-constituents in the phases is different from the initially prepared DES. Their distribution is concentration dependent and changes with the system composition. One of the biphasic systems was tested in CPC: High stationary phase retention was obtained and pulse injections of model compounds with different octanol/water-partition coefficients proved that the biphasic system was suitable for the separation of hydrophobic substances.

Table of Contents

Acknowledgements 3

Abstract 5

Table of Contents 7

1. Introduction and motivation 9

2. Theoretical background 13

2.1. Liquid-liquid chromatography 13

2.2. Biphasic solvent systems for liquid-liquid chromatography 18

2.2.1. Aqueous two-phase systems 20

2.2.2. Deep eutectic solvent-based biphasic systems 21

2.3. Thermodynamics 24

2.3.1. Thermodynamic equilibrium 24

2.3.2. Liquid-liquid equilibrium 24

2.3.3. Solid-liquid equilibrium 26

2.4. Solvent screening using a predictive thermodynamic model 27

2.4.1. Conductor-like screening model (COSMO) and conductor-like screening model for realistic solvation (COSMO-RS) 29

2.4.2. Representation of DESs in COSMO-RS 30

3. Results 33

3.1. Paper I 33

Ionic liquids as modifying agents for protein separation in centrifugal partition chromatography 35

3.2. Paper II 45

Assessing solute partitioning in deep eutectic solvent-based biphasic systems using the predictive thermodynamic model COSMO-RS 47

3.3. Paper III 59

Computational solvent system screening for the separation of tocopherols with centrifugal partition chromatography using deep eutectic solvent-based biphasic systems 61

3.4. Paper IV 67

Liquid-liquid equilibria of *n*-heptane, methanol and deep eutectic solvents composed of carboxylic acid and monocyclic terpenes 69

3.5. Paper V 79

A water-free solvent system containing an L-menthol-based deep eutectic solvent for centrifugal partition chromatography applications 80

3.6. List of other published manuscripts 86

4. Overall discussion 87

4.1. Aqueous two-phase systems 87

4.2. DES-based biphasic systems 88

5. Conclusion 91

6. Outlook 93

7. Symbols 95

8. Abbreviations 97

9. List of Figures and Tables 99

10. References 101

Appendix 111

1. Introduction and motivation

Liquid-liquid chromatography (LLC) is a versatile preparative technology that combines features of liquid-liquid extraction and chromatography [1]. It is a valued technique in natural product separation, fractionation and purification of plant extracts, and in the discovery of new active ingredients from natural resources [2]. The term LLC refers to two different column types that share the same separation principle: countercurrent chromatography (CCC) and centrifugal partition chromatography (CPC). LLC is used in this work whenever it is referred to both column types, the terms CPC or CCC are used when only one of the column types is addressed. In both column types, a biphasic solvent system is applied for the separation of target compounds. The biphasic system is prepared by the user prior to the separation by mixing and equilibration of the respective solvents. The two liquid phases are then split into separate reservoirs, one is used as stationary and the other as mobile phase. The stationary phase is kept inside a specially designed column by a centrifugal field while the mobile phase is pumped through [3]. The feed solution is introduced via an injection loop or a feed pump. The technology has several advantages compared to other chromatography types. LLC has a high column capacity since the whole volume of the liquid stationary phase is accessible for solutes compared to classic chromatography where the solutes can only interact with the surface of the solid stationary phase [3]. No irreversible adsorption of target compounds can occur. The stationary phase can easily be removed from the column and replaced with a fresh or different one due to the liquid nature of the stationary phase [4]. LLC is also non-sensitive to particles in the feed solution making it possible to inject crude plant extracts. Furthermore, the scale-up of LLC separations is fast and easy. Since the users prepare the biphasic systems themselves by mixing two to four solvents, the technology is very versatile and a nearly countless number of different solvent systems is available for use. However, this advantage comes with a drawback: Solvent system selection can be very time consuming due to the large number of possible solvent combinations. The solvent system needs to be chosen and prepared by the user depending on the properties of target compounds and impurities that have to be separated. It can easily result in a disappointing and long search when the selection is done by trial and error methods [5].

Solvent systems for the separation of medium polar compounds that are neither very hydrophobic nor very hydrophilic are well characterized. The most abundantly used solvent systems for LLC are mixtures of two to three organic solvents and water [2]. For very polar and non-polar compounds, however, the number of solvent systems suitable for LLC that can be found in literature is limited. Looking at the properties of the desired natural products or active ingredients, a disparity becomes obvious: A large number of active ingredients and natural substances are rather hydrophobic and cannot be separated with the above-mentioned characterized solvent systems [6, 7]. A similar problem exists for the separation of another class of target molecules: Biomolecules, such as proteins, are often not chemically stable in mixtures containing organic solvents and thus, biphasic solvent systems with organic solvents are not applicable for separations of such molecules [8, 9].

The aim of this thesis is to extend the existing pool of solvent systems for LLC and to explore potential novel biphasic solvent systems for the separation of hydrophobic compounds and

proteins. The thesis focuses on alternative biphasic solvent systems with so-called designer solvents, namely ionic liquids (ILs) and deep eutectic solvents (DESs). ILs can be used to form aqueous two-phase systems (ATPSs), also known as aqueous biphasic systems (ABSs), when mixed with water and a kosmotropic salt [10]. In particular, ILs have gained a lot of attention due to their favourable properties, such as their high solvation capacity, their low vapour pressure and the fact that they are non-flammable and non-explosive. Besides, the cation and anion combination that forms the IL can be selected specifically for a separation task. This fact offers the possibility to create tailor-made ILs, and thus tailor-made biphasic solvent systems when mixed with water, and kosmotropic salts [10-16]. However, ATPSs formed by ILs and salts also have certain drawbacks. In many cases relatively large amounts of IL and salt are needed to form the biphasic solvent system: Usually at least 15-20 wt% are required for hydrophilic ILs and the salts [11, 12, 17, 18]. Since ILs can be quite expensive, such biphasic solvent systems require high investment and thus are often avoided on industrial scale. In this thesis, ATPSs with only small amounts of ILs are investigated and their potential use in LLC is evaluated. The aim is to combine the beneficial properties of ILs while keeping the costs of the biphasic solvent systems lower than in previously mentioned ATPSs with high IL-content. Such ATPSs with low IL-content have been applied in liquid-liquid extraction and have been proposed for a use in LLC in previous work [17, 19]. In this work, they are applied in LLC for the first time (chapter 3.1, **Paper I**). Protein partition coefficients and stationary phase retention inside a CPC column are investigated. Further options to increase the productivity of the protein separation with CPC are presented.

The second part of the thesis focuses on the use of biphasic systems containing DESs in LLC. DESs are mixtures of hydrogen bond donors and hydrogen bond acceptors that show a strong melting point depression compared to the pure constituents when combined in a certain molar ratio [20]. DESs have similar properties as ILs: They are non-flammable, have low vapour pressure and show a high solvation capacity for a large number of compounds [21]. Additionally to the properties they share with ILs, they have several other advantages. For example, relatively inexpensive compounds from natural sources, such as sugars, alcohols and polyols, or quaternary ammonium salts, can form DESs. DESs formed from such natural ingredients, so-called natural deep eutectic solvents (NADES), are considered non-toxic, often referred to as green solvents, and can be produced from food grade bulk chemicals [22, 23]. The main difference between ILs and DESs is that ILs are chemical compounds made up by cations and anions connected by ionic bonds while DESs are mixtures of two or more different compounds that may be ionic or neutral. The mixed DES-constituents form a hydrogen bond network that is considered to be the reason for the melting point depression [24].

It is possible to select DESs that are liquid at room temperature and to form non-aqueous biphasic solvent systems by combining them with organic solvents. DES-based biphasic systems can be used in LLC-separations and they are particularly suitable for the separation of hydrophobic target compounds [25]. Unfortunately, use of DES-based biphasic systems is not yet common in LLC. The main reason for this is probably the high number of degrees of freedom for the selection of DES-based biphasic systems. The ratio between the constituents can be varied within a certain range in which a liquid mixture is obtained. Furthermore, the

user has to select two or more organic solvents to combine with the DES. Finally, the composition of the biphasic system, that means the ratio of the solvents and the DES in the mixture, has to be selected. The high number of degrees of freedom easily results in a combinatorial explosion and experimental solvent system search without a rational systematic approach is highly laborious. As a part of this thesis, it was evaluated whether computational solvent system screening using a thermodynamic model, namely the Conductor-like Screening Model for Realistic Solvation (COSMO-RS), can be applied to DES-based biphasic systems (chapter 3.2, **Paper II**). For this matter, different modelling strategies for DESs were compared. In order to evaluate the applicability of the screening approach, activity coefficients, liquid-liquid equilibria and solute partition coefficients were predicted and compared to literature data. Other reasons why DES-based biphasic systems are not yet widely used in LLC are the lack of applications in literature that show the benefits of the systems and the lack of liquid-liquid equilibrium data of DES-based biphasic systems that are known to be applicable in LLC. The tested solvent system screening approach has thus been applied to select DES-based biphasic systems for the separation of poorly water-soluble tocopherols (chapter 3.3, **Paper III**). This was on the one hand done to show the potential of model-based solvent screening for DES-based biphasic systems in LLC and on the other hand to promote the use of the biphasic systems by showing an example application. Additionally, the limited liquid-liquid equilibrium data impedes the use of DES-based biphasic systems in LLC. So far, only biphasic systems designed for liquid-liquid extraction were available in literature. Therefore, novel DES-based biphasic systems were designed (chapter 3.4, **Paper IV**) and their applicability in LLC was tested (chapter 3.5, **Paper V**).

Objective and structure of this thesis

The objective of this thesis is to explore alternative biphasic solvent systems for the separation of either very hydrophilic or hydrophobic target compounds with CPC. The work focuses on biphasic systems with so-called designer solvents, namely ILs and DESs, to enlarge the existing established pool of solvent systems.

The thesis is divided into theoretical background (Chapter 2), results (Chapter 3), a general discussion (Chapter 4) and conclusions and outlook (Chapter 5 and 6). In Chapter 2 general relevant theory and methods are summarized. Additional subject specific literature, state of the art, and detailed method descriptions are covered in each paper.

Sections 3.1 to 3.5 contain a short summary for each paper and the published manuscripts. The connections between the published manuscripts are highlighted. Chapter 4 contains a general discussion of the results of Papers I-V. In Chapter 5, a conclusion is drawn and Chapter 6 contains an outlook for future work.

2. Theoretical background

This chapter contains the principle of operation of liquid-liquid chromatography and describes biphasic solvent systems that can be used as stationary and mobile phases, with focus on biphasic systems that contain DESs or ILs. Further, the basic thermodynamic principles are explained and a short introduction to the thermodynamic model used in this work is given.

2.1. Liquid-liquid chromatography

Liquid-liquid chromatography is a separation technology which uses the two liquid phases of a biphasic solvent system as stationary and mobile phases for a chromatographic separation [1, 26]. The column has a special geometrical design and a centrifugal field is applied to keep one of the liquid phases stationary. The peripheral setup is usually the same as in other chromatography methods and samples are introduced via an injection loop or a feed pump. The biphasic system is prepared by the user by mixing the appropriate amounts of the solvents. The two phases are equilibrated before use. Next, the phases are split and one of them is used as stationary and the other one as mobile phase for the separation. At the beginning, the column is completely filled with the stationary phase and rotation is started. After full rotational speed is reached, the mobile phase is pumped through the column with the desired volumetric flow rate. The mobile phase replaces parts of the stationary phase inside that column until hydrodynamic equilibrium is reached. After that point the ratio of mobile to stationary phase inside the column is supposed to stay constant and the feed mixture may be injected. The underlying separation principle is the different distribution of solutes between the liquid mobile and stationary phases. The retention volume or elution volume of compound *i* is determined by the volume of stationary (V_{SP}) and mobile phase (V_{MP}) inside the column and the partition coefficient P_i, as described in Equation 1 [3, 5].

$$V_{R,i} = V_{MP} + P_i V_{SP} \qquad \text{(Equation 1)}$$

The partition coefficient of a target compound *i* can be determined in shake flask experiments (Equation 2) or can be calculated from the chromatogram (Equation 3).

$$P_i = \frac{c_i^{SP}}{c_i^{MP}} \qquad \text{(Equation 2)}$$

$$P_i = \frac{V_{R,i} - V_{MP}}{V_{SP}} \qquad \text{(Equation 3)}$$

To determine partition coefficients in shake flask experiments, a small amount of solute, approximately 1-5 mmol l^{-1}, is dissolved in the biphasic solvent system (with equal volume of upper and lower phase) and the concentration of the solute in each phase is measured. For such low solute concentrations, it is expected that the partition coefficient is constant and independent of concentration. In LLC, each of the two phases of a biphasic system, upper or lower phase, may be used as stationary phase. In case the upper phase is used as stationary phase and the lower phase as mobile phase the operation mode is called *descending mode* (dsc). In *ascending mode* (asc) the lower phase is used as stationary phase and the upper phase as mobile phase. The user may decide which of the phases is used as stationary phase.

According to the definition of P_i introduced in Equation 3, two different solute partition coefficient values are obtained for the same biphasic system in the two operation modes. The inverse relationship between the partition coefficients from descending mode and ascending mode is described in Equation 4.

$$P_i^{asc} = \left(P_i^{dsc}\right)^{-1} \quad \text{(Equation 4)}$$

The best operating range for partition coefficients is within 0.4 to 2.5. This range is called the *sweet spot* in analogy to a baseball bat, as illustrated in Figure 1. For larger partition coefficients the productivity of the separation process decreases, since runtime and eluent consumption become higher. For smaller partition coefficients, usually the resolution is not sufficient. In order to evaluate whether two compounds can be separated, the separation factor α_{ji} can be used.

$$\alpha_{ji} = \frac{P_j}{P_i} \quad \text{(Equation 5)}$$

The minimum α_{ji} with which baseline separated peaks can be achieved depends on the axial dispersion and mass transfer in the column and, is thus connected to the number of theoretical stages of the column (see Equation 7).

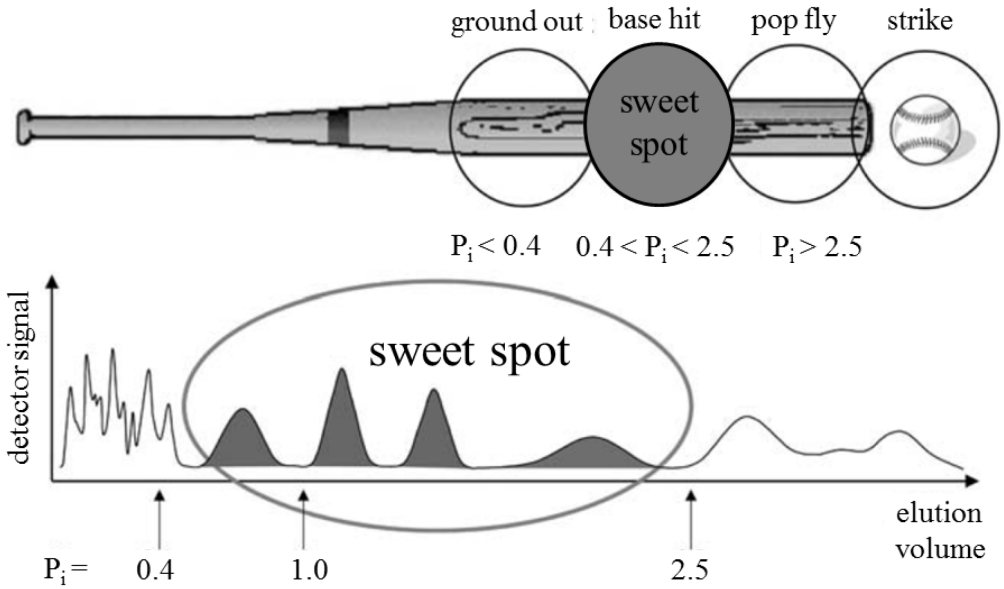

Figure 1: Schematic illustration of the s*weet spot*; partition coefficients below the chromatogram correspond to the plotted elution volume. Partition coefficients values between 0.4 and 2.5 result in the best separation performance for countercurrent and centrifugal partition chromatography[27]

Other than by the partition coefficient, the separation is also strongly influenced by the stationary phase retention S_f. S_f refers to the volume fraction of the total column volume V_c that is occupied by the stationary phase. There are two ways to determine S_f: It can either be derived from eluted phase volumes or via injection of a tracer. The first method employs the following procedure: First, the column is completely filled with stationary phase and the column rotation is started. Then, mobile phase is pumped through the column with the

selected flow rate. A part of the stationary phase inside the column is replaced by mobile phase and collected at the outlet of the column. When hydrodynamic equilibrium is reached, no more stationary phase elutes from the column. The volume of the eluted stationary phase is determined and the system dead volume, i.e. the volume of the tubing before and after the column, is subtracted. The resulting volume corresponds to the volume of the mobile phase in the column. After the separation, the remaining stationary phase is pushed out of the column and its volume is determined. S_f can then be calculated according to Equation 6.

$$S_f = \frac{V_{SP}}{V_c} = \frac{V_c - V_{MP}}{V_c} \qquad \text{(Equation 6)}$$

A tracer is a substance that is not retained by the stationary phase and passes the column with the mobile phase. The partition coefficient of a tracer is zero. S_f can also be determined from a tracer injection: The retention volume of the tracer is determined from the chromatogram. According to Equation 1, if P_{tracer} is equal to zero, the retention volume is equal to the volume of the mobile phase inside the column. S_f can then be calculated with the mobile phase volume and the column volume using Equation 6.

Stationary phase retention depends on the mobile phase flow rate, the physical properties of the biphasic system, the rotational speed and the column geometry. There are two basic ways to construct the column in liquid-liquid chromatography: hydrodynamic and hydrostatic columns. The hydrodynamic column is also called countercurrent chromatography (CCC) while the hydrostatic column is referred to as centrifugal partition chromatography (CPC).

Most hydrodynamic devices were developed by Prof. Ito [3] and have two axes of rotation. They are composed of tubing wound around a cylindrical drum that is mounted in a planetary gear [1]. Along the column tubing, there are alternating settling and mixing zones due to changes in the direction of the centrifugal field in the planetary motion, as illustrated in Figure 2. An advantage of this column type is the fact that the two phases are in contact with each other within the whole column volume. This enables mass transfer between the stationary and mobile phases along the whole column. Due to the simple geometry of the tubing, reasonable stationary phase retention can only be achieved with low flow rates, usually in the range of a few millilitres per minute for laboratory scale devices. The largest reported CCC column has a column volume of 18 l and was operated with up to 850 ml min^{-1} with a stationary phase retention of 66% prior to injection. It has to be mentioned though, that stationary phase loss occurred during separation and S_f decreased to 31% at the end of the separation [28]. Different column designs based on Ito's original hydrodynamic CCC have been developed to improve stationary phase retention. Among these further developed devices are toroidal coils [29], conical colums [30], and spiral CCC [31, 32], or tubing modifications [33, 34].

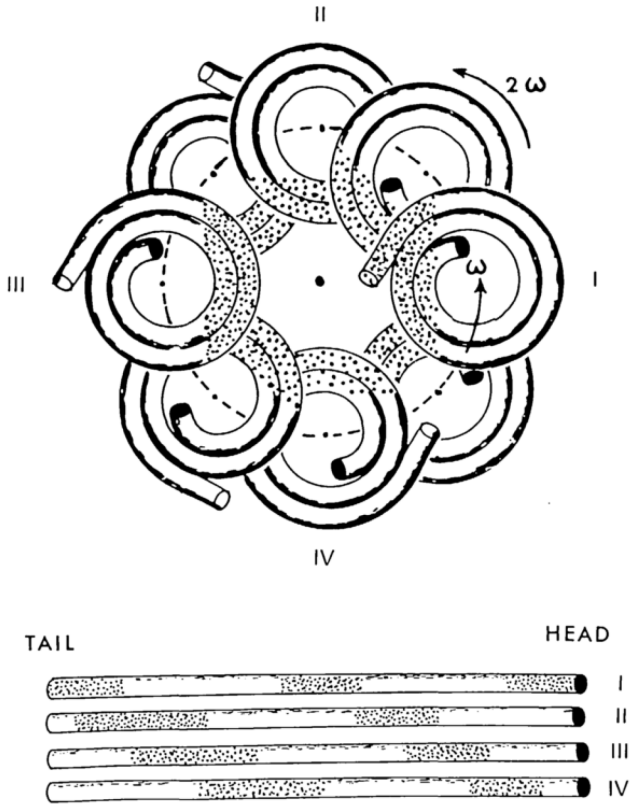

Figure 2: Formation of mixing and settling zones along a hydrodynamic CCC column [35].

Hydrostatic columns, within this work referred to as CPC columns, have a single axis of rotation that can either be mounted vertically or horizontally. They consist of a number of disks with connected cells that are alternatingly stacked with annular plates as shown in Figure 3. The annular plates are usually made from Teflon and act as a seal between the annular disks. The plates have an inlet and outlet opening that connects the last cell of a previous disk with the first cell of the following disk in the stack. The geometry of the cells in CPC columns has been subject to optimization and several designs have been introduced to the market, such as Z-cells [36] or twin cells with different cell volume [37]. Three examples of different cell geometries can be seen in Figure 4. In hydrostatic CPC columns higher mobile phase flow rates can be used compared to the hydrodynamic CCC columns at reasonable stationary phase retention. The mobile and stationary phases are only in contact with each other in the cells, the connecting ducts between the cells are exclusively filled with mobile phase. This means, mass transfer between the stationary and mobile phases is possible in the cells, but not in the connecting ducts. In this work, a hydrostatic CPC column was used to perform the separations shown in **Papers I, III, and V** in Chapter 3.

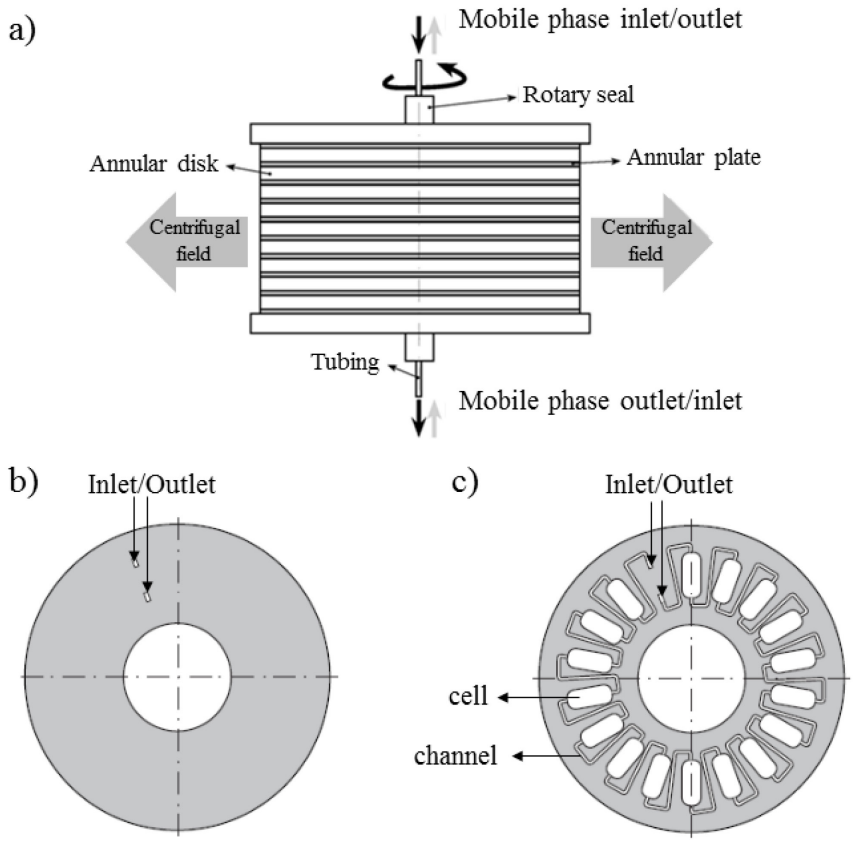

Figure 3: (a) Hydrostatic CPC column; (b) annular plate; (c) annular disk with cells and connecting channels [36]

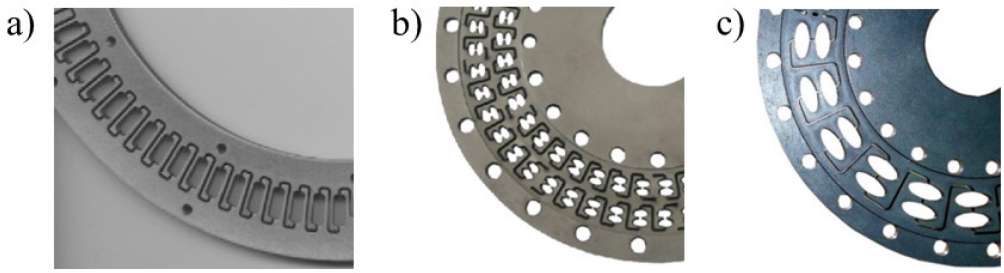

Figure 4: Different designs of cells and channels on annular disks of CPC: (a) Z-cell from Kromaton [36], (b) twin cell of an SCPC250 from Gilson with a twin cell volume of 0.101 ml [37], (c) twin cell geometry of an SCPC 250 BIO with larger cell volume of 0.961 ml from Gilson [37]

Both LLC column designs combine the advantages of liquid-liquid extraction and chromatography. The technology is located between the two unit operations in terms of theoretical separation stages N_i (Equation 7).

$$N_i = \left(\frac{t_{R,i}}{\sigma_i}\right)^2 \qquad \text{(Equation 7)}$$

The retention time $t_{R,i}$ and the variance σ_i^2 of the peak can be determined from the chromatogram. Usually, the number of theoretical stages of CCC and CPC columns is in the range of a few hundreds to a few thousands.

The liquid nature of the stationary phase enables several unique operational modes that are not possible with solid stationary phases. Elution extrusion, for example, combines a chromatographic elution with a subsequent extrusion step where additional stationary phase is pumped to elute compounds remaining in the column [38]. A similar approach is back extrusion where the stationary phase is also eluted after a regular separation, but in contrast to elution extrusion the mobile phase is used to push the stationary phase out of the column. Both methods are suited to elute highly retained solutes. One of the main differences is that in elution extrusion the direction of the flow is maintained while in back extrusion the flow direction is changed [39].

When assigned with a separation task, the LLC user needs to select a stationary and mobile phase that gives partition coefficients preferably in the *sweet spot*, high enough separation factors and sufficiently high stationary phase retention [40, 41]. The mobile and stationary phase cannot be chosen independently, since they are in equilibrium and a change in composition of one of the phases will also change the other liquid phase. Hence, the user needs to select a biphasic solvent system.

2.2. Biphasic solvent systems for liquid-liquid chromatography

Biphasic solvent systems that are used as stationary and mobile phases for CCC and CPC separations are usually composed of three or more solvents. The requirements to the solvent system differ quite a lot from liquid-liquid extraction looking at the solute partition coefficient values. In liquid-liquid extraction, target compounds have either very large or very small partition coefficients, while in CCC and CPC moderate partition coefficients between 0.4 and 2.5 within the *sweet spot* are favourable. It depends on the molecular structure of the substances in a mixture that needs to be separated what kind of biphasic solvent system can be used.

Usually, the selection of the biphasic solvent system is the most time consuming task in the design of a LLC separation. Selection of an appropriate solvent system can require a lot of time and effort if it is done with experimental trial and error methods. In most cases the solvent system selection is done by researching literature for structurally similar target compounds and selecting the same or similar solvent systems. If this does not lead to an appropriate biphasic solvent system, solvent system families are consulted most of the times. The term “solvent system family” refers to a group of solvent systems composed of the same constituents with different mixing ratios. These systems are organized according to their polarity. The most commonly used solvent system families in LLC are the Arizona system family composed of *n*-heptane, ethyl acetate, methanol and water and the HEMWat family containing *n*-hexane, ethyl acetate, methanol, and water.

For the separation of a range of target compounds with medium polarity, biphasic systems composed of water and organic solvents are commonly used. In fact, HEMWat and Arizona systems are the overall most abundantly used biphasic systems in CCC and CPC. HEMWat systems make up more than one third (35 %) and Arizona systems account for 16 % of all biphasic systems used in literature [2].

Even though they cover a certain polarity range, these solvent system families are not applicable for very hydrophobic molecules, i.e. molecules with large octanol/water partition coefficients (log $P^{o/w}$), or very hydrophilic molecules, i.e. molecules with very small octanol/water partition coefficients. For the separation of hydrophobic molecules, water-free biphasic solvent systems are applied. Examples for such non-aqueous solvent systems are *n*-hexane/chloroform/acetonitrile, *n*-hexane/ethyl acetate/acetonitrile, *n*-hexane/acetonitrile/ethanol, and *n*-hexane/benzotrifluoride/acetonitrile [2, 42]. The number of reported non-aqueous solvent systems is limited and they make up only 3 % of the solvent systems used in literature [2]. Recently, non-aqueous biphasic solvent systems composed of organic solvents and DESs have been introduced as potential candidates for the separation of hydrophobic species in CCC and CPC [25]. For the separation of very hydrophilic molecules, either biphasic systems composed of polar organic solvents and water, such as *n*-butanol/methanol/water, or solvent systems completely without organic solvents, namely ATPSs are used [43, 44]. Small molecules are mostly stable in organic solvents. Biomacromolecules, such as proteins, may undergo denaturation and contact with organic solvents has to be avoided. A scheme of possible classification and solvent system selection according to octanol/water partition coefficients of the target compounds is shown in Figure 5. Solvent systems for medium polar target compounds make up the majority of the reported biphasic systems for CCC and CPC. However, many active ingredients are hydrophobic compounds and they cannot be separated with such systems. And on the side of hydrophilic molecules, separation of native therapeutic proteins is still a challenging task and growing field. There is a need to expand the number of potential biphasic systems for the separation of very hydrophobic and hydrophilic compounds.

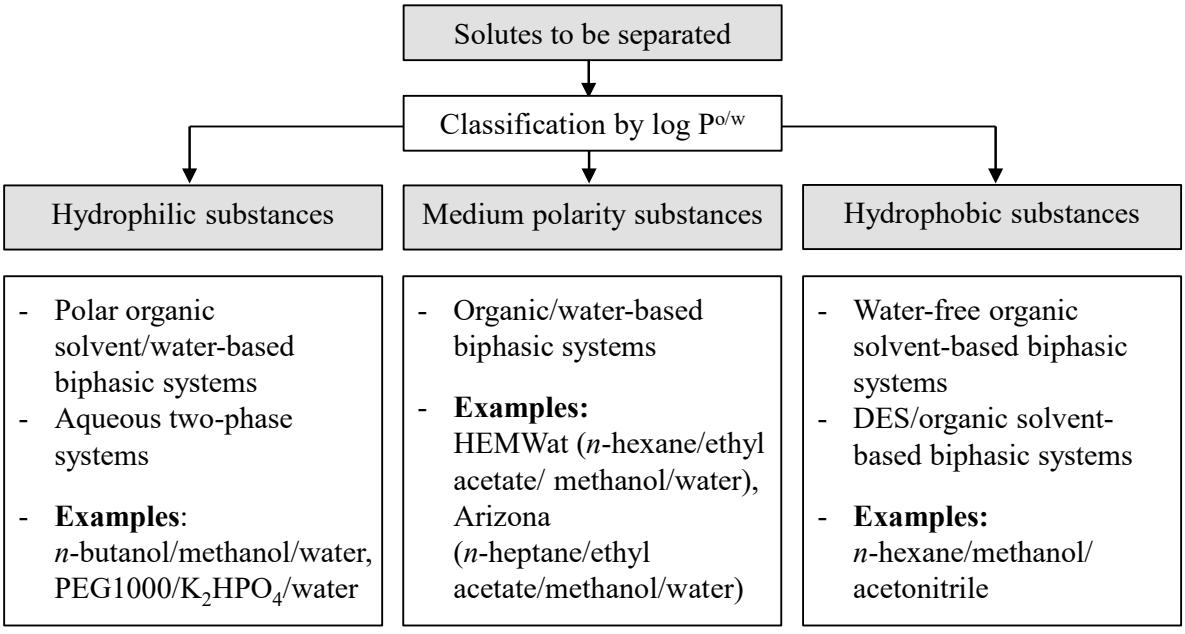

Figure 5: Selection of a solvent system class according to target compound octanol-water partition coefficients

2.2.1. Aqueous two-phase systems

ATPSs are created when phase forming compounds are mixed with water, for example a combination of polymers and salts, two or more different kinds of polymers, ILs and salts, and even DESs and salts [8-10, 45]. In an ATPS, both liquid phases are mainly composed of water. They are especially suitable for the separation of biomolecules due to the absence of organic solvents that may cause proteins to denature.

ILs are salts with melting points below 373 K and are exclusively composed of ions [46]. They can be tailored for different applications by variation of their cation and anion-combination [47]. ILs have gained attention due to their properties, including excellent solvation capacity, non-flammability, and low vapour pressure [48]. Still, their high price impedes large scale industrial application [23].

ATPSs are formed due to the salting out effect of the phase forming compounds. The salting out capacity of ions is ranked in the Hofmeister series for anions and cations and, for example derived for ATPSs with ILs and salts, follows the order [16]:

$$PO_4^{3-} > C_6H_5O_7^{3-} > HPO_4^{2-} \approx CO_3^{2-} > SO_4^{2-} \approx SO_3^{2-} > C_4H_4O_6^{2-} >> H_2PO_4^{-} > OH^{-} > CH_3COO^{-} \approx HSO_4^{-} \approx HCO_3^{-} > Cl^{-}$$

$$Mg^{2+} \approx Ni^{2+} \approx Sr^{2+} > Ca^{2+} >> Na^{+} > K^{+} > Cs^{+}$$

The series above are exemplary lists. Other studies have derived series with varying cations and anions for different purposes [11, 12, 49-51]. The ions on the left sides of the two series cause a stronger salting out effect and are referred to as kosmotropes. The ions on the other side of the series are causing salting-in and are called chaotropes.

The preparation of an ATPS is illustrated in Figure 6 for an example system containing water, polyethylene glycol 1000 (PEG 1000), and dipotassium hydrogen phosphate (K_2HPO_4). When sufficient amounts of PEG 1000 and K_2HPO_4 are dissolved in water and the mixture forms two phases. When solutes that are added to the biphasic system they are distributed according to their affinity to the phases [47].

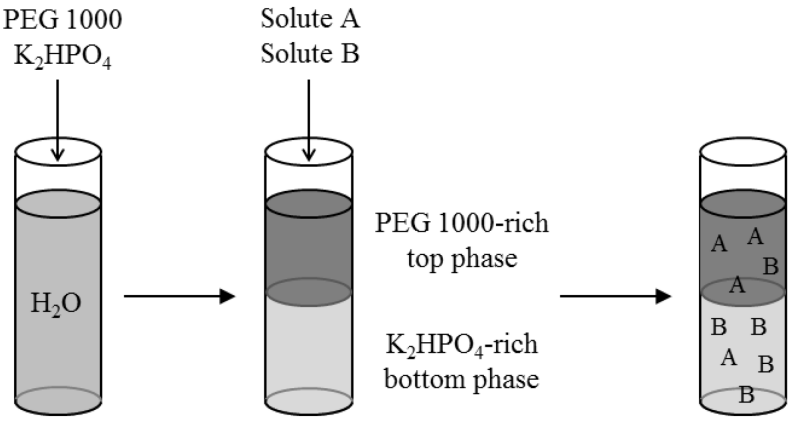

Figure 6: Schematic illustration of the distribution of phase forming compounds in an ATPS.

2.2.2. Deep eutectic solvent-based biphasic systems

DESs are a new class of designer solvents. They are composed of hydrogen bond donors (HBD) and hydrogen bond acceptors (HBA) and when combined in certain molar ratio, the mixture shows a substantial melting point depression compared to the pure compounds [20, 24]. In Figure 7, a schematic diagram of a solid-liquid phase equilibrium of a binary mixture is presented.

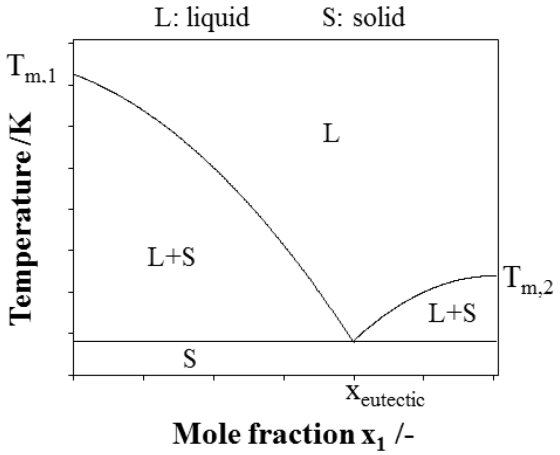

Figure 7: Schematic solid-liquid equilibrium phase diagram for a binary simple eutectic.

DESs can be prepared from non-toxic species, or often food-grade bulk chemicals, such as sugars, carboxylic acids, organic salts, and alcohols [22, 52-54]. Natural deep eutectic solvents (NADES) are a subclass of DESs and prepared from natural compounds. An exemplary list of molecules that have been used as HBA and HBD to form DESs and NADESs is presented in Figure 8. DESs and NADESs share many favourable properties with ILs while they can be produced at a lower price. They are considered non-flammable, have low vapour pressure, and show high solvation capacity for a large variety of target compounds. Their physical properties can be adjusted by choosing suitable HBD and HBA combinations. DESs are also easy to prepare: HBA and HBD are mixed in the appropriate molar ratio and energy is introduced to the system in forms of heating or grinding [55] to speed up phase transition. Table 1 lists a few examples of HBA and HBD combinations with respective molar ratio and melting temperature of the mixture. Due to their versatility, DESs have been used for many applications, for example as reaction medium [56], in solid phase extraction [57-59], biodiesel production [60-63] or in chromatography [64, 65]. DESs can also be applied to form liquid biphasic systems which can be exploited in separation technologies, such as liquid-liquid extraction [66-71]. These systems are usually selected in such a way that DES constituents are solely located in one of the phases. It was also shown that DES-based biphasic systems are suitable to be used as stationary and mobile phases in centrifugal partition chromatography, especially for the separation of hydrophobic target compounds [25].

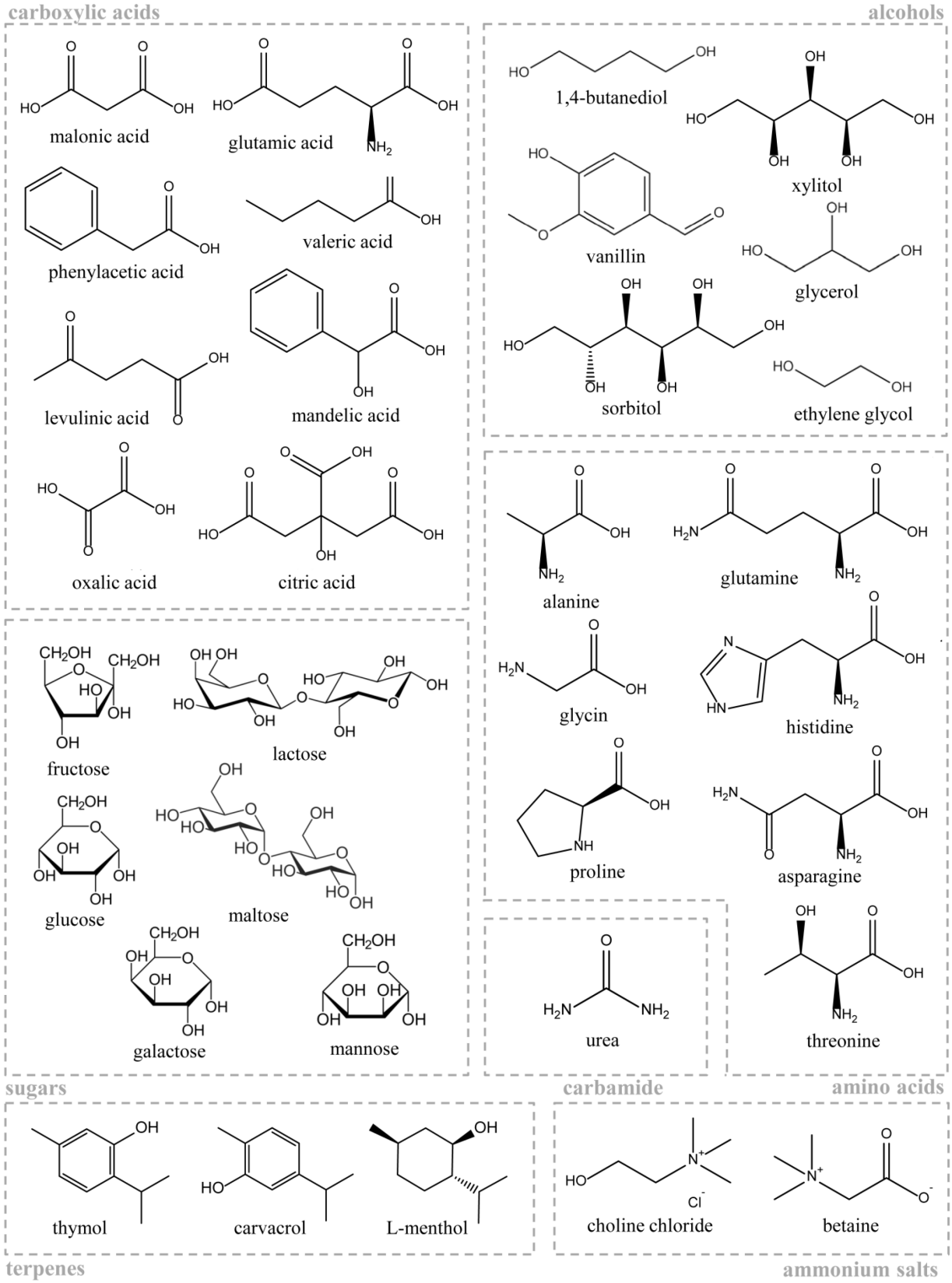

Figure 8: Molecular structures of possible DES-constituents

Table 1: Examples of HBA and HBD combinations with molar ratio and melting temperatures

HBA and HBD	molar ratio	melting temperature /°C	reference
choline chloride – urea	1:2	12	[24]
choline chloride – glycerol	1:2	-40	[72]
choline chloride – malonic acid	1:1	10	[20]
choline chloride – oxalic acid	1:1	34	[20]
choline chloride – phenylacetic acid	1:2	25	[20]
choline chloride – tartaric acid	1:2	47	[56]
choline chloride - glucose	1:2	14	[56]
L-proline – oxalic acid	1:1	-14.5	[56]
L-menthol – levulinic acid	1:1	0.2	[73]

2.3. Thermodynamics

In this chapter, the thermodynamic principles and equations used in this work are summarized. Detailed descriptions and derivations of the Equations 8 to 26 can be found in [74].

2.3.1. Thermodynamic equilibrium

According to Gibbs, there are three equilibrium conditions for a heterogeneous closed system that is made up of two or more phases φ. The conditions for thermal, mechanical and chemical equilibrium are given in Equations 8 to 10, respectively [74].

$$T^1 = T^2 = \cdots = T^\varphi \qquad \text{(Equation 8)}$$

$$p^1 = p^2 = \cdots = p^\varphi \qquad \text{(Equation 9)}$$

$$\begin{matrix} \mu_1^1 = \mu_1^2 = \cdots = \mu_1^\varphi \\ \vdots \quad \vdots \qquad\quad \vdots \\ \mu_m^1 = \mu_m^2 = \cdots = \mu_m^\varphi \end{matrix} \qquad \text{(Equation 10)}$$

Temperature T, pressure p and chemical potential μ of m chemical species have to be uniform throughout the system in order to fulfil equilibrium conditions.

The chemical potential is the partial molar Gibbs' energy G (Equation 11)

$$\mu_i = \left(\frac{\partial G}{\partial n_i}\right)_{T,p,n_j} \qquad \text{with} \quad n_i \neq n_j \qquad \text{(Equation 11)}$$

where n_i is the amount of substance of compound i.

Applying the concept of fugacity (f_i), which was introduced by Lewis, the chemical potential can be expressed via Equation 12

$$\mu_i = \mu_{i,ideal\ gas}^0(\mathrm{T}, \mathrm{p}^+) + RT \ln \frac{f_i}{\mathrm{p}^+} \qquad \text{(Equation 12)}$$

where f_i^0 and μ_i^0 are the reference state fugacity and chemical potential, respectively. In Equation 12 the pure ideal gas at system temperature and a pressure p^+ of 1 atm is selected as the reference state.

Introducing the fugacity, Equation 10 can be substituted with the so-called iso-fugacity criterion (Equation 13). The iso-fugacity criterion follows from the equality of chemical potentials, if the reference state is the same in all phases.

$$f_i^1 = f_i^2 = \cdots = f_i^\varphi \qquad \text{with} \quad i = 1 \ldots m \qquad \text{(Equation 13)}$$

2.3.2. Liquid-liquid equilibrium

The liquid-liquid equilibrium between two phases can be described with Equation 14 which is derived from the iso-fugacity criterion (Equation 13)

$$x_i^\alpha \gamma_i^\alpha f_i^0 = x_i^\beta \gamma_i^\beta f_i^0 \qquad \text{with} \quad i = 1 \ldots m \qquad \text{(Equation 14)}$$

where x_i is the mole fraction and γ_i the activity coefficient of a compound i in the respective phase.

Since the reference state fugacity is a pure compound property and the same in both phases, the relation simplifies to Equation 15.

$$x_i^{\alpha}\gamma_i^{\alpha} = x_i^{\beta}\gamma_i^{\beta} \qquad \text{with} \quad i = 1 \dots m \qquad \text{(Equation 15)}$$

The distribution of a compound between the two phases can be described by the partition coefficient. The partition coefficient of compound i between two phases β and α that is calculated using mole fractions (Equation 16) is denoted with $K_i^{x,\alpha\beta}$.

$$K_i^{x,\alpha\beta} = \frac{x_i^{\alpha}}{x_i^{\beta}} = \frac{\gamma_i^{\beta}}{\gamma_i^{\alpha}} \qquad \text{(Equation 16)}$$

For low solute concentrations, $x_i \to 0$, the partition coefficient can be considered a constant which is independent of solute concentration. In practical applications, such as CPC and CCC, it is more common to calculate the partition coefficient based on solute concentration c_i than on mole fraction (Equation 17).

$$P_i^{\alpha\beta} = \frac{c_i^{\alpha}}{c_i^{\beta}} \qquad \text{(Equation 17)}$$

It is a frequently used assumption to use the concentration-based solute partition coefficient $P_i^{\alpha\beta}$ in the linear range of the partition equilibrium for the selection of biphasic systems and design of CCC and CPC processes. This simplification is reasonable since low solute concentrations are normally used to design a separation process and the injection concentration is increased in a later step.

The mole fraction-based partition coefficient and concentration-based partition coefficient can be converted into each other with the molar volumes of the phases ν^{α} and ν^{β} using Equation 18.

$$P_i^{\alpha\beta} = \frac{\nu^{\beta}}{\nu^{\alpha}} K_i^{x,\alpha\beta} \qquad \text{(Equation 18)}$$

The molar volumes of the phase ν^{φ} can be calculated with the composition of the phases, the molar volume of the pure solvents ν_i^0, and the excess volume of mixing ν^E, as shown in Equation 19.

$$\nu^{\varphi} = \sum x_i \nu_i^0 + \nu^E \qquad \text{(Equation 19)}$$

For screening purposes, the molar volume is often approximated with the ideal volume of mixing and ν^E is neglected.

2.3.3. Solid-liquid equilibrium

Similar to the liquid-liquid equilibrium, the solid-liquid equilibrium can be described starting from the iso-fugacity criterion.

$$f_i^S = f_i^L \qquad \text{with} \quad i = 1 \dots m \qquad \text{(Equation 20)}$$

This relation can also be expressed via mole fractions, activity coefficients, and standard fugacities for solid and liquid phase (Equation 21).

$$x_i^S \gamma_i^S f_i^{0S} = x_i^L \gamma_i^L f_i^{0L} \qquad \text{(Equation 21)}$$

In order to calculate the solubility of a solid in the liquid phase or vice versa with Equation 21, information about the non-ideality in the considered system, i.e. activity coefficients in solid and liquid phase, as well as the ratio of standard fugacities are necessary. For a simple eutectic, when the solid phase is always a pure solid, the equation can be simplified, as shown in Equation 22.

$$f_i^{0S} = x_i^L \gamma_i^L f_i^{0L} \qquad \text{(Equation 22)}$$

The ratio of standard fugacities can be obtained from the Gibbs' energy of the solid-liquid phase transition Δg_{SL}.

$$\Delta g_{SL} = RT \ln \frac{f_i^{0L}}{f_i^{0S}} \qquad \text{(Equation 23)}$$

The Gibbs' energy of the solid-liquid phase transition can also be expressed through Equation 24, as it is related to the change in enthalpy Δh_{SL} and entropy Δs_{SL} of the phase transition process.

$$\Delta g_{SL} = \Delta h_{SL} - T \Delta s_{SL} \qquad \text{(Equation 24)}$$

The solid-liquid phase transition can be divided into three steps: heating from the system temperature to the triple point temperature, melting of the solid at triple point temperature T_{tr}, and cooling to the subcooled liquid at system temperature.

That means the change in enthalpy Δh_{SL} in Equation 24 contains an enthalpy contribution due to the heating from system temperature to T_{tr} and cooling back to system temperature, and a change in enthalpy due to melting, the enthalpy of fusion $\Delta_{fus} h$ at the triple point temperature. The change in entropy can be estimated in a similar way via entropy of fusion and a heat capacity (c_p) dependent term for the temperature change from T to T_{tr}. In Equation 25 the aforementioned expressions are introduced to Equation 24 and the entropy of fusion is replaced by $\Delta_{fus} h$ divided by the triple point temperature T_{tr}; Δc_p is the difference between the heat capacity of the liquid and the solid phase.

$$\ln \frac{f_i^{0L}}{f_i^{0S}} = \frac{\Delta_{fus} h}{RT} \left(\frac{T_{tr}}{T} - 1 \right) - \frac{\Delta c_p}{R} \left(\frac{T_{tr}}{T} - 1 \right) + \frac{\Delta c_p}{R} \ln \frac{T_{tr}}{T} \qquad \text{(Equation 25)}$$

Equation 25 is commonly applied in a simplified form: Instead of the triple point properties, melting properties are used. Triple point properties are usually not available, and thus the melting temperature T_m and $\Delta_{fus} h$ at melting temperature are used instead of the triple point temperature values. Further, the two heat capacity dependent terms are neglected as they tend

to have similar values and nearly cancel each other out, especially close to the triple point temperature. A detailed derivation can be found in [74, 75].

Solubility depends on the melting properties of the pure compounds, T_m and $\Delta_{fus}h$, and the activity coefficient. Measurement or estimation of melting properties can be laborious and come with high uncertainty. For solvent system screening it is often enough to get a qualitative estimation of solubility to choose a suitable solvent from a selection. The solvent capacity C_i^∞ is a useful qualitative estimation and can be calculated from limiting activity coefficients with Equation 26.

$$C_i^\infty = \frac{1}{\gamma_i^\infty} \qquad \text{(Equation 26)}$$

High solvent capacity is obtained for limiting activity coefficients smaller than unity, meaning the attractive interactions of solute and solvent molecules are stronger than in an ideal solution. Solvent capacity is a tool to estimate the relative solubility of a solute in different solvents. It has successfully been applied in solvent system screening for LLC [40]. This approach can on the one hand be used to obtain a relative estimation of the solubility of target compounds, on the other hand limiting activity coefficients can also be used to estimate the relative solubility of a solvent in another liquid solvent.

2.4. Solvent screening using a predictive thermodynamic model

The number of possible solvent combinations that can form a biphasic system is nearly limitless. Trial and error methods are very time consuming and require high experimental effort. Models can help to reduce this workload by narrowing down the number of solvent systems to consider. There is a large number of different models to choose from. Thermodynamic models for the prediction of phase equilibria can be divided into two subclasses: equation of state (EoS) or excess Gibb's energy model (g^E-model). The first group includes cubic EoS, such as Peng-Robinson or Redlich-Kwong Equation, or statistical EoS, such as variations of the Statistical Associating Fluid Theory (SAFT) equations. Examples for g^E-models are Non-Random Two-Liquid (NRTL) Theory, Wilson Equation, or Universal Quasichemical (UNIQUAC) Equation. For many applications, it is of a particular advantage to have a predictive model. This also applies for CCC and CPC where in many cases there are no pure substances available for experimental determination of parameters. Predictive g^E-Models include Universal Quasichemical Functional-group Activity Coefficients (UNIFAC) equation and the Conductor-like Screening Model for Realistic Solvation (COSMO-RS, formerly also Conductor-like Screening Model for Real Solvents).

The necessary tasks for the selection of a DES-based biphasic system for CPC separations are illustrated in Figure 9. First, possible HBA-HBD combinations have to be chosen. In the second step, the stoichiometric ratio has to be selected for each HBA-HBD combination. It has to be noted, that this ratio needs to yield a liquid mixture at ambient temperature, but it does not necessarily need to be the eutectic composition. At the moment, the first two steps are done based on literature review. Further, a pool of organic solvents is needed that is selected according to process or safety requirements. Next, possible combinations of DES and organic solvents need to be chosen (step 4 in Figure 9). This can be done via limiting activity

coefficient screening. In addition to the solvent combination - usually three to four different species are combined - the stoichiometric composition of the biphasic system has to be selected in step 5. For this purpose, the liquid-liquid equilibrium is calculated for each previously selected combination of DES and organic solvents. In the last step, solute partition coefficients of target compounds and impurities are calculated for different compositions of the biphasic system. The biphasic system and its composition are selected according to the partition coefficient values, which are desired to be in the *sweet spot*. In this work, COSMO-RS was selected for the calculation of thermodynamic properties based on previous work in the field of CPC and CCC [40, 41, 76]. It was used to calculated limiting activity coefficients for the selection of combinations of organic solvents in step 4, illustrated in Figure 9, for the prediction of LLE in step 5 and the calculation of solute partition coefficients in step 6.

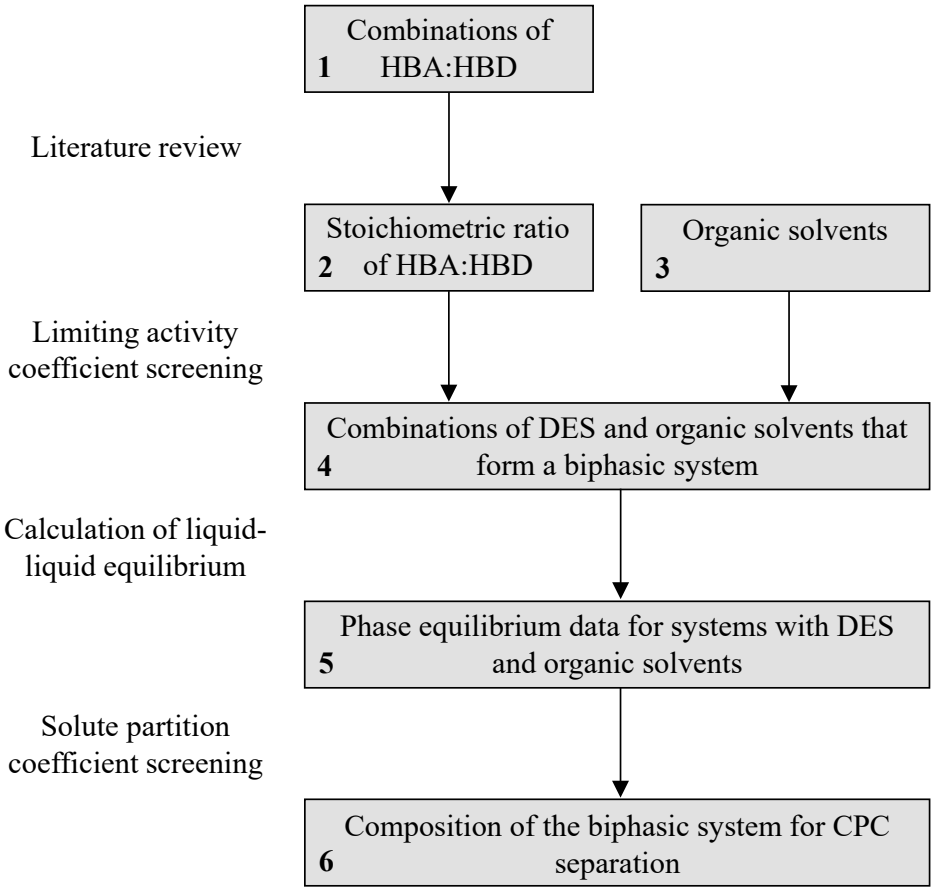

Figure 9: Necessary steps for the selection of a DES-based biphasic system for CPC separations.

2.4.1. Conductor-like screening model (COSMO) and conductor-like screening model for realistic solvation (COSMO-RS)

The conductor-like screening model (COSMO) is a continuum solvation model developed by Klamt [77]. It combines quantum chemistry and statistical thermodynamics in order to predict thermodynamic properties of pure compounds and mixtures solely based on molecular structure. The model requires sets of molecular conformations for the considered chemical species and the following calculations are performed for each structure of the set: A cavity is constructed around the molecule that is surrounded by a continuum with dielectric constant ε corresponding to an ideal conductor. DFT calculations are performed for each molecule in order to obtain the screening charge density. The screening charge density is divided into discrete surface segments. The surface segments are defined by their area, screening charge, spatial coordinates and screening charge density. This information is stored in a database. Thus, the described calculations have to be performed only once for each chemical compound [78].

COSMO was expanded to the conductor-like screening model for realistic solvation (COSMO-RS) by Klamt in order to account for intermolecular interactions in mixtures. This is achieved by breaking down the interactions of an ensemble of molecules in a mixture to an ensemble of pair-wise interacting surface segments. The information of the ensemble of surface segments of a molecule is stored in the sigma profile $p_i(\sigma)$, a histogram of the segment surface polarization charge density σ. Examples for *n*-hexane and water are shown in Figure 10.

The $p_S(\sigma)$ of a mixture can be calculated from the $p_i(\sigma)$ of each molecule, the respective mole fraction x_i and the molecular surface area A_i of each molecule [79].

$$p_S(\sigma) = \frac{\sum_i x_i \, p_i(\sigma)}{\sum_i x_i \, A_i} \qquad \text{(Equation 27)}$$

The chemical potential μ_S^X of a solute X in a solvent S is calculated by integration of the σ-potential $\mu_S(\sigma)$ over the surface of the solute. A detailed derivation of $\mu_S(\sigma)$ can be found in [79]. The number of surface contacts of the molecules in the mixture is denoted with k, T is the temperature of the system, and $\gamma_{comb,S}$ the combinatorial term of the activity coefficient.

$$\mu_S^X = \int d\sigma p_X(\sigma)\mu_S(\sigma) + kT \ln\left(x + \gamma_{comb,S}\right) \qquad \text{(Equation 28)}$$

Liquid-liquid equilibria, capacity and solute partition coefficients are derived from activity coefficients. They can be obtained from the chemical potential using Equation 29

$$\gamma_i = exp\left(\frac{\mu_S^X - \mu_i^0}{RT}\right) \qquad \text{(Equation 29)}$$

where μ_S^X is the calculated chemical potential, μ_i^0 is the chemical potential of the COSMO standard state, and R is the universal gas constant.

The term COSMO-RS refers to the model theory and COSMOtherm denotes the implementation of the model into the commercially available software from Cosmologic GmbH & Co. KG.

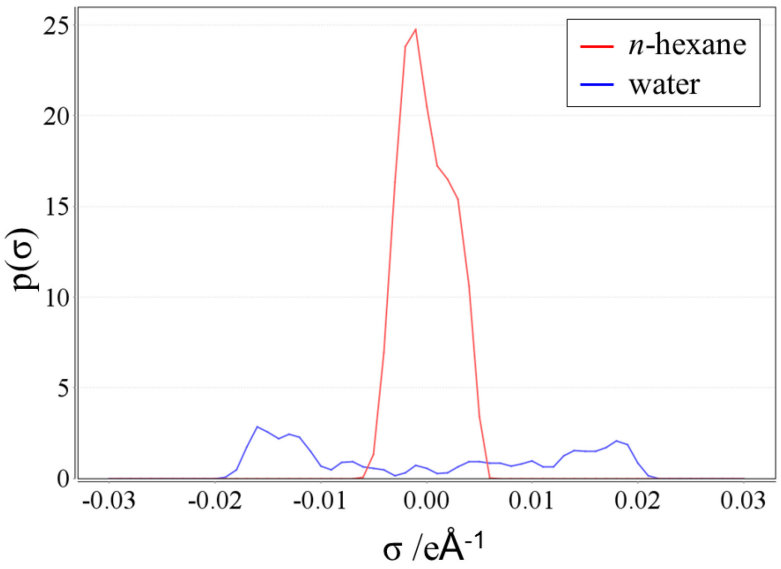

Figure 10: Sigma profiles of *n*-hexane and water taken from COSMOtherm software, Cosmologic GmbH & Co. KG.

2.4.2. Representation of DESs in COSMO-RS

There are different ways to treat ionic molecules in COSMO-RS [80]. An ionic species can be described as a non-dissociated molecule and COSMO calculations are performed for the ion pair as one molecule. The cation and anion can also be treated as an electroneutral mixture of fully dissociated ions. The third option is to treat the ions as individual species in the quantum chemical calculations, but the information is then combined in a so-called metafile. Since many DESs contain ionic species, the approaches were adapted as illustrated in Figure 11, where ν is the stoichiometric factor of different constituents, namely cation (c), anion (a), HBA, and HBD.

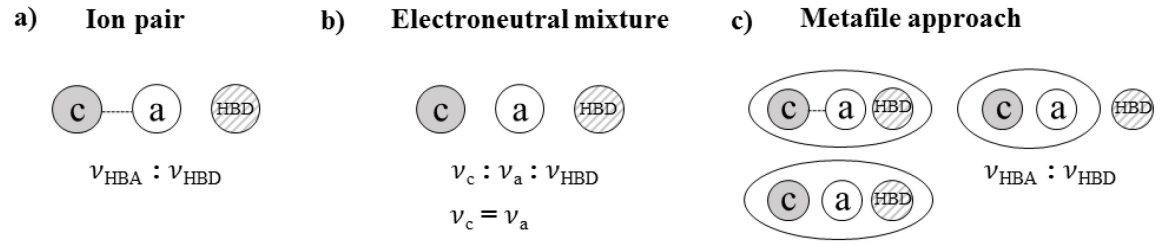

Figure 11: Different molecular representations of DESs in COSMO-RS: (a) ion pair approach, (b) representation as electroneutral mixture, and (c) metafile approach.

When ions or mixtures with ions are considered in COSMO-RS, the results have to be rescaled to the experimental definitions according to Equation 30.

$$x_i^{exp}\gamma_i^{exp} = x_i^{calc}\gamma_i^{calc} \qquad \text{(Equation 30)}$$

x_i^{calc} and γ_i^{calc} are the mole fraction and activity coefficient calculated with COSMO-RS, and x_i^{exp} and γ_i^{exp} are the mole fraction and activity coefficient obtained from experiment.

Details about the molecular representation of DESs in COSMO-RS and scaling from COSMO-RS calculated values to experimental framework can be found in the manuscript "Assessing solute partitioning in deep eutectic solvent-based biphasic systems using the predictive thermodynamic model COSMO-RS" (**Paper II**) in section 3.6.2.

3. Results

3.1. Paper I

Ionic liquids as modifying agents for protein separation in centrifugal partition chromatography

Citation

F. Bezold, S. Roehrer, M. Minceva, Ionic Liquids as Modifying Agents for Protein Separation in Centrifugal Partition Chromatography, Chemical Engineering & Technology, 42 (2019) 474-482.

https://doi.org/10.1002/ceat.201800369

Summary

Previous work has shown that ATPSs with ILs as phase forming compounds, with concentrations around 20 wt% of IL, were not suitable for CCC and CPC since protein partition coefficients are too high [17]. In this manuscript, ATPSs composed of polyethylene glycol 1000, phosphate salts, water, and small amounts of IL, were studied. The aim of this work was to utilize the capability of ILs to tune protein partition coefficients and make use of this phenomenon in CPC separations. Partition coefficients of two model proteins, myoglobin and lysozyme, were determined in shake flask experiments and the effect of small amounts of 1-ethyl-3-methylimidazolium chloride ([EMIM]Cl) or 1-butyl-3-methylimidazolium chloride ([BMIM]Cl) was investigated. The ILs and proteins were selected based on previous work, where myoglobin, lysozyme and BSA were used. BSA was omitted in the present study since preliminary CPC experiments showed that BSA lowers the interfacial tension of the biphasic system and causes complete stationary phase loss after injection. In the shake flask experiments conducted in this work, it was shown that myoglobin distribution was not altered while the partition coefficient of lysozyme decreased when IL was added and was shifted to the *sweet spot*. Stationary phase retention of the ATPS without and with additional IL was then determined and it was found that the effect of amounts up to 1.5 wt% of [EMIM]Cl on stationary phase retention was negligible. The decreasing effect of the IL on the partition coefficient of lysozyme was confirmed in CPC separation experiments. The biphasic system was stable enough to increase the injection volume to 50 ml, 20 % of the total column volume. Process simulations were then performed in order to evaluate further increase of the injection volume and the results indicated that this may be possible. The findings of this work may also impact other research areas and may be used in different applications, such as the separation of glucosides, nanotubes, monoclonal antibodies, peptides, DNA or virus-like particles.

The work was part of a project funded by the German Research Foundation (Deutsche Forschungsgemeinschaft, DFG-ProjektMI1340/3-1). The authors thank the German Research Foundation for providing the financial support for this work.

Contributions

The author of this dissertation had a leading role in this work. She planned and coordinated the work, conducted or supervised all data acquisition, and interpreted the data. The author selected the ILs and phase forming compounds, system compositions, and process parameters for the CPC separations. S. Roehrer performed the simulations in collaboration with the author. W. Stelzer conducted the circular dichroism measurements with the author and helped with circular dichroism data analysis and interpretation. The manuscript was written by the author and discussed with Prof. Minceva.

Chemical Engineering & Technology Research Article 474

Franziska Bezold
Simon Roehrer
Mirjana Minceva*

Ionic Liquids as Modifying Agents for Protein Separation in Centrifugal Partition Chromatography

Aqueous two-phase systems (ATPSs) can be applied in centrifugal partition chromatography (CPC) to separate biomolecules. Two ionic liquids (ILs) served as modifying agents to tune partition coefficients in the separation of two model proteins, myoglobin and lysozyme. Myoglobin was not affected by the ILs, while the partition coefficient of lysozyme was lowered with addition of IL. High stationary phase retention was achieved with ATPSs in a CPC column with cell size and geometry specially designed for unstable biphasic systems. When ILs were used as modifying agents, no notable decrease in stationary phase retention was observed. The injection volume was increased to 20 % of the total column volume and process simulations indicate that a further increase in the injection volume is possible.

Keywords: Aqueous two-phase systems, Ionic liquids, Liquid-liquid chromatography, Protein separation

Received: July 20, 2018; *revised:* November 22, 2018; *accepted:* December 12, 2018

DOI: 10.1002/ceat.201800369

Supporting Information available online

1 Introduction

Aqueous two-phase systems (ATPSs) are biphasic liquid systems with both phases mainly consisting of water. They provide mild conditions for the separation of biomolecules and are used for the purification of virus-like particles, monoclonal antibodies, and other proteins [1–7]. ATPSs can be formed by two polymers, i.e., kosmotropic salt and polymer, kosmotropic salt and ionic liquid (IL), or IL and polymer in water. Polyethylene glycol (PEG) and phosphate salts are among the most commonly used phase-forming compounds for ATPSs for extraction and separation of proteins [8]. The main application field of ATPSs is liquid-liquid extraction. However, there is a growing interest in ATPSs in the field of liquid-liquid chromatography since they enable the separation of proteins and other hydrophilic biomolecules.

Liquid-liquid chromatography is a chromatographic technique that uses two liquid phases as stationary and mobile phases. The columns for performing liquid-liquid chromatography separations can be divided into two subgroups: hydrodynamic countercurrent chromatography (CCC) or hydrostatic centrifugal partition chromatography (CPC). Both column designs share the same separation principle. One of the phases is kept stationary inside the column with the help of a centrifugal field, while the other phase is pumped through the column. Target compounds are separated according to the difference in their distribution between the stationary and mobile phases.

Partition coefficients between 0.4 and 2.5 are in the optimum separation region, the so-called "sweet spot". Thus, it is desirable to select the biphasic solvent system as such that the partition coefficients of target compounds are in the sweet spot, in order to achieve high productivity and sufficient resolution. The separation performance strongly depends on the volume of the stationary phase that can be held inside the column [9]. A higher stationary phase volume leads to higher separation resolution. Due to the low interfacial tension and quite viscous nature of ATPSs compared to organic solvents it has been challenging to achieve high stationary phase retention at reasonable flow rates in conventional CCC and CPC columns. There are two strategies to overcome this problem: (1) the development of new column designs, and (2) tuning the physical properties of the ATPS, e.g., by varying composition, using additives, and using novel phase-forming components.

In recent years, several new CCC and CPC column designs have been developed to overcome the difficulties when working with ATPSs. Hydrodynamic CCC devices are composed of tubing wound around a cylindrical drum that is mounted in a planetary gear [10]. One approach to improve stationary phase retention in hydrodynamic machines is spiral CCC, where the tubing is wound in a special spiral support [11, 12]. The stationary phase retention of ATPSs can be further increased by tubing modifications in the spiral CCC setup [13, 14] or adjustments in the design which include toroidal [15] and conical columns [16].

Franziska Bezold, Simon Roehrer, Dr. Mirjana Minceva
mirjana.minceva@tum.de
Technical University of Munich, Biothermodynamics, TUM School of Life and Food Sciences Weihenstephan, Maximus-von-Imhof-Forum 2, 85354 Freising, Germany.

However, in hydrodynamic CCC devices, ATPSs can only be employed with low mobile phase flow rates (2 mL min^{-1} with a 280-mL column [17]) without stationary phase loss.

In contrast to CCC, in hydrostatic CPC setups the column is composed of small chambers with interconnecting channels [9]. Due to the geometrical design, CPC devices show higher back pressure, and in regular setups only biphasic solvent systems with low viscosity can be used. To overcome this issue, a column geometry with bigger cells has been designed, allowing the use of more viscous biphasic solvent systems containing low-molecular-weight polymers, ILs or deep eutectic solvents [18, 19]. With the new developments in apparatus design, many general problems of ATPSs, such as low stationary phase retention or high back pressure, have been addressed.

In addition to apparatus design, there are approaches to improve the separation performance by adjusting the properties of ATPSs. Besides the most frequently used polymer-polymer-based and polymer-salt-based ATPSs, ATPSs composed of ILs, salts, and water or IL, polymer, and water have been developed [20, 21]. Recently, ATPSs containing inorganic salts and deep eutectic solvents have been introduced [22–24]. To achieve the desired separation factor, ATPSs can be tailored, e.g., by varying ATPS composition, the polymer chain length, or functional groups in polymer-based ATPSs [25, 26], choosing different inorganic salt species according to the Hofmeister series or by selecting cations or anions in IL-based ATPS [27–29].

However, the options for tailoring are more limited for application of ATPSs in CPC. Increasing polymer chain length results in high back pressure due to higher viscosity, and variation of inorganic salt species strongly influences the size and position of the biphasic region as well as solute distribution. Similarly, cation and anion of IL-based ATPS can be varied to tune the properties of the biphasic system. However, in previous work, it has been shown that the partition coefficients of the model proteins used in this study were too high for an application in CPC or CCC in APTSs composed of ILs, phosphate, and water [30].

In general, it is difficult to improve both the physical properties and the partition coefficient at the same time. Better physical properties for an application in CPC and CCC are usually achieved for system compositions far from the plait point and with longer tie lines, while partition coefficients are favorable for systems closer to the plait point. Other than by the above-mentioned possibilities, the properties of ATPSs can also be tuned by additives or modifying agents. Additives or modifying agents are present in small amounts and, hence, alter solute partition coefficient while having little influence on the physical properties of the ATPS and the location of the binodal.

Commonly used modifications to alter the partition coefficient of a target compound are, e.g., pH adjustment [31, 32] and addition of sodium chloride [4]. Adjustment of pH has a great influence on proteins since their net charge changes with pH. Addition of small amounts of ILs has been shown to positively influence the partition coefficient of antioxidants for application of ATPSs in liquid-liquid extraction [33].

In this work, the effect of ILs on protein partition coefficients and the application of this effect in CPC separations were investigated. The novel CPC design with bigger cells described above was used for the CPC experiments to achieve high stationary phase retention at larger flow rates than in typical separations with ATPSs and CCC. The focus of this work is the application of ILs as modifying agents for the separation of proteins with ATPSs in CPC. 1-Ethyl-3-methylimidazolium chloride ([EMIM]Cl) and 1-butyl-3-methylimidazolium chloride ([BMIM]Cl) have been selected as modifying agents. Shake-flask experiments were conducted to show the potential of ILs to tune the protein partition coefficient in the ATPSs, and CPC experiments were conducted with the most promising systems.

2 Materials and Methods

2.1 Chemicals

Myoglobin (from horse muscle, 95–100 %, pH(I) = 6.8–7.2, M_W = 16 951.49 Da), 1-ethyl-3-methylimidazolium chloride ([EMIM]Cl, ≥ 95 %), and 1-butyl-3-methylimidazolium chloride ([BMIM]Cl, ≥ 95 %) were obtained from Sigma Aldrich (Germany). PEG 1000 (average M_W = 950–1050 g mol^{-1}), KH_2PO_4 (≥ 99.5 %), and $K_2HPO_4 \cdot 3H_2O$ (≥ 99.0 %) were purchased from Merck KGaA (Germany). Ultrapure-grade lysozyme (pH(I) = 11.35, M_W = 14 307.0 Da) was from Amresco (USA), acetonitrile (HPLC (high-performance liquid chromatography)-grade) from J. T. Baker (USA), and trifluoroacetic acid (approx. 100 %) from VWR Chemicals (Germany). Purified water was prepared using a MilliQ filter system from Merck KGaA (Germany).

2.2 Preparation of ATPSs for Shake-Flask and CPC Experiments

For the preparation of the biphasic systems, all components were weighed out. The total sample mass was 12–15 g and the system composition was PEG 1000/K_2HPO_4/KH_2PO_4/H_2O 15.00:9.68:5.32:70.00 (w/w/w/w). At first, K_2HPO_4 and KH_2PO_4 in a ratio of 1.82:1 (w/w), water and PEG 1000, molten in a 50 °C water bath, were weighed in and completely dissolved. The amount of water was adjusted to account for water added with IL- and protein stock solutions in a later step. The mixture was allowed to cool to ambient temperature before further use. For biphasic systems containing modifiers, [EMIM]Cl or [BMIM]Cl was added in form of a stock solution containing 80 wt % of IL and 20 wt % of water.

For shake-flask experiments and the feed solutions for the CPC experiments, protein was added from stock solution in the last step. The two separate stock solutions both contained a concentration of 10 mg mL^{-1} of lysozyme or myoglobin in water. The ATPSs were then put on an automatic shaker or magnetic stirrer for 30 min and equilibrated for at least 2 h at ambient temperature (23.0 ± 1.0 °C).

2.3 Determination of Partition Coefficients

The partition coefficients of lysozyme and myoglobin as well as the distribution of the ILs in the different ATPSs were deter-

mined by shake-flask experiments. After preparation and equilibration, the phases were split and the UV absorbance of myoglobin or lysozyme, respectively, was measured. Partition coefficients were determined at least in triplicate; different concentrations between 0.3 and 0.7 mg g^{-1} (0.35–0.82 mg mL^{-1}) of either myoglobin or lysozyme were used to check for linearity of the partition coefficient. The partition coefficients of ILs were determined in ATPSs with 0.5, 1.0, 1.5, and 2.5 wt % of added ILs.

A Shimadzu Prominence HPLC system was employed for analysis with an RP-C18 column from Phenomenex (Kinetex C-18 core shell reversed-phase column, 100×4.6 mm, particle size 5 µm, pore size 100 Å) equipped with a diode array detector. Gradient-grade acetonitrile and water with 0.05 % TFA each served as eluents for linear gradient elution starting from 21.5 to 40 % acetonitrile in 10 min with a mobile phase flow rate of 0.4 mL min^{-1}, followed by a washing step. Chromatograms were analyzed at 230 nm.

2.4 CPC Experiments

The centrifugal partition chromatography experiments were performed with a CPC 250 PRO SPECIAL BIO VERSION unit, formerly called SCPE-250-BIO, from Gilson Purification SAS. The column consists of 12 stainless-steel disks with Teflon coating for biocompatibility and has a total column volume of 250 mL. The maximum rotational speed is 3000 rpm and the maximum pressure of the system is 100 bar (1450 psi). The column was connected to two HPLC pumps (pump 305, 50SC head, Gilson, USA) with a maximum flow rate of 50 mL min^{-1} and a DAD detector (171 diode array detector, Gilson, USA).

Biphasic solvent systems for the chromatographic separations were prepared as described in Sect. 2.2. After equilibration, the phases were separated, put into two reservoirs, and degassed before the CPC experiments. To determine the stationary phase retention, the column was first completely filled with stationary phase. After the rotation was started, the mobile phase was pumped through the column. The volume of stationary phase eluted from the column until hydrodynamic equilibrium was reached was determined. At the end of each experiment, the remaining amount of stationary phase was pumped out of the column and its volume was noted.

The protein feed solution was dissolved in an equal volume of upper and lower phase. Preparation of the feed mixture only in the mobile phase was not possible since the solubility of lysozyme in the lower phase (mobile phase) was too low to dissolve a sufficient amount of the protein to achieve a visible peak in the UV detector. Therefore, the stationary phase retention was measured for each experiment prior to the injection and then recalculated including the volume of stationary phase coming from the injection. The feed contained 2 mg g^{-1} (2.3 mg mL^{-1}) of lysozyme and 2 mg g^{-1} (2.3 mg mL^{-1}) of myoglobin for all CPC experiments. All chromatograms shown in the results were recorded at 230 nm with 470 nm set as reference wavelength for the detector.

2.5 Simulations

Simulations were performed by numerically solving the equilibrium cell model equations using gPROMS Model Builder v4.2 software from Process Systems Enterprise (London, UK). As introduced by Martin and Synge [34], the column is described as a cascade of N[1)] ideal stirred-tank reactors (theoretical stages) with a volume of V_C/N. Under the assumption of ideal mixing, the mass balance of component i for each theoretical stage is solved according to Eq. (1). The concentration of solute i in stage k is denoted as $c_{i,k}$ for mobile (MP) and stationary phase (SP), respectively; V is the volume of the corresponding phase, t is the time, and F is the mobile phase flow rate. The number of stages N describes peak-broadening effects due to axial dispersion and mass transfer resistance and was determined from the experimental data, i.e., elution profiles.

$$\frac{V_{MP}}{N}\frac{dc_{i,k}^{MP}}{dt}+\frac{V_{SP}}{N}\frac{dc_{i,k}^{SP}}{dt}=F\left(c_{i,k-1}^{MP}-c_{i,k}^{MP}\right)\quad k=1,\ldots,N \tag{1}$$

Details about the model can be found in [35–37]. In the experiments, the stationary phase was injected with the feed and it was observed that this additional stationary phase volume slowly elutes over the whole separation run. No additional loss of stationary phase was detected besides the injected volume. Hence, for the simulation, the stationary phase retention was recalculated according to $S_f = (V_{SP} + V_{SP,injection})/V_{column}$ and a linear function for the loss of stationary phase that was injected with the sample ($V_{SP,injection}$) was assumed. The linear function was specific for each system and flow rate and determined from the experimental data, i.e., elution profiles.

Simulated chromatograms were taken to select the switching time for the dual-mode experiment presented in Sect. 3.3. In dual mode, the separation mode is switched at a certain time and the roles of stationary and mobile phase are exchanged. In this work, the separation started in descending mode with the upper phase being the stationary phase for the chromatographic separation. The mode should be switched after the first protein elutes. When the role of stationary and mobile phase is exchanged, the pumping direction inside the column is also reversed, and the compound remaining in the column is eluted. Additionally, in Sect. 3.4 the effect of increasing injection volume was studied in experiment and simulations.

3 Results and Discussion

3.1 Influence of ILs on Protein Distribution

One of the most important parameters in the design of a CPC separation is the partition coefficient of target compounds and impurities in the biphasic solvent system used as stationary and mobile phases. In CPC and CCC, the partition coefficient is defined as the ratio of the solute concentration in the stationary phase (c_i^{SP}) and the solute concentration in the mobile phase (c_i^{MP}) at thermodynamic equilibrium.

1) List of symbols at the end of the paper.

$$P_i = \frac{c_i^{SP}}{c_i^{MP}} \quad (2)$$

Since the user may choose which one of the two phases of a biphasic system is the stationary and which the mobile phase, there are two possible operation modes. In descending mode (DSC), the upper phase of the liquid biphasic system is used as the stationary phase, and the lower phase acts as the mobile phase. In ascending mode (ASC), the lower phase serves as stationary phase and the upper phase as mobile phase.

The partition coefficient can also be determined from pulse injections:

$$P_i = \frac{V_R - V_{MP}}{V_{SP}} \quad (3)$$

where V_R is the retention volume of the target compound, and V_{MP} and V_{SP} are the volumes of mobile and stationary phase inside the column during the separation, respectively. The retention volume was determined by multiplying the mean retention time of the peak with the mobile phase flow rate. The mean retention time was calculated by the first absolute momentum μ_t by Eq. (4).

$$\mu_t = \frac{\int_0^\infty tc(t)dt}{\int_0^\infty c(t)dt} \quad (4)$$

The partition coefficients were determined for descending mode. The system composed of PEG 1000/K_2HPO_4/KH_2PO_4/H_2O 15:9.68:5.32:70 (w/w/w/w) with a ratio of K_2HPO_4/KH_2PO_4 equal to 1.82 was used as reference system without modifier. In this ATPS, the pH value in the upper phase was 7.3 ± 0.1, and 7.1 ± 0.1 in the lower phase, measured at a temperature of 23.1 ± 0.3 °C. The addition of [EMIM]Cl or [BMIM]Cl with the concentrations used in this work did not change the pH values in both phases.

The influence of the ILs [EMIM]Cl and [BMIM]Cl on the protein partition coefficients was investigated in shake-flask experiments. ATPSs with a composition of PEG 1000/K_2HPO_4/KH_2PO_4/H_2O 15:9.68:5.32:70 (w/w/w/w) were prepared with additional varying amounts of ILs. The amount of ILs was kept low, i.e., between 0.5 and 2.5 wt %, to find the minimal effective concentrations and keep the cost for modifiers as low as possible.

Figs. 1 a and b indicate the partition coefficients of myoglobin and lysozyme in the ATPSs with different amounts of [EMIM]Cl or [BMIM]Cl. The partition coefficient of myoglobin was not altered when [EMIM]Cl or [BMIM]Cl were added. For lysozyme, the partition coefficient decreases from a value of 2.9 to 2.0 for 2.5 wt % of [EMIM]Cl and to 1.9 for 2.5 wt % [BMIM]Cl. In addition to the protein distribution, the partition coefficient of ILs in the ATPSs was determined. Fig. 1 c shows the results for the IL partition coefficients.

The partition coefficient of [EMIM]Cl stays constant with a mean partition coefficient of 0.89 ± 0.02 for amounts of ILs between 0.5 and 2.5 wt %. This means the IL is located in both phases in the ATPS. For [BMIM]Cl a mean partition coefficient of 1.38 ± 0.09 was obtained. Hydrophilic ILs, such as

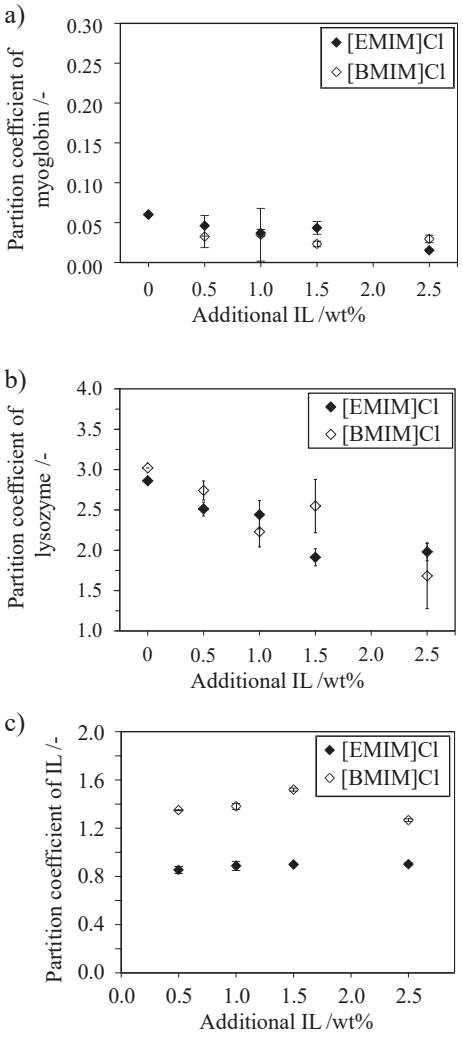

Figure 1. Partition coefficients of (a) myoglobin and (b) lysozyme in the biphasic system PEG 1000/K_2HPO_4/KH_2PO_4/H_2O 15.00:9.68:5.32:70.00 (w/w/w/w) with and without additional [EMIM]Cl or [BMIM]Cl. (c) Partition coefficients of [EMIM]Cl and [BMIM]Cl.

[BMIM]Cl and [EMIM]Cl, are present as individual solvated ions in diluted aqueous solutions and thus the dissociated cation and anion can interact directly with protein surfaces [38, 39].

Lysozyme has an isoelectric point of 11.35 and is positively charged in both phases of the ATPS. It was shown by Gokarn et al. that anions, such as chloride, accumulate at the surface of lysozyme [40]. Due this effect, the chloride anions are shielding the positive charges of the protein. $[EMIM]^+$ can be considered a chaotropic cation which are stabilizing enzymes in aqueous mixtures [38] and has been shown to enhance the stability of lysozyme, as described by Buchfink et al. [41]. The chaotropicity decreases from $[EMIM]^+$ to $[BMIM]^+$ [42]. These stabilizing interactions cause lysozyme to be distributed more evenly between the two phases than without the modifying agent.

For some imidazolium derivates, inhibition of lysozyme activity was found above certain concentrations [43]. It is generally advisable to remove the IL, PEG, and salts after separation by dialysis to prevent partial inhibition. However, it could be demonstrated for [EMIM]Cl that the structure of lysozyme and myoglobin is not changed by exposure to small concentrations of the IL (Figs. S2 and S3 in the Supporting Information). It is interesting to note that the addition of ILs has an adverse effect compared to NaCl, which is commonly used as a modifying agent to increase the solubility of proteins, on the lysozyme partition coefficient. The effect of NaCl on the protein partition coefficients is indicated in Fig. S1 and Tab. S3.

3.2 Stationary Phase Retention

Prior to the separation of proteins, the stationary phase retention S_f of the ATPS was determined. S_f is defined as the ratio of the stationary phase inside the column during the separation and the total column volume V_c ($S_f = V_{SP}/V_c$). The results for S_f at a rotational speed of 2000 rpm for the ATPS without modifier, PEG 1000/K_2HPO_4/KH_2PO_4/H_2O 15:9.68:5.32:70 (w/w/w/w), are presented in Fig. 2a. S_f decreases from 0.79 for 5 mL min^{-1} to 0.61 for 20 mL min^{-1} in descending mode. In ascending mode, the same S_f value as in descending mode is achieved for a mobile phase flow rate of 5 mL min^{-1}, whereas

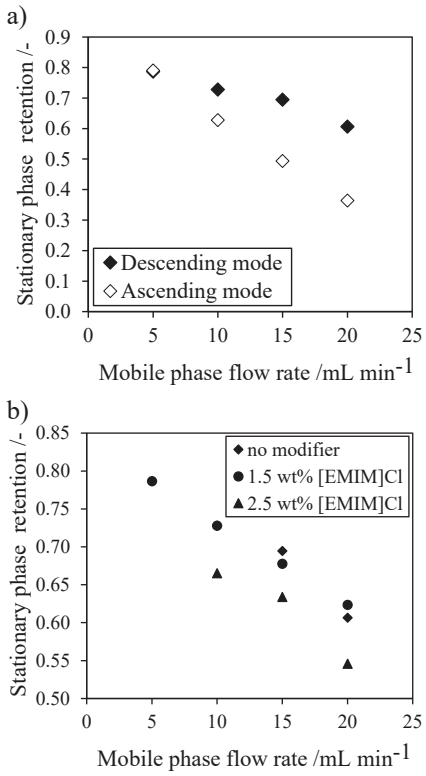

Figure 2. (a) Stationary phase retention of PEG 1000/K_2HPO_4/KH_2PO_4/H_2O 15.00:9.68:5.32:70.00 (w/w/w/) at a rotational speed of 2000 rpm. (b) Comparison of S_f for PEG 1000/K_2HPO_4/KH_2PO_4/H_2O 15.00:9.68:5.32:70.00 (w/w/w/w) without and with additional [EMIM]Cl.

for higher mobile phase flow rates a steeper decline of S_f was observed.

In Fig. 2 b, the stationary phase retention values of PEG 1000/K_2HPO_4/KH_2PO_4/H_2O 15:9.68:5.32:70 (w/w/w/w) with additional amounts of [EMIM]Cl are indicated. For the system without IL and with 1.5 wt % [EMIM]Cl very similar S_f values were observed. When 2.5 wt % of [EMIM]Cl are added to the APTS, the measured values of stationary phase retention were approximately 5 % lower than for the ATPS without IL or with 1.5 wt % of [EMIM]Cl.

3.3 Separation of Lysozyme and Myoglobin without Modifier

In this section, CPC experiments are performed for the ATPS without modifier. First, protein separation in descending mode is conducted, and then dual-mode separation is presented to demonstrate a potential method to increase productivity and throughput. Evaluating the partition coefficients of myoglobin and lysozyme from the shake-flask experiments presented in Sect. 3.1 indicates that it is preferable to perform the injection in descending mode.

Fig. 3 presents the chromatogram of a 10-mL batch injection of the protein feed mixture at a rotational speed of 2000 rpm and a mobile phase flow rate of 10 mL min^{-1}. S_f of 0.74 was calculated after injection. Myoglobin eluted close to the dead volume, while lysozyme eluted later as a broad peak. With the injection, 5 mL of additional stationary phase was injected. No additional stationary phase loss was observed except for the amount injected with the feed. The additionally injected stationary phase did not elute from the column right after injection, but eluted slowly over the whole separation time. Therefore, a linear decrease in S_f was assumed for the calculations of the protein partition coefficients.

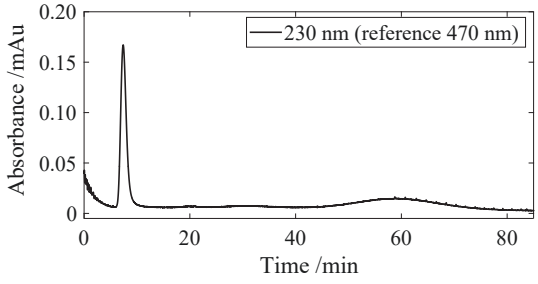

Figure 3. Chromatogram of myoglobin and lysozyme separation using PEG 1000/K_2HPO_4/KH_2PO_4/H_2O 15.00:9.68:5.32:70.00 (w/w/w/w). Batch separation was performed with an injection volume of 10 mL, 2000 rpm, feed concentration of 2 mg g^{-1} (2.3 mg mL^{-1}) for each protein, mobile phase flow rate of 10 mL min^{-1}, and an initial S_f of 0.74.

Partition coefficients of 0.04 for myoglobin and 3.02 for lysozyme were calculated from the chromatogram. The total separation time was 85 min for a mobile phase flow rate of 10 mL min^{-1}; however, the separation could be shortened by applying dual-mode separation. In dual mode, the separation

mode and thus the role of stationary and mobile phase are interchanged during the run. In this example, the separation was first started in descending mode at 10 mL min^{-1} and then switched to ascending mode with 20 mL min^{-1}. In previous experiments, an S_f between 0.72 and 0.74 was obtained for descending mode (Fig. 2 a). Thus, the lower phase occupies around 26–28 % of the column volume. The volumetric flow rate of 20 mL min^{-1} was selected for ascending mode since an S_f value of 0.28 can be guaranteed for this flow rate (Fig. 2 a). Flow rates higher than 20 mL min^{-1} were not feasible due to the high back pressure in ascending mode.

Prior to the experiment, the separation was simulated to determine the switching time. It was assumed that the volume of the phases stays the same before and after switching the modes. The simulated and experimental chromatogram are displayed in Fig. 4. From the simulations a switching time of 9 min was selected for the experiments. Due to limitations of the experimental setup, the flow could not directly be switched from 10 mL min^{-1} of the lower phase to 20 mL min^{-1}. Instead, the mobile phase flow took 1.5 min after switching to reach a volumetric flow of 20 mL min^{-1} of the upper phase. Thus, a deviation from the simulated chromatogram due to the start-up behavior of the pump is to be expected. In the dual-mode separation, lysozyme eluted shortly after myoglobin, leading to a separation time below 20 min. The small peak in front of the lysozyme peak in Fig. 4 is a result from pressure change due to switching the mode.

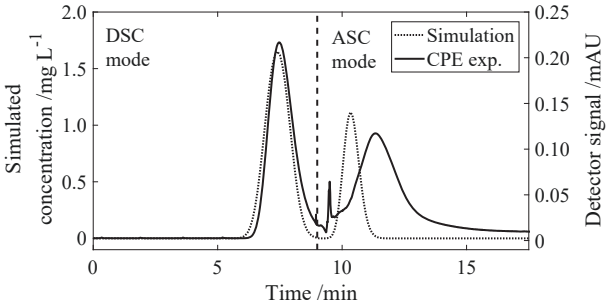

Figure 4. Simulated and experimental dual-mode separation with a feed concentration of 2 mg g^{-1} (2.3 mg mL^{-1}) for each protein, injection volume of 10 mL, 2000 rpm, and mobile phase flow rate of 10 mL min^{-1} in DSC mode and 20 mL min^{-1} in ASC mode. The separation mode was switched from DSC to ASC mode after 9 min (indicated with a dashed line).

3.4 Separation of Lysozyme and Myoglobin with Modifying Agent

The goal of the following CPC injections was to evaluate the applicability of IL-modifiers in the process. PEG 1000/K_2HPO_4/KH_2PO_4/H_2O 15:9.68:5.32:70 (w/w/w/w) was prepared with an additional 2.5 or 1.5 wt % [EMIM]Cl. Fig. 5 a presents a chromatogram of the protein separation with additional 2.5 wt % [EMIM]Cl. The initial S_f value was 0.67 including the volume of stationary phase injected with the sample. The partition coefficients of myoglobin and lysozyme calculated from the chromatogram were 0.07 and 1.84, respectively. Compared to the injection without IL in the ATPS, the partition coefficient of lysozyme decreased from 3.02 to 1.84. From shake-flask experiments, a mean partition coefficient of lysozyme of 1.96 was obtained for the ATPS with 2.5 wt % [EMIM]Cl. The protein partition coefficients from both methods are similar, the small deviation may be caused from the assumption of linear behavior of the stationary phase stripping.

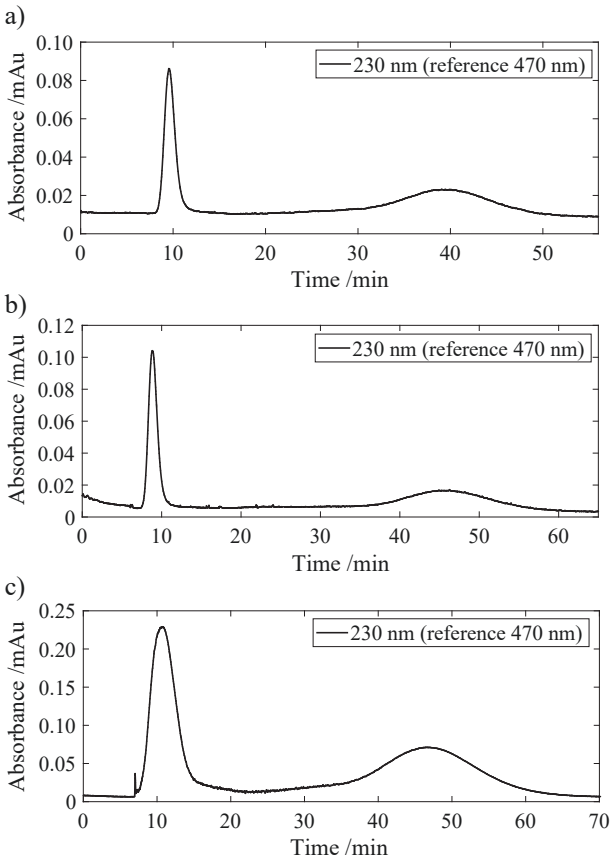

Figure 5. Chromatogram of myoglobin and lysozyme separation with a concentration of 2 mg g^{-1} (2.3 mg mL^{-1}) for each protein, mobile phase flow rate of 10 mL min^{-1} at 2000 rpm for PEG 1000/K_2HPO_4/KH_2PO_4/H_2O 15.00:9.68:5.32:70.00 (w/w/w/w) with (a) 2.5 wt % [EMIM]Cl, $V_{injection}$ = 10 mL, initial S_f of 0.67; $P_{myoglobin}$ was 0.07 and $P_{lysozyme}$ 1.84; (b) 1.5 wt % [EMIM]Cl, $V_{injection}$ = 10 mL, initial S_f of 0.72, $P_{myoglobin}$ was 0.11 and $P_{lysozyme}$ 2.17; (c) 1.5 wt % [EMIM]Cl, $V_{injection}$ = 50 mL, initial S_f of 0.72, $P_{myoglobin}$ was 0.22 and $P_{lysozyme}$ 2.11.

Another CPC run was performed using PEG 1000/K_2HPO_4/KH_2PO_4/H_2O with additional 1.5 wt % [EMIM]Cl (Fig. 5 b). The initial S_f value was 0.72 after injection, and the partition coefficients of myoglobin and lysozyme were 0.11 and 2.17, respectively. As expected from shake-flask experiments, the addition of IL does not change the partition coefficients of myoglobin while the lysozyme partition coefficient decreased compared to the system without IL. The trend of the lysozyme partition coefficients from shake-flask experiments with

[EMIM]Cl could be confirmed. The lysozyme partition coefficient obtained from the injection with 1.5 wt % of [EMIM]Cl was higher than for 2.5 wt % of [EMIM]Cl; however, in both ATPSs with additional IL a decrease in the partition coefficient of lysozyme to the sweet spot was observed.

High productivity and throughput are strongly desired for preparative and industrial application. Solubility of the proteins is a limiting factor; however, since the two proteins are well baseline-separated, there is opportunity to use larger injection volumes of the sample to increase productivity. In Fig. 5c, the injection volume was increased by a factor of 5 from 10 to 50 mL, i. e., from 4 to 20 % of the total column volume. The other operating conditions were identical to the previous experiments. With the sample, 25 mL of stationary phase were injected. During the separation, 27 mL of stationary phase eluted from the column, making the total net stationary phase loss just 2 mL despite the large injection volume. The two proteins were still baseline-separated. This leads to the conclusion that even larger volumes of sample could be injected into the column for batch separation.

To support this hypothesis, simulations for batch injections with even larger injection volumes were performed. For small injection volumes, the difference in the stationary phase retention due to the injection might be negligible, whereas for larger injection volumes the peaks are shifted in the experiment. Therefore, the additionally injected volume of stationary phase was accounted for in the simulations. During the experiments with 10 and 50 mL injection volume, a steady stripping of the additionally injected stationary phase was observed rather than a rapid loss at the beginning of the separation. Hence, a term for linear loss of the additionally injected stationary phase as a function of time was implemented in the model to reflect this behavior. It was assumed for the calculations that no further stationary phase is lost except for the amount injected with the feed and that the initial S_f value was reached at the end of the separation run.

Fig. 6 presents a comparison between the simulated chromatograms and the experiments. Feed concentration, protein partition coefficients, and initial S_f were derived from the experiment. Taking the possible error resulting from the assumption of linear stripping of additionally injected stationary phase into account, the simulated peaks agree very well with the experiment. Therefore, in the next step, the injection volume was further increased to 75, 100, and 125 mL in the simulations. This corresponds to an injection of 174.4, 232.5, and 290.6 mg of each protein. For higher injection volumes, a different modeling strategy has to be applied since the column cannot take up more than 250 mL of stationary phase in total. In this case, extrusion of the stationary phase would have to be considered.

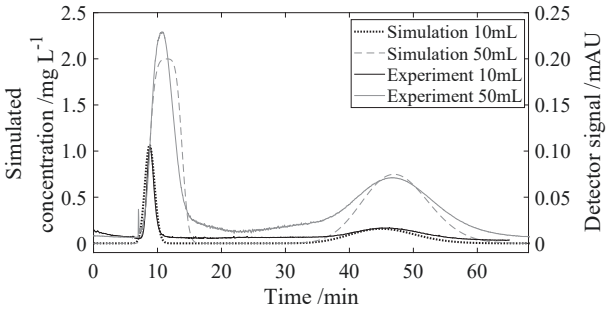

Figure 6. Comparison of experimental chromatograms and simulated pulse injections of myoglobin and lysozyme for 10 and 50 mL injection volume with PEG 1000/(K_2HPO_4/KH_2PO_4)/H_2O with 1.5 wt % [EMIM]Cl with 10 mL min^{-1}, 2000 rpm.

The simulated chromatograms are displayed in Fig. 7. As the injection volume rises, also the additionally injected volume of stationary phase increases. Thus, in agreement with Eq. (2), the maximum of the lysozyme peak is shifted to higher retention time for a constant partition coefficient. The simulations in Fig. 7 indicate that theoretically injection volumes up to 50 % are possible.

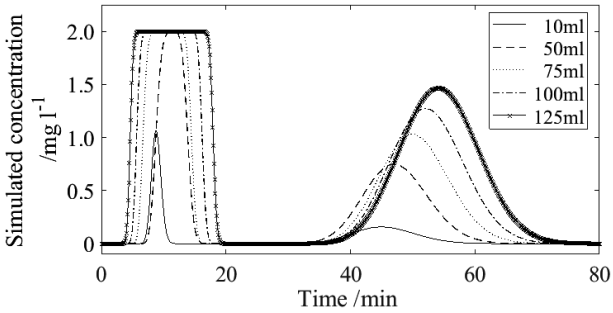

Figure 7. Simulated chromatograms with injection volumes of 10, 50, 75, 100, and 125 mL for PEG 1000/K_2HPO_4/KH_2PO_4/H_2O 15.00:9.68:5.32:70.00 (w/w/w/w) with 1.5 wt % [EMIM]Cl; mobile phase flow rate 10 mL min^{-1}.

4 Conclusions

The effect of IL addition on the partition coefficients of two model proteins, namely, lysozyme and myoglobin, in polymer/salt-based ATPSs was investigated. Even small amounts of ILs used in this work move the partition coefficient of lysozyme closer to the so-called sweet spot ($0.4 < P_i < 2.5$), while myoglobin was not affected by the addition of ILs.

The new CPC column design with bigger twin cells allows the use of ATPS as stationary and mobile phase with high flow rates not only in elution, but also in dual mode. The findings from the shake-flask experiments with IL as modifying agent were confirmed in CPC experiments with either 1.5 or 2.5 wt % of [EMIM]Cl as stationary and mobile phases for the separation of myoglobin and lysozyme.

ATPSs with IL as modifying agent were successfully applied to shift the partition coefficient of the proteins towards the sweet spot in a protein separation with CPC while maintaining high stationary phase retention at reasonable flow rates. Since the separation factor was still high, the injection volume was increased to achieve higher productivity. A sample volume up to 20 % of the total column volume was injected without a decrease in stationary phase retention.

The stability of the hydrodynamic equilibrium in the column proves the potential of ATPSs in CPC to be used for large sample amounts. Simulations show the capacity for further increase

of the injection volume and, thus, further raise of productivity. In the publication by Oelmeier et al. [44], it is demonstrated that CPC can be used for monoclonal antibody purification, however, only with low mobile phase flow rates [44]. The methodology proposed in this work has high potential to be applied to other products sensitive to organic solvents, such as monoclonal antibodies, to increase separation productivity.

Acknowledgment

The authors thank the Deutsche Forschungsgemeinschaft for financial support (German Research Foundation, DFG-Projekt MI1340/3-1), and Ms. Jahyun Yang, Ms. Swati Agrawal, and Mr. Alex Gorochow for their participation in the experiments. We thank Mr. Walter Stelzer and Prof. Langosch (Chair of Biopolymer Chemistry, Technical University of Munich) for their help with the circular dichroism (CD) measurements and Sigma-Aldrich Chemie GmbH (subsidiary of Merck KGaA) for providing [EMIM]Cl for the experiments presented in this work.

The authors have declared no conflict of interest.

Symbols used

c	[mg g^{-1}]	concentration
F	[mL min^{-1}]	mobile phase flow rate
N	[–]	number of theoretical plates (column efficiency)
P	[–]	partition coefficient
S_f	[–]	stationary phase retention
t	[min]	time
V	[mL]	volume

Greek letter

μ	[min]	first absolute momentum

Sub- and superscripts

i	[–]	compound *i*
k	[–]	stage
MP	mobile phase	
R	retention	
SP	stationary phase	

Abbreviations

ASC	ascending mode
ATPS	aqueous two-phase system
BMIM	1-butyl-3-methylimidazolium
CCC	countercurrent chromatography
CD	circular dichroism
CPC	centrifugal partition chromatography
DAD	diode array detector
DSC	descending mode
EMIM	1-ethyl-3-methylimidazolium
HPLC	high-performance liquid chromatography
IL	ionic liquid
PEG	polyethylene glycol

References

[1] P. A. J. Rosa et al., *Biotechnol. J.* **2013**, *8 (3)*, 352–362. DOI: https://doi.org/10.1002/biot.201200031

[2] C. Ladd Effio et al., *J. Chromatogr., A* **2015**, *1383*, 35–46. DOI: https://doi.org/10.1016/j.chroma.2015.01.007

[3] J. Dos Reis Coimbra, J. Thömmes, M. R. Kula, *J. Chromatogr., A* **1994**, *668 (1)*, 85–94. DOI: https://doi.org/10.1016/0021-9673(94)80095-2

[4] C. Schwienheer, A. Prinz, T. Zeiner, J. Merz, *J. Chromatogr., B* **2015**, *1002*, 1–7. DOI: https://doi.org/10.1016/j.jchromb.2015.07.050

[5] A. S. Schmidt, A. M. Ventom, J. A. Asenjo, *Enzyme Microb. Technol.* **1994**, *16 (2)*, 131–142. DOI: https://doi.org/10.1016/0141-0229(94)90076-0

[6] A. M. Azevedo et al., *Sep. Purif. Technol.* **2009**, *65 (1)*, 14–21. DOI: https://doi.org/10.1016/j.seppur.2007.12.010

[7] J. Benavides, O. Aguilar, B. H. Lapizco-Encinas, M. Rito-Palomares, *Chem. Eng. Technol.* **2008**, *31 (6)*, 838–845. DOI: https://doi.org/10.1002/ceat.200800068

[8] M. Iqbal et al., *Biol. Proced. Online* **2016**, *18 (1)*, 18. DOI: https://doi.org/10.1186/s12575-016-0048-8

[9] A. Berthod, D. W. Armstrong, *J. Liq. Chromatogr.* **1988**, *11 (3)*, 547–566. DOI: https://doi.org/10.1080/01483918808068331

[10] Y. Ito, *J. Biochem. Biophys. Methods* **1981**, *5 (2)*, 105–129. DOI: https://doi.org/10.1016/0165-022X(81)90011-7

[11] M. Knight et al., *J. Chromatogr., A* **2011**, *1218 (36)*, 6148–6155. DOI: https://doi.org/10.1016/j.chroma.2011.06.007

[12] D. Dasarathy, Y. Ito, *J. Chromatogr., A* **2015**, *1418*, 77–82. DOI: https://doi.org/10.1016/j.chroma.2015.09.033

[13] Y. Yang, H. A. Aisa, Y. Ito, *J. Chromatogr., A* **2009**, *1216 (27)*, 5265–5271. DOI: https://doi.org/10.1016/j.chroma.2009.05.024

[14] Y. Ito, R. Clary, *Separations* **2016**, *3 (4)*. 31. DOI: https://doi.org/10.3390/separations3040031

[15] Y. H. Guan, D. Fisher, I. A. Sutherland, *J. Chromatogr., A* **2010**, *1217 (21)*, 3525–3530. DOI: https://doi.org/10.1016/j.chroma.2010.03.034

[16] J. Ding et al., *J. Chromatogr., A* **2017**, *1499*, 101–110. DOI: https://doi.org/10.1016/j.chroma.2017.03.076

[17] Y. Shibusawa, Y. Ito, *J. Chromatogr., A* **1991**, *550*, 695–704. DOI: https://doi.org/10.1016/S0021-9673(01)88575-7

[18] J. Goll, G. Audo, M. Minceva, *J. Chromatogr., A* **2015**, *1406*, 129–135. DOI: https://doi.org/10.1016/j.chroma.2015.05.077

[19] S. Roehrer, F. Bezold, E. M. Garcia, M. Minceva, *J. Chromatogr., A* **2016**, *1434*, 102–10. DOI: https://doi.org/10.1016/j.chroma.2016.01.024

[20] K. E. Gutowski et al., *J. Am. Chem. Soc.* **2003**, *125 (22)*, 6632–6633. DOI: https://doi.org/10.1021/ja0351802

[21] M. G. Freire et al., *Chemistry* **2012**, *18 (6)*, 1831–1839. DOI: https://doi.org/10.1002/chem.201101780

[22] K. Xu et al., *Anal. Chim. Acta* **2015**, *864*, 9–20. DOI: https://doi.org/10.1016/j.aca.2015.01.026

[23] N. Li et al., *Talanta* **2016**, *152*, 23–32. DOI: https://doi.org/10.1016/j.talanta.2016.01.042
[24] H. Passos et al., *ACS Sustainable Chem. Eng.* **2016**, *4 (5)*, 2881–2886. DOI: https://doi.org/10.1021/acssuschemeng.6b00485
[25] P.-Å. Albertsson, *Adv. Protein Chem.* **1970**, *24*, 309–341.
[26] W. Zhang et al., *Thermochim. Acta* **2013**, *560*, 47–54. DOI: https://doi.org/10.1016/j.tca.2013.02.015
[27] S. P. M. Ventura et al., *J. Phys. Chem. B* **2009**, *113 (27)*, 9304–9310. DOI: https://doi.org/10.1021/jp903286d
[28] S. P. M. Ventura et al., *J. Chem. Eng. Data* **2011**, *56 (11)*, 4253–4260. DOI: https://doi.org/10.1021/je200714h
[29] S. P. M. Ventura et al., *J. Chem. Eng. Data* **2012**, *57 (2)*, 507–512. DOI: https://doi.org/10.1021/je2010787
[30] F. Bezold, J. Goll, M. Minceva, *J. Chromatogr., A* **2015**, *1388*, 126–132. DOI: https://doi.org/10.1016/j.chroma.2015.02.021
[31] C. Schwienheer, J. Merz, G. Schembecker, *J. Liq. Chromatogr. Relat. Technol.* **2015**, *38 (9)*, 929–941. DOI: https://doi.org/10.1080/10826076.2014.951765
[32] A. E. Visser, R. P. Swatloski, R. D. Rogers, *Green Chem.* **2000**, *2 (1)*, 1–4. DOI: https://doi.org/10.1039/A908888A
[33] M. R. Almeida et al., *Sep. Purif. Technol.* **2014**, *128*, 1–10. DOI: https://doi.org/10.1016/j.seppur.2014.03.004
[34] A. J. P. Martin, R. L. M. Synge, *Biochem. J.* **1941**, *35 (12)*, 1358–1368.
[35] J. Völkl, W. Arlt, M. Minceva, *AIChE J.* **2013**, *59 (1)*, 241–249. DOI: https://doi.org/10.1002/aic.13812
[36] E. Hopmann, M. Minceva, *J. Chromatogr., A* **2012**, *1229*, 140–147. DOI: https://doi.org/10.1016/j.chroma.2011.12.102
[37] J. Goll, A. Frey, M. Minceva, *J. Chromatogr., A* **2013**, *1284*, 59–68. DOI: https://doi.org/10.1016/j.chroma.2013.01.116
[38] H. Zhao, *J. Chem. Technol. Biotechnol.* **2015**, *91 (1)*, 25–50. DOI: https://doi.org/10.1002/jctb.4837
[39] M. Sha et al., *J. Phys. Chem. Lett.* **2015**, *6 (18)*, 3713–3720. DOI: https://doi.org/10.1021/acs.jpclett.5b01513
[40] Y. R. Gokarn et al., *Protein Sci.* **2011**, *20 (3)*, 580–587. DOI: https://doi.org/10.1002/pro.591
[41] R. Buchfink et al., *J. Biotechnol.* **2010**, *150 (1)*, 64–72. DOI: https://doi.org/10.1016/j.jbiotec.2010.07.003
[42] H. Zhao et al., *Tetrahedron: Asymmetry* **2006**, *17 (3)*, 377–383. DOI: https://doi.org/10.1016/j.tetasy.2006.01.015
[43] M. Shinitzky, E. Katchalski, V. Grisaro, N. Sharon, *Arch. Biochem. Biophys.* **1966**, *116*, 332–343. DOI: https://doi.org/10.1016/0003-9861(66)90039-7
[44] S. A. Oelmeier, C. Ladd-Effio, J. Hubbuch, *J. Chromatogr., A* **2013**, *1319*, 118–126. DOI: https://doi.org/10.1016/j.chroma.2013.10.043

3.2. Paper II

Assessing solute partitioning in deep eutectic solvent-based biphasic systems using the predictive thermodynamic model COSMO-RS

Citation

F. Bezold, M.E. Weinberger, M. Minceva, Assessing solute partitioning in deep eutectic solvent-based biphasic systems using the predictive thermodynamic model COSMO-RS, Fluid Phase Equilibria, 437 (2017) 23-33

https://doi.org/10.1016/j.fluid.2017.01.001

Summary

The objective of this work was to evaluate the application of solvent system screening with COSMO-RS for biphasic systems containing DESs. Limiting activity coefficients of volatile organic compounds in DESs, liquid-liquid equilibria of systems containing DES and organic solvents, and solute partition coefficients in DES-based biphasic systems were predicted and compared to experimental data. The calculations were performed for three different approaches for the molecular representation of DESs: electroneutral mixture, ion pair representation, and metafile approach. The metafile approach was omitted since it did not lead to consistent results for LLE calculations and thus was not applicable for solvent screening. The results of the other two approaches were compared for two parametrizations, the triple-zeta valence polarized basis set (TZVP) and TZVPD-FINE with the additional diffuse basis function and fine grid marching tetrahedron cavity construction. These are two different parametrization sets for the calculations of the screening charge density. It has to be noted, that there are also differences in the implementation of COSMO-RS for the two parametrizations in the COSMOtherm software. In the experimental data used for validation of the predictions, the DESs were treated as pseudo-compounds. The stoichiometry of the systems with DESs in the experiment and the stoichiometry in the COSMO-RS calculations was different, the results of the calculations needed to be scaled to pseudo-compound definition to match the experimental data for comparison.

Overall, the TZVP parametrization together with the electroneutral approach was recommended for screening of DES-based biphasic systems. Even though the predictions with TZVPD-FINE parametrization showed smaller deviations for some cases, the calculations for the TZVP parametrization were up to ten times faster and the algorithm for solving the LLE had a lower likelihood of non-convergence.

The investigated systems contained DES-constituents predominantly in one of the phases, while in the second phase, no substantial amounts of DES-constituents were determined. Calculations for one system, where ternary predictions were not satisfying, showed that treating the system as quaternary mixture, composed of two organic solvents, HBD, and

HBA, may be more suitable in this case. Quaternary calculations showed that the ratio of HBD to HBA is expected to change and that part of the HBD molecules are expected to be located in the upper phase of the system. However, no quaternary experimental data existed to compare the quaternary system predictions. Additionally, solute partition coefficients, the most important thermodynamic properties in the solvent system selection for CPC and CCC, were calculated and compared to experimental data. These results showed that the trend in solute partitioning was generally represented. Good quantitative predictions were obtained within and close to the so-called *sweet spot* of CPC and CCC. Although the evaluation was restricted to pseudo-ternary DES-based biphasic systems, the prediction accuracy was high enough to perform a solvent system screening for CPC or CCC separations.

Contributions

The author was the lead scientist in all parts of the work. She planned and coordinated the work, supervised all data acquisition, and had a leading role in data interpretation. M. Weinberger conducted data acquisition supervised by the author. The author and co-author each performed parts of the DFT-calculations. The quaternary calculations were done by the author. The manuscript was written by the author and discussed with Prof. Minceva.

Fluid Phase Equilibria 437 (2017) 23–33

Contents lists available at ScienceDirect

Fluid Phase Equilibria

journal homepage: www.elsevier.com/locate/fluid

Assessing solute partitioning in deep eutectic solvent-based biphasic systems using the predictive thermodynamic model COSMO-RS

Franziska Bezold, Maria E. Weinberger, Mirjana Minceva*

Biothermodynamics, TUM School of Life and Food Sciences Weihenstephan, Technische Universität München, 85354 Freising, Germany

ARTICLE INFO

Article history:
Received 16 September 2016
Received in revised form
14 December 2016
Accepted 1 January 2017
Available online 3 January 2017

Keywords:
Deep eutectic solvents
Liquid-liquid equilibrium
Partition coefficient
Countercurrent chromatography
Centrifugal partition chromatography

ABSTRACT

The prediction quality of COSMO-RS for the thermodynamic properties needed for the design of a liquid-liquid chromatographic process was evaluated for systems containing deep eutectic solvents (DES). Therefore activity coefficients, liquid-liquid equilibrium data, and partition coefficients of different solutes were computed and compared to experimental data from literature or measurements. The calculations were performed using TZVP and TZVPD-FINE parameterizations and fully dissociated and non-dissociated representations of the H-bond acceptor molecules. It was found that the predictions qualitatively resemble the trend of the experimental data. The TZVPD-FINE parameterization did not yield significantly lower deviations from the experimental values than TZVP, while calculations with the latter were up to ten times faster. Although DES constituents exhibit strong H-bond interactions, the representation as an electroneutral mixture is preferable. It could be shown that the predictions of partition coefficients are in good agreement with the measured values in the preferred working range of liquid-liquid chromatography. The overall prediction quality is sufficient to use the predictive model for the screening procedure for the solvent system selection.

1. Introduction

Deep eutectic solvents (DES) are a combination of hydrogen bond donor (HBD) and hydrogen bond acceptor molecules (HBA), which in mixture have a substantially lower melting point than the pure components. The term refers to such combinations with a melting point below 100 °C. After Abbott et al. reported the interesting properties of this new solvent class in 2003, DES gained a lot of attention [1]. Because of their high solving capacity, low volatility and relatively low price, many new applications have been described and their number is rapidly increasing [2–7]. The most abundantly used HBA is choline chloride, a non-toxic quaternary ammonium salt. It can be combined to form a DES with various HBD, such as urea, carboxylic acids and sugar-based polyols [8]. The resulting mixtures are considered biocompatible and less environmentally harmful green solvents [3]. Those advantages also led to the application of biphasic solvent systems containing DES in solid-support free liquid-liquid chromatography [9]. This technique, also known as countercurrent or centrifugal partition chromatography (CCC or CPC), uses the two liquid phases of a biphasic solvent system in thermodynamic equilibrium as the mobile and stationary phases for a chromatographic separation process [10]. A mixture can be separated according to the difference in the partition coefficient of each component in this liquid biphasic system. DES can be used to form water free biphasic liquid systems with, for example, alkanes and alcohols or nitriles, which can be utilized for the separation of hydrophobic compounds [9]. Since DES have shown interesting characteristics, it is worth increasing the accessibility of DES-based biphasic systems. Due to the large number of possible combinations of DES and possible biphasic solvent systems formed with DES and other solvents, systematic screening methods are needed for solvent system selection.

In liquid-liquid chromatography the most crucial step in the design of a separation process is the selection of a biphasic liquid system, which phases will be used as the mobile and stationary phases for the separation. Choosing such a system may involve many experiments if it is done by a trial and error approach. Therefore the exploration of systematic methods to reduce the efforts for this selection process came into the focus of research. There are many strategies for solvent system selection, for example by classifying the large amount of possible biphasic solvent systems by their composition or by comparison of the partition coefficient

* Corresponding author.
E-mail address: mirjana.minceva@tum.de (M. Minceva).

http://dx.doi.org/10.1016/j.fluid.2017.01.001
0378-3812/

of different standard substances in those systems [10–13]. These solvent system evaluations have significantly eased the selection process; however, they can only assess a finite number of solvent systems and still involve a lot of measurements until a final solvent system is chosen. In many cases no pure substances from the mixture to be separated are available to determine partition coefficients in many different solvent systems. Due to those limitations, model-based approaches for the selection of a biphasic solvent system were developed. Thermodynamic models have been used to predict liquid-liquid equilibria (LLE) of multicomponent mixtures and the partitioning of solutes between the phases of a biphasic system. In previous work, our group has shown that thermodynamic models can drastically reduce the experimental effort in the solvent system selection process [14,15].

Publications on the application of thermodynamic models to systems involving DES have rapidly increased in the last few years. Gonzalez et al. performed a correlation to reflect the phase behavior of two different DES combined with hexane and benzene, toluene or ethyl acetate with varying temperature using UNIQUAC [16]. The group of Hadj-Kali investigated the extraction of aromatics from aliphatics and denitrification of diesel using NRTL and COSMO-RS for LLE calculation [17–19]. Rodriguez et al. presented phase equilibrium data for chloride quaternary ammonium salts and polyol-based DES and performed COSMO-RS calculations to predict the phase equilibria [20]. Gouveia et al. investigated an application of DES as azeotrope breakers for mixtures of aliphatics and aromatics using COSMO-RS and experimentally [21], and Aissaoui et al. used COSMO-RS in the investigation of DES for an application in natural gas dehydration [22]. Since the interactions between the HBA and HBD are of great interest for the choice of a DES for a specific process, molecular dynamics simulations have been applied to study the characteristics of DES solutions, such as self-diffusion or hydrogen bonding. The most abundantly investigated DES, choline chloride-urea, was used to gain an insight into the hydrogen bonding between the donor and acceptor molecules and later molecular dynamics and experimental analysis were performed for three further HBD [23,24]. Ullah et al. investigated the intermolecular interactions in the DES composed of choline chloride and levulinic acid, which was used in CO_2 capturing, and characterized a network of H-bonds between the donor and acceptor molecules [25]. Although predictive models have been applied in the design of different separation processes, they have not yet been applied to solvent system screening involving DES-based solvent systems for liquid-liquid chromatography. The most important properties needed for the design of a liquid-liquid chromatographic separation process are LLE and partition coefficients of target molecules within a biphasic system. In contrast to extraction processes a moderate partition coefficient in the range of $-0.4 < \log P_i < 0.4$ is preferred and usually biphasic systems closer to the plait point are used. It has been shown that COSMO-RS can be applied in the selection of a biphasic solvent system composed of water and organic solvents for a liquid-liquid chromatographic separation [14,15,26]. However, the approach needs to be validated for complex biphasic systems containing DES.

In this work the prediction quality of COSMO-RS is evaluated for solvent systems containing DES. The most important thermodynamic parameters for the design of a liquid-liquid chromatographic separation process are calculated and compared to experimental data taken from literature or measurements. Those thermodynamic properties include activity coefficients, LLE data and partition coefficients. For the COSMO-RS calculations different parameterizations and methods to represent the DES in the software are compared.

2. Material and methods

2.1. Experimental details

2.1.1. Chemicals

Choline chloride, betaine and levulinic acid were purchased from Alfa Aesar. All compounds used for the DES had purities ≥ 98%. Methanol, 1-propanol and heptane (99.9%) were purchased from VWR Chemicals, ethanol (≥99.9%) was obtained from Merck KGaA, acetonitrile (≥99.9%) from J.T. Baker. Vanillin (99%) and α-tocopherol (≥97%) from Alfa Aesar and β-ionone (96%) from Aldrich were used for the partitioning experiments.

2.1.2. Preparation of deep eutectic solvents

For the DES preparation HBA and HBD were weighed in at a molar ratio of 1:2 and heated to 80–85 °C in a hermetically closed vial for approximately 25 min. The mixtures were stirred and heated until a clear homogenous liquid was obtained. A more detailed description of the procedure can be found in Ref. [9]. Betaine or choline chloride were used as HBA, the HBD in both cases was levulinic acid. The DES composed of betaine and levulinic acid (1:2 mol:mol) will further be referred to as BLA, the DES containing choline chloride and levulinic acid (1:2 mol:mol) as CLA.

2.1.3. Biphasic solvent systems

The biphasic solvent systems were prepared by mixing the solvents in the respective amounts. The composition of the solvent systems and the solutes used for the shake flask experiments can be found in Table 1. The biphasic systems were mixed using an automatic shaker for 30 min and were afterwards allowed to settle for another 1.5 h.

2.1.4. Partition coefficients

The partition coefficient K of a solute i is defined as the ratio of the solute's mole fraction in each phase at thermodynamic equilibrium:

$$K_i^{\alpha\beta} = \frac{x_i^{\alpha}}{x_i^{\beta}} = \frac{\gamma_i^{\beta}}{\gamma_i^{\alpha}} \tag{1}$$

where x_i and γ_i are the mole fraction and activity coefficient of compound i, and α and β are the two phases of a biphasic liquid system. For low concentration of the solute in the biphasic system the solute distribution shows linear behavior and the partition coefficient can be assumed as a constant.

In experimental screenings of the partition coefficient it is more convenient to use concentrations c instead of mole fractions:

$$P_i^{\alpha\beta} = \frac{c_i^{\alpha}}{c_i^{\beta}} = \frac{x_i^{\alpha}\rho^{\alpha}}{x_i^{\beta}\rho^{\beta}} \tag{2}$$

where ρ is the molar density of the phase.

For the calculation of the partition coefficient the compositions of the two phases without solute has to be known. These were taken from literature data or calculated using the LLE function in COSMOtherm.

The experimental partition coefficients of vanillin, β-ionone and α-tocopherol were determined using the shake flask method described in our previous work [9]. For the shake flask experiments α-tocopherol, vanillin or β-ionone were added to the systems at a concentration of 5 mmol l^{-1}. UV–Vis spectroscopy was utilized to assess the concentrations of the respective solute in the phases of the solvent systems. The experiments were conducted in triplicate.

Table 1
Composition of the solvent systems for the measurement of the partition coefficients of vanillin, β-ionone and α-tocopherol.

Solute	DES	Amount of DES /wt%	Alkane	Amount of alkane /wt%	Alcohol or nitrile	Amount of alcohol or nitrile /wt%
vanillin or β-ionone	CLA	37.5	heptane	37.5	methanol	25.0
	CLA	37.5	heptane	37.5	ethanol	25.0
	CLA	37.5	heptane	37.5	acetonitrile	25.0
	BLA	37.5	heptane	37.5	methanol	25.0
	BLA	37.5	heptane	37.5	ethanol	25.0
	BLA	37.5	heptane	37.5	propanol	25.0
	BLA	37.5	heptane	37.5	acetonitrile	25.0
α-tocopherol	CLA	30.0	heptane	30.0	methanol	40.0
	CLA	30.0	heptane	30.0	ethanol	40.0
	BLA	30.0	heptane	30.0	methanol	40.0
	BLA	30.0	heptane	30.0	ethanol	40.0
	BLA	30.0	heptane	30.0	propanol	40.0

2.2. Computational details

2.2.1. Representation of molecules

Diedenhofen et al. described three modelling approaches for the representation of ionic liquids in the COSMO-RS framework [27]. The HBA of the DES investigated in this work is in most cases an ionic molecule composed of an anion and cation. An ionic liquid or salt can be described as a single non-dissociated molecule, the so-called ion pair approach, or as an electroneutral mixture of cations and anions. These approaches represent the completely non-dissociated or fully dissociated forms of an ionic species. As a third approach the ions can be treated as separate molecules at the quantum chemical level, but afterwards they are combined for the COSMO-RS calculations. This procedure is called metafile approach in the following sections. Thereby the σ-profiles, areas and volumes are summed up and written in a metafile [27]. These approaches can be extended to the representation of DES containing an ionic HBA. Fig. 1 shows a schematic representation of the three approaches adapted from Ref. [27] for the representation of DES in COSMO-RS calculations. For the metafile approach three different options can be considered, as shown in Fig. 1c. Either all DES-constituents from the electroneutral approach or from the ion pair approach can be combined into a metafile or a metafile can be created only for the ionic HBA and the HBD is considered separately. However, only one molecular conformation of each species can be used in the metafile. The approach has been considered (data not shown), but was dismissed due to several reasons: The consideration of only one conformation per metafile was not satisfactory since the molecules show very different conformations, e.g. intramolecular hydrogen bonding in glycerol; The metafile approaches did not lead to consistent results for the miscibility gap when employing different concentration grids for the calculations of LLE points.

The ratio of cation and anion of the HBA and the HBD, respectively, must be fixed to represent the stoichiometry of the DES in the input for COSMO-RS. In an experiment, the DES is for example prepared by mixing 1 mol choline chloride and n mol of the HBD, whereas in the input for COSMO-RS for electroneutral mixtures the DES is composed of 1 mol of choline cations, 1 mol of chloride anions and n mol of the HBD. In the COSMO-RS input all those constituents contribute to the total number of moles. Therefore, as described by Hizzadin et al. [17], it is necessary to convert the molar fractions obtained from the COSMO-RS calculations to reflect the experimental composition.

The activity coefficient of a component *i* received from COSMO-RS calculations (γ_i^{calc}) can be converted to the laboratory framework (γ_i^{exp}) according to Equation (3).

$$x_i^{exp}\gamma_i^{exp} = x_i^{calc}\gamma_i^{calc} \tag{3}$$

The experimental definition of the mole fraction of a component *i*, x_i^{exp}, is given by Equation (4).

$$x_i^{exp} = \frac{n_i}{n_i + n_{DES} + \sum_{j\neq i, j\neq DES} n_j} \tag{4}$$

In the COSMO-RS framework the mole fraction, x_i^{calc}, is defined according to Equation (5) for single molecule or non-dissociated HBA (ion pair) and according to Equation (6) for dissociated HBA (electroneutral). The molar amount of DES (n_{DES}) is composed of stochimetric amounts of HBA and HBD.

$$x_i^{non-diss,calc} = \frac{n_i}{n_i + (\nu_{HBA} + \nu_{HBD})n_{DES} + \sum_{j\neq i, j\neq DES} n_j} \tag{5}$$

$$x_i^{diss,calc} = \frac{n_i}{n_i + (\nu_c + \nu_a + \nu_{HBD})n_{DES} + \sum_{j\neq i, j\neq DES} n_j} \tag{6}$$

In equation (5) ν_i represents the stoichiometric coefficient of each DES constituent. The stoichiometric coefficients of HBA and HBD are fixed for each DES. For the electroneutral approach used in

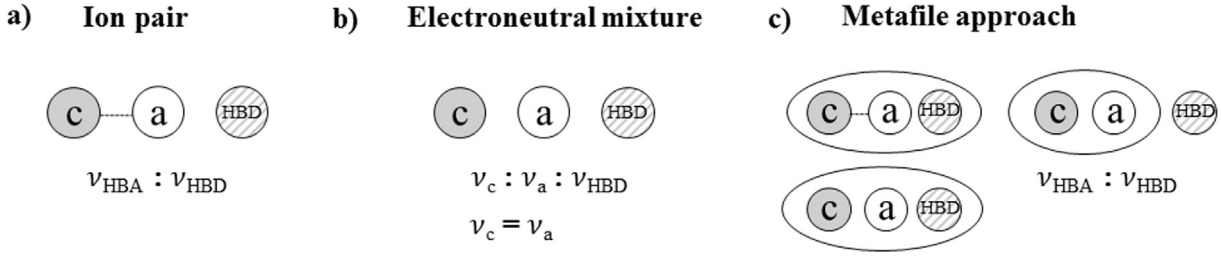

Fig. 1. Schematic illustration of ion pair (a), electroneutral (b) and metafile (c) representation of DES adapted from Ref. [27], ν_i represents the stoichiometric coefficient of each constituent, cations are labelled with c, anions with a. For c) three different options to build the metafile can be considered.

Equation (6), ν_{HBA} is split into the sum of the stoichiometric coefficient of cations ν_c and the stoichiometric coefficient of anions ν_a (see Equation (4)). Since the mixture has to be electroneutral, the molar amounts of anions and cations have to be equal. For the calculations of pseudo-ternary LLE containing DES the assumption has been applied that the initial ratio of HBA and HBD stays the same in both phases.

The molar fractions calculated in the COSMO-RS framework can then be converted to the laboratory scale [28]:

$$x_i^{exp} = \frac{\frac{x_i^{calc}}{\nu_i}}{\frac{x_i^{calc}}{\nu_i} + \sum_{j \neq i}\left(\frac{x_j^{calc}}{\nu_j}\right)} = \frac{\frac{x_i^{calc}}{\nu_i}}{\sum_k \left(\frac{x_k^{calc}}{\nu_k}\right)} \tag{7}$$

with $\nu_k = \begin{cases} 1, & k \text{ not a DES} \\ \nu, & k \text{ is a DES} \end{cases}$

Equation (7) is valid for all components except the DES. The coefficient ν corresponds to the sum of the stoichiometric coefficient of all DES-constituents. For example, in the case of the DES choline chloride-levulinic acid in a molar ratio of 1:2 and electroneutral approach, the DES is composed of one part choline cations, one part chloride anions and 2 parts of levulinic acid molecules. That means ν will have a value of four. With Equations (5) and (9) the activity coefficients can be converted according to Equation (8).

$$\gamma_i^{exp} = \gamma_i^{calc} \sum_k \left(\frac{x_k^{calc}}{\nu_k}\right) \tag{8}$$

In pure DES, for activity coefficients of a solute at infinite dilution, Equation (9) simplifies to

$$\gamma_i^{\infty,exp} = \frac{1}{\nu}\gamma_i^{\infty,calc} \tag{9}$$

2.2.2. COSMO-RS calculations

COSMOconf (Version 4.0, COSMOlogic, Germany) was applied to generate the molecular structures and the Balloon algorithm, implemented in the software, was used for the generation of conformers, which were considered as a Boltzmann-weighted mixture of conformers for the calculations. The maximum number of conformers was set to 20 within an energy window of 25 kcal/mol from the lowest energy structure. Full DFT optimization was performed for all conformers in TURBOMOLE (Version 6.6, COSMOlogic, Germany) using the Becke-Perdew (BP) functional with resolution of the identity (RI) approximation. The calculations were performed twice with either the triple-zeta valence polarized basis set (TZVP) or TZVPD-FINE with the additional diffuse basis function and the fine grid marching tetrahedron cavity construction. The activity coefficients, LLE and partition coefficients were then computed using the commercially available software COSMOtherm (Version C30 Release 15.01., COSMOlogic, Germany).

2.2.3. Comparison of prediction qualities

To evaluate the prediction quality of the COSMO-RS calculations with the different approaches described in section 2.2.1 the root mean square deviation (RMSD) was calculated.

$$\text{RMSD} = 100 \sqrt{\sum_{k=1}^{m}\sum_{i=1}^{c}\sum_{j=1}^{2} \frac{\left(x_{i,k}^{j,exp} - x_{i,k}^{j,calc}\right)^2}{2mc}} \tag{10}$$

For LLE predictions the RMSD was calculated according to Equation (10) where m is the number of tie lines, c is the number of components and j the number of phases. The DES were considered as one single pseudo component. To calculate the RMSD for limiting activity coefficients of different solvents in different DES γ_{solv}^{∞}, Equation (11) was used with N as the number of considered activity coefficients.

$$\text{RMSD} = 100 \sqrt{\sum_{i=1}^{N} \frac{\left(\gamma_{solv,i}^{\infty,\,exp} - \gamma_{solv,i}^{\infty,calc}\right)^2}{N}} \tag{11}$$

3. Results and discussion

3.1. Prediction of activity coefficients

As a first step in the evaluation of the prediction quality of COSMO-RS, limiting activity coefficients of different solvents in DES were calculated and compared to experimental data taken from Ref. [29]. The considered DES were choline chloride-glycerol in a molar ratio of 1:1 and 1:2. Calculations of the activity coefficients at infinite dilution were carried out for the TZVP and TZVPD-FINE parameterization considering different representations of the DES. The so-called ion pair approach reflects the non-dissociated form of the HBA choline chloride. Herein the geometry optimization is performed for choline cation and chloride anion together. For the electroneutral approach, which represents a fully dissociated form, the geometry optimization for cation and anion is performed separately. An example for sigma surfaces obtained from these two approaches is shown in Fig. S1 in supporting information. The resulting activity coefficients obtained with these approaches are listed in Table 2.

By just comparing the mean RMSD (see Table 2) the predictions made with the TZVP parameterization show generally smaller deviations from the experimentally determined activity coefficients than the predictions made with the TZVPD-FINE parameterization. For the TZVPD-FINE parameterization (Fig. 2), the limiting activity coefficients of alkanes in DES are significantly overestimated, whereas for the more polar solvents like alcohols and ketones the limiting activity coefficients are slightly underestimated in this set of data. A parity plot of the results (see Fig. 2 for TZVPD-FINE and Fig. 3 for TZVP parameterization) gives a better overview of the prediction quality for different values of the activity coefficients. Up to logarithmic activity coefficients of approximately 5 the predicted values are in good agreement with the experimentally determined ones for TZVPD-FINE. For the non-cyclic alkanes, namely octane, n-decane, dodecane and tetradecane, the deviation of the predicted and experimental values increases with the alkane chain length. Using the TZVP parameterization the deviation between computed and experimental activity coefficients for non-cyclic alkanes is significantly smaller than for values obtained with TZVPD-FINE. However, considering the other species, the overestimation of the interactions between the solvent molecules and the DES is higher for this parameterization. It has to be noted that deviations in the calculations with TZVP and TZVPD-FINE are not only caused by the different parameterizations in the DFT calculations, but also by the differences in the COSMO-RS model implemented for those two parameterizations in COSMOtherm. The same tendencies hold true for calculations of activity coefficients of the same compounds in a DES containing choline chloride and glycerol in a molar ratio of 1:1. Tabulated values for this DES are given in supporting information in Table S1.

TZVPD-FINE was introduced in 2011 and designed to improve predictions for specific compound classes, e. g. secondary or tertiary amines. Key feature compared to TZVP are new hydrogen

Table 2
Logarithmic limiting activity coefficients of different solvents in the DES choline chloride-glycerol (1:2) calculated with COSMO-RS and TZVP and TZVPD-FINE parameterization. Experimental values taken from Ref. [29].

Solvent	Experimental	Parameterization	Ion pair	Electroneutral
octane	5.72	TZVP	5.16	4.06
		TZVPD-FINE	7.79	7.27
n-decane	6.22	TZVP	6.36	5.06
		TZVPD-FINE	9.59	8.94
dodecane	6.59	TZVP	7.54	6.04
		TZVPD-FINE	11.36	10.55
tetradecane	7.00	TZVP	8.71	7.01
		TZVPD-FINE	13.13	12.14
benzene	2.93	TZVP	1.42	0.97
		TZVPD-FINE	2.37	2.26
toluene	3.79	TZVP	1.98	1.43
		TZVPD-FINE	3.33	3.19
cyclohexane	4.88	TZVP	3.10	2.30
		TZVPD-FINE	4.92	4.59
methanol	0.00	TZVP	−1.12	−1.76
		TZVPD-FINE	−1.20	−1.35
ethanol	0.59	TZVP	−0.72	−1.40
		TZVPD-FINE	−0.40	−0.64
propanol	1.39	TZVP	−0.32	−1.13
		TZVPD-FINE	0.29	0.08
1-butanol	2.08	TZVP	0.14	−0.77
		TZVPD-FINE	0.93	0.71
1-pentanol	3.11	TZVP	0.60	−0.42
		TZVPD-FINE	1.80	1.58
propanone	1.28	TZVP	−0.19	−0.26
		TZVPD-FINE	0.08	−0.37
methyl isobutyl ketone	3.56	TZVP	1.44	1.00
		TZVPD-FINE	2.53	2.04
acetonitrile	0.74	TZVP	−0.28	−0.24
		TZVPD-FINE	−0.52	−0.78
ethyl acetate	2.83	TZVP	0.76	0.50
		TZVPD-FINE	1.47	1.21
tetrahydrofuran	1.79	TZVP	0.32	0.03
		TZVPD-FINE	1.02	0.47
pyridine	1.10	TZVP	0.05	−0.09
		TZVPD-FINE	0.10	−0.32
RMSD		TZVP	1.56	2.03
		TZVPD-FINE	2.25	2.05

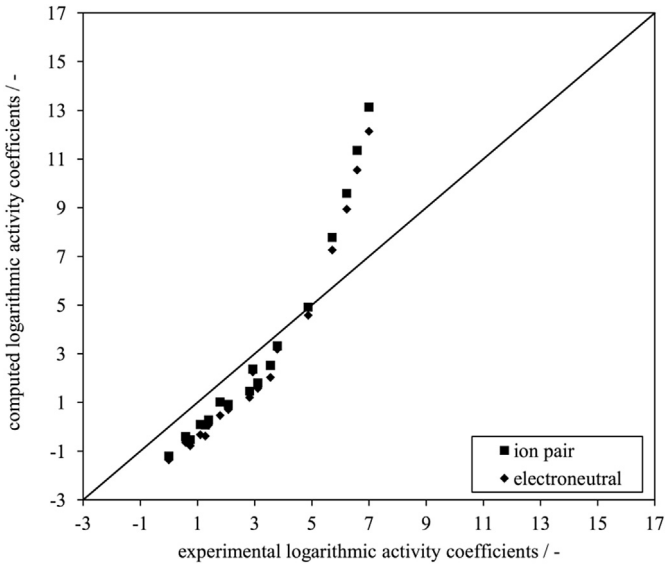

Fig. 2. Computed versus experimental logarithmic activity coefficients of different compounds in choline chloride-glycerol 1:2 for TZVPD-FINE.

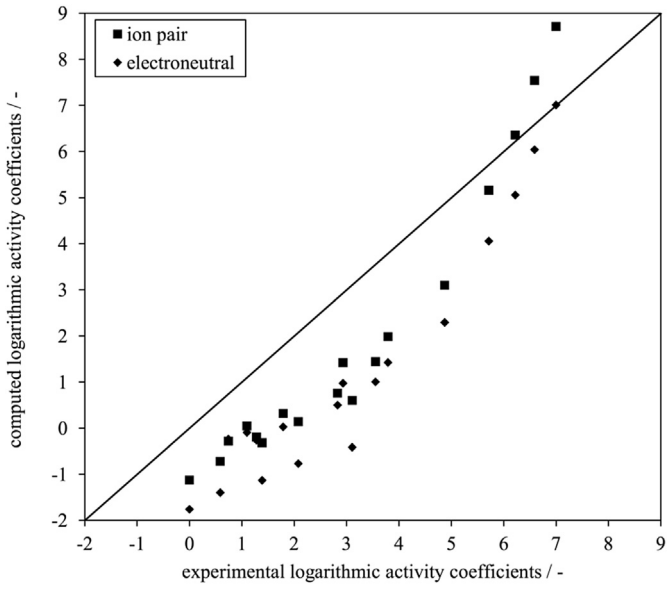

Fig. 3. Computed versus experimental logarithmic activity coefficients of different compounds in choline chloride-glycerol 1:2 for TZVP.

binding physics and improved cavity constructions [30]. As expected, the TZVPD-FINE parameterization gives better results for polar interactions where H-bond formation plays an important role. The predicted and experimental activity coefficients are also in very good agreement for cyclic molecules, such as benzene or toluene. For the prediction of the activity coefficients of long chain alkanes the TZVP parameterization is preferable considering the investigated data set. The variation between the limiting activity coefficients calculated with the different representation approaches of the DES is relatively high for this set of data. A reason for this could be the different conformations of the investigated HBA in electroneutral and ion pair approach. In the studied ion pair the partially positive surface charges at the hydroxyl groups are shielded by the chloride anion for half of the conformers used for the calculations. The chloride anion bound in the ion pair also has a weaker negative charged surface than the individual chloride in the electroneutral representation. The conformer sets for the choline chloride ion pair include quite different 3D-structures and a larger number of conformations than in the electroneutral representation of the HBA.

The findings of these predictions for pseudo binary systems composed of the DES and a solute may help elucidating the behavior of more complex ternary or multinary systems.

3.2. Liquid-liquid equilibria

For the evaluation of the prediction quality of COSMO-RS for biphasic liquid systems, LLE-data was collected from literature and the experimental values were compared to the calculated phase equilibria. The miscibility of twelve different systems was computed and the RMSD for experimental and predicted tie lines was calculated. In this section the quaternary systems composed of two organic solvents, HBA and HBD were treated as pseudo ternary systems. The ratio of HBA and HBD was kept constant in both phases during the calculations and the results were converted to the ternary definition using Equation (7). Table 3 lists the biphasic systems and their literature reference, as well as the RMSD for the fully dissociated and non-dissociated representation of the HBA both computed with the TZVP and TZVPD-FINE parameterizations. Two data sets for LLE are shown in this section, ternary diagrams of all calculated LLE can be found in the supporting information Figs. S2–S13.

The biphasic systems investigated in this section mainly use choline chloride as HBA, except for two liquid systems containing tetrabutylphosphonium bromide. The systems with the numbers 1–3 and 9–10 are composed of heptane, ethanol and DES containing choline chloride and different HBD (see Table 3). The calculated tie lines for the systems containing choline chloride-levulinic acid (CLA, system no. 1), choline chloride-ethylene glycol 1:2 (CEG, system no. 2), or choline chloride-lactic acid (CLC, system no. 9) represent the experimental tie lines very well, as can be seen by the relatively low RMSD (see Table 3). For the systems with glycerol (CGL, system no. 3) and glycolic acid (CGY, system no. 8) as HBD the fraction of ethanol in the lower, DES-rich phase is overestimated by COSMO-RS. Therefore the predicted fraction of ethanol in the upper, heptane-rich phase is too low compared to the experimentally determined phase compositions.

For most of the biphasic systems the deviation of the calculated and experimentally determined phase equilibria is similar for all four approaches. Fig. 4 shows ternary plots of the results for the four modelling approaches for the biphasic system composed of heptane/ethanol/CLA (system no. 1). It has to be noted that the DES used to determine this LLE were prepared by heating. When choline chloride and carboxylic acids are heated, esters and hydrochloric acid occur as impurities. A part of the deviation of the calculated and experimental LLE for this system, and also the other systems containing carboxylic acids, may be due to those impurities in the experiment which are not accounted for in the calculations. However, the predicted tie lines are in good agreement with the experimental LLE data for the system heptane/ethanol/CLA. The RMSD for the prediction is lowest for the TZVPD-FINE parameterization with non-dissociated representation of the choline chloride ion (compare Table 3). However, the difference in RMSD for the modelling approaches is small. Accounting for the calculation times of the LLE the calculations for the TZVP-parameterization are approximately ten times faster than for TZVPD-FINE. Because of this the TZVP-parameterization is to be preferred for most of the biphasic systems. However, in some systems there is a significant difference between the two parameterizations. Fig. 5 gives an example for such a case and shows the biphasic system heptane/toluene/tetrabutylphosphonium bromide-sulfolane. In this example, the size of the miscibility gap received from the calculations with the TZVP parameterization is underestimated for both ion pair and electroneutral approach. For the TZVPD-FINE parameterization the predicted miscibility gap is in good agreement with the experimental data concerning the size of the biphasic region, even though the slope of the tie lines still differs from the experiment. One of the investigated systems, namely heptane/toluene/

Table 3
RMSD for COSMO-RS calculations using TZVP or TZVPD-FINE and different molecular representations; systems are numbered for easier referencing.

System no.	Reference	System	RMSD TZVP ion pair/%	RMSD TZVP electroneutral/%	RMSD TZVPD-FINE ion pair/%	RMSD TZVPD-FINE electroneutral/%
1	[31]	ChCl-levulinic acid 1:2 - heptane - ethanol	6.85	7.56	6.76	6.97
2	[31]	ChCl-ethylene glycol 1:2 - heptane - ethanol	5.09	5.82	5.16	5.16
3	[31]	ChCl-glycerol 1:2 - heptane - ethanol	12.97	13.69	12.63	12.82
4	[16]	ChCl-glycerol 1:2 - hexane - benzene	7.85	10.65	1.96	2.25
5	[16]	ChCl-Lactic acid 1:2 - hexane - benzene	8.19	10.69	5.21	4.71
6	[16]	ChCl-lactic acid 1:2 - hexane - ethyl acetate	21.73	16.51	32.13	35.29
7	[32]	ChCl-lactic acid 1:2 - hexane - ethanol	7.06	7.86	6.53	7.08
8	[32]	ChCl-glycolic acid 1:1 - hexane - ethanol	14.21	15.84	10.91	13.18
9	[32]	ChCl-lactic acid 1:2 - heptane - ethanol	4.48	5.16	1.54	3.66
10	[32]	ChCl-glycolic acid 1:1 - heptane - ethanol	8.80	9.85	6.60	8.12
11	[33]	TBPBr-sulfolane 1:2 - heptane - toluene	17.60	18.81	7.63	8.26
12	[33]	TBPBr-ethylene glycol 1:2 - heptane - toluene	14.29	15.72	9.44	6.68

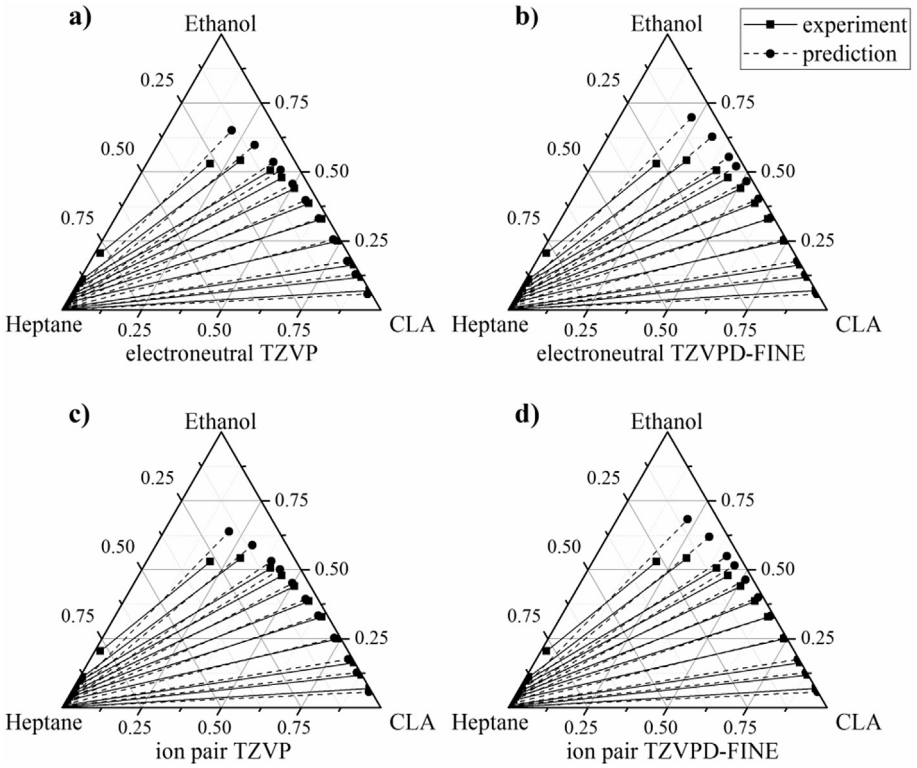

Fig. 4. Experimental vs. predicted LLE for the system composed of heptane, ethanol and CLA (system no. 1); dashed lines mark COSMO-RS predicted tie lines with (a) TZVP parameterization with electroneutral, (b) TZVPD-FINE parameterization with electroneutral, (c) TZVP parameterization and ion pair, and (d) TZVPD-FINE parameterization with ion pair representation of DES molecules.

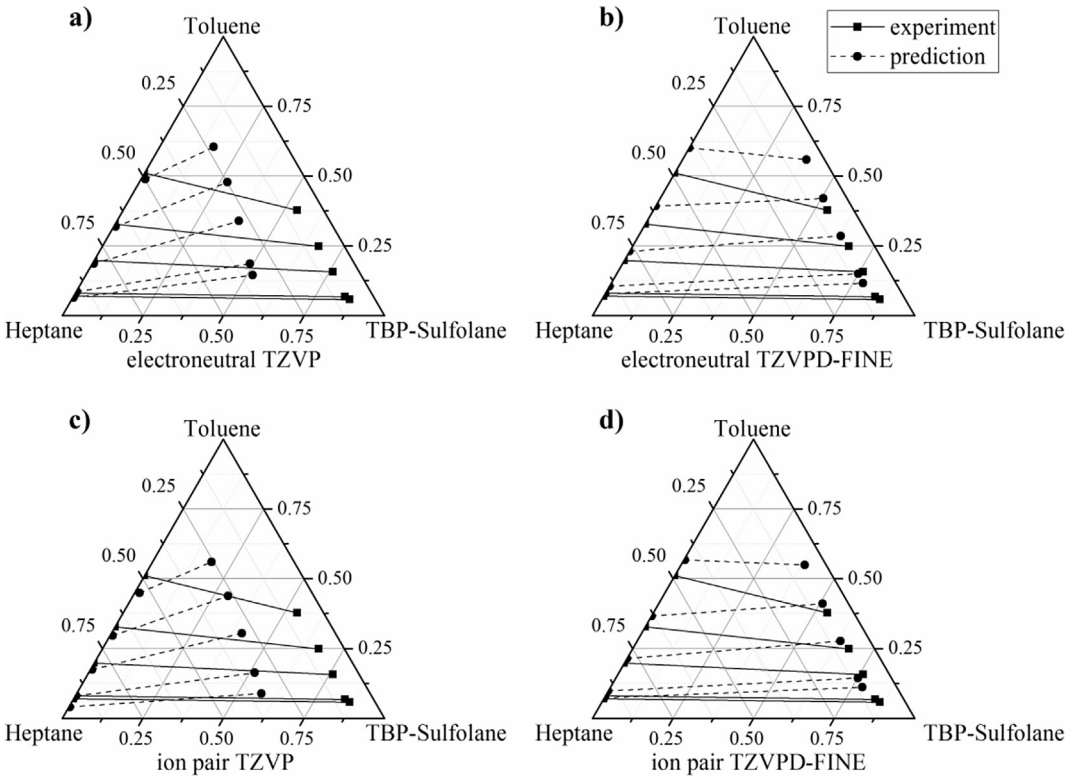

Fig. 5. Experimental vs. predicted LLE for the system composed of heptane, toluene and tetrabutylphosphonium bromide-sulfolane (system no. 11), dashed lines mark COSMO-RS predicted tie lines with (a) TZVP parameterization with electroneutral, (b) TZVPD-FINE parameterization with electroneutral, (c) TZVP parameterization and ion pair, and (d) TZVPD-FINE parameterization with ion pair representation of DES molecules.

tetrabutylphosphonium bromide-ethylene glycol, was also calculated with COSMO-RS by the group of Hadj-Kali [17]. The RMSD for this system is reported with 4.91% in their work. The calculations performed in this works yield a minimum RMSD of 6.68%. The reasons for this discrepancy are the different versions of TURBOMOLE and COSMOtherm used in the works and the different conformers included for the calculations.

The difference in the prediction quality of the TZVP- and TZVPD-FINE-parameterizations becomes easier to see when the RMSD for each approach is plotted individually for both phases, i.e. the organic solvent-rich phase and the DES-rich phase. The plot in Fig. 6 shows the RMSD for the calculated phase compositions in upper organic-rich phase and lower DES-rich phase. The bars include 99% of the values, while the boxes mark the 75% and 25% quartile, the horizontal line in the box marks the median and the cross represents the mean value of the RMSD. In this plot, it becomes easy to see that the mean values of the RMSD do not differ very much. However, the scattering of the values for the lower phase is higher for the TZVP parameterization than for TZVPD-FINE. The lowest RMSD is achieved for predictions of the phase composition in the DES-rich phase with TZVPD-FINE parameterization and electroneutral approach, except for one phase composition, namely the system composed of hexane/ethyl acetate/CLC (system no. 6). In the upper phase all parameterizations and representations of the DES show similar deviations from the experimental phase compositions. The scattering of the RMSD for the TZVP parameterization is significantly lower for calculations of the phase composition of the organic solvent-rich upper phase than of the lower phase for the investigated biphasic systems. Comparing the results of the LLE predictions with the prediction quality of activity coefficients investigated in section 3.1 a similar trend can be observed. The TZVPD-FINE-parameterization gives smaller deviations for the lower phase where polar molecules and H-bond interactions play an important role, while the TZVP-parameterization leads to comparable deviations for both the polar lower and less polar upper phase. In biphasic systems both types of molecules and interactions play an important role.

For some input compositions, the algorithm to solve the equilibrium used by COSMOtherm (VLE/LLE job type) did not converge and led to missing tie lines in the miscibility gap. This problem can be overcome by slightly varying the global input concentration of a system. The error for further calculations resulting from this approach to predict the phase composition is shown in supporting information (Fig. S15). The convergence problem occurred especially for TZVPD-FINE-parameterization in combination with the non-dissociated representation of the HBA (ion pair approach) and least for TZVP and fully dissociated HBA (electroneutral approach).

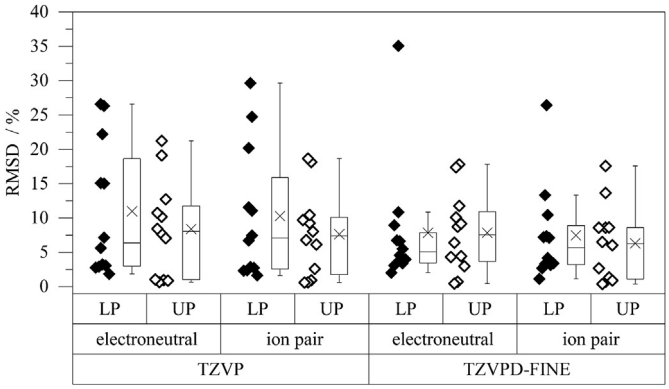

Fig. 6. RMSD for the lower (LP) and upper (UP) phase compositions of the LLE computed with TZVP and TZVPD-FINE parameterizations with fully and non-dissociated representation of the HBA.

3.2.1. Consideration as quaternary liquid-liquid equilibria

From a physical point of view it is more reasonable to treat a LLE of a DES and two other solvents as a quaternary system than as a pseudo ternary system. However, this consideration comes with some restraints. Equations (5)–(9) of section 2.2.1 cannot be used to convert the mole fractions of DES from COSMO-RS framework to laboratory framework, since they are restricted for the assumption that the stoichiometric coefficients of the DES-constituents stay the same in both phases. Therefore it is difficult to compare the results of the quaternary LLE calculations with the experimentally determined LLE. However, the distribution of the individual DES constituents is a very interesting matter.

Calculations of three tie lines each of the biphasic systems heptane/ethanol/CLA (system no. 1) and hexane/ethyl acetate/CLC were performed with TZVP and TZVPD-FINE for the ion pair approach using the multinary liquid-liquid equilibrium option in COSMOtherm. The results of both calculations are tabulated in Tables S2 and S3 in the supporting information. The calculated phase composition for the heptane/ethanol/CLA system (system no. 6) shows that the ratio of HBD and HBA stays constant in the DES-rich phase since the amount of DES constituents in the heptane-rich phase is negligible. The systems 2 to 5 and 7 to 12 can be assumed to yield similar results since the amount of DES is very small in the upper phases of those systems. In those systems the assumption that the ratio of HBD and HBA stays constant is acceptable. In system no. 6 the amount of DES constituents in the hexane-rich phase is not negligible. The results of the calculations for the quaternary systems in Table S3 show that the ratio of HBD and HBA in the DES-rich phase decreases with increasing amount of ethyl acetate. The decrease is stronger pronounced for the calculations with TZVPD-FINE than with TZVP. Unfortunately, it is not possible to say which results describe the LLE better since there is no experimental data available on the individual distribution of HBA and HBD in this system.

3.3. Partition coefficients of different solutes in DES-Based biphasic systems

Since the separation of a mixture in liquid-liquid chromatography is based on the difference in the distribution of the target compounds or impurities within a biphasic liquid system, the partition coefficient of these molecules is one of the most important physicochemical properties to consider in the design of the process. To assess the prediction quality of COSMO-RS for solute partitioning in biphasic systems containing DES, the partition coefficients of nine natural components from the G.U.E.S.S.-mix [11] were calculated and compared to experimentally determined values. The experimental data for the partition coefficients in the system heptane/ethanol/CLA were taken from Ref. [9]. The calculations were performed using experimental and predicted phase composition data for a global composition of 30/40/30 wt/wt/wt. Fig. 7 shows the predicted and experimental partition coefficients of α-tocopherol, arbutin, β-ionone, caffeine, coumarin, naringenin, retinol, R-carvone and vanillin using experimental LLE data for the input of the phase composition. The solutes are ordered according to their octanol-water partition coefficient in Fig. 7, starting from lowest to highest from left to right. For β-ionone, caffeine, coumarin, naringenin, carvone and vanillin the predicted partition coefficients are in good agreement with the experimentally determined partition coefficients. The values of predicted and measured partition coefficients show higher deviations for α-tocopherol, arbutin and retinol. It can be seen that the highest deviation of predicted and experimental values is obtained for the most

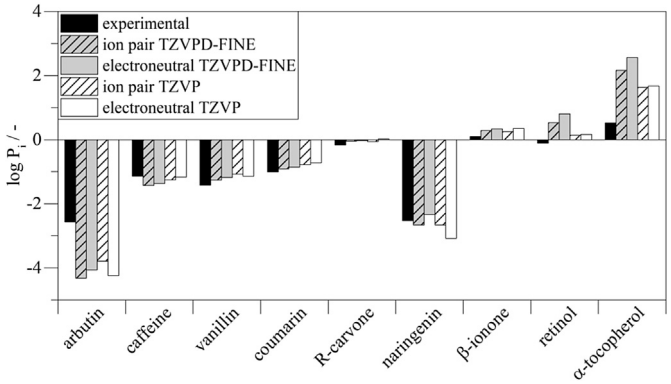

Fig. 7. Experimental and predicted logarithmic partition coefficients of solutes with different polarity in the biphasic system composed of Heptane/Ethanol/CLA with a composition of 30/40/30 wt/wt/wt calculated using COSMO-RS with experimental LLE data.

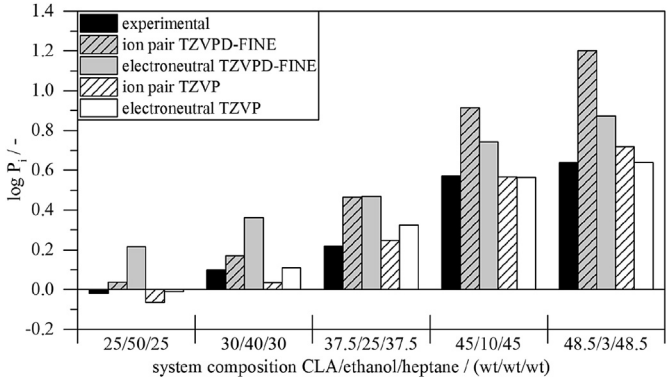

Fig. 8. Experimental and predicted logarithmic partition coefficients of β-ionone in the biphasic system composed of Heptane/Ethanol/CLA with varying compositions; LLE data was received from COSMO-RS calculations.

hydrophilic molecule of the selected solutes, i.e. arbutin, and the most hydrophobic molecules, i.e. α-tocopherol and retinol, according to their octanol-water partition coefficients. Despite the higher deviations for those three molecules, the overall trend of the distribution of the different natural compounds within the DES-based biphasic system is well represented. Except for retinol, the predicted partition coefficients within the preferred range in liquid-liquid chromatography, i.e. $-0.4 < \log P_i < 0.4$, are in good agreement with the experimentally determined partition coefficients.

Availability of LLE-data for biphasic systems containing DES is limited and measuring phase diagrams can be very time consuming, especially considering biphasic solvent system screening. Hence, the partition coefficients were also computed using predicted LLE data. Fig. 9 shows partition coefficients calculated with COSMO-RS using experimental and predicted LLE data. By reason of clarity only the results for the TZVP-parameterization are shown. A similar plot for the TZVPD-FINE parameterization can be found in the supporting information, Fig. S14. The partition coefficients received by calculations using predicted LLE data only differ slightly from the predicted partition coefficients using experimentally determined phase compositions as input for solutes within or close to the preferred range of partition coefficients in liquid-liquid chromatography. The results show that using predicted LLE data does not introduce a significant, additional deviation from the experimentally determined partition coefficients for the investigated biphasic DES-based system.

In liquid-liquid chromatography it is common practice to choose a biphasic solvent system on the basis of solute partition coefficients and then fine tune the composition of the system by choosing a well-suited tie line in the miscibility gap to achieve a stable and economic process. Hence, the partition coefficient of one of the model substances, namely β-ionone, has been calculated for varying global compositions of the biphasic system heptane/ethanol/CLA (system no. 1 in Table 3). The results displayed in Fig. 8 show that the partition coefficient of β-ionone increases with the tie line length and the distance of the global system composition from the plait point. This trend is also reflected in the predicted partition coefficients. The TZVP parameterization also leads to good quantitative values. The results of these calculations show that COSMO-RS can be used to predict the variation of the partition coefficient with the phase composition in biphasic systems containing DES.

Eventually the predictive model was used to calculate partition

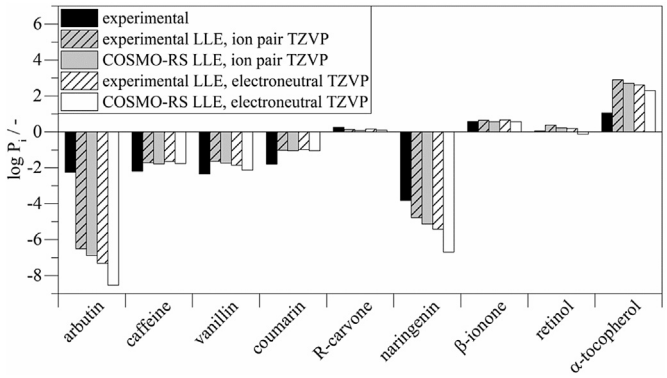

Fig. 9. Experimental and predicted logarithmic partition coefficients of solutes with different polarity in the biphasic system composed of heptane/ethanol/CLA with a composition of 45/10/45 wt/wt/wt calculated using COSMO-RS with the TZVP parameterization and experimental and predicted LLE data.

coefficients in DES-based biphasic solvent systems with no LLE data available. The solvent system compositions used in this data set are listed in section 2.1.3, Table 1. The predicted and experimentally determined partition coefficients of the three model compounds vanillin, β-ionone, and α-tocopherol are given in Fig. 10. Betaine is a zwitterion and therefore the representation as two dissociated separate ions was not applicable. The predicted results for the zwitterion were put into the same diagram with the data of the ion pair representation, although betaine is not an ion pair. The results confirm the previous observation, that the partition coefficients of β-ionone and vanillin show less deviation from the experimental values, while the calculated partition of α-tocopherol in the biphasic systems are generally overestimated, especially for the TZVPD-FINE parameterization. However, the TZVP parameterization combined with the electroneutral representation of the HBA gives reasonable results for a solvent system screening. Although the partition coefficients of α-tocopherol are overestimated, the trend in the distribution behavior of the solute can be reproduced using the TZVP-parameterization and the electroneutral representation of the HBA (TZVP and ion pair for biphasic systems containing BLA respectively). For β-ionone the predicted partition coefficients are in good agreement with the experimentally determined values for TZVP parameterization and electroneutral approach, with the exception of biphasic systems containing acetonitrile (ACN) or propanol (PrOH). Best prediction quality is observed for vanillin, a small polar molecule.

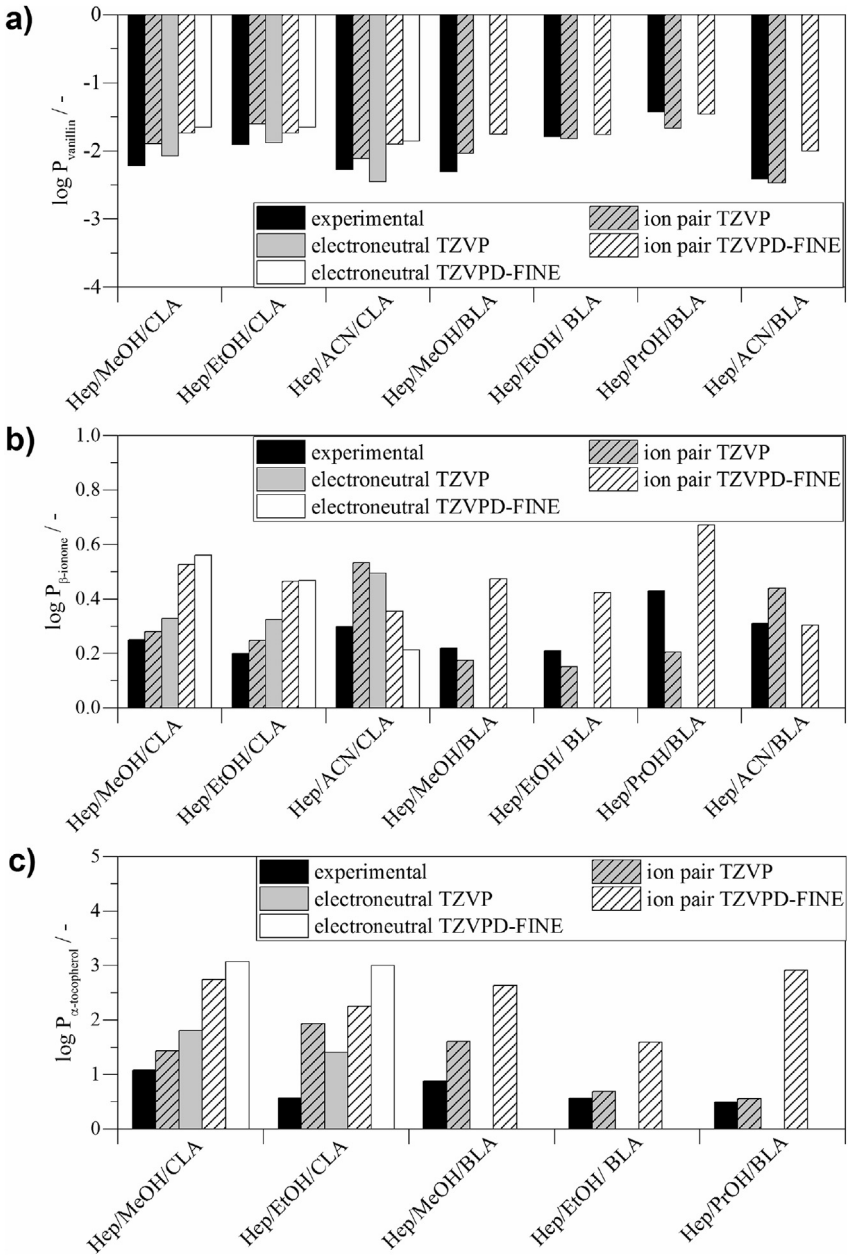

Fig. 10. Predicted and experimentally determined partition coefficients of a) vanillin, b) β-ionone and c) α-tocopherol in different DES-based biphasic solvent systems listed in Table 1; LLE data for partition coefficient calculations were received from COSMO-RS calculations.

4. Conclusion

The evaluation of the prediction quality of COSMO-RS for limiting activity coefficients has shown that using different parameterizations, i.e. TZVP or TZVPD-FINE, leads to significantly different results. These deviations occur not only due to the differences in the parameterization, but also due to the differences in the implementation of COSMO-RS for the different parameterizations in COSMOtherm. Compared to this the difference resulting from the used representation of the ionic HBA is small. The TZVPD-FINE-parameterization yields better predictions for polar or small organic molecules, but high deviations from the experimental activity coefficients for long chain, non-polar alkanes. For the investigated set of data the TZVP-parameterization is better suited to predict activity coefficients of molecules with low polarity in DES. Limiting activity coefficients calculated with TZVPD-FINE show smaller deviations from the experiment than calculations with the TZVP-parameterization for the investigated substances with ln γ_i^∞ up to 5.

For LLE calculations of biphasic systems containing DES, where both polar and non-polar interactions are of great importance, both parameterizations yield similar RMSD. However, the prediction quality is high enough in most cases to receive qualitative and quantitative results for the phase compositions of biphasic systems containing DES. The assumption that the ratio of HBD and HBA stays constant is reasonable for systems with a negligible amount of DES in one of the phases. For systems with a non-negligible amount the treatment as pseudo ternary system is not satisfactory. However, there is a need for quaternary experimental LLE data to evaluate how well the modeling approaches reproduce the actual distribution of all constituents. The best prediction results for partition coefficients are received for moderate partition

coefficients. Since the preferred working range for partition coefficients in liquid-liquid chromatography lies between $-0.4 < \log Pi < 0.4$ these results suit the requirements very well. Using predicted LLE data did not lead to further deviation from the experimental partition coefficients compared to when experimental LLE data was used. In conclusion, it can be summarized that the prediction quality of COSMO-RS is high enough to use the predictive model in a screening of DES-based biphasic solvent systems and partition coefficients. It could be shown that the application of COSMO-RS in the selection of a biphasic solvent system for liquid-liquid chromatography can be extended to DES-based biphasic systems.

Nomenclature

$K_i^{\alpha\beta}$	partition coefficient of compound i (mole fractions)
$P_i^{\alpha\beta}$	partition coefficient of compound i (concentration)
α, β	phases of a biphasic liquid system
x_i^{α}	mole fraction of compound i in phase α
γ_i^{α}	activity coefficient of compound i in phase α
c_i^{α}	concentration of compound i in phase α in g/l
ρ^{α}	molar density of phase α in mol/m^3
ν_i	stoichiometric coefficient of a constituent in a mixture
n_{DES}	molar amount of DES in the laboratory framework (treated as one pseudo compound) in mol
ν_a	stoichiometric coefficient of the anion
ν_c	stoichiometric coefficient of the cation
x_i^{exp}	mole fraction of compound i in the laboratory framework
γ_i^{exp}	activity coefficient of compound i in the laboratory framework
x_i^{calc}	mole fraction of compound i in the COSMO-RS framework
γ_i^{calc}	activity coefficient of compound i in the COSMO-RS framework
$x_i^{non-diss,calc}$	mole fraction of compound i in the COSMO-RS framework for ion pair approach
$x_i^{diss,calc}$	mole fraction of compound i in the COSMO-RS framework for electroneutral approach
ν	sum of the stoichiometric coefficient of all DES-constituents
γ_i^{∞}	limiting activity coefficient of compound i
COSMO-RS	Conductor-Like Screening Model for Realistic Solvation
DFT	density functional theory
DES	deep eutectic solvent
HBA	hydrogen bond acceptor
HBD	hydrogen bond donor
CLA	choline chloride-levulinic acid 1:2
CLC	choline chloride-lactic acid 1:2
CEG	choline chloride-ethylene glycol 1:2
CGY	choline chloride-glycolic acid 1:1
CGL	choline chloride-glycerol 1:2
TBP	tetrabutylphosphonium bromide
TBP-EG	tetrabutylphosphonium bromide-ethylene glycol 1:2
BLA	Betaine-levulinic acid 1:2

Appendix A. Supplementary data

Supplementary data related to this article can be found at http://dx.doi.org/10.1016/j.fluid.2017.01.001.

References

[1] A.P. Abbott, et al., Novel solvent properties of choline chloride/urea mixtures, Chem. Commun. (1) (2003) 70–71.
[2] E.L. Smith, A.P. Abbott, K.S. Ryder, Deep eutectic solvents (DESs) and their applications, Chem. Rev. 114 (21) (2014) 11060–11082.
[3] M. Francisco, A. van den Bruinhorst, M.C. Kroon, Low-Transition-temperature mixtures (LTTMs): a new generation of designer solvents, Angew. Chem. Int. Ed. 52 (11) (2013) 3074–3085.
[4] E. Durand, J. Lecomte, P. Villeneuve, From green chemistry to nature: the versatile role of low transition temperature mixtures, Biochimie 120 (January 2016) 119–123.
[5] Ru, B. Konig, Low melting mixtures in organic synthesis - an alternative to ionic liquids? Green Chem. 14 (11) (2012) 2969–2982.
[6] Q. Zhang, et al., Deep eutectic solvents: syntheses, properties and applications, Chem. Soc. Rev. 41 (21) (2012) 7108–7146.
[7] B. Tang, H. Zhang, K.H. Row, Application of deep eutectic solvents in the extraction and separation of target compounds from various samples, J. Sep. Sci. 38 (6) (2015) 1053–1064.
[8] Z. Maugeri, P. Dominguez de Maria, Novel choline-chloride-based deep-eutectic-solvents with renewable hydrogen bond donors: levulinic acid and sugar-based polyols, RSC Adv. 2 (2) (2012) 421–425.
[9] S. Roehrer, et al., Deep eutectic solvents in countercurrent and centrifugal partition chromatography, J. Chromatogr. A 1434 (2016) 102–110.
[10] A. Foucault, L. Chevolot, Counter-current chromatography: instrumentation, solvent selection and some recent applications to natural product purification, J. Chromatogr. A 808 (1) (1998) 3–22.
[11] J.B. Friesen, G.F. Pauli, G.U.E.S.S.—a generally useful estimate of solvent systems for CCC, J. Liq. Chromatogr. Relat. Technol. 28 (17) (2005) 2777–2806.
[12] J.B. Friesen, G.F. Pauli, Rational development of solvent system families in counter-current chromatography, J. Chromatogr. A 1151 (1–2) (2007) 51–59.
[13] J.B. Friesen, S. Ahmed, G.F. Pauli, Qualitative and quantitative evaluation of solvent systems for countercurrent separation, J. Chromatogr. A 1377 (2015) 55–63.
[14] E. Hopmann, W. Arlt, M. Minceva, Solvent system selection in counter-current chromatography using conductor-like screening model for real solvents, J. Chromatogr. A 1218 (2) (2011) 242–250.
[15] E. Hopmann, A. Frey, M. Minceva, A priori selection of the mobile and stationary phase in centrifugal partition chromatography and counter-current chromatography, J. Chromatogr. A 1238 (2012) 68–76.
[16] A.S.B. Gonzalez, et al., Liquid–liquid equilibrium data for the systems {LTTM + benzene + hexane} and {LTTM + ethyl acetate + hexane} at different temperatures and atmospheric pressure, Fluid Phase Equilibria 360 (2013) 54–62.
[17] H.F. Hizaddin, et al., Evaluating the performance of deep eutectic solvents for use in extractive denitrification of liquid fuels by the conductor-like screening model for real solvents, J. Chem. Eng. Data 59 (11) (2014) 3470–3487.
[18] S. Mulyono, et al., Separation of BTEX aromatics from n-octane using a (tetrabutylammonium bromide + sulfolane) deep eutectic solvent - experiments and COSMO-RS prediction, RSC Adv. 4 (34) (2014) 17597–17606.
[19] H.F. Hizaddin, et al., Coupling the capabilities of different complexing agents into deep eutectic solvents to enhance the separation of aromatics from aliphatics, J. Chem. Thermodyn. 84 (2015) 67–75.
[20] N.R. Rodriguez, et al., Experimental determination of the LLE data of systems consisting of {hexane + benzene + deep eutectic solvent} and prediction using the Conductor-like Screening Model for Real Solvents, J. Chem. Thermodyn. 104 (2017) 128–137.
[21] A.S.L. Gouveia, et al., Deep eutectic solvents as azeotrope breakers: liquid–liquid extraction and COSMO-RS prediction, ACS Sustain. Chem. Eng. 4 (10) (2016) 5640–5650.
[22] T. Aissaoui, I.M. AlNashef, Y. Benguerba, Dehydration of natural gas using choline chloride based deep eutectic solvents: COSMO-RS prediction, J. Nat. Gas Sci. Eng. 30 (2016) 571–577.
[23] S.L. Perkins, P. Painter, C.M. Colina, Molecular dynamic simulations and vibrational analysis of an ionic liquid analogue, J. Phys. Chem. B 117 (35) (2013) 10250–10260.
[24] S.L. Perkins, P. Painter, C.M. Colina, Experimental and computational studies of choline chloride-based deep eutectic solvents, J. Chem. Eng. Data 59 (11) (2014) 3652–3662.
[25] R. Ullah, et al., A detailed study of cholinium chloride and levulinic acid deep eutectic solvent system for CO2 capture via experimental and molecular simulation approaches, Phys. Chem. Chem. Phys. 17 (32) (2015) 20941–20960.
[26] A. Frey, E. Hopmann, M. Minceva, Selection of biphasic liquid systems in liquid-liquid chromatography using predictive thermodynamic models, Chem. Eng. Technol. 37 (10) (2014) 1663–1674.
[27] M. Diedenhofen, A. Klamt, COSMO-RS as a tool for property prediction of IL mixtures—a review, Fluid Phase Equilibria 294 (1–2) (2010) 31–38.
[28] F. Eckert, COSMOtherm Reference Manual, COSMOlogic GmbH & Co. KG, Leverkusen, Germany, 2014.
[29] S.P. Verevkin, et al., Separation performance of BioRenewable deep eutectic solvents, Industrial Eng. Chem. Res. 54 (13) (2015) 3498–3504.
[30] C.G.C. KG, COSMOtherm Version C3.0 Release 12.01, 2012.
[31] F.S. Oliveira, et al., Deep eutectic solvents as extraction media for azeotropic mixtures, Green Chem. 15 (5) (2013) 1326–1330.
[32] N.R. Rodriguez, B.S. Molina, M.C. Kroon, Aliphatic + ethanol separation via liquid–liquid extraction using low transition temperature mixtures as extracting agents, Fluid Phase Equilibria 394 (2015) 71–82.
[33] M.A. Kareem, et al., Phase equilibria of toluene/heptane with tetrabutylphosphonium bromide based deep eutectic solvents for the potential use in the separation of aromatics from naphtha, Fluid Phase Equilibria 333 (2012) 47–54.

3.3. Paper III

Computational solvent system screening for the separation of tocopherols with centrifugal partition chromatography using deep eutectic solvent-based biphasic systems

Citation

F. Bezold, M.E. Weinberger, M. Minceva, Computational solvent system screening for the separation of tocopherols with centrifugal partition chromatography using deep eutectic solvent-based biphasic systems, Journal of Chromatography A, 1491 (2017) 153-158.

https://doi.org/10.1016/j.chroma.2017.02.059

Summary

Tocopherols are vitamin E derivates that are poorly soluble in water. The objective of this work was to select a suitable DES-based biphasic system for tocopherol separation and to fractionate a mixture of different tocopherols with CPC using the selected system. The mixture used in the work contained mainly α-, and γ-tocopherol with traces of β- and δ-tocopherol. α-Tocopherol is the most valuable for human diet among the structurally similar molecules. The sigma-surfaces of the tocopherols can be seen in Figure 12, the tocopherols differ in the position of the methyl groups at their chromane ring. In order to achieve the set goal to find a DES-based biphasic system, the solvent system selection approach with COSMO-RS that was evaluated in **Paper II** (section 3.2) was applied. LLE of 21 DES-based systems and tocopherol partition coefficients in the systems were predicted with COSMO-RS.

The results of the calculations suggested three DES-based biphasic systems where partition coefficients of β-, γ- and δ-tocopherol within the sweet spot were found. The partition coefficient of α-tocopherol was above the sweet spot range for all investigated systems. From previous work, it was expected that partition coefficients of α-tocopherol are overestimated [81]. Therefore, a system was selected where the partition coefficients of β-, γ- and δ-tocopherol were located within *sweet spot* and where α-tocopherol was closest to it.

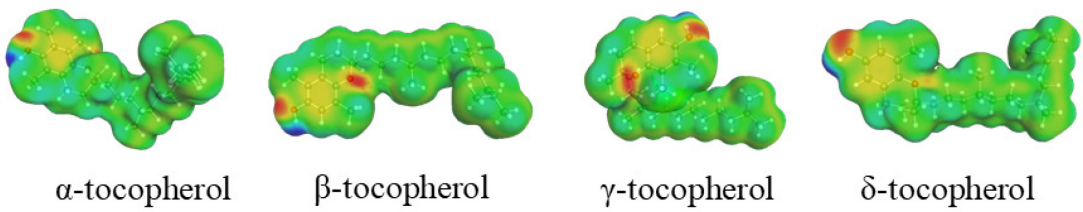

Figure 12: Sigma surfaces of α-, β-, γ- and δ-tocopherol for TZVP parametrization (images obtained from COSMOtherm 15.01)

The best candidate from the computational screening was the system composed of *n*-heptane, ethanol, and the DES formed by choline chloride and 1,4-butandiol (1:3 mol:mol) with a composition of 30/40/30 wt/wt/wt. Pulse injections were then performed with the biphasic

systems and the tocopherol mixture and separation of α- and γ-tocopherol was obtained. The biphasic system that was selected from the screening with COSMO-RS yielded a separation factor of 1.74 for α- and γ-tocopherol. Furthermore, high stationary phase retention was obtained with 0.76 for a flow rate of 20 ml min^{-1} and high concentrations of tocopherols were soluble in the phases. No shake flask experiments needed to be performed prior to the separation with CPC. The computational solvent system screening substantially reduced the experimental effort for the selection of the DES-based biphasic system.

Contributions

The author was the lead scientist in the experiments. She planned and coordinated the work, supervised all data acquisition, had a leading role in data interpretation, and performed the DFT-calculations. M. Weinberger conducted the remaining data acquisition supervised by the author. The manuscript was written by the author and discussed with Prof. Minceva.

Journal of Chromatography A, 1491 (2017) 153–158

Contents lists available at ScienceDirect

Journal of Chromatography A

journal homepage: www.elsevier.com/locate/chroma

Computational solvent system screening for the separation of tocopherols with centrifugal partition chromatography using deep eutectic solvent-based biphasic systems☆

Franziska Bezold, Maria E. Weinberger, Mirjana Minceva*

Biothermodynamics, TUM School of Life and Food Sciences Weihenstephan, Technische Universität München, 85354 Freising, Germany

ARTICLE INFO

Article history:
Received 23 December 2016
Received in revised form 20 February 2017
Accepted 23 February 2017
Available online 27 February 2017

Keywords:
Centrifugal partition chromatography
Vitamin E
Deep eutectic solvents
Tocopherols
Biphasic solvent system screening
COSMO-RS

ABSTRACT

Tocopherols are a class of molecules with vitamin E activity. Among those, α-tocopherol is the most important vitamin E source in the human diet. The purification of tocopherols involving biphasic liquid systems can be challenging since these vitamins are poorly soluble in water. Deep eutectic solvents (DES) can be used to form water-free biphasic systems and have already proven applicable for centrifugal partition chromatography separations. In this work, a computational solvent system screening was performed using the predictive thermodynamic model COSMO-RS. Liquid-liquid equilibria of solvent systems composed of alkanes, alcohols and DES, as well as partition coefficients of α-tocopherol, β-tocopherol, γ-tocopherol, and σ-tocopherol in these biphasic solvent systems were calculated. From the results the best suited biphasic solvent system, namely heptane/ethanol/choline chloride-1,4-butanediol, was chosen and a batch injection of a tocopherol mixture, mainly consisting of α- and γ-tocopherol, was performed using a centrifugal partition chromatography set up (SCPE 250-BIO). A separation factor of 1.74 was achieved for α- and γ-tocopherol.

1. Introduction

Tocopherols are a class of molecules which are known for their vitamin E activity. Their antioxidative capacity and the fact that they act as free radical scavenger make tocopherols an interesting class of molecules for human health and food supplement industry [1,2]. Among the tocopherols, α-tocopherol is the most important vitamin E source in the human diet [3]. Hence, there is a great interest in separation methods that can provide purified α-tocopherol [4–12]. Besides chromatographic methods, liquid-liquid separation technologies, such as countercurrent distribution or countercurrent chromatography, have been applied for tocopherol purification [13,14]. The purification of tocopherols involving biphasic liquid systems can be challenging since these vitamins are poorly soluble in water. Therefore, a water-free separation method is favorable. Deep eutectic solvents (DES) can be used to form water-free biphasic systems and have already proven applicable for centrifugal partition chromatography (CPC) separations [15]. DESs are formed when hydrogen bond donor (HBD) and hydrogen bond acceptor (HBA) molecules are combined in a certain molar ratio. The resulting mixture has a substantially lower melting point than the pure components. The term refers to such combinations with a melting point below 100 °C. They gained increasing attention after Abbott et al. described properties of DESs in 2003 [16,17]. The high solvation capacity, low volatility, and low cost of DESs led to many new applications in extraction and separation processes [18–20]. The number of possible combinations of HBA and HBD is nearly limitless. Typical HBA are quaternary ammonium or phosphonium salts, which are combined with HBD, such as urea, carboxylic acids and sugar-based polyols [8]. The resulting mixtures are considered biocompatible and less environmentally harmful green solvents [3].

In previous work, we have shown that the predictive thermodynamic model COSMO-RS (Conductor-like Screening Model for Realistic Solvation) can be used to drastically reduce the experimental effort in the solvent system selection process for centrifugal partition chromatography [21–23]. With this model, thermodynamic properties, such as liquid-liquid equilibria and partition coefficients can be calculated based on the molecular structure of the compounds in the system. This method has also proven applicable for DES-based biphasic solvent systems [24]. In this work, the computational screening method is applied for the selection of

☆ Selected paper from the 9th International Counter-current Chromatography Conference (CCC 2016), 1–3 August 2016, Chicago, IL, USA.

* Corresponding author.
E-mail address: mirjana.minceva@tum.de (M. Minceva).

http://dx.doi.org/10.1016/j.chroma.2017.02.059
0021-9673/

a DES-based biphasic solvent system for the separation of a mixture consisting primarily of α-tocopherol and γ-tocopherol, with β-tocopherol and σ-tocopherol in small amounts. In the screening, 21 solvent systems composed of alkanes, alcohols and DESs were considered. The most promising system from the computational solvent system screening was then used in a centrifugal partition chromatography experiment in a 250 ml CPC (SCPE 250-BIO, also called centrifugal partition extractor). The separation performance was compared to a reference DES-based biphasic solvent system, which has been used for the separation of hydrophobic natural compounds in our previous work [15].

2. Material and methods

2.1. Chemicals

Ethanol and *n*-heptane (liquid-chromatography grade) were obtained from Merck KGaA and VWR International GmbH. Choline chloride, betaine, 1,4-butanediol, and levulinic acid were purchased from Alfa Aesar with purities ≥98%. Commercial α-tocopherol with a purity of ≥97% was obtained from Alfa Aesar and a synthetic tocopherol mixture was kindly provided by Sigma-Aldrich Chemie GmbH. The tocopherol content was 37 wt% of α-, and 37 wt% of γ-tocopherol, 1 wt% of β-tocopherol and 7 wt% of δ-tocopherol. Structures of the tocopherol homologues contained in the mixture are shown in Fig. 1.

2.2. Preparation of the DES

To prepare the DES, HBA and HBD were weighed in at a specific molar ratio listed in Table 1 for each DES, and the sealed flask was heated to 80–85 °C. The mixtures were stirred and heated until a clear homogenous liquid was obtained. A more detailed description of the procedure can be found in [15]. Choline chloride was used as HBA. The HBD levulinic acid was used in the first and 1,4-butanediol in the second experiment.

2.3. Biphasic solvent systems

The biphasic solvent systems considered in the computational screening are listed in Table 1. The proportions of the components of the biphasic solvent systems were chosen from the experimental ternary diagram of heptane/ethanol/CLA [25]. The compositions 30/40/30 wt/wt/wt and 37.5/25/37.5 wt/wt/wt of different alkane/alcohol/DES-systems for the screening were chosen because they have been used in our previous work for shake flask experiments, and with heptane/ethanol/CLA a good stationary volume retention ratio has been achieved for the composition of 30/40/30 wt/wt/wt [15]. For the experimental validation of the selected biphasic solvent systems, DES and solvents were mixed in the respective amounts. The system was stirred in a sealed flask for at least one hour at room temperature and allowed to settle for a minimum time of 30 min afterwards. The phases were then separated into two reservoirs for their use as mobile and stationary phases of the chromatographic separation.

2.4. Partition coefficient

For the calculation of solute partition coefficients in a biphasic solvent system, the composition of the phases (solute-free) has to be known. The equilibrium phase composition can be taken from literature or determined by solving the liquid-liquid equilibrium (LLE) conditions defined by Eq. (1)

$$x_i^{SP}\gamma_i^{SP} = x_i^{MP}\gamma_i^{MP} \tag{1}$$

where x_i is the mole fraction, γ_i the activity coefficient of compound *i*, and *SP* and *MP* are the two phases of a biphasic solvent system used as stationary phase (*SP*) and mobile phase (*MP*) for the chromatographic separation.

The partition coefficient *K* of a solute *i* is defined as the ratio of the mole fraction of the solute in the phases at thermodynamic equilibrium:

$$K_i = \frac{x_i^{SP}}{x_i^{MP}} = \frac{\gamma_i^{\infty,MP}}{\gamma_i^{\infty,SP}} \tag{2}$$

where γ_i^{∞} is the limiting activity coefficient of the solute *i*.

In this work, the partition coefficients were all calculated for descending mode, i.e. *SP* is the upper phase and *MP* the lower phase of the considered biphasic system. At low solute concentrations, the distribution shows linear behavior and the partition coefficient is assumed to be constant.

For centrifugal partition chromatography the partition coefficient is expressed using concentrations *c* instead of mole fractions (see Eq. (3)). K_i can be converted to P_i using the molar densities ρ of the two phases.

$$P_i = \frac{c_i^{SP}}{c_i^{MP}} = \frac{x_i^{SP}\rho^{SP}}{x_i^{MP}\rho^{MP}} \tag{3}$$

The partition coefficient P_i can be experimentally determined by pulse injections in centrifugal partition chromatography. It is calculated from the chromatogram using the following equation:

$$P_i = \frac{V_R - V_{MP}}{V_{SP}} \tag{4}$$

where V_R is the retention volume, V_{MP} is the volume of the mobile phase and V_{SP} is the volume of stationary phase in the column. In centrifugal partition chromatography moderate partition coefficients in the range of $-0.4 < \log P_i < 0.4$ or close to that range are preferred. Smaller partition coefficients result in early eluting peaks with low resolution, whereas for high partition coefficients the target components elute late and in broad peaks.

The separation factor is calculated as the ratio of the partition coefficient of two consecutive peaks of compounds *i* and *j* where $P_j > P_i$.

$$\alpha_{ij} = \frac{P_j}{P_i} \tag{5}$$

2.5. Computational details

2.5.1. COSMO-RS

In this work, the Conductor-Like Screening Model for Realistic Solvation (COSMO-RS) was used to calculate LLE, i.e. the composition of the phases of the investigated biphasic solvent systems, and the partition coefficients of tocopherol homologues in these systems. The predictive thermodynamic model COSMO-RS combines quantum mechanical calculations and statistical thermodynamics. For each molecular conformer of the solutes and solvents of the biphasic systems, the screening charge density is computed using the density functional theory (DFT). These calculations only have to be performed once per molecule. From the screening charge density, the charge distribution (σ-profile) is obtained. From the σ-profile thermodynamic properties, such as activity coefficients and chemical potential can be obtained based solely on the molecular structure of the molecules in the mixture. From these properties LLE and partition coefficients can be computed. Detailed information about COSMO-RS can be found in [26].

2.5.2. Modelling of the DES in COSMO-RS

For the computational screening of partition coefficients of the tocopherol homologues in DES-based biphasic systems, the DES

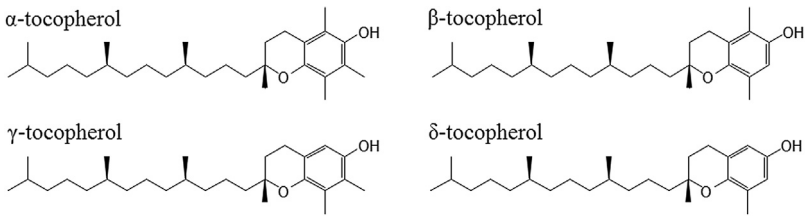

Fig. 1. Chemical structure of α-tocopherol, β-tocopherol, γ-tocopherol, and δ -tocopherol.

Table 1
List of DES-based biphasic systems considered as mobile and stationary phases for the liquid-liquid chromatographic separation of tocopherols. The selected systems are marked in bold.

Alkane	Alcohol	DES	Ratio of HBA:HBD/mol:mol	Abbreviation of the DES	Composition (wt/wt/wt)	System abbreviation
n-Heptane	Methanol	Choline chloride – levulinic acid	1:2	CLA	30/40/30	Hep/MeOH/CLA
n-Heptane	Methanol	Choline chloride – levulinic acid	1:2	CLA	37.5/25/37.5	Hep/MeOH/CLA
n-Heptane	**Ethanol**	**Choline chloride – levulinic acid**	**1:2**	**CLA**	**30/40/30**	**Hep/EtOH/CLA**
n-Heptane	Ethanol	Choline chloride – levulinic acid	1:2	CLA	37.5/25/37.5	Hep/EtOH/CLA
n-Hexane	Ethanol	Choline chloride – levulinic acid	1:2	CLA	30/40/30	Hex/EtOH/CLA
n-Heptane	Propanol	Choline chloride – levulinic acid	1:2	CLA	30/40/30	Hep/PrOH/CLA
n-Heptane	Propanol	Choline chloride – levulinic acid	1:2	CLA	37.5/25/37.5	Hep/PrOH/CLA
n-Hexane	Propanol	Choline chloride – levulinic acid	1:2	CLA	30/40/30	Hex/PrOH/CLA
n-Heptane	Methanol	Betaine – levulinic acid	1:2	BLA	30/40/30	Hep/MeOH/BLA
n-Heptane	Methanol	Betaine – levulinic acid	1:2	BLA	37.5/25/37.5	Hep/MeOH/BLA
n-Heptane	Ethanol	Betaine – levulinic acid	1:2	BLA	30/40/30	Hep/EtOH/BLA
n-Heptane	Ethanol	Betaine – levulinic acid	1:2	BLA	37.5/25/37.5	Hep/EtOH/BLA
n-Heptane	Ethanol	Choline chloride – ethylene glycol	1:2	CEG	30/40/30	Hep/EtOH/CEG
n-Heptane	Ethanol	Choline chloride – ethylene glycol	1:2	CEG	37.5/25/37.5	Hep/EtOH/CEG
n-Heptane	Ethanol	Choline chloride – glycerol	1:2	CGL	30/40/30	Hep/EtOH/CGL
n-Heptane	Ethanol	Choline chloride – glycerol	1:2	CGL	37.5/25/37.5	Hep/EtOH/CGL
n-Heptane	Ethanol	Choline chloride – malonic acid	1:1	CMA	30/40/30	Hep/EtOH/CMA
n-Hexane	Ethanol	Choline chloride – malonic acid	1:1	CMA	30/40/30	Hex/EtOH/CMA
n-Heptane	Ethanol	Choline chloride – lactic acid	1:2	CLC	30/40/30	Hep/EtOH/CLC
n-Heptane	**Ethanol**	**Choline chloride – 1,4-butanediol**	**1:3**	**CBD**	**30/40/30**	**Hep/EtOH/CBD**
n-Hexane	Ethanol	Choline chloride – 1,4-butanediol	1:3	CBD	30/40/30	Hex/EtOH/CBD

was treated as stoichiometric mixture of the HBD and ionic HBA modelled as a fully dissociated electroneutral mixture. The LLE was calculated as a pseudo ternary mixture composed of two solvents and the DES. The ratio between HBA cation and anion and the HBD was kept constant during the calculations. The molar fractions calculated in the COSMO-RS framework were then converted to the laboratory scale according to Eq. (6) [27]

$$x_i^{exp} = \frac{\frac{x_i^{calc}}{\nu_i}}{\frac{x_i^{calc}}{\nu_i} + \sum_{j \neq i}\left(\frac{x_j^{calc}}{\nu_j}\right)} = \frac{\frac{x_i^{calc}}{\nu_i}}{\sum_k \left(\frac{x_k^{calc}}{\nu_k}\right)} \quad (6)$$

$$\text{with } \nu_k = \begin{cases} 1, k\, not\ \ a\ \ DES \\ \nu, k\ \ is\ \ a\ \ DES \end{cases}$$

where x_i^{exp} is the experimental mole fraction of compound *i*, x_i^{calc} is the calculated mole fraction of compound *i*, ν_k is the stoichiometric coefficient of compound *k*, and ν denotes the sum of the stoichiometric coefficients of the DES. A detailed explanation for the conversion can be found in our previous work [24].

2.5.3. Software

For the generation of conformers of tocopherols, organic solvents, and DES-constituents, COSMOconf (Version 4.0, COSMOlogic, Germany) was used with the Balloon algorithm, implemented in the software. The conformers were considered as a Boltzmann-weighted mixture of conformers for the calculations. The maximum number of conformers was set to 20 within an energy window of 25 kcal/mol from the lowest energy structure. For the different molecular conformations full DFT optimization was performed in TURBOMOLE (Version 6.6, COSMOlogic, Germany) using the Becke-Perdew (BP) functional with resolution of the identity (RI) approximation and the triple-zeta valence polarized basis set (TZVP). LLE and partition coefficients were then computed using the commercially available software COSMOtherm (Version C30 Release 15.01., COSMOlogic, Germany).

2.6. CPE experiments

A centrifugal partition chromatography unit (SCPE 250-BIO) from Armen Instruments, France, was used to conduct the batch injections of the tocopherol mixtures. The separations were performed at room temperature in descending mode, i.e. the upper phase of the biphasic solvent systems was used as stationary phase and the lower phase was used as mobile phase. Due to the special cell geometry, this column is suitable for biphasic solvent systems with higher viscosity than organic/water-based solvent systems. The column is built of 11 stainless steel disks with 20 twin-cells per disk and has a total column volume of 250 ml. The maximum rotational speed is 3000 rpm and separations at a pressure up to 100 bar can conducted. A detailed description of the column can be found in [15,28]. The rotational speed was set to 2000 rpm. A flow rate of the mobile phase of 20 ml/min and an injection volume of 2 ml were used for both experiments.

3. Results and discussion

3.1. Biphasic solvent system screening using COSMO-RS

For the selection of a suitable DES-based biphasic solvent system, the partition coefficients of α-, β-, γ-, and δ-tocopherol

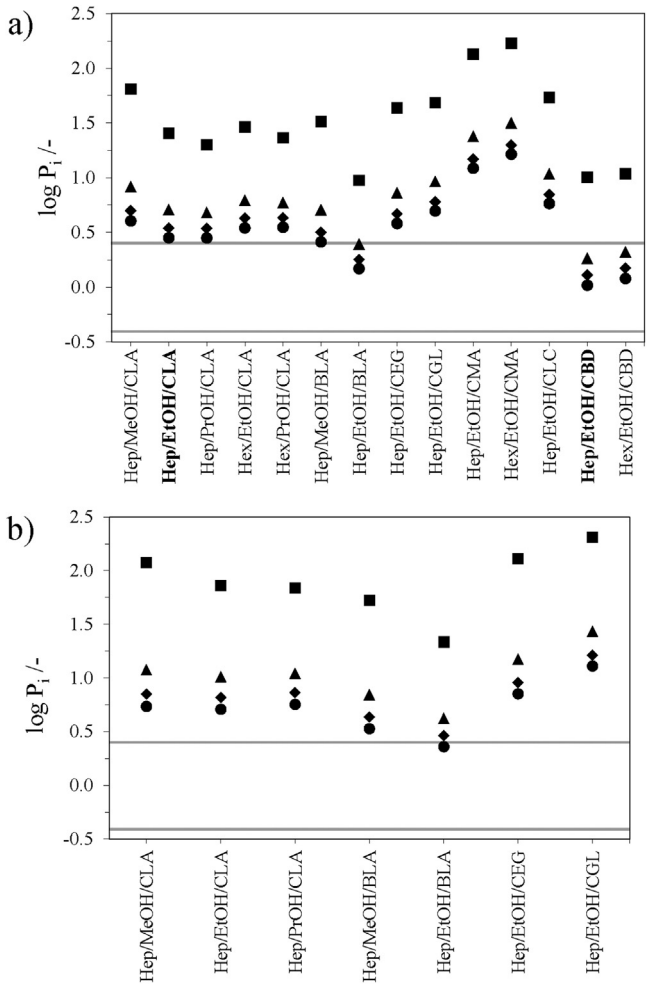

Fig. 2. Partition coefficient of α-tocopherol (■), β-tocopherol (▲), γ-tocopherol (♦), and δ-tocopherol (●) calculated with COSMO-RS for a) systems with composition 30/40/30 (wt/wt/wt), and b) systems with composition 37.5/25/37.5 (wt/wt/wt); selected systems are marked in bold.

were calculated in 21 DES-based water-free solvent systems using COSMO-RS. In previous work, we have shown that the prediction quality of COSMO-RS is high enough to use the model in a computational solvent system screening for DES-based biphasic systems for centrifugal partition chromatography [24]. It could be shown that partition coefficients of α-tocopherol in DES-based systems were overestimated, but the trend of the solute distribution was well reflected in the predicted values. For the screening study the global compositions of 30/40/30 (wt/wt/wt) and 37.5/25/37.5 (wt/wt/wt) were chosen based on results from our previous publication [15]. In the first step the LLE was calculated for each system listed in Table 1 to obtain the composition of the phases of the biphasic systems, since experimental LLE data was only available for one system [25]. The phase composition was then used to calculate the partition coefficient at infinite dilution. Predicted partition coefficients for the investigated systems with a global composition of 30/40/30 (wt/wt/wt) (a) and 37.5/25/37.5 (wt/wt/wt) (b) are displayed in Fig. 2. From the results different trends in tocopherol distribution can be observed. For example, when heptane and CLA are kept constant and different alcohols are used, the calculated logarithmic partition coefficients of the tocopherol homologues decrease from methanol to ethanol (Hep/MeOH/CLA to Hep/EtOH/CLA in Fig. 2a). From ethanol to propanol the logarithmic partition coefficient slightly decreases for α-, β-, and γ-tocopherol and stays constant for δ-tocopherol. Similar behavior, i.e. strong decrease in the logarithmic partition coefficient from methanol to ethanol, and smaller decrease from ethanol to propanol, can be observed for systems with *n*-hexane instead of *n*-heptane. The findings are in good agreement with experimental observations from [24]. When the alkane and alcohol in the biphasic system are kept constant, it can be seen that the DESs CGL, CMA and CLC lead to high logarithmic partition coefficients, while values closest to the preferred range, indicated with grey lines in Fig. 2a and b, were observed for CBD, CLA and BLA. Comparing the different system compositions of 30/40/30 wt/wt/wt and 37.5/25/37.5 wt/wt/wt, the logarithmic partition coefficients of the tocopherol homologues are generally higher for systems with higher concentrations of alkanes and DES. Systems with *n*-hexane show generally higher partition coefficients of the tocopherols and smaller selectivity than the corresponding biphasic systems with *n*-heptane.

As mentioned in Section 2.4, the optimum range for the solute partition coefficient in centrifugal partition chromatography is $-0.4 < \log P_i < 0.4$. Among the calculated results, the solvent systems composed of heptane/ethanol/CBD and heptane/ethanol/BLA (both for the composition 30/40/30 (wt/wt/wt)) show the lowest partition coefficients. The system heptane/ethanol/BLA was not considered for CPE-experiments because the lower phase showed higher viscosity than the other selected biphasic solvent systems.

3.2. Batch separation of tocopherols using a centrifugal partition extractor

The most promising biphasic solvent system for the separation of the tocopherol mixture from the computational screening, namely heptane/ethanol/CBD 30/40/30 (wt/wt/wt), was experimentally evaluated in the next step. The calculated logarithmic partition coefficients in this system were $\log P_{\alpha\text{-tocopherol}} = 1.00$, $\log P_{\beta\text{-tocopherol}} = 0.26$, $\log P_{\gamma\text{-tocopherol}} = 0.11$, and $\log P_{\delta\text{-tocopherol}} = 0.02$. Additionally, a centrifugal partition chromatography experiment with the system heptane/ethanol/CLA 30/40/30 (wt/wt/wt) was conducted. This solvent system has been used in our previous work [15] and it could be shown that the partition coefficient of α-tocopherol was close to the preferred range, namely $\log P_{\alpha\text{-tocopherol}} = 0.52 \pm 0.1$ ($P_{\alpha\text{-tocopherol}} = 3.31$). Hence, heptane/ethanol/CLA was used as a reference system for comparison with the biphasic solvent system chosen from the COSMO-RS calculations. The calculated values for the logarithmic partition coefficients in this system were $\log P_{\alpha\text{-tocopherol}} = 1.41$, $\log P_{\beta\text{-tocopherol}} = 0.71$, $\log P_{\gamma\text{-tocopherol}} = 0.54$, and $\log P_{\delta\text{-tocopherol}} = 0.45$. Fig. 3a shows the chromatogram of the experiment conducted with the reference system heptane/ethanol/CLA 30/40/30 (wt/wt/wt). The upper, heptane-rich phase was used as the stationary phase and the lower, DES-rich phase was used as the mobile phase with 20 ml/min. The stationary phase volume retention ratio for the experiment was 0.74. The injection volume was 2 ml and the feed contained 35.7 g/l of α-tocopherol, 0.6 g/l of β-tocopherol, 36.5 g/l of γ-tocopherol, and 7.0 g/l of δ-tocopherol. In the chromatogram, two main peaks can be seen, which correspond to α- and γ-tocopherol, that are present in the highest concentrations in the feed. An injection of pure α-tocopherol (data not shown) confirmed that the second large peak is caused by α-tocopherol. Consequently, the first peak is γ-tocopherol, because only α- and γ-tocopherol are present in high enough amounts to cause the two larger peaks. The small shoulder at the front of the first peak is possibly caused by δ-tocopherol. The elution order is consistent with the partition coefficients obtained from the COSMO-RS calculations (see Fig. 2). From the chromatogram, partition coefficients of 2.37 for the first and 3.62 for the second peak are obtained and a value of 1.53 was obtained for the separation factor.

For the second biphasic system, heptane/ethanol/CBD 30/40/30 (wt/wt/wt), a similar stationary phase volume retention ratio

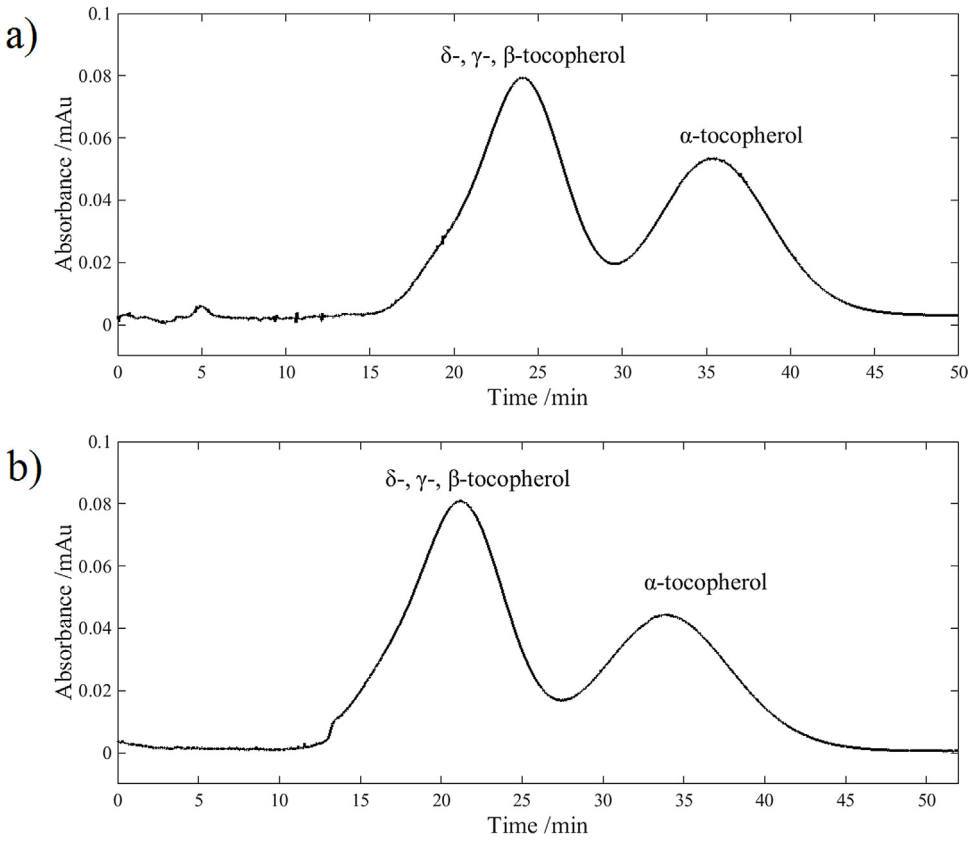

Fig. 3. Chromatogram for the injection of the tocopherol feed in descending mode using the biphasic solvent system heptane/ethanol/CLA 30/40/30 (wt/wt/wt) (a) and heptane/ethanol/CBD 30/40/30 (wt/wt/wt) (b); rotational speed = 2000 rpm; mobile phase flow rate = 20 ml min^{-1}, 2 ml injection volume, detector wavelength = 292 nm, stationary phase volume retention ratio a) 0.74 and b) 0.76.

of 0.76 could be achieved at 20 ml/min and the same sample volume was injected as in the previous run (2 ml). The feed contained 36.2 g/l of α-tocopherol, 0.6 g/l of β-tocopherol, 36.0 g/l of γ-tocopherol, and 6.9 g/l of δ-tocopherol. Fig. 3b shows the chromatogram of the separation experiment. At first sight the chromatogram in Fig. 3b looks very similar to the injection using the biphasic system heptane/ethanol/CLA 30/40/30 (wt/wt/wt) in Fig. 3a; however, slightly different partition coefficients were obtained. For the first peak a value of 2.00 and for the second peak 3.47 were calculated for the partition coefficient from the chromatogram. The separation factor for those two peaks was 1.74. Both partition coefficients were smaller than in the first injection, which decreased the solvent consumption. In addition a higher separation factor could be obtained using heptane/ethanol/CBD.

For the second peak a mean $P_{\alpha\text{-tocopherol}}$ of 3.55 was obtained from the two chromatograms. In previous work, a logarithmic partition coefficient of α-tocopherol of 0.52 ± 0.1 ($P_{\alpha\text{-tocopherol}}$ = 3.31) in heptane/ethanol/CLA 30/40/30 wt/wt/wt was obtained from shake flask experiments [15]. This means the partition coefficient of α-tocopherol is overestimated by COSMO-RS in this system. This is very likely also the case for the other biphasic systems investigated in this study. However, in [24] it could be demonstrated that the trend of tocopherol partitioning in DES-based biphasic solvent systems can be reproduced by COSMO-RS. The tocopherol homologues show different partition behavior most likely due to their different affinity to hydrogen bonding as proposed by Yang et al. [29]. In their work, it is proposed that the tocopherol homologues have different affinity to hydrogen bonding with the chloride anion of an ionic liquid in a biphasic system composed of hexane, methanol and ionic liquid used in liquid-liquid extraction. The predominant phenomenon for the formation of DESs is proposed to be the formation of a hydrogen bond network [30]. Hence, in the DES-rich lower phase, which is used as the mobile phase, hydrogen bonding plays an important role. The OH-groups of the tocopherol molecules are capable of forming hydrogen bonds with the chloride anion of choline chloride. The degree of steric hindrance of the OH-group varies at the chromane ring of the tocopherols because of the different positions of methyl groups. This might be the dominant cause which leads to a difference in the partition coefficients of the tocopherol homologues in DES-based biphasic solvent systems.

4. Conclusion

Biphasic solvent systems based on DESs for the separation of a mixture consisting mainly of α-tocopherol and γ-tocopherol have been selected using the predictive thermodynamic model COSMO-RS. Although the partition coefficient of α-tocopherol was clearly overestimated by the model, the trend of the tocopherol distribution was reproduced for the experimentally validated values. The most promising biphasic system from the computational screening, namely heptane/ethanol/CBD 30/40/30 (wt/wt/wt), was selected to perform a centrifugal partition chromatography experiment in a 250 ml centrifugal partition extractor. It was demonstrated that DES-based biphasic systems can be used for the separation of α- and γ-tocopherol. Furthermore, the experimental effort for the solvent system selection could be drastically reduced by the model-based solvent system selection approach.

References

[1] A. Kamal-Eldin, L.-Å. Appelqvist, The chemistry and antioxidant properties of tocopherols and tocotrienols, Lipids 31 (1996) 671–701.

[2] M.G. Traber, J. Atkinson, Vitamin E, antioxidant and nothing more, Free Radic. Biol. Med. 43 (2007) 4–15.
[3] A. Hosomi, M. Arita, Y. Sato, C. Kiyose, T. Ueda, O. Igarashi, H. Arai, K. Inoue, Affinity for α-tocopherol transfer protein as a determinant of the biological activities of vitamin E analogs, FEBS Lett. 409 (1997) 105–108.
[4] S. Peper, M. Johannsen, G. Brunner, Preparative chromatography with supercritical fluids: comparison of simulated moving bed and batch processes, J. Chromatogr. A 1176 (2007) 246–253.
[5] T. Adachi, E. Isobe, Use of synthetic adsorbents in preparative normal-phase liquid chromatography, J. Chromatogr. A 989 (2003) 19–29.
[6] A. Bruns, D. Berg, A. Werner-Busse, Isolation of tocopherol homologues by preparative high-performance liquid chromatography, J. Chromatogr. A 450 (1988) 111–113.
[7] J. Wan, W. Zhang, B. Jiang, Y. Guo, C. Hu, Separation of individual tocopherols from soybean distillate by low pressure column chromatography, J. Am. Oil Chem. Soc. 85 (2008) 331–338.
[8] G. Brunner, T. Malchow, K. Stürken, T. Gottschau, Separation of tocopherols from deodorizer condensates by countercurrent extraction with carbon dioxide, J. Supercrit. Fluids 4 (1991) 72–80.
[9] Y.M. Choo, A.N. Ma, H. Yahaya, Y. Yamauchi, M. Bounoshita, M. Saito, Separation of crude palm oil components by semipreparative supercritical fluid chromatography, J. Am. Oil Chem. Soc. 73 (1996) 523–525.
[10] A. Pyka, J. Sliwiok, Chromatographic separation of tocopherols, J. Chromatogr. A 935 (2001) 71–76.
[11] F. Wei, B. Shen, M. Chen, X. Zhou, Y. Zhao, Separation of α-tocopherol with a two-feed simulated moving bed, Chin. J. Chem. Eng. 20 (2012) 673–678.
[12] M. Saito, Y. Yamauchi, K. Inomata, W. Kottkamp, Enrichment of tocopherols in wheat germ by directly coupled supercritical fluid extraction with semipreparative supercritical fluid chromatography, J. Chromatogr. Sci. 27 (1989) 79–85.
[13] H. Rosenkrantz, A.T. Milhorat, M. Farber, Counter-current distribution in identification of tocopherol compounds in feces, J. Biol. Chem. 192 (1951) 9–15.
[14] S. Hammann, A. Kröpfl, W. Vetter, More than 170 polyunsaturated tocopherol-related compounds in a vitamin E capsule: countercurrent chromatographic enrichment, gas chromatography/mass spectrometry analysis and preliminary identification of the potential artefacts, J. Chromatogr. A 1476 (2016) 77–87.
[15] S. Roehrer, F. Bezold, E.M. Garcia, M. Minceva, Deep eutectic solvents in countercurrent and centrifugal partition chromatography, J. Chromatogr. A 1434 (2016) 102–110.
[16] A.P. Abbott, G. Capper, D.L. Davies, R.K. Rasheed, V. Tambyrajah, Novel solvent properties of choline chloride/urea mixtures, Chem. Commun. (2003) 70–71.
[17] A.P. Abbott, D. Boothby, G. Capper, D.L. Davies, R.K. Rasheed, Deep eutectic solvents formed between choline chloride and carboxylic acids: versatile alternatives to ionic liquids, J. Am. Chem. Soc. 126 (2004) 9142–9147.
[18] B. Tang, H. Zhang, K.H. Row, Application of deep eutectic solvents in the extraction and separation of target compounds from various samples, J. Sep. Sci. 38 (2015) 1053–1064.
[19] Q. Zhang, K. De Oliveira Vigier, S. Royer, F. Jerome, Deep eutectic solvents: syntheses, properties and applications, Chem. Soc. Rev. 41 (2012) 7108–7146.
[20] B. Ru, Konig, Low melting mixtures in organic synthesis – an alternative to ionic liquids? Green Chem. 14 (2012) 2969–2982.
[21] E. Hopmann, W. Arlt, M. Minceva, Solvent system selection in counter-current chromatography using conductor-like screening model for real solvents, J. Chromatogr. A 1218 (2011) 242–250.
[22] E. Hopmann, A. Frey, M. Minceva, A priori selection of the mobile and stationary phase in centrifugal partition chromatography and counter-current chromatography, J. Chromatogr. A 1238 (2012) 68–76.
[23] A. Frey, E. Hopmann, M. Minceva, Selection of biphasic liquid systems in liquid-liquid chromatography using predictive thermodynamic models, Chem. Eng. Technol. 37 (2014) 1663–1674.
[24] F. Bezold, M.E. Weinberger, M. Minceva, Assessing solute partitioning in deep eutectic solvent-based biphasic systems using the predictive thermodynamic model COSMO-RS, Fluid Phase Equilib. 437 (2017) 23–33.
[25] F.S. Oliveira, A.B. Pereiro, L.P.N. Rebelo, I.M. Marrucho, Deep eutectic solvents as extraction media for azeotropic mixtures, Green Chem. 15 (2013) 1326–1330.
[26] A. Klamt, Conductor-like screening model for real solvents: a new approach to the quantitative calculation of solvation phenomena, J. Phys. Chem. 99 (1995) 2224–2235.
[27] F. Eckert, COSMOtherm Reference Manual, COSMOlogic GmbH & Co. KG, Leverkusen, Germany, 2014.
[28] J. Goll, G. Audo, M. Minceva, Comparison of twin-cell centrifugal partition chromatographic columns with different cell volume, J. Chromatogr. A 1406 (2015) 129–135.
[29] Q. Yang, H. Xing, Y. Cao, B. Su, Y. Yang, Q. Ren, Selective separation of tocopherol homologues by liquid- liquid extraction using ionic liquids, Ind. Eng. Chem. Res. 48 (2009) 6417–6422.
[30] M. Francisco, A. van den Bruinhorst, M.C. Kroon, Low-transition-temperature mixtures (LTTMs): a new generation of designer solvents, Angew. Chem. Int. Ed. 52 (2013) 3074–3085.

3.4. Paper IV

Liquid-liquid equilibria of *n*-heptane, methanol and deep eutectic solvents composed of carboxylic acid and monocyclic terpenes

Citation

F. Bezold, M. Minceva, Liquid-liquid equilibria of n-heptane, methanol and deep eutectic solvents composed of carboxylic acid and monocyclic terpenes, Fluid Phase Equilibria, 477 (2018) 98-106.

https://doi.org/10.1016/j.fluid.2018.08.020

Summary

In almost all DES-based biphasic systems that are available in literature, DES-constituents are only present in only one of the phases in considerable concentrations. The DES-constituents remain in one of the liquid phases. Therefore, the ratio between HBA and HBD is constant and stays the same as for the initially prepared DES. Hence, such systems are often treated as pseudo-ternary systems. This manuscript follows the recommendation of **Paper II** to measure quaternary LLE containing DES-constituents in both phases. At first, a hydrophobic DES composed of L-menthol and levulinic acid in a ratio of 1:1 mol:mol (MLA) was selected for the experiments in accordance with Florindo et al. [82]. In order to find suitable organic solvents to form a biphasic system with the DES, a screening of limiting activity coefficients was performed: Limiting activity coefficients are a possibility to estimate the miscibility of two solvents. For their prediction, the method recommended in [81] was applied. The results are shown in Figure 13. The dashed line marks a border between solvents that are miscible with MLA and solvents that build a second liquid phase when mixed with MLA. Values below the dashed line indicate complete miscibility. To form a quaternary biphasic system, methanol was selected as a miscible solvent and *n*-heptane as a solvent that is not completely miscible with MLA. Additionally, the two terpenes thymol or carvacrol that are structurally similar to L-menthol were used to form eutectic mixtures with levulinic acid. They also formed biphasic systems with *n*-heptane and methanol.

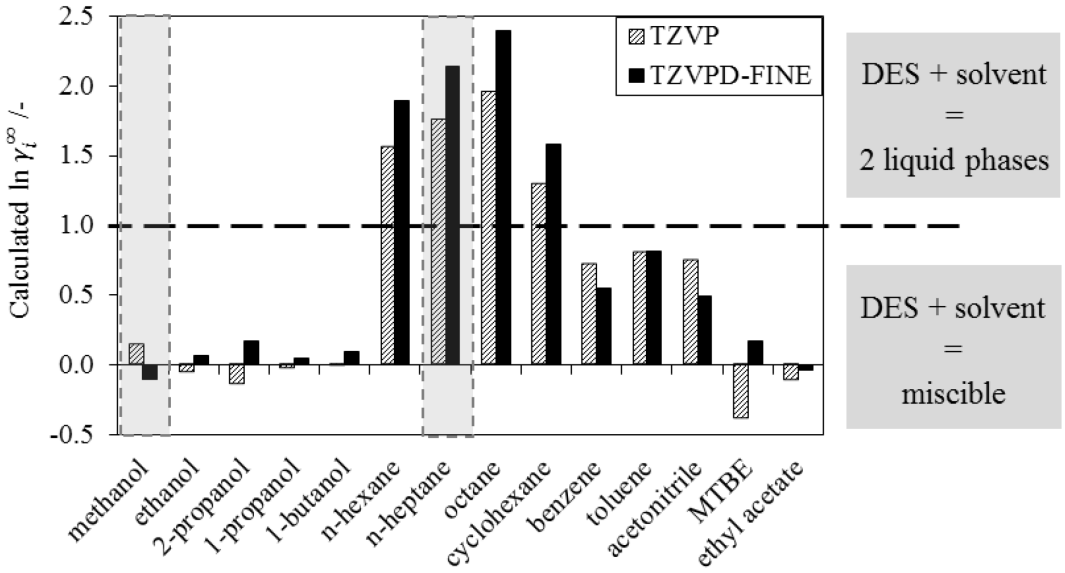

Figure 13: Limiting activity coefficients of organic solvents in L-menthol-levulinic acid (1:1 ml:mol) calculated with COSMO-RS. Solvents with values below the dashed line are miscible with the DES and mixtures with solvents with values above the dashed line show two liquid phases.

Liquid-liquid equilibria were then measured for the three quaternary systems *n*-heptane/methanol/L-menthol/levulinic acid, *n*-heptane/methanol/thymol/levulinic aicd, and *n*-heptane/methanol/carvacrol/levulinic acid. In previous publications, it was assumed that the ratio of DES-constituents is constant and stays the same as in the initially prepared DES in both phases of an LLE. However, for the systems investigated in this work, it was shown that the ratio of DES-constituents in the phases is not the same as for the initially prepared DES, and that the distribution of the DES-constituents changes with the composition of the biphasic system. Unfortunately, COSMO-RS predictions did not give satisfactory results for the quaternary systems. Further effort in model improvement or selection of different thermodynamic models has to be taken to improve a-priori predictions.

Contributions

The author of this dissertation had a leading role in this work. The author selected the solvents that were used for the quaternary biphasic systems. The author performed all laboratory work needed for determination of the LLE-data shown in this work, including design of the experiments, selection of the system compositions, sample preparation, GC calibration and measurements, and analysed the data. The GC-method was developed in collaboration with Petra Kiefer (Lehrstuhl für Thermische Verfahrenstechnik, FAU-Erlangen). Ahmad Alhadid determined the data for the three thermograms that are shown in supplementary information. The author wrote the manuscript and discussed it with Prof. Minceva.

Fluid Phase Equilibria 477 (2018) 98–106

Contents lists available at ScienceDirect

Fluid Phase Equilibria

journal homepage: www.elsevier.com/locate/fluid

Liquid-liquid equilibria of *n*-heptane, methanol and deep eutectic solvents composed of carboxylic acid and monocyclic terpenes

Franziska Bezold, Mirjana Minceva*

Biothermodynamics, TUM School of Life Sciences Weihenstephan, Technical University of Munich, 85354, Freising, Germany

ARTICLE INFO

Article history:
Received 27 June 2018
Received in revised form
30 August 2018
Accepted 31 August 2018
Available online 1 September 2018

Keywords:
Hydrophobic deep eutectic solvents
Quaternary liquid-liquid equilibrium
L-menthol-based eutectic solvent
Monocyclic terpenes

ABSTRACT

Driven by the absence of quaternary LLE data for systems containing deep eutectic solvents (DES), phase equilibrium data has been determined for systems composed of *n*-heptane, methanol, and hydrophobic DES. Three DES were studied; levulinic acid was used as hydrogen bond acceptor (HBA) and L-menthol, thymol and carvacrol were used as hydrogen bond donors (HBDs). It is a commonly used assumption that the ratio of HBA and HBD is the same as the initial DES composition and equal in both phases. However, it was shown that the ratio of HBD and HBA is not constant and changes with initial concentration of the eutectic mixture in the system. Carvacrol- and thymol-based systems show a larger miscibility gap than L-menthol-based systems. This is caused by stronger HBD-HBA interactions of thymol-levulinic acid and carvacrol-levulinic acid which keep a larger fraction of the DES constituents together in the lower phase than in the L-menthol-levulinic acid-based systems. The investigated systems are promising candidates for separation technologies where high solubility of target compounds is desired in both liquid phases, as in centrifugal partition chromatography, for example.

1. Introduction

Deep eutectic solvents (DES) have gained a lot of attention as new designer solvents within the movement towards sustainable production and green solvents. DES are composed of hydrogen bond acceptor (HBA) and hydrogen bond donor (HBD) molecules which show strong eutectic behavior when combined in the right molar ratio. Their properties are similar to ionic liquids, for example, they are non-flammable and have a high solvation capacity for a large number of target compounds. A subclass of DES is natural deep eutectic solvents (NADES) which are composed of natural compounds and are considered to be non-toxic green solvents [1,2]. Furthermore, NADES can be produced from relatively inexpensive chemical species compared to ionic liquids and many compounds able to form NADES can be obtained as food grade bulk chemicals. DES have successfully been used in upstream and downstream processing, as well as analytical methods. They can, for example, be used as reaction media [3], additives in HPLC eluents [4], entrainers in distillation [5], extractant for solid-phase extraction [6–8] or liquid-liquid extraction [9–11], and in biphasic liquid systems for centrifugal partition chromatography [12,13]. Many downstream technologies require liquid-liquid equilibrium (LLE) data for process design. Most of the LLE-data of DES-based biphasic systems available in literature was determined for different applications of liquid-liquid extraction [9,11,14–18]. In liquid-liquid extraction biphasic systems with DES are usually composed of a DES-rich and an alkane-rich phase. It is desirable to retain the DES exclusively in one of the phases and thus ionic HBAs, such as choline chloride [19], betaine [20], or tetrabutylphosphonium bromide [15], are often applied because they are usually poorly soluble in the second, alkane-rich, phase. Such ionic HBAs cannot be analyzed by gas chromatography, a commonly applied method for determining LLE data. In these cases the concentration of the volatile compounds in the mixture are analyzed and the ionic HBA content in the phases is either calculated from mass balance or it is assumed that the HBA and HBD ratio stays the same as in the initial DES and only the HBD is analyzed [11,15,17]. In the examples from literature both methods or assumptions are valid since the DES constituents are only present in one of the phases. Biphasic systems like this with DES constituents solely present in one of the phases can be represented as pseudo ternary phase diagrams and the DES can be treated as a pseudo compound in thermodynamic models [21]. To our knowledge, up to now no LLE data of quaternary water-free biphasic systems containing DES are available in

* Corresponding author.
E-mail address: mirjana.minceva@tum.de (M. Minceva).

https://doi.org/10.1016/j.fluid.2018.08.020
0378-3812/

literature. However, such data is needed to gain deeper understanding of the behavior of DES in complex systems and such biphasic systems are interesting for applications where moderate solute partition coefficients of target compounds between the two phases are beneficial. In centrifugal partition chromatography, for example, target compounds are desired to have partition coefficients between 0.4 and 2.5 to achieve maximum productivity. Hence, the solvent system should provide high solubility of target compounds in both phases. Furthermore, quaternary LLE data is needed to improve modelling and prediction of phase diagrams for DES-based biphasic systems [21]. In order to form true quaternary systems, DES has to be combined with at least two other solvents in which it is partly soluble. This criterion can be fulfilled by DES composed of non-charged constituents, such as so-called hydrophobic DES which are, for example, composed of carboxylic acids and hydrophobic small molecules. Hydrophobic DES were first introduced by Ribeiro et al. [22] and have gained interest for the extraction of compounds with low water solubility [2,23].

In this work, quaternary phase diagrams of hydrophobic eutectic mixtures composed of carboxylic acids and monocyclic terpenes, *n*-heptane and methanol are determined in order to investigate the behavior of the DES constituents in the complex system. Levulinic acid was used as HBA and L-menthol, and the two structural similar terpenes thymol and carvacrol were used as HBDs. HBA and HBD were combined in molar ratios of 1:1, 2:3, and 3:2, then mixed with *n*-heptane and methanol. As all of the DES constituents used in this work can be evaporated, the phase composition was analyzed by gas chromatography (GC) and the distributions of all chemical species in the mixture between the two phases, as well as the ratio of the DES constituents in the each of the liquid phases, were investigated.

2. Material and methods

2.1. Chemicals

Purity and supplier of the chemicals used in this work are listed in Table 1. L-Menthol, thymol and carvacrol from natural source were used for the experiments. All chemicals were used as obtained without further purification.

2.2. DES and biphasic system preparation

For DES preparation the constituents (see Fig. 1) were combined in the appropriate amounts, heated to 45 °C for 20–30 min in a water bath and mixed with a magnetic stirrer. After this procedure a stable liquid solution was obtained under ambient conditions. For each of the HBD and HBA combinations (L-menthol-levulinic acid, thymol-levulinic acid, and carvacrol-levulinic acid) three different compositions of 1:1 mol:mol, 3:2 mol:mol, and 2:3 mol:mol were prepared.

Each biphasic sample composition was prepared in triplicate. Biphasic system compositions were chosen in the following way: The weight fraction of *n*-heptane was kept constant at 50 wt%. Starting from 50 wt% *n*-heptane and 50 wt% methanol the weight fraction of DES was increased stepwise, while the weight fraction of methanol was decreased. For the 1:1 mol:mol composition the DES content was changed in 5 wt% steps and in 10 wt% steps for DES compositions with ratios of 2:3 mol:mol and 3:2 mol:mol. All system compositions used in this work are listed in Table 2. Biphasic samples for LLE determination were prepared by weighing DES, methanol, and *n*-heptane in falcon tubes using a Satorius Entris balance with a repeatability of 0.1 mg. The samples were then mixed for 45 min in an automatic shaker in a temperature controlled environment and allowed to settle for at least 3.5 h. Temperature was measured with a digital thermometer during equilibration and temperature variation during sample preparation and equilibration did never exceed 0.15 K. In order to make sure the biphasic samples were settled, they were centrifuged for 3 min at 3000 rpm in a temperature controlled centrifuge and samples of the phases were taken with syringe needles and diluted with THF for GC-analysis.

2.3. Analysis of phase composition

The phase composition was analyzed using a Nexis GC 2030 with flame ionization detection (FID) from Shimadzu and a Restek Rxi-17Sil MS capillary column (30 m length, 0.25 mm inner diameter, 0.25 μm film thickness) in split mode. Helium was used as carrier gas with a linear velocity controlled flow of 23 cm/s. The inlet temperature was set to 300 °C with a split-ratio of 50 for injection. After an isothermal step at 50 °C for 1.5 min, oven temperature was increased with 30 K/min to 140 °C, followed by another isothermal step with 140 °C held for 9 min. FID temperature was set to 300 °C.

Consistency of the results of the phase composition analysis was checked by evaluating the shortest distance Δw^i (Equation (1)) between each tie line and the initial system composition according to the method proposed by Ref. [24].

$$\Delta w^i = 100 \cdot \left(w^\alpha - w^i\right) - \left(\left(w^\alpha - w^i\right)\frac{w^\beta - w^\alpha}{w^\beta - w^\alpha}\right)\frac{w^\beta - w^\alpha}{w^\beta - w^\alpha} \quad (1)$$

w^i, w^α, and w^β are vectors containing the initial composition and the composition of the phases α and β.

The combined uncertainty $u_{c,i}$ of the measurement was assessed according to the method proposed by Konieczka and Jacek [25] with the following formula

$$u_{c,i} = \sqrt{\left(u_{r,w}\right)^2 + \left(u_{r,cal,i}\right)^2 + \left(u_{r,GC}\right)^2} \quad (2)$$

where $u_{r,w}$ is the relative standard uncertainty of the balance used for sample preparation, $u_{r,cal,i}$ the relative standard uncertainty of the calibration for compound *i*, and $u_{r,GC}$ the relative standard uncertainty of the gas chromatograph. The uncertainty of the balance $u_{r,w}$ was calculated assuming a rectangular distribution and

Table 1
Source, purity, and purity analysis method provided by the supplier for the chemicals used in this work.

Chemical	Source	Purity/wt%	Analysis method
L-menthol	Alfa Aesar	99	gas chromatography
carvacrol	Sigma Aldrich	99	gas chromatography
thymol	VWR International GmbH	>99	gas chromatography
methanol	VWR International GmbH	>99	gas chromatography
n-heptane	VWR International GmbH	>99	gas chromatography
tetrahydrofuran (THF)	Alfa Aesar	99.9; stabilized with 250–350 ppm BHT	gas chromatography

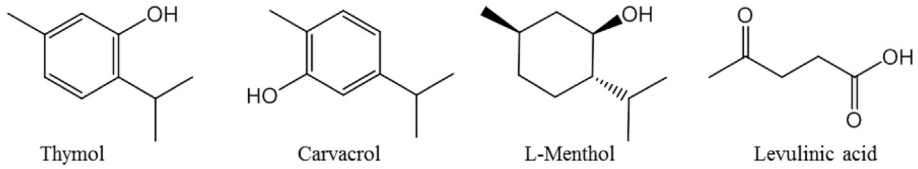

Fig. 1. Molecular structures of DES constituents.

Table 2
Selected system composition for GC-analysis.

System number	Molar ratio HBD:HBA	$w_{n\text{-heptane}}$	$w_{methanol}$	w_{DES}	Number of phases		
					L-Menthol	Thymol	Carvacrol
1	1:1	0.50	0	0.50	2 phases	2 phases	2 phases
2	1:1	0.50	0.05	0.45	2 phases	2 phases	2 phases
3	1:1	0.50	0.10	0.40	2 phases	2 phases	2 phases
4	1:1	0.50	0.15	0.35	2 phases	2 phases	2 phases
5	1:1	0.50	0.20	0.30	2 phases	2 phases	2 phases
6	1:1	0.50	0.25	0.25	2 phases	2 phases	2 phases
7	1:1	0.50	0.30	0.20	2 phases	2 phases	2 phases
8	1:1	0.50	0.35	0.15	2 phases	2 phases	2 phases
9	1:1	0.50	0.40	0.10	2 phases	2 phases	2 phases
10	1:1	0.50	0.45	0.05	2 phases	2 phases	2 phases
11	–	0.50	0.50	0	2 phases	2 phases	2 phases
12	3:2	0.50	0.40	0.10	2 phases[a]	2 phases	2 phases
13	3:2	0.50	0.30	0.20	1 phase	2 phases	2 phases
14	3:2	0.50	0.20	0.30	1 phase	2 phases	2 phases
15	3:2	0.50	0.10	0.40	2 phases	2 phases	2 phases
16	2:3	0.50	0.40	0.10	2 phases	2 phases	2 phases
17	2:3	0.50	0.30	0.20	1 phase	2 phases	2 phases
18	2:3	0.50	0.20	0.30	2 phases	2 phases	2 phases
19	2:3	0.50	0.10	0.40	2 phases	2 phases	2 phases

[a] Volume of lower phase too small for analysis.

repeatability data given by the manufacturer, $u_{r,cal,i}$ was calculated from the calibration curves according to Equation (3) and $u_{r,GC}$ was determined from repeated measurements of aliquots of the same samples. The values of the concentration were far above the limit of detection of the GC-method and it was assumed that the analytes are completely recovered from the column.

$$u_{r,cal,i} = \frac{S_{xy}}{bc_i}\sqrt{1+\frac{1}{n}+\frac{(c_i-c_m)^2}{\sum_j (c_j-c_m)^2}} \quad (3)$$

S_{xy} is the residual standard deviation, n is the number of samples for calibration, c_m is the mean concentration of all samples for calibration, c_i is the calculated concentration, c_j are the concentration levels used in the calibration curve, and b is the coefficient of the calibration curve. All concentrations are in mg/ml.

Molar distribution coefficients of the compounds between the phases α and β were calculated using the following equation:

$$K_i^{x,\beta\alpha} = \frac{x_i^{\beta}}{x_i^{\alpha}} \quad (4)$$

x_i^{β} and x_i^{α} are the mole fractions of compound i in the n-heptane-rich phase β and methanol-rich α. The n-heptane-rich phase was the upper phase in all investigated biphasic systems and the methanol- or DES-rich phase was the lower phase.

The binary system n-heptane/methanol was included in the measurements in order to test the analytical method by comparing the obtained results with literature data. Literature data was calculated from the fitted equation for temperature dependent mutual solubility of n-heptane and methanol given in Ref. [26]. The values from literature are compared with own measurements in Table 3 and are in reasonable agreement with the values determined in this work.

3. Results and discussion

The eutectic mixture of D,L-menthol and levulinic acid with a ratio of 1:1 mol:mol was first reported by Florindo et al. [23]. In this work, however, L-menthol ($T_m = 42.1$ °C [27]) was combined with levulinic acid. Three different molar ratios of the DES constituents were used, namely 1:1, 2:3, and 3:2. The experimentally determined phase compositions of the system composed of n-heptane, methanol, L-menthol, and levulinic acid are listed in Table 4. The tie lines are plotted in Fig. 2a, for clarity only the tie lines with the smallest Δw_i-value (see Table 4) of a triplicate were plotted. As the ratio of L-menthol and levulinic acid is not the same in the coexisting phases, they cannot be combined as in pseudo-ternary systems shown in other work [9,11,14–17] and, thus, the tie lines are plotted in a tetrahedron phase diagram. From the phase diagram it can be seen that the plane built up by the tie lines with an initial molar ratio of L-menthol:levulinic acid of 1:1 has an hourglass-like shape. For systems 12, 13, 14, and 17 only one phase was obtained, or the compositions were too close to the miscible region (see Table 2). Systems 16, 18, and 19 contain an excess of levulinic acid in the initial composition of the eutectic mixture. The tie lines obtained for this initial composition of the eutectic mixture are longer than for the other systems 1–10, indicating a wider miscibility gap. System 15 contains an excess of L-menthol in the initial eutectic mixture and this causes the tie line length to decrease.

The second quaternary system investigated in this work contains thymol instead of L-menthol. Thymol and menthol differ in their ring structure; thymol has three double bonds while menthol has only single bonds (see Fig. 1). The melting point of pure thymol

Table 3
Comparison of literature data and measurements from this work for mutual solubility of *n*-heptane and methanol.

Temperature/K	$x^{\beta}_{Methanol}$ - from literature [26]	$x^{\beta}_{Methanol}$ - measured	$x^{\alpha}_{Methanol}$ - from literature [26]	$x^{\alpha}_{Methanol}$ - measured
293.95 K	0.1447	0.1414 ± 0.0014	0.9034	0.9085 ± 0.0002
295.15 K	0.1509	0.1493 ± 0.0010	0.9007	0.9070 ± 0.0014

Table 4
Liquid-liquid equilibrium phase composition from GC-analysis for (1) *n*-heptane/(2) methanol/(3) L-menthol/(4) levulinic acid at T = 293.95 K and atmospheric pressure (1.01 bar).

Initial system composition				Upper phase composition				Lower phase composition				Δw^i
w_1	w_2	w_3	w_4	w_1	w_2	w_3	w_4	w_1	w_2	w_3	w_4	
0.5000	0.0000	0.2869	0.2131	0.5606	0.0000	0.3163	0.1232	0.0424	0.0000	0.1893	0.7684	1.96
0.5003	0.0000	0.2867	0.2130	0.5589	0.0000	0.3175	0.1236	0.0422	0.0000	0.1890	0.7687	2.10
0.5000	0.0000	0.2869	0.2132	0.5585	0.0000	0.3175	0.1240	0.0421	0.0000	0.1890	0.7689	2.08
0.4995	0.0508	0.2580	0.1917	0.5856	0.0343	0.2740	0.1060	0.0689	0.1159	0.2102	0.6050	1.79
0.5001	0.0503	0.2579	0.1916	0.5906	0.0346	0.2714	0.1034	0.0663	0.1150	0.2145	0.6042	1.74
0.4996	0.0510	0.2578	0.1916	0.5891	0.0341	0.2746	0.1022	0.0703	0.1109	0.2097	0.6092	1.82
0.5000	0.1001	0.2295	0.1705	0.5946	0.0675	0.2444	0.0936	0.1142	0.1882	0.2272	0.4704	2.22
0.5003	0.0999	0.2294	0.1704	0.5951	0.0673	0.2446	0.0929	0.1143	0.1892	0.2273	0.4691	2.23
0.4997	0.1000	0.2296	0.1706	0.5943	0.0674	0.2449	0.0934	0.1132	0.1873	0.2278	0.4717	2.26
0.5001	0.1505	0.2004	0.1489	0.6146	0.0999	0.2063	0.0792	0.1744	0.2579	0.2248	0.3429	1.95
0.4995	0.1506	0.2007	0.1492	0.6136	0.1002	0.2067	0.0796	0.1770	0.2590	0.2245	0.3396	1.90
0.4997	0.1506	0.2006	0.1491	0.6149	0.1004	0.2057	0.0790	0.1750	0.2568	0.2253	0.3429	1.91
0.5002	0.1998	0.1721	0.1279	0.6559	0.1255	0.1618	0.0568	0.2369	0.3231	0.2015	0.2385	0.84
0.5002	0.2005	0.1717	0.1276	0.6557	0.1260	0.1606	0.0578	0.2358	0.3216	0.2006	0.2420	0.78
0.5003	0.1999	0.1720	0.1278	0.6537	0.1213	0.1672	0.0578	0.2315	0.3202	0.2069	0.2414	1.38
0.4994	0.2500	0.1438	0.1068	0.7037	0.1354	0.1215	0.0394	0.2834	0.3704	0.1739	0.1723	0.43
0.4997	0.2502	0.1435	0.1066	0.7026	0.1298	0.1278	0.0398	0.2791	0.3700	0.1770	0.1738	0.99
0.4994	0.2504	0.1435	0.1066	0.7018	0.1298	0.1283	0.0400	0.2800	0.3670	0.1791	0.1739	1.15
0.4992	0.2999	0.1152	0.0856	0.7656	0.1274	0.0856	0.0214	0.3055	0.4307	0.1419	0.1219	0.83
0.5005	0.2996	0.1147	0.0852	0.7670	0.1262	0.0857	0.0211	0.3056	0.4312	0.1409	0.1222	0.80
0.4997	0.3005	0.1146	0.0852	0.7671	0.1224	0.0886	0.0220	0.2995	0.4295	0.1458	0.1252	1.02
0.5004	0.3498	0.0860	0.0639	0.8268	0.1082	0.0548	0.0103	0.3020	0.5000	0.1074	0.0906	1.61
0.5000	0.3503	0.0859	0.0638	0.8302	0.1031	0.0562	0.0104	0.2968	0.5018	0.1113	0.0901	1.76
0.4997	0.3503	0.0861	0.0640	0.8296	0.1035	0.0565	0.0105	0.2976	0.5009	0.1107	0.0907	1.73
0.5003	0.3998	0.0573	0.0426	0.8772	0.0884	0.0304	0.0040	0.2889	0.5813	0.0727	0.0571	2.35
0.4994	0.4000	0.0578	0.0429	0.8773	0.0882	0.0304	0.0040	0.2839	0.5821	0.0768	0.0571	2.35
0.5009	0.3989	0.0575	0.0427	0.8800	0.0839	0.0318	0.0043	0.2852	0.5812	0.0758	0.0578	2.31
0.4996	0.4501	0.0289	0.0214	0.9216	0.0654	0.0128	0.0003	0.2611	0.6721	0.0374	0.0294	1.74
0.4996	0.4499	0.0290	0.0215	0.9230	0.0639	0.0129	0.0003	0.2629	0.6665	0.0392	0.0314	1.74
0.5000	0.4493	0.0291	0.0216	0.9158	0.0702	0.0130	0.0010	0.2665	0.6643	0.0380	0.0312	1.93
0.4994	0.5006	0.0000	0.0000	0.9494	0.0506	0.0000	0.0000	0.2401	0.7599	0.0000	0.0000	0.07
0.5001	0.4999	0.0000	0.0000	0.9506	0.0494	0.0000	0.0000	0.2391	0.7609	0.0000	0.0000	0.14
0.5000	0.3999	0.0669	0.0331	0.8439	0.1123	0.0387	0.0051	0.3458	0.5332	0.0801	0.0409	2.04
0.5006	0.3994	0.0669	0.0331	0.8468	0.1102	0.0387	0.0043	0.3374	0.5409	0.0817	0.0400	2.20
0.5004	0.3997	0.0668	0.0331	0.8480	0.1090	0.0386	0.0045	0.3381	0.5416	0.0814	0.0389	2.21
0.4999	0.1000	0.1892	0.2109	0.6976	0.0472	0.1964	0.0589	0.0793	0.1929	0.1836	0.5443	2.05
0.4994	0.1010	0.1890	0.2106	0.6981	0.0465	0.1976	0.0578	0.0756	0.1969	0.1812	0.5463	2.03
0.4996	0.1006	0.1890	0.2107	0.6980	0.0459	0.1976	0.0585	0.0744	0.1952	0.1806	0.5498	2.05
0.4997	0.3006	0.0945	0.1053	0.8365	0.0836	0.0643	0.0156	0.2197	0.4798	0.1212	0.1793	1.64
0.5005	0.3001	0.0943	0.1051	0.8407	0.0819	0.0635	0.0140	0.2159	0.4850	0.1229	0.1761	1.66
0.5005	0.3004	0.0942	0.1050	0.8406	0.0821	0.0635	0.0138	0.2170	0.4861	0.1223	0.1746	1.67
0.4991	0.4005	0.0475	0.0529	0.9008	0.0717	0.0237	0.0038	0.2487	0.6138	0.0617	0.0758	1.97
0.4995	0.4003	0.0474	0.0528	0.9035	0.0691	0.0237	0.0037	0.2432	0.6190	0.0629	0.0748	1.91
0.4997	0.3996	0.0476	0.0531	0.9029	0.0695	0.0239	0.0037	0.2453	0.6183	0.0622	0.0743	1.97

Mean combined uncertainties are $u(T) = 0.15$ K, $u_c(x_{heptane}) = 0.0100$, $u_c(x_{methanol}) = 0.0109$, $u_c(x_{L\text{-}menthol}) = 0.0038$, $u_c(x_{levulinic\ acid}) = 0.0026$ for the upper phase and $u_c(x_{heptane}) = 0.0844$, $u_c(x_{methanol}) = 0.0866$, $u_c(x_{L\text{-}menthol}) = 0.0364$, $u_c(x_{levulinic\ acid}) = 0.0451$ for the lower phase, the shortest distance between tie line and initial composition Δw^i is listed in wt%.

is reported with 49.6 °C [27]. It is capable of forming a eutectic mixture with levulinic acid and liquid mixtures at room temperature can be obtained with molar ratios of 1:1, 3:2, and 2:3. Fig. 2b shows the quaternary phase diagram of *n*-heptane, methanol, thymol, and levulinic acid, the composition of the phases is listed in Table 5. The miscibility gap is larger than for the system *n*-heptane/methanol/L-menthol/levulinic acid (see Fig. 2) and shifted to *n*-heptane. A larger fraction of thymol is located in the lower phase compared to the menthol-based systems. The tie line length follows a similar trend as the L-menthol-based system and increases for higher initial levulinic acid content (systems 16–19 in Table 2). System 12 has the shortest tie line and system 12 and 13 are close to the one-phase region.

The third eutectic mixture is composed of the terpene carvacrol ($T_m = 2.5$ °C [27]) and levulinic acid. Carvacrol differs from thymol only in the position of the hydroxyl group in the benzene ring (see Fig. 1). The phase diagram is presented in Fig. 2c and the determined phase compositions are presented in Table 6. This system shows the largest miscibility gap for the investigated initial compositions. As in the other two systems the tie line length increases for higher initial levulinic acid content in the eutectic mixture, i.e. systems 16 to 19 in Table 2. System 12 and 13 still show longer tie

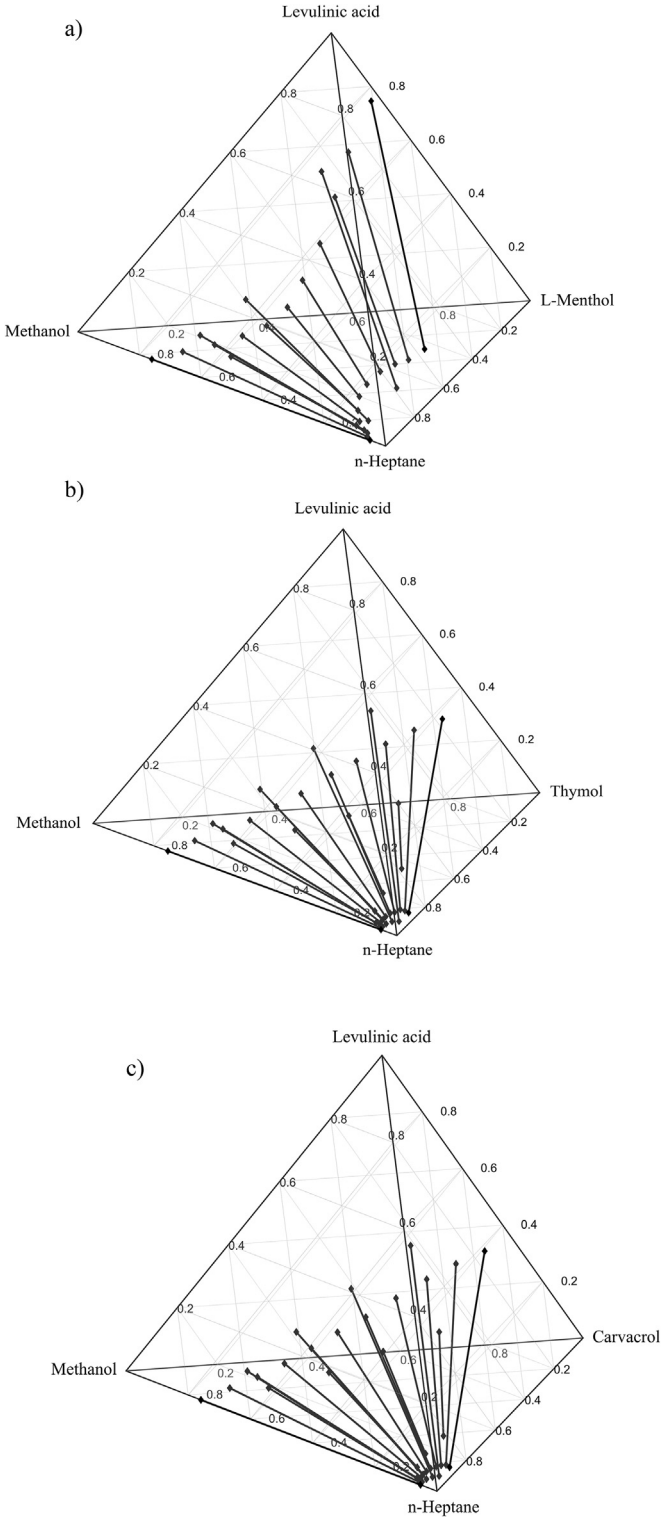

Fig. 2. LLE phase diagram of (a) *n*-heptane, methanol, L-menthol, levulinic acid, (b) *n*-heptane, methanol, thymol, levulinic acid, and (c) *n*-heptane, methanol, carvacrol, levulinic acid.

lines and are farther from the one-phasic region than for *n*-heptane/methanol/thymol/levulinic acid.

For easier visual assessment of the distribution of all components between the two phases the logarithmic distribution coefficients, calculated according to Equation (4), are plotted against the initial methanol mole fraction. The logarithmic distribution coefficients for the system *n*-heptane/methanol/L-menthol/levulinic acid are shown in Fig. 3. Levulinic acid is mainly located in the lower phase, while L-menthol is distributed more equally between the phases with a logarithmic distribution coefficient ranging from −0.28 to 0.47. The distribution coefficient of L-menthol has similar values for all biphasic systems independent of the initial molar ratio of the eutectic mixture. For levulinic acid concentration dependent partitioning is observed. The distribution coefficients are smaller for higher levulinic acid content in the initial eutectic mixture (L-menthol-levulinic acid 2:3, systems 12–15) and vice versa. Besides the distribution constants, the molar ratio of HBD to HBA in the phases was calculated and can be found in Supplementary Information, Table S4. The ratio of the mole fractions of L-menthol to levulinic acid in the upper phase increases from 1.91 for system 1 (*n*-heptane/methanol/L-menthol/levulinic acid 50.0/0/28.7/21.3 wt/wt/wt/wt) to 35.86 in system 10 (*n*-heptane/methanol/L-menthol/levulinic acid 50.0/0.45/0.029/0.021 wt/wt/wt/wt). In the lower phase the ratio of L-menthol:levulinic acid is 0.18 in system 1 and increases to 0.93 in system 10.

The logarithmic distribution coefficients in Fig. 4 show that thymol mainly partitions to the lower phase, however, the upper phase still contains up to 9.5 wt% for the systems with initial eutectic mixture ratio of 1:1, and up to 20.2 wt% for higher initial thymol:levulinic acid ratio (see Table 5). For lower initial methanol content, the logarithmic distribution coefficient of thymol shows a stronger concentration dependency for different initial molar ratios of the eutectic mixture that becomes less pronounced when the methanol content is increased. The same effect is observed for *n*-heptane and methanol, and occurs strongest for levulinic acid.

Fig. 5 shows the logarithmic distribution coefficients of the system composed of *n*-heptane, methanol, carvacrol, and levulinic acid. The components show similar behavior to the thymol-based LLE. All species have a concentration dependent distribution that is more pronounced for high initial concentrations of the carvacrol - levulinic acid mixture. Similar to the thymol-based LLE, levulinic acid also shows the strongest change in its logarithmic distribution coefficients for different HBD:HBA ratios. The molar ratio of HBD to HBA in the phases is listed in Supplementary Information Table S4. In the upper phase of system 1 the carvacrol to levulinic acid ratio is 3.39 and increases to 5.80 in system 10, in the lower phase the ratio stays more or less constant with values in the range of 0.91–1.00 in systems 1–10.

Overall, L-menthol-levulinic acid shows the highest deviation from its initial molar HBD:HBA ratio in the lower phases (see Table S4 in Supplementary Information). Especially for systems with high initial DES content, levulinic acid is present in excess in the lower phase. For thymol-levulinic acid and carvacrol-levulinic acid, the molar ratio of HBD:HBA stays more or less constant for systems with an initial DES composition of 1:1 with values ranging from 0.89 to 1.00. A similarity between thymol-levulinic acid-based and carvacrol-levulinic acid-based systems can also be observed for the lower phases of systems 12 to 19, with initial molar DES constituent ratios of 3:2 and 2:3. Concerning the upper phase, the molar ratio of HBD:HBA is smaller in the L-menthol–based systems than in the thymol- or carvacrol-based systems. Due to the higher solubility of L-menthol in *n*-heptane, generally larger amounts of L-menthol and levulinic acid are present in the upper phase. This can also be seen from the ratio of the volume of upper and lower phase (Table S5) which is quite high (7.83 ± 0.02 for system 1) for L-menthol-based systems compared to thymol- and carvacrol-based systems (1.17 ± 0.01 and 1.27 ± 0.03 for system 1). Considering that the ratio of DES-constituents is not constant in the two phases and is not equal to the ratio with which the DES was prepared, the question is raised whether the HBA and HBD molecules in the

Table 5
Liquid-liquid equilibrium phase composition from GC-analysis for (1) *n*-heptane/(2) methanol/(3) thymol/(4) levulinic acid at T = 295.15 K and atmospheric pressure (1.01 bar).

Initial system composition				Upper phase composition				Lower phase composition				Δw^i
w_1	w_2	w_3	w_4	w_1	w_2	w_3	w_4	w_1	w_2	w_3	w_4	
0.4998	0.0000	0.2821	0.2181	0.8873	0.0000	0.0920	0.0207	0.1703	0.0000	0.4642	0.3655	2.03
0.4997	0.0000	0.2822	0.2181	0.8825	0.0000	0.0954	0.0221	0.1683	0.0000	0.4631	0.3685	1.99
0.5004	0.0000	0.2818	0.2179	0.8847	0.0000	0.0914	0.0239	0.1702	0.0000	0.4584	0.3713	1.67
0.5005	0.0506	0.2532	0.1957	0.8651	0.0116	0.0965	0.0269	0.1724	0.0745	0.4127	0.3404	1.77
0.5006	0.0511	0.2529	0.1954	0.8656	0.0117	0.0963	0.0265	0.1733	0.0749	0.4128	0.3390	1.81
0.4999	0.0502	0.2538	0.1962	0.8708	0.0123	0.0917	0.0253	0.1751	0.0752	0.4090	0.3406	1.55
0.4995	0.1006	0.2256	0.1743	0.8588	0.0260	0.0896	0.0256	0.1871	0.1496	0.3583	0.3050	1.55
0.4995	0.1009	0.2254	0.1742	0.8589	0.0261	0.0896	0.0253	0.1861	0.1514	0.3583	0.3042	1.51
0.5001	0.1007	0.2252	0.1740	0.8593	0.0262	0.0891	0.0254	0.1879	0.1511	0.3573	0.3037	1.48
0.4994	0.1509	0.1972	0.1524	0.8675	0.0364	0.0757	0.0204	0.2007	0.2377	0.3103	0.2512	1.22
0.5009	0.1499	0.1970	0.1523	0.8669	0.0365	0.0763	0.0203	0.1988	0.2359	0.3126	0.2527	1.30
0.4995	0.1502	0.1975	0.1527	0.8658	0.0390	0.0751	0.0200	0.2020	0.2333	0.3087	0.2560	1.08
0.4998	0.1998	0.1695	0.1310	0.8668	0.0497	0.0656	0.0179	0.2184	0.2995	0.2621	0.2200	1.28
0.5001	0.1991	0.1697	0.1311	0.8656	0.0496	0.0667	0.0181	0.2173	0.2994	0.2629	0.2204	1.29
0.4997	0.1998	0.1695	0.1310	0.8666	0.0497	0.0659	0.0178	0.2177	0.2998	0.2618	0.2207	1.27
0.5000	0.2498	0.1411	0.1091	0.8812	0.0565	0.0505	0.0118	0.2342	0.3886	0.2139	0.1633	1.21
0.5003	0.2500	0.1409	0.1089	0.8828	0.0553	0.0500	0.0118	0.2328	0.3902	0.2130	0.1640	1.16
0.5000	0.2503	0.1408	0.1089	0.8788	0.0582	0.0504	0.0126	0.2350	0.3849	0.2114	0.1688	0.90
0.4996	0.3004	0.1128	0.0872	0.8900	0.0622	0.0389	0.0089	0.2467	0.4493	0.1683	0.1356	1.14
0.4998	0.3002	0.1128	0.0872	0.8899	0.0626	0.0388	0.0088	0.2473	0.4516	0.1674	0.1336	1.11
0.5001	0.2997	0.1129	0.0873	0.8899	0.0625	0.0388	0.0088	0.2448	0.4493	0.1691	0.1369	1.16
0.4997	0.3502	0.0847	0.0655	0.9030	0.0652	0.0268	0.0050	0.2559	0.5251	0.1237	0.0953	1.53
0.5001	0.3499	0.0846	0.0654	0.9027	0.0652	0.0269	0.0052	0.2570	0.5257	0.1227	0.0945	1.54
0.4994	0.3505	0.0846	0.0654	0.9029	0.0649	0.0269	0.0052	0.2566	0.5265	0.1225	0.0944	1.54
0.4996	0.4003	0.0565	0.0437	0.9195	0.0626	0.0157	0.0022	0.2506	0.5980	0.0837	0.0676	1.67
0.4999	0.3998	0.0566	0.0437	0.9204	0.0619	0.0155	0.0022	0.2494	0.5998	0.0834	0.0674	1.63
0.4999	0.3998	0.0566	0.0437	0.9188	0.0627	0.0159	0.0026	0.2513	0.6010	0.0809	0.0668	1.65
0.5006	0.4495	0.0282	0.0218	0.9339	0.0586	0.0068	0.0007	0.2520	0.6771	0.0402	0.0308	1.36
0.4990	0.4501	0.0287	0.0222	0.9330	0.0593	0.0070	0.0007	0.2530	0.6753	0.0406	0.0311	1.41
0.4997	0.4501	0.0284	0.0219	0.9333	0.0587	0.0071	0.0009	0.2493	0.6784	0.0401	0.0321	1.32
0.5003	0.4997	0.0000	0.0000	0.9476	0.0524	0.0000	0.0000	0.2465	0.7535	0.0000	0.0000	0.19
0.4999	0.5001	0.0000	0.0000	0.9466	0.0534	0.0000	0.0000	0.2465	0.7535	0.0000	0.0000	0.23
0.4998	0.1000	0.2641	0.1361	0.6574	0.0640	0.2011	0.0776	0.3735	0.1190	0.3328	0.1747	4.85
0.4998	0.1003	0.2639	0.1360	0.6604	0.0639	0.1986	0.0771	0.3724	0.1202	0.3323	0.1751	4.74
0.4997	0.1006	0.2638	0.1359	0.6549	0.0649	0.2016	0.0786	0.3727	0.1196	0.3328	0.1748	4.79
0.5001	0.2000	0.1980	0.1020	0.7483	0.0955	0.1200	0.0363	0.3560	0.2532	0.2579	0.1329	4.12
0.5004	0.1999	0.1978	0.1019	0.7495	0.0953	0.1194	0.0359	0.3547	0.2547	0.2563	0.1344	3.99
0.5001	0.2004	0.1977	0.1018	0.7487	0.0957	0.1198	0.0358	0.3545	0.2544	0.2576	0.1335	4.03
0.5001	0.2996	0.1322	0.0682	0.8304	0.0979	0.0588	0.0128	0.3382	0.4010	0.1723	0.0886	1.06
0.5000	0.3002	0.1318	0.0679	0.8288	0.0966	0.0613	0.0133	0.3379	0.3976	0.1758	0.0887	1.18
0.4995	0.3001	0.1322	0.0682	0.8298	0.0959	0.0613	0.0130	0.3379	0.3983	0.1759	0.0879	1.18
0.5010	0.3993	0.0658	0.0340	0.8978	0.0783	0.0213	0.0026	0.3040	0.5712	0.0864	0.0384	2.21
0.4987	0.4010	0.0661	0.0341	0.8982	0.0784	0.0210	0.0023	0.3061	0.5705	0.0865	0.0369	2.27
0.4999	0.3997	0.0662	0.0342	0.8999	0.0767	0.0209	0.0025	0.2976	0.5748	0.0901	0.0374	2.23
0.4997	0.1013	0.1848	0.2143	0.9192	0.0144	0.0521	0.0143	0.1169	0.1687	0.3214	0.3931	1.18
0.5003	0.1004	0.1849	0.2144	0.9223	0.0143	0.0502	0.0132	0.1174	0.1675	0.3219	0.3931	1.12
0.4999	0.0995	0.1855	0.2151	0.9228	0.0148	0.0491	0.0133	0.1184	0.1605	0.3197	0.4013	1.14
0.4992	0.2007	0.1390	0.1612	0.9178	0.0310	0.0404	0.0108	0.1543	0.3310	0.2314	0.2833	1.10
0.4990	0.2016	0.1386	0.1607	0.9177	0.0309	0.0405	0.0108	0.1516	0.3351	0.2314	0.2819	1.08
0.5000	0.2001	0.1388	0.1610	0.9165	0.0326	0.0397	0.0113	0.1520	0.3310	0.2287	0.2884	0.98
0.5005	0.2996	0.0926	0.1074	0.9224	0.0454	0.0259	0.0064	0.1940	0.4912	0.1438	0.1710	1.20
0.4995	0.3001	0.0928	0.1076	0.9228	0.0452	0.0257	0.0062	0.1939	0.4923	0.1437	0.1702	1.25
0.5000	0.2999	0.0927	0.1075	0.9212	0.0462	0.0258	0.0068	0.1942	0.4871	0.1440	0.1748	1.07
0.5029	0.3955	0.0470	0.0546	0.9320	0.0534	0.0119	0.0027	0.2281	0.6261	0.0686	0.0772	1.47
0.5000	0.4000	0.0463	0.0537	0.9320	0.0530	0.0121	0.0028	0.2287	0.6241	0.0691	0.0780	1.34
0.4997	0.3996	0.0466	0.0541	0.9324	0.0527	0.0121	0.0028	0.2285	0.6239	0.0685	0.0791	1.33

Mean combined uncertainties are $u(T) = 0.1$ K, $u_c(x_{heptane}) = 0.0146$, $u_c(x_{methanol}) = 0.0131$, $u_c(x_{L\text{-menthol}}) = 0.0084$, $u_c(x_{levulinic\ acid}) = 0.0028$ for the upper phase and $u_c(x_{heptane}) = 0.0831$, $u_c(x_{methanol}) = 0.0915$, $u_c(x_{L\text{-menthol}}) = 0.0684$, $u_c(x_{levulinic\ acid}) = 0.0387$ for the lower phase, the shortest distance between tie line and initial composition Δw^i is listed in wt%.

phases can still be referred to as DES. Further studies, such as molecular dynamics simulations, are needed to fully answer this question on a molecular level. However, for biphasic systems with low initial DES content and strong deviation of the ratio of HBD:HBA in the phases from the initially prepared DES it is recommended to refer to DES-constituents or individual species rather than DES.

Both the quaternary phase diagrams and logarithmic distribution coefficients show that the miscibility gap is smaller for L-menthol than for the systems with one of the two other monocyclic terpenes and also that the HBD:HBA ratio changes the most for the systems with L-menthol. In these systems, the H-bonding seems to be disrupted more easily causing a larger fraction of L-menthol to be located in the upper phase than thymol or carvacrol. This indicates that the interaction between L-menthol and levulinic acid is weaker than the interaction between either thymol or carvacrol with levulinic acid. This hypothesis is backed up by comparing the thermograms of 1:1 mol:mol L-menthol-levulinic acid, thymol-

Table 6
Liquid-liquid equilibrium phase composition from GC-analysis for (1) *n*-heptane/(2) methanol/(3) carvacrol/(4) levulinic acid at T = 295.15 K and atmospheric pressure (1.01 bar).

Initial system composition				Upper phase composition				Lower phase composition				Δw^i
w_1	w_2	w_3	w_4	w_1	w_2	w_3	w_4	w_1	w_2	w_3	w_4	
0.5002	0.0000	0.2819	0.2179	0.8846	0.0000	0.0943	0.0210	0.1447	0.0000	0.4722	0.3831	1.67
0.5012	0.0000	0.2814	0.2175	0.8834	0.0000	0.0948	0.0218	0.1455	0.0000	0.4715	0.3830	1.67
0.5003	0.0000	0.2818	0.2179	0.8839	0.0000	0.0943	0.0218	0.1432	0.0000	0.4717	0.3851	1.58
0.4995	0.0508	0.2536	0.1961	0.8690	0.0112	0.0961	0.0236	0.1490	0.0751	0.4238	0.3522	1.80
0.4994	0.0511	0.2536	0.1960	0.8690	0.0117	0.0958	0.0235	0.1495	0.0753	0.4229	0.3523	1.77
0.4997	0.0506	0.2536	0.1961	0.8702	0.0114	0.0951	0.0233	0.1499	0.0755	0.4245	0.3501	1.81
0.4999	0.1002	0.2256	0.1744	0.8668	0.0237	0.0873	0.0222	0.1612	0.1529	0.3729	0.3129	1.76
0.5004	0.1001	0.2253	0.1742	0.8651	0.0235	0.0886	0.0228	0.1631	0.1524	0.3726	0.3119	1.82
0.5000	0.0999	0.2257	0.1744	0.8642	0.0234	0.0894	0.0230	0.1618	0.1513	0.3737	0.3132	1.86
0.4996	0.1506	0.1973	0.1525	0.8681	0.0355	0.0767	0.0197	0.1796	0.2332	0.3204	0.2668	1.62
0.5053	0.1482	0.1954	0.1511	0.8683	0.0354	0.0769	0.0195	0.1797	0.2349	0.3196	0.2657	1.51
0.5000	0.1500	0.1974	0.1526	0.8684	0.0357	0.0765	0.0194	0.1791	0.2319	0.3215	0.2675	1.64
0.4997	0.2007	0.1690	0.1307	0.8713	0.0480	0.0644	0.0163	0.2015	0.3143	0.2646	0.2197	1.11
0.5005	0.1998	0.1690	0.1307	0.8722	0.0477	0.0641	0.0160	0.2012	0.3117	0.2663	0.2209	1.19
0.4994	0.2008	0.1691	0.1307	0.8710	0.0473	0.0643	0.0174	0.1993	0.3126	0.2665	0.2217	1.25
0.4997	0.2502	0.1411	0.1090	0.8823	0.0559	0.0501	0.0117	0.2175	0.3864	0.2114	0.1847	0.96
0.4996	0.2503	0.1411	0.1090	0.8823	0.0553	0.0502	0.0122	0.2182	0.3867	0.2113	0.1837	0.95
0.4999	0.2499	0.1411	0.1091	0.8822	0.0553	0.0502	0.0122	0.2166	0.3860	0.2127	0.1847	1.01
0.4996	0.3005	0.1127	0.0872	0.8923	0.0610	0.0380	0.0086	0.2308	0.4548	0.1700	0.1444	1.30
0.4999	0.3004	0.1126	0.0871	0.8933	0.0605	0.0377	0.0084	0.2310	0.4579	0.1685	0.1427	1.20
0.4998	0.3000	0.1129	0.0873	0.8932	0.0609	0.0374	0.0085	0.2321	0.4574	0.1676	0.1429	1.16
0.5004	0.3501	0.0843	0.0652	0.9053	0.0627	0.0266	0.0054	0.2429	0.5311	0.1229	0.1031	1.46
0.4999	0.3500	0.0847	0.0655	0.9057	0.0625	0.0265	0.0054	0.2434	0.5301	0.1231	0.1035	1.45
0.4993	0.3504	0.0847	0.0655	0.9058	0.0625	0.0263	0.0053	0.2417	0.5266	0.1266	0.1050	1.52
0.5008	0.3991	0.0564	0.0436	0.9192	0.0613	0.0166	0.0029	0.2474	0.6019	0.0833	0.0675	1.63
0.5007	0.3992	0.0565	0.0437	0.9194	0.0615	0.0163	0.0028	0.2478	0.6039	0.0816	0.0668	1.62
0.4993	0.4001	0.0568	0.0439	0.9189	0.0620	0.0162	0.0028	0.2475	0.6023	0.0830	0.0672	1.63
0.5001	0.4498	0.0282	0.0218	0.9324	0.0593	0.0073	0.0009	0.2447	0.6799	0.0408	0.0346	1.26
0.4997	0.4498	0.0284	0.0220	0.9329	0.0586	0.0074	0.0011	0.2449	0.6794	0.0410	0.0347	1.25
0.4997	0.4503	0.0282	0.0218	0.9328	0.0589	0.0074	0.0009	0.2449	0.6789	0.0412	0.0350	1.27
0.4997	0.5003	0.0000	0.0000	0.9468	0.0532	0.0000	0.0000	0.2406	0.7594	0.0000	0.0000	0.03
0.5003	0.4997	0.0000	0.0000	0.9469	0.0531	0.0000	0.0000	0.2408	0.7592	0.0000	0.0000	0.03
0.5006	0.4994	0.0000	0.0000	0.9465	0.0535	0.0000	0.0000	0.2396	0.7604	0.0000	0.0000	0.01
0.4999	0.1003	0.2639	0.1360	0.7245	0.0509	0.1725	0.0521	0.3010	0.1307	0.3686	0.1997	1.88
0.5001	0.1001	0.2639	0.1360	0.7251	0.0502	0.1726	0.0520	0.3017	0.1322	0.3693	0.1968	1.97
0.5003	0.0999	0.2639	0.1360	0.7254	0.0501	0.1725	0.0519	0.3010	0.1317	0.3690	0.1983	1.91
0.4997	0.2003	0.1980	0.1020	0.7881	0.0805	0.1039	0.0275	0.3071	0.2708	0.2693	0.1528	1.72
0.4995	0.2007	0.1978	0.1019	0.7883	0.0809	0.1034	0.0274	0.3109	0.2726	0.2665	0.1501	1.77
0.4999	0.1997	0.1982	0.1021	0.7886	0.0807	0.1034	0.0273	0.3093	0.2718	0.2673	0.1517	1.71
0.4999	0.2999	0.1322	0.0681	0.8473	0.0873	0.0546	0.0109	0.3119	0.4116	0.1801	0.0965	0.48
0.4992	0.3005	0.1322	0.0681	0.8460	0.0876	0.0553	0.0111	0.3119	0.4142	0.1782	0.0957	0.37
0.5000	0.2994	0.1324	0.0682	0.8466	0.0874	0.0550	0.0110	0.3101	0.4114	0.1804	0.0981	0.45
0.4996	0.4002	0.0661	0.0341	0.9040	0.0729	0.0207	0.0023	0.2869	0.5772	0.0917	0.0441	2.01
0.5004	0.3990	0.0664	0.0342	0.9033	0.0734	0.0206	0.0026	0.2864	0.5763	0.0915	0.0458	1.99
0.5002	0.4002	0.0657	0.0339	0.9043	0.0732	0.0201	0.0024	0.2862	0.5795	0.0901	0.0442	2.02
0.5002	0.1003	0.1850	0.2145	0.9224	0.0144	0.0503	0.0129	0.1069	0.1603	0.3244	0.4084	1.35
0.5004	0.0999	0.1851	0.2146	0.9222	0.0142	0.0504	0.0131	0.1076	0.1608	0.3243	0.4074	1.30
0.4995	0.1009	0.1850	0.2145	0.9226	0.0142	0.0500	0.0132	0.1080	0.1646	0.3225	0.4049	1.17
0.5000	0.1995	0.1392	0.1613	0.9172	0.0312	0.0403	0.0113	0.1417	0.3293	0.2335	0.2955	1.21
0.4999	0.1999	0.1391	0.1612	0.9192	0.0312	0.0396	0.0100	0.1439	0.3333	0.2318	0.2909	0.99
0.4993	0.2004	0.1391	0.1612	0.9192	0.0309	0.0394	0.0104	0.1424	0.3309	0.2329	0.2938	1.15
0.5007	0.2996	0.0925	0.1072	0.9230	0.0448	0.0258	0.0063	0.1868	0.4911	0.1449	0.1771	1.02
0.4998	0.3005	0.0925	0.1072	0.9236	0.0447	0.0256	0.0061	0.1876	0.4894	0.1452	0.1778	1.00
0.4993	0.3002	0.0928	0.1076	0.9236	0.0447	0.0254	0.0064	0.1854	0.4894	0.1463	0.1789	0.99
0.4986	0.3987	0.0476	0.0551	0.9322	0.0530	0.0123	0.0025	0.2242	0.6268	0.0687	0.0802	1.35
0.4996	0.3999	0.0465	0.0539	0.9331	0.0525	0.0119	0.0025	0.2234	0.6311	0.0677	0.0778	1.34
0.4994	0.4005	0.0464	0.0537	0.9329	0.0528	0.0118	0.0025	0.2244	0.6287	0.0693	0.0776	1.32

Mean combined uncertainties are $u(T) = 0.1$ K, $u_c(x_{heptane}) = 0.0147$, $u_c(x_{methanol}) = 0.0128$, $u_c(x_{L\text{-}menthol}) = 0.0088$, $u_c(x_{levulinic\ acid}) = 0.0028$ for the upper phase and $u_c(x_{heptane}) = 0.0832$, $u_c(x_{methanol}) = 0.0911$, $u_c(x_{L\text{-}menthol}) = 0.0717$, $u_c(x_{levulinic\ acid}) = 0.0391$ for the lower phase, the shortest distance between tie line and initial composition Δw^i is listed in wt%.

levulinic acid, and carvacrol-levulinic acid (see Fig. S1 in Supplementary Information). For thymol-levulinic acid and carvacrol-levulinic acid drastically lower melting temperatures are obtained than for L-menthol-levulinic acid. The more severe depression of the melting point shows that there are strong intermolecular interactions stabilizing the liquid phase. For L-menthol two peaks can be seen in the thermogram, the first corresponding to the eutectic and the second one to the liquidus melting temperature. The higher melting temperature indicates that interactions are weaker.

4. Conclusion

LLE data is presented for three quaternary systems containing eutectic mixtures. The DES used in this work are composed of a hydrophobic HBD, namely L-menthol, thymol, or carvacrol, and

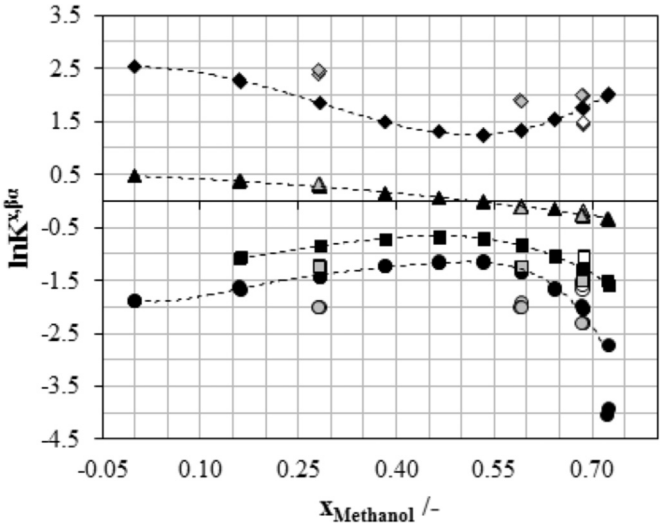

Fig. 3. Logarithmic distribution coefficient of *n*-heptane (◆), methanol (■), L-menthol (▲), and levulinic acid (●); molar ratio of L-menthol:levulinic acid 1:1 (black), 3:2 (white), and 2:3 (grey), $x_{Methanol}$ is the initial mole fraction of methanol in the system.

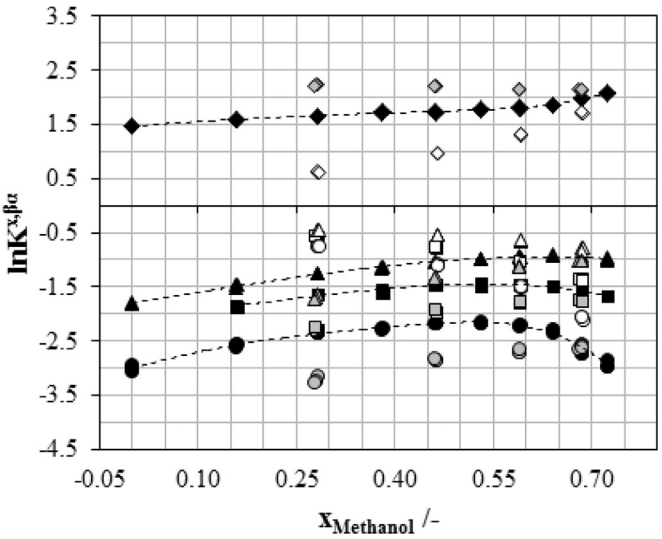

Fig. 4. Logarithmic distribution coefficient of *n*-heptane (◆), methanol (■), thymol (▲), and levulinic acid (●); molar ratio of thymol:levulinic acid 1:1 (black), 3:2 (white), and 2:3 (grey), $x_{Methanol}$ is the initial mole fraction of methanol in the system.

levulinic acid as HBA. Biphasic systems with different initial molar ratios of HBD to HBA (1:1, 2:3, and 3:2) were investigated. DES constituents are present in both phases of the investigated systems. It is shown that the ratio of HBD to HBA changes with the initial concentration of the eutectic mixtures in the systems. Their ratio cannot be assumed constant in the two phases and is not equal to the ratio with which the DES was prepared. The biphasic region increases respectively from the systems containing L-menthol, to thymol, and to carvacrol for the investigated initial compositions. This indicates that the interactions between L-menthol and levulinic acid are weaker than the interactions between thymol or carvacrol and levulinic acid. The biphasic systems are high potential candidates for downstream technologies, such as for the separation of hydrophobic compounds with centrifugal partition chromatography, where it would be favorable to have DES in both phases. DES constituents in both phases could act as solubilizing agents for

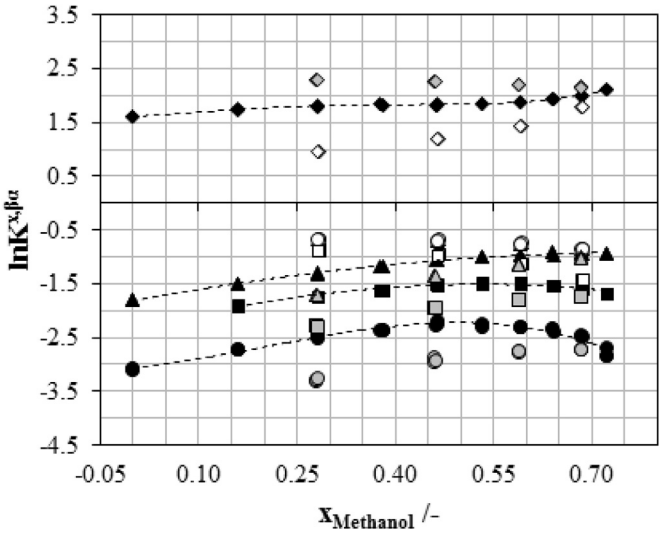

Fig. 5. Logarithmic distribution coefficient of *n*-heptane (◆), methanol (■), carvacrol (▲), and levulinic acid (●); molar ratio of carvacrol:levulinic acid 1:1 with black, 3:2 with white, and 2:3 with grey symbols, $x_{Methanol}$ is the initial mole fraction of methanol in the system.

target compounds and increase their solubility in both phases, and thus the overall productivity of a separation process.

Acknowledgement

We thank Prof. Wolfgang Arlt, Mrs. Petra Kiefer, and Dr. Liudmila Mokrushina (Lehrstuhl for Thermische Verfahrenstechnik, Friedrich-Alexander Universität Erlangen Nürnberg) for their support with the development of the analytical method and scientific discussion of the results. We thank Martin Hübner for his help in preliminary measurements and discussion of the results and Ahmad Alhadid for conducting the dynamic scanning calorimetry measurement.

Appendix A. Supplementary data

Supplementary data related to this article can be found at https://doi.org/10.1016/j.fluid.2018.08.020.

References

[1] Y. Dai, J. van Spronsen, G.-J. Witkamp, R. Verpoorte, Y.H. Choi, Natural deep eutectic solvents as new potential media for green technology, Anal. Chim. Acta 766 (2013) 61–68.
[2] C. Florindo, L. Romero, I. Rintoul, L.C. Branco, I.M. Marrucho, From phase change materials to green solvents: hydrophobic low viscous fatty acid–based deep eutectic solvents, ACS Sustain. Chem. Eng. 6 (2018) 3888–3895.
[3] D.A. Alonso, A. Baeza, R. Chinchilla, G. Guillena, I.M. Pastor, D.J. Ramón, Deep eutectic solvents: the organic reaction medium of the century, Eur. J. Org Chem. 2016 (2016) 612–632.
[4] T. Tan, M. Zhang, Y. Wan, H. Qiu, Utilization of deep eutectic solvents as novel mobile phase additives for improving the separation of bioactive quaternary alkaloids, Talanta 149 (2016) 85–90.
[5] Y. Peng, X. Lu, B. Liu, J. Zhu, Separation of azeotropic mixtures (ethanol and water) enhanced by deep eutectic solvents, Fluid Phase Equil. 448 (2017) 128–134.
[6] A.K. Das, M. Sharma, D. Mondal, K. Prasad, Deep eutectic solvents as efficient solvent system for the extraction of κ-carrageenan from Kappaphycus alvarezii, Carbohydr. Polym. 136 (2016) 930–935.
[7] H. Lores, V. Romero, I. Costas, C. Bendicho, I. Lavilla, Natural deep eutectic solvents in combination with ultrasonic energy as a green approach for solubilisation of proteins: application to gluten determination by immunoassay, Talanta 162 (2017) 453–459.
[8] Y. Dai, G.-J. Witkamp, R. Verpoorte, Y.H. Choi, Natural deep eutectic solvents as a new extraction media for phenolic metabolites in Carthamus tinctorius L, Anal. Chem. 85 (2013) 6272–6278.

[9] M.A. Kareem, F.S. Mjalli, M.A. Hashim, I.M. AlNashef, Liquid–liquid equilibria for the ternary system (phosphonium based deep eutectic solvent–benzene–hexane) at different temperatures: a new solvent introduced, Fluid Phase Equil. 314 (2012) 52–59.
[10] F.S. Oliveira, A.B. Pereiro, L.P.N. Rebelo, I.M. Marrucho, Deep eutectic solvents as extraction media for azeotropic mixtures, Green Chem. 15 (2013) 1326–1330.
[11] A.S.B. Gonzalez, M. Francisco, G. Jimeno, S.L.G. de Dios, M.C. Kroon, Liquid–liquid equilibrium data for the systems {LTTM + benzene + hexane} and {LTTM + ethyl acetate + hexane} at different temperatures and atmospheric pressure, Fluid Phase Equil. 360 (2013) 54–62.
[12] S. Roehrer, F. Bezold, E.M. Garcia, M. Minceva, Deep eutectic solvents in countercurrent and centrifugal partition chromatography, J. Chromatogr., A 1434 (2016) 102–110.
[13] F. Bezold, M.E. Weinberger, M. Minceva, Computational solvent system screening for the separation of tocopherols with centrifugal partition chromatography using deep eutectic solvent-based biphasic systems, J. Chromatogr. A 1491 (2017) 153–158.
[14] N.R. Rodriguez, T. Gerlach, D. Scheepers, M.C. Kroon, I. Smirnova, Experimental determination of the LLE data of systems consisting of {hexane + benzene + deep eutectic solvent} and prediction using the conductor-like screening model for real solvents, J. Chem. Therm. 104 (2017) 128–137.
[15] M.A. Kareem, F.S. Mjalli, M.A. Hashim, M.K.O. Hadj-Kali, F.S.G. Bagh, I.M. Alnashef, Phase equilibria of toluene/heptane with tetrabutylphosphonium bromide based deep eutectic solvents for the potential use in the separation of aromatics from naphtha, Fluid Phase Equil. 333 (2012) 47–54.
[16] M.A. Kareem, F.S. Mjalli, M.A. Hashim, M.K.O. Hadj-Kali, F.S. Ghareh Bagh, I.M. Alnashef, Phase equilibria of toluene/heptane with deep eutectic solvents based on ethyltriphenylphosphonium iodide for the potential use in the separation of aromatics from naphtha, J. Chem. Therm. 65 (2013) 138–149.
[17] N.R. Rodriguez, B.S. Molina, M.C. Kroon, Aliphatic + ethanol separation via liquid–liquid extraction using low transition temperature mixtures as extracting agents, Fluid Phase Equil. 394 (2015) 71–82.
[18] N.R. Rodriguez, J. Ferre Guell, M.C. Kroon, Glycerol-based deep eutectic solvents as extractants for the separation of MEK and ethanol via liquid–liquid extraction, J. Chem. Eng. Data 61 (2016) 865–872.
[19] M. Hayyan, T. Aissaoui, M.A. Hashim, M.A. AlSaadi, A. Hayyan, Triethylene glycol based deep eutectic solvents and their physical properties, Journal of the Taiwan Institute of Chemical Engineers 50 (2015) 24–30.
[20] N. Li, Y. Wang, K. Xu, Y. Huang, Q. Wen, X. Ding, Development of green betaine-based deep eutectic solvent aqueous two-phase system for the extraction of protein, Talanta 152 (2016) 23–32.
[21] F. Bezold, M.E. Weinberger, M. Minceva, Assessing solute partitioning in deep eutectic solvent-based biphasic systems using the predictive thermodynamic model COSMO-RS, Fluid Phase Equil. 437 (2017) 23–33.
[22] B.D. Ribeiro, C. Florindo, L.C. Iff, M.A.Z. Coelho, I.M. Marrucho, Menthol-based eutectic mixtures: hydrophobic low viscosity solvents, ACS Sustain. Chem. Eng. 3 (2015) 2469–2477.
[23] C. Florindo, L.C. Branco, I.M. Marrucho, Development of hydrophobic deep eutectic solvents for extraction of pesticides from aqueous environments, Fluid Phase Equil. 448 (2017) 135–142.
[24] T. Gerlach, I. Smirnova, Liquid–liquid equilibria of quaternary systems composed of 1,3-propanediol, short-chain alcohol, water, and salt, J. Chem. Eng. Data 61 (2016) 3548–3558.
[25] P. Konieczka, J. Namieśnik, Estimating uncertainty in analytical procedures based on chromatographic techniques, J. Chromatogr. A 1217 (2010) 882–891.
[26] D.G. Shaw, A. Skrzecz, J.W. Lorimer, A. Maczynski, Solubility data series - alcohols and hydrocarbons, International Union of Pure and Applied Chemistry 56 (1994) 154–176.
[27] W.M. Haynes, CRC Handbook of Chemistry and Physics, 93rd Edition, CRC Press, Boca Raton, 2014.

3.5. Paper V

A water-free solvent system containing an L-menthol-based deep eutectic solvent for centrifugal partition chromatography applications

Citation

F. Bezold, M. Minceva, A water-free solvent system containing an L-menthol-based deep eutectic solvent for centrifugal partition chromatography applications, Journal of Chromatography A, 1587 (2018) 166-171.

https://doi.org/10.1016/j.chroma.2018.11.083

Summary

Eventually, one of the quaternary biphasic systems proposed in **Paper IV** was evaluated for its use in CPC separations. This publication describes the first application of a quaternary biphasic solvent system with DES-constituents in both phases as stationary and mobile phases for CPC. Model compounds with different octanol/water partition coefficients were selected for the study to cover a wide range of substances from very hydrophilic to very hydrophobic molecules. First, shake flask experiments were conducted to determine the partition coefficients of the model compounds in the biphasic system composed of *n*-heptane/methanol/L-menthol/levulinic acid. Considering the set of experimental data of the model compounds used in this work, it was found that the biphasic system was suitable for the separation of substances with logarithmic octanol/water partition coefficients in the range of 2.1 to 12. The partition coefficients of these compounds were found to be within the *sweet spot* range. In other DES-based biphasic systems that were previously used in CPC the partition coefficients of the same solutes were higher [25]. High stationary phase retention was obtained in a CPC column and pulse injections showed that the selected model compounds could be separated. Additionally, the stability of different system compositions in presence of water was tested. L-menthol is poorly soluble in water and when water is added to the mixture of L-menthol and levulinic acid, L-menthol precipitated. It was found that contact with water should be avoided for systems with high content of L-menthol and levulinic acid while water is not critical for systems with low initial content of the DES-constituents.

Contributions

The author of this dissertation had a leading role in this work. The author did the conceptual design of the work and conducted the experiments. The author selected the system compositions, model substances, and parameters for the CPC separations. The author wrote the manuscript and discussed it with Prof. Minceva.

Journal of Chromatography A, 1587 (2019) 166–171

Contents lists available at ScienceDirect

Journal of Chromatography A

journal homepage: www.elsevier.com/locate/chroma

A water-free solvent system containing an L-menthol-based deep eutectic solvent for centrifugal partition chromatography applications

F. Bezold, M. Minceva*

Biothermodynamics, TUM School of Life Sciences Weihenstephan, Technical University of Munich, 85354 Freising, Germany

ARTICLE INFO

Article history:
Received 25 September 2018
Received in revised form
15 November 2018
Accepted 20 November 2018
Available online 11 December 2018

Keywords:
Non-aqueous solvent systems
Deep eutectic solvents
Liquid-liquid chromatography
Centrifugal partition chromatography
Countercurrent-chromatography

ABSTRACT

Centrifugal partition chromatography (CPC) is a well-established technology for natural compound separation. However, the separation of hydrophobic compounds is still challenging since the number of non-aqueous biphasic systems that can be used in CPC is limited. In this work, we evaluate quaternary solvent systems composed of *n*-heptane, methanol, and a eutectic solvent composed of L-menthol and levulinic acid, containing DES-constituents in both phases. It was evaluated whether the phases of the systems can be used as stationary and mobile phases for CPC separations. For this purpose, solutes that cover a broad range of octanol-water partition coefficients, i.e. hydrophobic to hydrophilic compounds, were used and shake flask experiments were performed to determine solute partition coefficients. The partition coefficients indicated that the more hydrophobic compounds were in the favored range for CPC and, thus, the systems are high potential candidates for the separation of hydrophobic compounds. In this particular solute set, the biphasic systems were most suitable for compounds with octanol-water partition coefficients between 2.1 and 12.0. It was shown that the biphasic systems with low initial DES-content are stable in presence of water, while L-menthol precipitates from the biphasic systems with high initial DES content when water is added. High stationary phase retention of up to 79.1% could be obtained and the selected model compounds were separated with high resolution in pulse injections, which confirmed the high potential of the biphasic solvent systems for CPC.

1. Introduction

Centrifugal partition chromatography (CPC) is a solid-support-free chromatographic technique that uses the two liquid phases of a biphasic solvent system as stationary and mobile phases [1]. One of the liquid phases is kept stationary inside the column due to a special column geometry and the application of a centrifugal field. The technology offers several advantages, such as high loading capacity, no irreversible adsorption, and tailored stationary and mobile phases that can be produced by the users themselves. Mixtures of target compounds are separated according to their partition coefficients between the stationary and mobile phases. The main requirements for the biphasic solvent system are the formation of two stable phases that do not form an emulsion in the column upon mixing and the partition coefficients of the target compounds in the biphasic solvent system should be in the so-called *sweet spot* [2]. Partition coefficients between 0.4 and 2.5 (-0.4 < log P_i < 0.4) are considered the range of the *sweet spot* which is usually one of the most important selection criteria for biphasic solvent systems. The fact that the user prepares a tailored solvent system is one of the features that make the technology so versatile, however, it also leaves the user with a nearly limitless number of possible solvent combinations and system compositions. The most often used are biphasic solvent systems from the HEMWat and Arizona system families [3]. These solvent systems composed of *n*-hexane or *n*-heptane, ethyl acetate, methanol and water can be used for a wide polarity range of target compounds. However, separations of mixtures of very hydrophilic or very hydrophobic compounds are most of the time not achieved with these solvent system families. Aqueous two-phase systems are applied for the separation of very hydrophilic compounds or molecules that are sensitive to organic solvents, such as proteins [4–7]. For the separation of hydrophobic compounds, such as certain carotenoids or fatty acids, non-aqueous biphasic systems are needed [8]. Unfortunately, the number of non-aqueous biphasic systems suitable for CPC in literature is quite limited [9]. In previous work, we have shown that non-aqueous biphasic systems containing deep eutectic solvents (DES) can be used for the separation of hydrophobic target compounds with CPC [10,11]. DES are composed of hydrogen bond donor (HBD) and acceptor (HBA) molecules that show

* Corresponding author.
E-mail address: Mirjana.minceva@tum.de (M. Minceva).

https://doi.org/10.1016/j.chroma.2018.11.083
0021-9673/

a strong melting point depression compared to the pure HBA and HBD when combined in a certain molar ratio. DES can be made from natural compounds (NADES) that are considered non-toxic and environmentally friendly and are non-flammable [12], have low vapor pressure, show high solvation capacity and overcome many of the drawbacks of ionic liquids [13], for example, they are low priced and easier to prepare.

In recent years, a drastic increase in research on applications of DES in liquid-liquid extraction could be observed and DES have been proposed, for example, for the separation of aromatics from aliphatics [14–18], glycerol from biodiesel [19–21], or extraction of phenolic compounds [22–24]. Most literature data on liquid-liquid equilibria of solvent systems containing DES originates from publications on liquid-liquid extraction. In liquid-liquid extraction it is desirable to keep the DES constituents exclusively in one of the phases. In CPC, however, it is not a prerequisite to have the DES-constituents only in one of the phases. Such biphasic systems with DES-constituents present in both phases have not yet been used in CPC and may be beneficial in order to achieve solute partition coefficients within the *sweet spot* range. However, at this point it is not known if reasonable stationary phase retention and partition coefficients can be obtained.

In this work, a new class of solvent systems with a DES that is composed of levulinic acid and poorly water-soluble L-menthol is evaluated. Potential application of the biphasic solvent systems as stationary and mobile phases in CPC is evaluated by partition coefficients that were determined in shake flask experiments. For this purpose eleven model compounds ranging from hydrophilic to hydrophobic were used. Stationary phase retention and stability in presence of water are investigated and, eventually, separations of model compounds with CPC are performed. The aim of this work is to apply this new class of DES-based biphasic systems that contain DES-constituents in both phases in CPC and to extend the pool of water-free biphasic solvent systems with DES for CPC users.

2. Material and methods

2.1. Chemicals

L-Menthol from natural source with 99% purity and levulinic acid with a purity of 99% were both obtained from Sigma Aldrich. Methanol and *n*-heptane (both liquid-chromatography grade) were purchased from VWR International GmbH. Caffeine, vanillin, coumarin, carvone, β-ionone, and β-carotene were selected as solutes from the GUESS mix reference standard [25] and cinnamaldehyde, retinol, and α-tocopherol were additionally selected for shake flask experiments. Octanol/water partition coefficients, purity and supplier of the solutes are listed in Table 1.

2.2. Preparation of DES and biphasic solvent systems

The DES used in this work was prepared by mixing L-menthol and levulinic acid in a molar ratio of 1:1. The mixture was heated to 45 °C in a water bath and agitated with a magnetic stirrer for about 20 min. After heating, the liquid DES was allowed to cool down to ambient temperature before further use. The obtained DES had a similar density to water (0.985 g cm^{-3}) and a viscosity of 30.1 mPas at 25 °C.

Biphasic solvent systems were prepared by weighing the appropriate amount of DES, methanol and *n*-heptane. The solvent mixture was stirred in a closed vessel for at least 2 h to equilibrate the phases. Afterwards the phases were separated using a separatory funnel. Even though a liquid DES was added to prepare the biphasic system, and not the separate DES-constituents, the quaternary notation is chosen to stress that the DES-constituents are distributed individually between the phases and the ratio between HBA and HBD changes for different system compositions. The composition of the biphasic solvent systems that were used in this work, details on the ratio of DES constituents in the phases and phase volume ratios can be found in [26]. The melting temperature of the mixture was 0.2 °C [26].

Table 1
List of solutes with octanol/water-partition coefficients log $P^{o/w}$, purity and producer.

Solute	log $P^{o/w}$ [a] /-	Purity /%	Supplier
Arbutin	−0.508	≥98	Alfa Aesar
Caffeine	−0.040	≥99	Sigma-Aldrich
Vanillin	1.284	99	Alfa Aesar
Coumarin	1.412	≥99	Sigma-Aldrich
Cinnamaldehyde	1.9[b]	≥98	Alfa Aesar
Carvone	2.103	≥98.5	Fluka
Naringenin	2.445	≥95	Sigma-Aldrich
β-Ionone	3.770	96	Sigma-Aldrich
Retinol	5.680[b]	≥95	Acros Organics
α-Tocopherol	12.000[c]	≥97	Alfa Aesar
β-Carotene	17.600[c]	≥97	Sigma-Aldrich

[a] [25] except cinnamaldehyde, retinol and α-tocopherol.
[b] Sigma-Aldrich material safety data sheet.
[c] PubChem database, physical properties of α-tocopherol (consulted 2018-07-05) http://pubchem.ncbi.nlm.nih.gov/rest/chemical/alpha-tocopherol.

2.3. Shake flask experiments

To prepare the samples for shake flask experiments 1–5 mmol l^{-1} of the solute were mixed with 5 ml upper phase and 5 ml lower phase of the biphasic system. The samples were put in an automatic shaker at 21.5 ± 0.5 °C and equilibrated for at least 2 h. After equilibration aliquots of the upper and lower phases were taken using a syringe needle and the concentration of the solutes in each of the phases was determined with UV–vis-spectroscopy. If dilution was necessary, the upper phase samples were diluted with *n*-heptane and the lower phase samples were diluted with methanol. All shake flask experiments were performed in triplicate.

The partition coefficient P of a solute i was calculated according to the following equation:

$$P_i^{\alpha\beta} = \frac{c_i^{\alpha}}{c_i^{\beta}} \quad (1)$$

β and α are the two phases of the biphasic solvent system, and c is the concentration of the solute i in the respective phase. All partition coefficients in the shake flask experiments (Section 3.1) were determined for descending mode, i.e. α is the upper phase and β the lower phase.

2.4. Centrifugal partition chromatography

Pulse injections were performed using a CPC 250 PRO SPECIAL BIO VERSION centrifugal partition chromatography unit from Gilson, USA. The column has a total volume of 250 ml and is composed of 11 Teflon-coated stainless steel disks with 20 twin-cells per disk. The column can be used with a pressure up to 100 bar and a maximum rotation of 3000 rpm. The separations in this work were performed at 21.5 ± 1.0 °C with a rotational speed of 2000 rpm. The injection volume was 5 ml for all experiments. For the feed solution, the solutes were weighed and dissolved in the mobile phase.

The stationary phase retention S_f was determined with

$$S_f = \frac{V_{SP}}{V_c} \quad (2)$$

where V_{SP} is the volume of stationary phase that can be retained in the column at a given rotation and mobile phase flow rate, and V_c

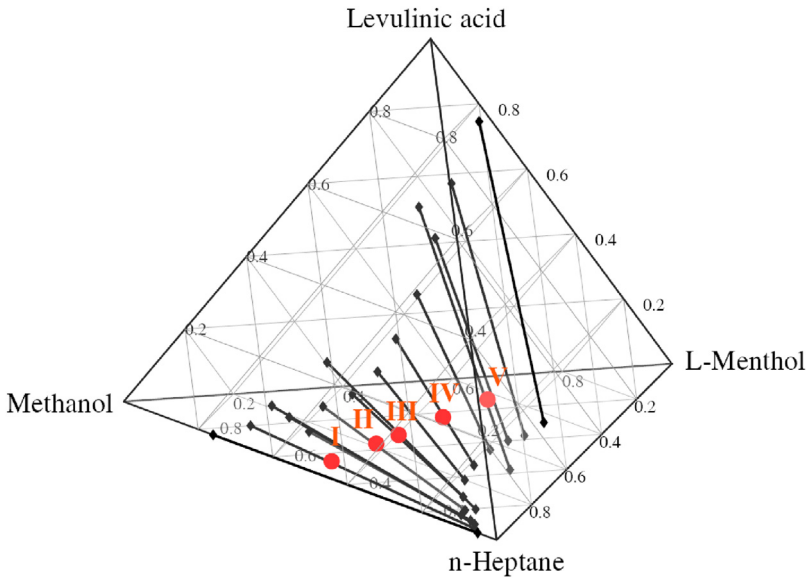

Fig. 1. Liquid-liquid phase diagram of *n*-heptan/methanol/L-menthol/levulinic acid [26] with the system composition used in this work marked with circles: I) 50.0/45.0/2.9/2.1 wt/wt/wt/wt (5 wt% DES), II) 50.0/35.0/8.6/6.4 wt/wt/wt/wt (15 wt% DES), III) 50.0/30.0/11.5/8.5 wt/wt/wt/wt (20 wt% DES), IV) 50.0/20.0/17.2/12.8 wt/wt/wt/wt (30 wt% DES), and V) 50.0/10.0/22.9/17.1 wt/wt/wt/wt (40 wt% DES).

is the total column volume. In ascending mode the upper phase of the biphasic solvent system is used as mobile phase and the lower phase is used as stationary phase, in descending mode the roles of the phases are switched, respectively. In order to determine the stationary phase retention, the column is first completely filled with stationary phase. Then, the rotation is turned on and the mobile phase is pumped through the column at the desired flow rate. The mobile phase replaces part of the volume of stationary phase inside the column up to a certain point when hydrodynamic equilibrium is reached. The eluted volume of stationary phase is measured and the volume of peripheral parts, i.e. volume of tubing before and after the column, is subtracted. At the end of the procedure, the remaining stationary phase is eluted from the column and the volume is determined.

Solute partition coefficients were calculated from the chromatograms using Eq. 3.

$$P_i = \frac{V_{R,i} - V_{MP}}{V_{SP}} \tag{3}$$

$V_{R,i}$ is the retention volume of compound i and V_{MP} is the volume inside the column taken up by the mobile phase. The retention volume is calculated by multiplying the retention time of a compound that has been determined from the chromatogram with the mobile phase flow rate.

The separation factor between two species i and j is calculated as the ratio between the partition coefficients of the two compounds (Eq. 4).

$$\alpha_{j,i} = \frac{P_j}{P_i} \tag{4}$$

The resolution of two peaks can be determined according to Eq. 5. The standard deviations σ and the retention times t_R of the compounds i and j are determined from the chromatogram.

$$R_{S,i-j} = \frac{t_{R,j} - t_{R,i}}{2\left(\sigma_j - \sigma_i\right)} \tag{5}$$

3. Results

3.1. Partition coefficients from shake flask experiments

In order to characterize the biphasic solvent system containing *n*-heptane, methanol, and the DES composed of L-menthol and levulinic acid, partition coefficients of ten different solutes were determined. The solutes were chosen by their octanol/water-partition coefficient in such way that a wide range of hydrophilic to hydrophobic compounds is covered (see Table 1). Five different system compositions within the biphasic region were selected for the shake flask experiments and their location in the phase diagram is shown in Fig. 1.

Fig. 2a shows the logarithmic partition coefficients of the model solutes for one fixed composition of the biphasic solvent system (*n*-heptane/methanol/L-menthol/levulinic acid 50.0/35.0/8.6/6.4 wt/wt/wt/wt with 15 wt% of DES-constituents in total). In this system, carvone, β-ionone, retinol, and α-tocopherol have partition coefficients in the *sweet spot*. The partition coefficients decrease with hydrophilicity of the compounds from carvone to arbutin. The low partition coefficient of naringenin is in agreement with previous results for other DES-based biphasic systems [10]. Compared to biphasic systems with DES present in only one of the phases, such as *n*-heptane/ethanol/choline chloride-levulinic acid [10], the partition coefficients of the model solutes are generally closer to the *sweet spot* for the system tested in this work with DES-constituents present in both phases.

In Fig. 2b the change of the partition coefficient of β-ionone is shown for the selected compositions of the biphasic solvent system composed of *n*-heptane, methanol, L-menthol, and levulinic acid. The partition coefficient of β-ionone increases from the system with 5 wt% to 20 wt% of L-menthol-levulinic acid. For higher L-menthol-levulinic acid content the partition coefficient of β-ionone slightly decreases again. This behavior corresponds to the hourglass-like shape of the miscibility gap with the narrowest region and shortest tie lines near 50.0/30.0/11.5/8.5 wt/wt/wt/wt. For these short tie lines the phases have a more similar composition than systems with long tie lines and, thus, solute partition coefficients approach uniform distribution in the biphasic system. Generally, the overall change in β-ionone partitioning is relatively

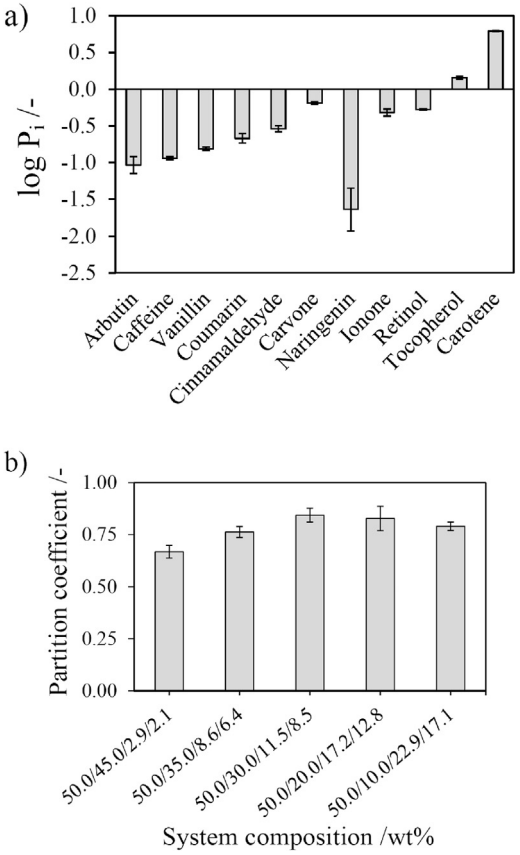

Fig. 2. (a) Logarithmic partition coefficients of model solutes with increasing octanol/water-partition coefficient from left to right in the system *n*-heptane/methanol/L-menthol/levulinic acid 50.0/35.0/8.6/6.4 wt/wt/wt/wt with 15 wt% DES; (b) Partition coefficient of β-ionone in different compositions of the biphasic solvent system composed of *n*-heptane/methanol/L-menthol/levulinic acid.

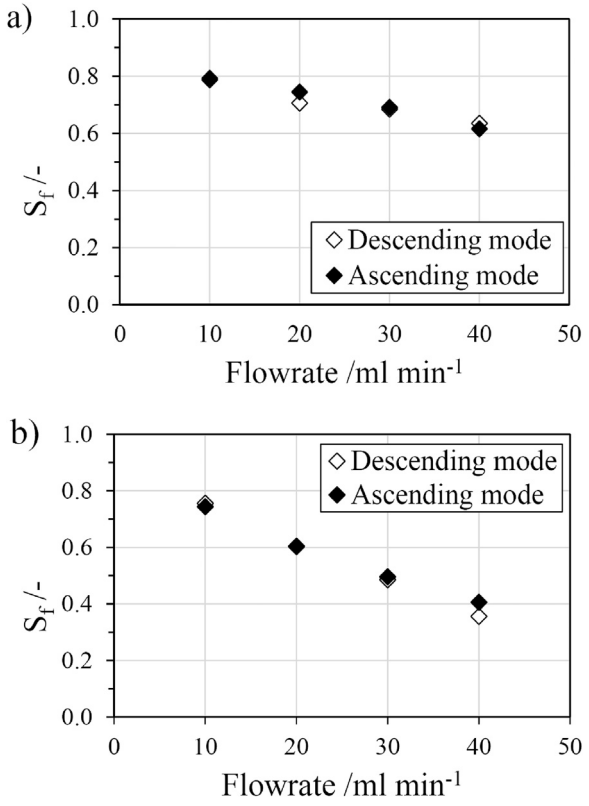

Fig. 3. Stationary phase retention (S_f) of (a) *n*-heptane/methanol/L-menthol/levulinic acid 50.0/45.0/2.9/2.1 wt/wt/wt/wt and (b) *n*-heptane/methanol/L-menthol/levulinic acid 50.0/35.0/8.6/6.4 wt/wt/wt/wt for different flow rates, in ascending and descending mode.

small compared to other systems where DES-constituents are only present in one of the phases [10].

3.2. Stability in presence of water

CPC columns are typically stored with methanol-water-mixtures inside. Thus, it is important to know if biphasic systems that are filled into the column are stable when in contact with water or whether the water has to be flushed out of the column before. Stability in presence of water can be an issue for DESs that contain hydrophobic species. When water is added to L-menthol-levulinic acid (1:1 mol:mol) hydrogen bonding between levulinic acid and water is more favorable than the interaction between L-menthol and levulinic acid and, thus, L-menthol is replaced by water. As L-menthol is not very soluble in aqueous environment, it precipitates above a certain amount of added water. This phenomenon may be used in DES recycling; however, precipitation has to be avoided inside the column or pumps during operation. To evaluate the stability of L-menthol in biphasic systems, water was gradually added to the biphasic systems. Three initial biphasic system compositions of *n*-heptane/methanol/L-menthol/levulinic acid with increasing DES content were selected: 50.0/40.0/5.7/4.3 wt/wt/wt/wt, 50.0/20.0/17.2/12.8 wt/wt/wt/wt, and 50.0/10.0/22.9/17.1 wt/wt/wt/wt. The water content was increased in steps from 2.5 wt% to 5.0 wt%, 10 wt%, 15 wt%, and eventually to 25 wt% and the mixture was vigorously shaken in-between each step. For the system composed of *n*-heptane/methanol/L-menthol/levulinic acid 50.0/40.0/5.7/4.3 wt/wt/wt/wt no precipitation occurred. For *n*-heptane/methanol/L-menthol/levulinic acid 50.0/20.0/17.2/12.8 wt/wt/wt/wt precipitation occurred at 15 wt% of water, however, the precipitate could be dissolved again after the mixture was shaken for some time. In the system *n*-heptane/methanol/L-menthol/levulinic acid 50.0/10.0/22.9/17.1 wt/wt/wt/wt precipitation was already observed at 5 wt% of water. The findings show that L-menthol is stable in solution in biphasic systems with high methanol content. When using biphasic systems with low methanol and high DES content, contact with water should be avoided.

3.3. Stationary phase retention

For the CPC experiments biphasic systems containing 5 wt% of DES (*n*-heptane/methanol/L-menthol/levulinic acid 50.0/45.0/2.9/2.1 wt/wt/wt/wt) and 15 wt% of DES (*n*-heptane/methanol/L-menthol/levulinic acid 50.0/35.0/8.6/6.4 wt/wt/wt/wt) were selected. Stationary phase retention was determined in ascending and descending mode for mobile phase flow rates between 10 and 40 ml min^{-1}.

The stationary phase retention for *n*-heptane/methanol/L-menthol/levulinic acid 50.0/45.0/2.9/2.1 wt/wt/wt/wt and 50.0/35.0/8.6/6.4 wt/wt/wt/wt is shown in Fig. 3a and b, respectively. For both biphasic systems stationary phase retention gave similar values in ascending and descending mode. With the biphasic system with 5 wt% of L-menthol-levulinic acid stationary phase retention was higher than 60% for all of the studied flow rates. Compared to that, lower stationary phase retention was observed for the biphasic system with 15 wt% L-menthol-levulinic acid and stationary phase retention decrease with flow rate was steeper. This can be explained by increasing viscosity of the phases with

higher content of DES-constituents in the system. These results indicate that systems with a lower content of DES-constituents may be superior in terms of S_f for performing CPC separations. Considering the results obtained for the partition coefficients in Section 3.1 and the obtained S_f -values, it is advisable to choose a system with low DES-content as a starting point for the selection of the system composition and then increase the DES-content if necessary.

3.4. Pulse injections in a centrifugal partition chromatography column

The applicability of the biphasic systems in centrifugal partition chromatography was tested by pulse injections. For injections in descending mode, coumarin, β-ionone, and α-tocopherol were selected according to the partition coefficients from shake flask experiments (see Fig. 2). The feed for the injection in descending mode was prepared by dissolving 3.7 g l^{-1} of coumarin, 4.9 g l^{-1} of β-ionone, and 32.0 g l^{-1} of α-tocopherol in the lower phase of the biphasic system. For the injection in ascending mode β-carotene was used instead of coumarin, and 0.16 g l^{-1} of β-carotene, 6.5 g l^{-1} of β-ionone, and 43.9 g l^{-1} of α-tocopherol were dissolved in upper phase to prepare the feed solution.

Fig. 4a and b show the pulse injections performed with the biphasic system *n*-heptane/methanol/L-menthol/levulinic acid 50.0/35.0/8.6/6.4 wt/wt/wt/wt in descending and ascending mode. A flow rate of 10 ml min^{-1} was selected for the pulse injections and stationary phase retention of 75.5% in descending mode and 73.2% in ascending mode was obtained after equilibration. In descending mode (Fig. 4a) coumarin (I), β-ionone (II), and α-tocopherol (III) were successfully separated. However, stationary phase loss occurred after injection and stationary phase retention decreased to around 56.1% at the end of the separation. The partition coefficients were calculated according to Eq. 3 with the mean value of the stationary phase retention at the beginning of the separation and at the time of the peak elution: $P_{coumarin} = 0.34$; $P_{\beta\text{-ionone}} = 0.83$; $P_{\alpha\text{-tocopherol}} = 1.32$. It has to be noted that deviations from the partition coefficients determined in the shake flask experiments in Section 3.1 are most probably caused by uncertainties due to the stationary phase stripping. Similar behavior for the stationary phase retention was observed for the separation in ascending mode, where stationary phase retention of 50.6% was obtained at the end of the separation. From the chromatogram in Fig. 4b the partition coefficients were calculated the same way as described above: $P_{\beta\text{-carotene}} = 0.28$; $P_{\alpha\text{-tocopherol}} = 0.90$; $P_{\beta\text{-ionone}} = 0.67$.

The descending mode separation has also been performed using the biphasic solvent system *n*-heptane/methanol/L-menthol/levulinic acid 50.0/45.0/2.9/2.1 wt/wt/wt/wt. At the beginning, stationary phase retention was 79.1% which dropped to 70.5% at the end of the separation. Although stationary phase loss was observed, it was less than with the biphasic system with 15 wt% menthol-levulinic acid. The partition coefficients from the chromatogram (Fig. 4c) were calculated the same way as described above: $P_{coumarin} = 0.22$; $P_{\beta\text{-ionone}} = 0.72$; $P_{\alpha\text{-tocopherol}} = 1.38$. Comparing the results from Fig. 4a and c, the separation factors $\alpha_{II,I}$ and $\alpha_{III,II}$ are higher for *n*-heptane/methanol/L-menthol/levulinic acid 50.0/45.0/2.9/2.1 wt/wt/wt/wt with values of 3.3 and 1.9 from Fig. 4c, compared to 2.4 and 1.6 derived from Fig. 4a. This shows that the solutes tend to distribute more evenly between the two phases when the content of DES-constituents is increased. Additionally, the resolution of the peaks was compared for the two biphasic systems. The separation resolution between peak II and I and between peak III and II were calculated according to Eq. 5 for Fig. 4a and c to compare the change in resolution with the percentage of DES-constituents in the biphasic system. For the system with 5 wt% of DES constituents (*n*-heptane/methanol/L-menthol/levulinic acid 50.0/45.0/2.9/2.1 wt/wt/wt/wt) the following values were obtained: $R_{S,II-I} = 6.6$ and $R_{S,III-II} = 3.2$. In the system with 15 wt% of DES constituents (*n*-heptane/methanol/L-menthol/levulinic acid 50.0/35.0/8.6/6.4 wt/wt/wt/wt) the resolutions decreased to $R_{S,II-I} = 4.1$ and $R_{S,III-II} = 2.9$. It can be seen that the separation resolution decreased with higher DES content in the system; however, the peaks are still very well separated. The change is more pronounced for the resolution of coumarin and β-ionone than for the resolution of β-ionone and α-tocopherol. From these first results, it can be concluded that the biphasic solvent systems composed of *n*-heptane/methanol/L-menthol/levulinic acid are useful candidates for water-free biphasic solvent systems for CPC.

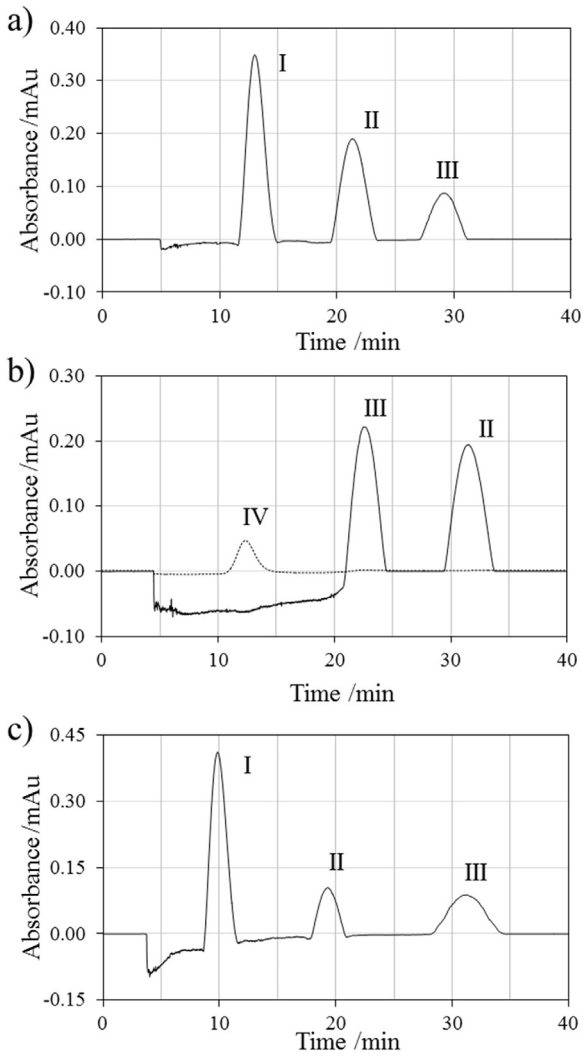

Fig. 4. Pulse injection of (a) coumarin (I), β-ionone (II), and α-tocopherol (III) in descending mode using the biphasic solvent system *n*-heptane/methanol/L-menthol/levulinic acid 50.0/35.0/8.6/6.4 wt/wt/wt/wt and (b) β-carotene (IV), α-tocopherol (III), and β-ionone (II) in ascending mode using *n*-heptane/methanol/L-menthol/levulinic acid 50.0/35.0/8.6/6.4 wt/wt/wt/wt; (c) pulse injection of coumarin (I), β-ionone (II), and α-tocopherol (III) in descending mode with the biphasic solvent system n-heptane/methanol/L-menthol/levulinic acid 50.0/45.0/2.9/2.1 wt/wt/wt/wt. All three separations were performed with a mobile phase flow rate of 10 ml min^{-1}; coumarin, β-ionone, and α-tocopherol were detected at 289 nm, β-carotene at 452 nm.

4. Conclusion

In the present work the applicability of quaternary non-aqueous biphasic solvent systems containing *n*-heptane, methanol, and a DES composed of L-menthol and levulinic acid as stationary and

mobile phases in CPC has been evaluated. In this biphasic system, DES constituents are present in both phases and cause the solute partition coefficients to shift towards the *sweet spot* compared to systems where DES-constituents are only present in one of the phases [10]. It was found that water addition does not cause precipitation of L-menthol for systems with low DES-content, while for system compositions with higher amounts of DES and less methanol precipitation occurs and contact with water should be avoided. Pulse injections affirmed the high potential of the biphasic systems for the separation of hydrophobic compounds and high stationary phase retention could be obtained for the separations. For higher amounts of L-menthol and levulinic acid in the biphasic system stationary phase loss was observed with injection, however, this could be reduced when only 5 wt% of the DES were used. The results of this work show the high potential of tailormade DES-based biphasic systems, which offer a whole new class of solvent systems for CPC. Nevertheless, strategies for solute recovery and recycling of the DES-constituents need to be developed in order to promote the application of such biphasic systems. Possible options to recover the solutes from the DES after removal of the volatile organic solvents are back extraction, diafiltration, and precipitation of the DES-constituents. Still, more research effort is needed to provide such strategies for different DES and solute groups.

Acknowledgement

The authors thank Ms. Eleni Papadopoulos for her valuable participation in parts of the experiments for this work.

References

[1] A. Berthod, D.W. Armstrong, Centrifugal partition chromatography. I. General Features, J. Liquid Chromatogr. 11 (1988) 547–566.
[2] J.B. Friesen, G.F. Pauli, G.U.E.S.S.—A generally useful estimate of solvent systems for CCC, J. Liquid Chromatogr. Related Technol. 28 (2005) 2777–2806.
[3] G.F. Pauli, S.M. Pro, J.B. Friesen, Countercurrent separation of natural products, J. Nat. Prod. 71 (2008) 1489–1508.
[4] J. Goll, G. Audo, M. Minceva, Comparison of twin-cell centrifugal partition chromatographic columns with different cell volume, J. Chromatogr. A 1406 (2015) 129–135.
[5] F. Bezold, J. Goll, M. Minceva, Study of the applicability of non-conventional aqueous two-phase systems in counter-current and centrifugal partition chromatography, J. Chromatogr. A 1388 (2015) 126–132.
[6] Y.H. Guan, D. Fisher, I.A. Sutherland, Protein separation using toroidal columns by type-J synchronous counter-current chromatography towards preparative separation, J. Chromatogr. A 1217 (2010) 3525–3530.
[7] Y. Shibusawa, Y. Ito, Protein separation with aqueous—aqueous polymer systems by two types of counter-current chromatographs, J. Chromatogr. A 550 (1991) 695–704.
[8] W. Vetter, S. Hammann, M. Müller, M. Englert, Y. Huang, The use of countercurrent chromatography in the separation of nonpolar lipid compounds, J. Chromatogr. A 1501 (2017) 51–60.
[9] J.B. Friesen, J.B. McAlpine, S.-N. Chen, G.F. Pauli, Countercurrent separation of natural products: an update, J. Nat. Prod. 78 (2015) 1765–1796.
[10] S. Roehrer, F. Bezold, E.M. Garcia, M. Minceva, Deep eutectic solvents in countercurrent and centrifugal partition chromatography, J. Chromatogr. A 1434 (2016) 102–110.
[11] F. Bezold, M.E. Weinberger, M. Minceva, Computational solvent system screening for the separation of tocopherols with centrifugal partition chromatography using deep eutectic solvent-based biphasic systems, J. Chromatogr. A 1491 (2017) 153–158.
[12] Y. Dai, J. van Spronsen, G.-J. Witkamp, R. Verpoorte, Y.H. Choi, Natural deep eutectic solvents as new potential media for green technology, Anal. Chim. Acta 766 (2013) 61–68.
[13] D.A. Alonso, A. Baeza, R. Chinchilla, G. Guillena, I.M. Pastor, D.J. Ramón, Deep eutectic solvents: the organic reaction medium of the century, Eur. J. Org. Chem. 2016 (2016) 612–632.
[14] S. Mulyono, H.F. Hizaddin, I.M. Alnashef, M.A. Hashim, A.H. Fakeeha, M.K. Hadj-Kali, Separation of BTEX aromatics from n-octane using a (tetrabutylammonium bromide + sulfolane) deep eutectic solvent - experiments and COSMO-RS prediction, RSC Adv. 4 (2014) 17597–17606.
[15] H.F. Hizaddin, M. Sarwono, M.A. Hashim, I.M. Alnashef, M.K. Hadj-Kali, Coupling the capabilities of different complexing agents into deep eutectic solvents to enhance the separation of aromatics from aliphatics, J. Chem. Thermodyn. 84 (2015) 67–75.
[16] M.A. Kareem, F.S. Mjalli, M.A. Hashim, I.M. AlNashef, Liquid–liquid equilibria for the ternary system (phosphonium based deep eutectic solvent–benzene–hexane) at different temperatures: a new solvent introduced, Fluid Phase Equilib. 314 (2012) 52–59.
[17] M.A. Kareem, F.S. Mjalli, M.A. Hashim, M.K.O. Hadj-Kali, F.S.G. Bagh, I.M. Alnashef, Phase equilibria of toluene/heptane with tetrabutylphosphonium bromide based deep eutectic solvents for the potential use in the separation of aromatics from naphtha, Fluid Phase Equilib. 333 (2012) 47–54.
[18] M.A. Kareem, F.S. Mjalli, M.A. Hashim, M.K.O. Hadj-Kali, F.S. Ghareh Bagh, I.M. Alnashef, Phase equilibria of toluene/heptane with deep eutectic solvents based on ethyltriphenylphosphonium iodide for the potential use in the separation of aromatics from naphtha, J. Chem. Thermodyn. 65 (2013) 138–149.
[19] A.P. Abbott, P.M. Cullis, M.J. Gibson, R.C. Harris, E. Raven, Extraction of glycerol from biodiesel into a eutectic based ionic liquid, Green Chem. 9 (2007) 868–872.
[20] K. Shahbaz, F.S. Mjalli, M. Hashim, I.M. Al-Nashef, Using deep eutectic solvents for the removal of glycerol from palm oil-based biodiesel, J. Appl. Sci. 10 (2010) 3349–3354.
[21] K.C. Ho, K. Shahbaz, W. Rashmi, F. Mjalli, M. Hashim, I. Alnashef, Removal of glycerol from palm oil-based biodiesel using new ionic liquids analogues, J. Eng. Sci. Technol. 10 (2015) 98–111.
[22] Y. Dai, G.-J. Witkamp, R. Verpoorte, Y.H. Choi, Natural deep eutectic solvents as a new extraction media for phenolic metabolites in Carthamus tinctorius L, Anal. Chem. 85 (2013) 6272–6278.
[23] A. García, E. Rodríguez-Juan, G. Rodríguez-Gutiérrez, J.J. Rios, J. Fernández-Bolaños, Extraction of phenolic compounds from virgin olive oil by deep eutectic solvents (DESs), Food Chem. 197 (2016) 554–561.
[24] Z. Lin, Y. Hou, S. Ren, Y. Ji, C. Yao, M. Niu, W. Wu, Phase equilibria of phenol + toluene + quaternary ammonium salts for the separation of phenols from oil with forming deep eutectic solvents, Fluid Phase Equilib. 429 (2016) 67–75.
[25] J.B. Friesen, G.F. Pauli, Rational development of solvent system families in counter-current chromatography, J. Chromatogr. A 1151 (2007) 51–59.
[26] F. Bezold, M. Minceva, Liquid-liquid equilibria of n-heptane, methanol and deep eutectic solvents composed of carboxylic acid and monocyclic terpenes, Fluid Phase Equilib. 477 (2018) 98–106.

3.6. List of other published manuscripts

Bezold, F., J. Goll, M. Minceva, “Study of the applicability of non-conventional aqueous two-phase systems in counter-current and centrifugal partition chromatography”, Journal of Chromatography A, 2015, 1388: p. 126-132.

Roehrer, S., F. Bezold, M. Minceva, “Deep eutectic solvents in countercurrent and centrifugal partition chromatography”, Journal of Chromatography A, 2016, 1434: p. 102-110.

Mainberger, S., M. Kindlein, F. Bezold, E. Elts, M. Minceva, H. Briesen, “Deep eutectic solvent formation: a structural view using molecular dynamics simulations with classical force fields”, Molecular Physics, 2017, 115: p. 1309-1321.

Kuhn, M., S. Lang, F. Bezold, M. Minceva, H. Briesen, “Time-resolved extraction of caffeine and trigonelline from finely-ground espresso coffee with varying particle sizes and tamping pressures”, Journal of Food Engineering, 2017, 206: p. 37-47

4. Overall discussion

The motivation of this thesis was to explore alternative solvent systems for the separation of very hydrophilic and hydrophobic target compounds with CPC. Within this work, ATPSs were investigated and applied in CPC to separate proteins. The second part of the thesis deals with the application of DES-based biphasic systems in CPC. Computational solvent system screening for DES-based biphasic systems was evaluated and applied to a separation task. Additionally, novel DES-based biphasic systems were developed and used as stationary and mobile phases in CPC separations.

4.1. Aqueous two-phase systems

ATPSs are biphasic systems with both phases mainly consisting of water. They are free of organic solvents and, thus, they can be applied for biomolecules, such as proteins. In this work, ATPSs composed of PEG 1000, K_2HPO_4, KH_2PO_4, water, and small amounts of an IL have been investigated. The fact that small amounts of IL can alter partition coefficients has been described for liquid-liquid extraction [19]. The objective of **Paper I** was to employ the effect that ILs can be used to tune protein partition coefficients in CPC separations. It was shown that the ILs [EMIM]Cl or [BMIM]Cl selectively altered the partition coefficients of the proteins myoglobin and lysozyme. This effect was used to change the elution time of lysozyme and shorten the separation time. The injection volume was increased to 20% of the column volume in order to increase the productivity of the separation. High stationary phase retention could be retained even with the increased injection volume. Simulations of separations with even larger injection volumes indicate that injections volumes up to 50% of the column volume may be applicable.

ILs may have a positive effect on the stability of proteins in solution [49, 83]. They have also been introduced as additives for protein refolding [84]. However, depending on the type of the IL and dissolved protein, ILs or other solutes may also have a destabilizing or inhibition effect [49, 83, 85, 86]. The stability of the biomolecules has to be assessed in the selection process of the ILs that are added to the ATPSs. Direct determination of the protein structure in the ATPSs with IL was not possible. Circular dichroism (CD) is a method that enables determination of secondary and tertiary structures of proteins to test for denaturation. The high phosphate content impeded CD measurements [87]. Due to the high ratio of phosphate salt to protein content, the protein concentration was too low for CD measurements after adjusting the phosphate concentration to a tolerable level by dilution. Therefore, myoglobin and lysozyme were each dissolved in buffer with a low salt concentration and the same [EMIM]Cl concentration as in the CPC experiments. The solution was stored at ambient temperature for around 1.5 h and then diluted for CD measurements. It could be shown that the protein structure remains unchanged with IL addition or if changes in the structure occur they are reversed by dilution.

ATPSs have also been used for the separation of monoclonal antibodies [88-90] and semiconducting single-wall carbon nanotubes [91, 92]. ATPSs have been applied in the downstream processing of virus-like particles [93] and enzymes, such as myrosinase [94], amylase [95], and laccases [96]. The results of **Paper I** may also be interesting for these

application areas. Especially the possibilities to increase the productivity could be transferred. For example, simulation based studies could be performed to increase the injection volume for other CPC separations, not only with ATPSs, but also with other biphasic systems.

4.2. DES-based biphasic systems

DES have gained a lot of attention during the last years due to their versatility and valuable solvent properties. It has been shown that DES-based biphasic systems are suitable for the separation of hydrophobic compounds in CPC [25]. In order to enhance the application of DES-based biphasic systems in CPC, several aspects, from solvent system selection to application and development of novel DES-based biphasic systems, were addressed.

Computational solvent system screening

Solvent system screening based on thermodynamic models has been applied for the selection of biphasic systems composed of organic solvents and water for CPC and CCC [40, 41]. In this thesis, the method was evaluated for the selection of DES-based biphasic systems. The purpose of the solvent system screening is to narrow down the number of possible biphasic systems from a nearly countless amount to a few choices that can be tested experimentally [40, 41, 76]. It was found that the prediction accuracy was high enough to use the screening approach for the selection of DES-based biphasic systems for CPC separations. With the method presented in **Paper II**, it is possible to select a DES-based biphasic solvent system for a CPC separation solely based on the molecular structure of target compounds and impurities.

However, some restrictions have to be made: The validity of the screening approach was confirmed for systems where the DES-constituents are mainly located in one of the phases, so called pseudo-ternary systems. Prior to publication of **Paper II**, only pseudo-ternary LLE data were available in literature for biphasic systems with DESs. That means, the DES was treated as a pseudo compound in the determination of the LLE data [69, 97-99], or only one DES-constituent was quantified and it was assumed that the stoichiometric ratio of HBA and HBD is constant and the same as in the initially prepared DES in all phases [67, 100, 101]. The resulting phase diagrams are plotted as ternary diagrams with the DES-constituents treated as a single compound instead of a quaternary system. First calculations have shown, that it has to be expected that the ratio of HBA and HBD is not constant in systems with DES-constituents present in both phases. This means, the assumption of a constant HBA:HBD-ratio is restricted to systems with DES-constituents located in one of the two phases. In cases where the behaviour of the biphasic system is already known, for example when additional tie lines for different global compositions are calculated, it is reasonable to assume fixed HBA:HBD ratio if applicable. A fixed stoichiometry of HBA and HBD also decreases the degree of freedom of the system. This decreases the time needed for the LLE calculation.

Considering the restrictions mentioned above, the solvent system selection approach that was validated in **Paper II** was applied to a separation task. In **Paper III**, a DES-based biphasic system for the separation of different tocopherols with CPC was selected. Besides the actual CPC separations, no experiments were conducted in the solvent system selection. The only inputs for the computational screening were the molecular structures of the DES-constituents,

solvents and the different tocopherols. Applying this screening approach substantially decreased the time and experimental effort needed to select the biphasic system for the CPC separation.

Liquid-liquid equilibrium data of systems with DES

During the literature research for LLE data of systems containing DESs, it became apparent that DESs were mainly treated as pseudo compounds in experiments and modelling. In **Paper IV**, novel biphasic systems with DES-constituents in both phases were developed. Three different DESs were selected: L-menthol-levulinic acid (1:1 mol:mol), thymol-levulinic acid (1:1 mol:mol), and carvacrol-levulinic acid (1:1 mol:mol). All DES-constituents are natural compounds and available as food-grade bulk chemicals. The HBDs, L-menthol, thymol, and carvacrol, are poorly soluble in water. The HBA, levulinic acid, is miscible with water. All DES-constituents can be evaporated and analysed by gas chromatography. LLE of different compositions of *n*-heptane, methanol, and L-menthol-levulinic acid, thymol-levulinic acid, or carvacrol-levulinic acid were determined. It was found that the biphasic systems behave as quaternary systems: DES-constituents are present in both phases and the ratio of HBD:HBA is different in the phases and changes with the global system composition. The obtained quaternary LLE-data may contribute to the understanding of the interactions between DES-constituents in complex solutions. The interactions of HBA and HBD are subject to current research [102-113]. When additional molecules are introduced to systems with DES, the interactions between all components of the mixture are complex: Systems of DESs and dissolved gases have been investigated [114-116], the behaviour of mixtures of DESs and water [117-119] or interaction of solutes with DESs [120, 121]. Yet, the behaviour of DESs and mixtures with DESs is not fully understood. The quaternary LLE may help to elucidate the interactions of DESs constituents in complex systems and may be used to test or improve existing thermodynamic models.

Application of DES-based biphasic systems in CPC separations

In **Paper IV**, novel biphasic systems with DES-constituents present in both phases were developed. In **Paper V**, one of these biphasic systems, namely *n*-heptan/methanol/ L-menthol/levulinic acid, was applied in CPC separations. Stationary phase retention and solute partition coefficients of compounds ranging from hydrophilic to hydrophobic were determined. The DES-based biphasic solvent system is in particular suitable for the separation of hydrophobic compounds.

Further, the stability of the biphasic system *n*-heptan/methanol/L-menthol/levulinic acid in presence of water was evaluated. Contact of L-menthol-levulinic acid (1:1 mol:mol) with water causes L-menthol to precipitate. Thus, it was investigated if precipitation also occurs in the quaternary biphasic system upon contact with water. Different global system compositions were prepared and mixed with water. It was found that in systems with high percentage of L-menthol and levulinic acid, precipitation occurs when water is added. Therefore, contact with water needs to be avoided for such systems. This can be a concern in daily laboratory praxis where CPC columns are often stored with mixtures of methanol and water when not in

use. For biphasic system compositions with low percentage of L-menthol and levulinic acid, contact with water is not critical.

DESs are applied in extraction of value-added compounds from plant material or other natural resources [58, 59, 122-131]. An additional benefit of DES-based biphasic systems would be obtained if the crude extract that is supposed to be separated with CPC would be prepared with the same DES that is used in the biphasic system. That way the process steps from natural source to final product could be reduced compared to processes where extracts need to be dried prior to further steps.

In general, a frequently encountered question concerning applications using DES-based biphasic systems is how to recover the products from the solvents. In the case of tocopherols, as discussed in **Paper III**, the separations are performed in descending mode. The fractionated tocopherols are present in the mobile phase which is the DES-rich, lower phase. It contains mainly ethanol and the DES-constituents, choline chloride and 1,4-butanediol. In this case, it is possible to use back extraction for tocopherol recovery: *n*-Heptane and water are added to the lower phase. The *n*-heptane leads to the formation of a second phase into which the tocopherols can be extracted. The added water is located in the lower DES-rich phase and causes tocopherol to partition into the upper *n*-heptane-rich phase. The *n*-heptane-rich upper phase can then be removed from the tocopherol by vacuum distillation. Another option would be to retain the tocopherols in the DES-rich lower phase and just remove ethanol by vacuum distillation. Depending on the desired product and the type of DES-constituents used, the tocopherol-DES-mixture could be directly applied in a formulation, for example in cosmetics or food supplements.

5. Conclusion

Biphasic systems with alternative solvents like ILs and DESs contribute to expand the application areas of CPC and CCC for the separation of hydrophobic and hydrophilic compounds. Although the solvent system selection requires more effort than for the conventionally used water and organic solvent-based biphasic systems, due to limited data and higher degree of freedom, it is worth taking it.

ATPSs provide a class of biphasic systems that can be applied for proteins that may denature in conventional water-organic solvent-based biphasic systems. ATPSs have scarcely been used in LLC because former CCC and CPC columns only allowed small flow rates; new column designs allow higher flow rates and make CPC separations with ATPSs more competitive to other technologies. The stationary phase retention is high enough to allow large injection volumes, which is another way to increase productivity of a protein separation.

The number of non-aqueous solvent systems for CPC and CCC in literature is limited and, thus, researchers are aiming to develop novel non-aqueous biphasic systems. DES-based biphasic systems are water-free and suitable for the separation of hydrophobic compounds and fit this unmet need. DESs can substitute organic solvents in water-free LLE, such as chloroform, dichloromethane, benzene or acetonitrile. DES-based biphasic systems for CPC and CCC are a relatively new development. It was investigated in this thesis whether solvent system screening approaches can be applied to them. It was shown in this work that for systems with DES-constituents only present in one of the phases, so-called pseudo ternary systems, the thermodynamic model COSMO-RS can be used. The prediction accuracy is sufficient for screening of limiting activity coefficients, liquid-liquid equilibria, and solute partition coefficients. Most reliable results were obtained when the ionic DESs were described as fully dissociated ions and with the TZVP parametrization. The screening approach was then applied to a mixture of tocopherols, mainly consisting of α- and γ-tocopherol, and LLE of 21 DES-based systems and tocopherol partition coefficients in the systems were predicted with COSMO-RS. The biphasic systems in the selection pool were all of the pseudo-ternary type. The best candidate from the computational screening was selected and CPC separation experiments were performed without further experimental screening. This example highlights how thermodynamic models can save time and experimental effort in the solvent system selection for CPC and CCC.

At the time of the publication of **Paper II and III**, only systems with DES-constituents solely present in one of the two phases were available in literature. First evaluations with COSMO-RS showed that DESs cannot be treated as a single entity in a simplified way in all cases. As no literature data of suitable LLE to prove this hypothesis were available, phase equilibrium data were determined for three new biphasic systems containing DES-constituents in both phases. It could be shown that DES-constituents are distributed between the two phases and that their molar ratio in the individual phases differs from the ratio initially used in the DES. Furthermore, it was found that the distribution of the DES-constituents in the biphasic system is concentration dependent. Unfortunately, COSMO-RS could not reproduce this behaviour as the miscibility gap was over-predicted. It was not possible to predict the distribution of the systems' constituents correctly. The applicability of such systems with DES-constituents in

both phases in CPC was tested and it could be shown that the evaluated biphasic system provided reasonable stationary phase retention and solute partition coefficients of hydrophobic model compounds in the *sweet spot*. The system was especially suitable for the tested model compounds with logarithmic octanol/water-partition coefficients between 2.1 and 12.

Up to now, the potential of biphasic systems with ILs or DESs is not yet fully exploited. This thesis shows the high potential of DES-based biphasic systems and contributes to making the use of biphasic systems with ILs and DESs more accessible. The findings of this work in the field of ATPSs are not only relevant for protein separation, but could be transferred to the separation of other target compounds that can be separated with ATPSs, such as peptides, monoclonal antibodies, or carbon nanotubes. DESs are a novel class of solvents which were successfully applied in CPC separations. For the application of DESs as solvents the complete process should be considered. DESs can also be used to produce crude plant extracts and could then directly be used as feed for CPC separations to decrease process steps and increase productivity.

6. Outlook

Although the prediction quality of COSMO-RS was sufficient to perform a solvent screening with biphasic systems that contain DES-constituents solely in one of the phases, the phase diagram predictions still have to be completely evaluated for biphasic systems with DES-constituents in both phases. However, to evaluate the prediction accuracy for such systems, and also to improve predictions, a larger set of LLE-data is needed. LLE data are crucial in order to develop new modelling approaches. The way to improve existing modelling approaches may lead through the combination of molecular dynamics simulations and thermodynamic models. Prediction methods of solid-liquid equilibria of DESs are not yet available. Reliable solid-liquid equilibrium prediction is another necessary step towards exploiting the full potential of DESs and selecting the most suitable HBA and HBD combinations for specific applications. Solid-liquid equilibrium prediction methods would enable model-based HBA and HBD selection and further decrease time and effort of solvent system selection.

From the viewpoint of application, the main obstacles that should be tackled in order to achieve a wider use of DES-based biphasic systems in CPC are the lack of separation examples and the limited number of DES-based biphasic systems that have been used in CPC. Both issues were addressed in this thesis, and further effort should be invested in the future to overcome these obstacles. Furthermore, solute recovery and solvent recycling are crucial for industrial scale application of DES-based biphasic systems. Thus, development of recovery and solvent reuse strategies are substantial.

For the separation of very hydrophilic biomolecules with CPC, ATPS were investigated. It was previously shown that ATPSs have potential to be used for protein separation in CPC and CCC [30-32, 37, 132-135]. Phase diagrams of different ATPSs were widely studied in literature [11, 12, 15, 16, 136-138] and different new CCC and CPC column designs have been developed for the handling of ATPS [30-32, 37, 135]. Protein stability measurements were conducted with ILs [49, 83, 84, 139, 140], however, to further promote the use of ATPSs in CCC and CPC, is necessary to investigate the stability of different proteins after exposure to shear forces in the column. Predictive thermodynamic models can be applied for process design. Currently, shake flask experiments are performed for the selection of an appropriate ATPS for CCC and CPC separations. Although proteins are too big to apply models that require DFT calculations for screening, other thermodynamic models that have shown to be useful for ATPSs, such as PC-SAFT, could be used to reduce experimental effort for the selection of ATPSs for CPC separations [141, 142]. Similar to DES-based biphasic systems, solute recovery and solvent recycling strategies are important for the application of CCC and CPC separations with ATPSs in large scale. Further research on this topic is desirable in order to promote the application of CCC and CPC separations with ATPSs.

7. Symbols

α_{ji}	Separation factor for the compounds *i* and *j*
A_i	Surface area
σ_i	Standard deviation of the peak of compound *i*
σ_i^2	Variance of the peak of compound *i*
c_i^{MP}	Concentration of solute *i* in the mobile phase
c_i^{SP}	Concentration of solute *i* in the stationary phase
C_i^{∞}	Solvent capacity
Δc_p	Difference between the heat capacity of the liquid and the solid phase
f_i^{φ}	Fugacity of compound *i* in phase φ
G	Gibbs' energy
Δg_{SL}	Molar Gibbs' energy of the solid-liquid phase transition
$\Delta_{fus}h$	Enthalpy of fusion
μ_m^{φ}	Chemical potential of the chemical species *m* in phase φ
v_i^0	Molar volume of the pure solvent *i*
v^{φ}	Molar volume of phase φ
v^E	Molar excess volume of mixing
N_i	Number of theoretical separation stages analysed for compound *i*
n_i	Amount of substance *i*
p^{φ}	Pressure of phase φ
P_i^{asc}	Partition coefficient of compound *i* determined for ascending mode
P_i^{dsc}	Partition coefficient of compound *i* determined for descending mode
$P_i^{\alpha\beta}$	Partition coefficient of compound *i* between phases α and β calculated with concentrations
$p_i(\sigma)$	Sigma profile of compound *i*
$K_i^{x,\alpha\beta}$	Partition coefficient of compound *i* between phases α and β calculated with mole fractions
S_f	Stationary phase retention
T^{φ}	Temperature of phase φ
T_m	Melting temperature
T_{tr}	Triple point temperature
$t_{R,i}$	Retention time of compound *i*
V_c	Column volume
V_{MP}	Volume of mobile phase inside the column

$V_{R,i}$	Retention volume of compound *i*
V_{SP}	Volume of stationary phase inside the column
x_i^{φ}	Mole fraction of compound *i* in phase φ
γ_i^{φ}	Activity coefficient of compound *i* in phase φ
γ_i^{∞}	Limiting activity coefficient of compound *i* in phase φ

8. Abbreviations

ATPS	Aqueous two-phase systems
BSA	Bovine serum albumin
CCC	Countercurrent chromatography
CD	Circular dichroism
COSMO	Conductor-like screening model
COSMO-RS	Conductor-like screening model for realistic solvation
CPC	Centrifugal partition chromatography
DES	Deep eutectic solvent
DFT	Density functional theory
EoS	Equation of state
GC	Gas chromatography
HBA	Hydrogen bond acceptor
HBD	Hydrogen bond donor
HEMWat	*n*-Hexane/ethyl acetate/methanol/water solvent system family
IL	ionic liquid
LLC	Liquid-liquid chromatography
LLE	Liquid-liquid equilibrium
MLA	L-Menthol-Levulinic acid
NRTL	Non-Random Two-Liquid theory
PC-SAFT	Perturbed Chain Statistical Associating Fluid Theory
PEG	Polyethylene glycol
SAFT	Statistical Associating Fluid Theory
UNIFAC	Universal Quasichemical Functional-group Activity Coefficients
UNIQUAC	Universal Quasichemical Equation

9. List of Figures and Tables

Figure 1: Schematic illustration of the s*weet spot*; partition coefficients below the chromatogram correspond to the plotted elution volume. Partition coefficients values between 0.4 and 2.5 result in the best separation performance for countercurrent and centrifugal partition chromatography[27] 14

Figure 2: Formation of mixing and settling zones along a hydrodynamic CCC column [35]. 16

Figure 3: (a) Hydrostatic CPC column; (b) annular plate; (c) annular disk with cells and connecting channels [36] 17

Figure 4: Different designs of cells and channels on annular disks of CPC: (a) Z-cell from Kromaton [36], (b) twin cell of an SCPC250 from Gilson with a twin cell volume of 0.101 ml [37], (c) twin cell geometry of an SCPC 250 BIO with larger cell volume of 0.961 ml from Gilson [37] 17

Figure 5: Selection of a solvent system class according to target compound octanol-water partition coefficients 19

Figure 6: Schematic illustration of the distribution of phase forming compounds in an ATPS. 20

Figure 7: Schematic solid-liquid equilibrium phase diagram for a binary simple eutectic..... 21

Figure 8: Molecular structures of possible DES-constituents 22

Figure 9: Necessary steps for the selection of a DES-based biphasic system for CPC separations. 28

Figure 10: Sigma profiles of n-hexane and water taken from COSMOtherm software, Cosmologic GmbH & Co. KG. 30

Figure 11: Different molecular representations of DESs in COSMO-RS: (a) ion pair approach, (b) representation as electroneutral mixture, and (c) metafile approach. 30

Figure 12: Sigma surfaces of α-, β-, γ- and δ-tocopherol for TZVP parametrization (images obtained from COSMOtherm 15.01) 59

Figure 13: Limiting activity coefficients of organic solvents in L-menthol-levulinic acid (1:1 ml:mol) calculated with COSMO-RS. Solvents with values below the dashed line are miscible with the DES and mixtures with solvents with values above the dashed line show two liquid phases. 68

Table 1: Examples of HBA and HBD combinations with molar ratio and melting temperatures 23

10. References

[1] Y. Ito, Countercurrent chromatography, Journal of Biochemical and Biophysical Methods, 5 (1981) 105-129.

[2] J.B. Friesen, J.B. McAlpine, S.-N. Chen, G.F. Pauli, Countercurrent Separation of Natural Products: An Update, Journal of Natural Products, 78 (2015) 1765-1796.

[3] A. Berthod, Countercurrent Chromatography, Elsevier Science, 2002.

[4] A. Berthod, Countercurrent Chromatography and the Journal of Liquid Chromatography: A Love Story, Journal of Liquid Chromatography & Related Technologies, 30 (2007) 1447-1463.

[5] A. Foucault, L. Chevolot, Counter-current chromatography: instrumentation, solvent selection and some recent applications to natural product purification, Journal of Chromatography A, 808 (1998) 3-22.

[6] P. Khadka, J. Ro, H. Kim, I. Kim, J.T. Kim, H. Kim, J.M. Cho, G. Yun, J. Lee, Pharmaceutical particle technologies: An approach to improve drug solubility, dissolution and bioavailability, Asian Journal of Pharmaceutical Sciences, 9 (2014) 304-316.

[7] V. Dhapte, P. Mehta, Advances in hydrotropic solutions: An updated review, St. Petersburg Polytechnical University Journal: Physics and Mathematics, 1 (2015) 424-435.

[8] P.Å. Albertsson, Partition of cell particles and macromolecules: separation and purification of biomolecules, cell organelles, membranes, and cells in aqueous polymer two-phase systems and their use in biochemical analysis and biotechnology, Wiley, 1986.

[9] R. Hatti-Kaul, Aqueous two-phase systems, in: Aqueous two-phase systems: methods and protocols, Springer, 2000, pp. 1-10.

[10] K.E. Gutowski, G.A. Broker, H.D. Willauer, J.G. Huddleston, R.P. Swatloski, J.D. Holbrey, R.D. Rogers, Controlling the Aqueous Miscibility of Ionic Liquids: Aqueous Biphasic Systems of Water-Miscible Ionic Liquids and Water-Structuring Salts for Recycle, Metathesis, and Separations, Journal of the American Chemical Society, 125 (2003) 6632-6633.

[11] S.P.M. Ventura, S.G. Sousa, L.S. Serafim, Á.S. Lima, M.G. Freire, J.A.P. Coutinho, Ionic Liquid Based Aqueous Biphasic Systems with Controlled pH: The Ionic Liquid Cation Effect, Journal of Chemical & Engineering Data, 56 (2011) 4253-4260.

[12] S.P.M. Ventura, S.G. Sousa, L.S. Serafim, Á.S. Lima, M.G. Freire, J.A.P. Coutinho, Ionic-Liquid-Based Aqueous Biphasic Systems with Controlled pH: The Ionic Liquid Anion Effect, Journal of Chemical & Engineering Data, 57 (2012) 507-512.

[13] Y. Pei, J. Wang, L. Liu, K. Wu, Y. Zhao, Liquid−Liquid Equilibria of Aqueous Biphasic Systems Containing Selected Imidazolium Ionic Liquids and Salts, Journal of Chemical & Engineering Data, 52 (2007) 2026-2031.

[14] Z. Li, Y. Pei, H. Wang, J. Fan, J. Wang, Ionic liquid-based aqueous two-phase systems and their applications in green separation processes, Trends in Analytical Chemistry, 29 (2010) 1336-1346.

[15] M.G. Freire, C.M.S.S. Neves, J.N. Canongia Lopes, I.M. Marrucho, J.A.P. Coutinho, L.P.N. Rebelo, Impact of Self-Aggregation on the Formation of Ionic-Liquid-Based Aqueous Biphasic Systems, The Journal of Physical Chemistry B, 116 (2012) 7660-7668.

[16] S. Shahriari, C.M.S.S. Neves, M.G. Freire, J.A.P. Coutinho, Role of the Hofmeister Series in the Formation of Ionic-Liquid-Based Aqueous Biphasic Systems, The Journal of Physical Chemistry B, 116 (2012) 7252-7258.

[17] F. Bezold, J. Goll, M. Minceva, Study of the applicability of non-conventional aqueous two-phase systems in counter-current and centrifugal partition chromatography, Journal of Chromatography A, 1388 (2015) 126-132.

[18] S.P.M. Ventura, C.M.S.S. Neves, M.G. Freire, I.M. Marrucho, J. Oliveira, J.A.P. Coutinho, Evaluation of Anion Influence on the Formation and Extraction Capacity of Ionic-Liquid-Based Aqueous Biphasic Systems, The Journal of Physical Chemistry B, 113 (2009) 9304-9310.

[19] M.R. Almeida, H. Passos, M.M. Pereira, Á.S. Lima, J.A.P. Coutinho, M.G. Freire, Ionic liquids as additives to enhance the extraction of antioxidants in aqueous two-phase systems, Separation and Purification Technology, 128 (2014) 1-10.

[20] A.P. Abbott, D. Boothby, G. Capper, D.L. Davies, R.K. Rasheed, Deep Eutectic Solvents Formed between Choline Chloride and Carboxylic Acids: Versatile Alternatives to Ionic Liquids, Journal of the American Chemical Society, 126 (2004) 9142-9147.

[21] E.L. Smith, A.P. Abbott, K.S. Ryder, Deep Eutectic Solvents (DESs) and Their Applications, Chemical Reviews, 114 (2014) 11060-11082.

[22] Y. Dai, J. van Spronsen, G.-J. Witkamp, R. Verpoorte, Y.H. Choi, Natural deep eutectic solvents as new potential media for green technology, Analytica Chimica Acta, 766 (2013) 61-68.

[23] Ru, B. Konig, Low melting mixtures in organic synthesis - an alternative to ionic liquids?, Green Chemistry, 14 (2012) 2969-2982.

[24] A.P. Abbott, G. Capper, D.L. Davies, R.K. Rasheed, V. Tambyrajah, Novel solvent properties of choline chloride/urea mixtures, Chemical Communications, (2003) 70-71.

[25] S. Roehrer, F. Bezold, E.M. Garcia, M. Minceva, Deep eutectic solvents in countercurrent and centrifugal partition chromatography, Journal of Chromatography A, 1434 (2016) 102-110.

[26] A.P. Foucault, Centrifugal partition chromatography, M. Dekker, 1995.

[27] J.B. Friesen, G.F. Pauli, G.U.E.S.S.—A Generally Useful Estimate of Solvent Systems for CCC, Journal of Liquid Chromatography & Related Technologies, 28 (2005) 2777-2806.

[28] I. Sutherland, P. Hewitson, S. Ignatova, New 18-l process-scale counter-current chromatography centrifuge, Journal of Chromatography A, 1216 (2009) 4201-4205.

[29] Y.H. Guan, D. Fisher, I.A. Sutherland, Protein separation using toroidal columns by type-J synchronous counter-current chromatography towards preparative separation, Journal of Chromatography A, 1217 (2010) 3525-3530.

[30] J. Ding, S. Li, Y. Zhao, Y.H. Guan, L. Deng, Q. Deng, Properties of hydrodynamic J-type countercurrent chromatography for protein separation using aqueous two-phase systems: With special reference to constructing conical columns, Journal of Chromatography A, 1499 (2017) 101-110.

[31] Y. Ito, M. Knight, T.M. Finn, Spiral Countercurrent Chromatography, Journal of chromatographic science, 51 (2013) 726-738.

[32] M. Knight, T.M. Finn, J. Zehmer, A. Clayton, A. Pilon, Spiral counter-current chromatography of small molecules, peptides and proteins using the spiral tubing support rotor, Journal of Chromatography A, 1218 (2011) 6148-6155.

[33] M. Englert, W. Vetter, Tubing modifications for countercurrent chromatography (CCC): Stationary phase retention and separation efficiency, Analytica Chimica Acta, 884 (2015) 114-123.

[34] Y. Yang, H.A. Aisa, Y. Ito, Flat-twisted tubing: Novel column design for spiral high-speed counter-current chromatography, Journal of Chromatography A, 1216 (2009) 5265-5271.

[35] Y. Ito, W.D. Conway, High-speed countercurrent chromatography, Critical Reviews in Analytical Chemistry, 17 (1986) 65-143.

[36] M. Minceva, Model-based design of preparative liquid-chromatography processes, Habilitation, FAU Erlangen-Nuremberg, Erlangen, 2013.

[37] J. Goll, G. Audo, M. Minceva, Comparison of twin-cell centrifugal partition chromatographic columns with different cell volume, Journal of Chromatography A, 1406 (2015) 129-135.

[38] A. Berthod, J.B. Friesen, T. Inui, G.F. Pauli, Elution-extrusion countercurrent chromatography: theory and concepts in metabolic analysis, Analytical Chemistry, 79 (2007) 3371-3382.

[39] Y. Lu, Y. Pan, A. Berthod, Using the liquid nature of the stationary phase in counter-current chromatography: V. The back-extrusion method, Journal of Chromatography A, 1189 (2008) 10-18.

[40] E. Hopmann, A. Frey, M. Minceva, A priori selection of the mobile and stationary phase in centrifugal partition chromatography and counter-current chromatography, Journal of Chromatography A, 1238 (2012) 68-76.

[41] A. Frey, E. Hopmann, M. Minceva, Selection of Biphasic Liquid Systems in Liquid-Liquid Chromatography Using Predictive Thermodynamic Models, Chemical Engineering & Technology, 37 (2014) 1663-1674.

[42] M. Englert, S. Hammann, W. Vetter, Isolation of β-carotene, α-carotene and lutein from carrots by countercurrent chromatography with the solvent system modifier benzotrifluoride, Journal of Chromatography A, 1388 (2015) 119-125.

[43] I.A. Sutherland, D. Heywood-Waddington, Y. Ito, Counter-current chromatography: Applications to the separation of biopolymers, organelles and cells using either aqueous—organic or aqueous—aqueous phase systems, Journal of Chromatography A, 384 (1987) 197-207.

[44] I.A. Sutherland, Review of centrifugal liquid-liquid chromatography using aqueous two-phase solvent systems: Its scale-up and prospects for the future production of high-value biologicals, Current Opinion in Drug Discovery & Development, 10 (2007) 540-549.

[45] W. Zhang, Y. Hu, Y. Wang, J. Han, L. Ni, Y. Wu, Liquid–liquid equilibrium of aqueous two-phase systems containing poly(ethylene glycol) of different molecular weights and several ammonium salts at 298.15K, Thermochimica Acta, 560 (2013) 47-54.

[46] J.S. Wilkes, M.J. Zaworotko, Air and water stable 1-ethyl-3-methylimidazolium based ionic liquids, Journal of the Chemical Society, Chemical Communications, (1992) 965-967.

[47] J.G. Huddleston, H.D. Willauer, R.P. Swatloski, A.E. Visser, R.D. Rogers, Room temperature ionic liquids as novel media for 'clean' liquid-liquid extraction, Chemical Communications, (1998) 1765-1766.

[48] S.P.M. Ventura, F.A. e Silva, M.V. Quental, D. Mondal, M.G. Freire, J.A.P. Coutinho, Ionic-Liquid-Mediated Extraction and Separation Processes for Bioactive Compounds: Past, Present, and Future Trends, Chemical Reviews, 117 (2017) 6984-7052.

[49] H. Zhao, Protein stabilization and enzyme activation in ionic liquids: specific ion effects, Journal of Chemical Technology & Biotechnology, 91 (2015) 25-50.

[50] H. Zhao, S.M. Campbell, L. Jackson, Z. Song, O. Olubajo, Hofmeister series of ionic liquids: kosmotropic effect of ionic liquids on the enzymatic hydrolysis of enantiomeric phenylalanine methyl ester, Tetrahedron: Asymmetry, 17 (2006) 377-383.

[51] M. Bončina, J. Reščič, V. Vlachy, Solubility of Lysozyme in Polyethylene Glycol-Electrolyte Mixtures: The Depletion Interaction and Ion-Specific Effects, Biophysical Journal, 95 (2008) 1285-1294.

[52] I.M. Aroso, A. Paiva, R.L. Reis, A.R.C. Duarte, Natural deep eutectic solvents from choline chloride and betaine – Physicochemical properties, Journal of Molecular Liquids, 241 (2017) 654-661.

[53] R. Xin, S. Qi, C. Zeng, F.I. Khan, B. Yang, Y. Wang, A functional natural deep eutectic solvent based on trehalose: Structural and physicochemical properties, Food chemistry, 217 (2017) 560-567.

[54] Y. Liu, J.B. Friesen, J.B. McAlpine, D.C. Lankin, S.-N. Chen, G.F. Pauli, Natural Deep Eutectic Solvents: Properties, Applications, and Perspectives, Journal of Natural Products, 81 (2018) 679-690.

[55] C. Florindo, F.S. Oliveira, L.P.N. Rebelo, A.M. Fernandes, I.M. Marrucho, Insights into the Synthesis and Properties of Deep Eutectic Solvents Based on Cholinium Chloride and Carboxylic Acids, ACS Sustainable Chemistry & Engineering, 2 (2014) 2416-2425.

[56] D.A. Alonso, A. Baeza, R. Chinchilla, G. Guillena, I.M. Pastor, D.J. Ramón, Deep Eutectic Solvents: The Organic Reaction Medium of the Century, European Journal of Organic Chemistry, (2016) 612-632.

[57] Y. Dai, G.-J. Witkamp, R. Verpoorte, Y.H. Choi, Natural Deep Eutectic Solvents as a New Extraction Media for Phenolic Metabolites in Carthamus tinctorius L, Analytical Chemistry, 85 (2013) 6272-6278.

[58] B.Y. Zhao, P. Xu, F.X. Yang, H. Wu, M.H. Zong, W.Y. Lou, Biocompatible deep eutectic solvents based on choline chloride: characterization and application to the extraction of rutin from Sophora japonica, ACS Sustainable Chemistry & Engineering, 3 (2015) 2746-2755.

[59] A.K. Das, M. Sharma, D. Mondal, K. Prasad, Deep eutectic solvents as efficient solvent system for the extraction of κ-carrageenan from Kappaphycus alvarezii, Carbohydrate Polymers, 136 (2016) 930-935.

[60] A.P. Abbott, P.M. Cullis, M.J. Gibson, R.C. Harris, E. Raven, Extraction of glycerol from biodiesel into a eutectic based ionic liquid, Green Chemistry, 9 (2007) 868-872.

[61] K. Shahbaz, F.S. Mjalli, M. Hashim, I.M. Al-Nashef, Using deep eutectic solvents for the removal of glycerol from palm oil-based biodiesel, Journal of Applied Sciences, 10 (2010) 3349-3354.

[62] A. Hayyan, M.A. Hashim, M. Hayyan, F.S. Mjalli, I.M. AlNashef, A novel ammonium based eutectic solvent for the treatment of free fatty acid and synthesis of biodiesel fuel, Industrial Crops and Products, 46 (2013) 392-398.

[63] A. Hayyan, M.A. Hashim, M. Hayyan, F.S. Mjalli, I.M. AlNashef, A new processing route for cleaner production of biodiesel fuel using a choline chloride based deep eutectic solvent, Journal of Cleaner Production, 65 (2014) 246-251.

[64] X. Li, K.H. Row, Exploration of Mesoporous Stationary Phases Prepared Using Deep Eutectic Solvents Combining Choline Chloride with 1,2-Butanediol or Glycerol for Use in Size-Exclusion Chromatography, Chromatographia, 78 (2015) 1321-1325.

[65] G. Li, T. Zhu, Y. Lei, Choline chloride-based deep eutectic solvents as additives for optimizing chromatographic behavior of caffeic acid, Korean Journal of Chemical Engineering, 32 (2015) 2103-2108.

[66] A.A. Samarov, M.A. Smirnov, M.P. Sokolova, E.N. Popova, A.M. Toikka, Choline chloride based deep eutectic solvents as extraction media for separation of n-hexane–ethanol mixture, Fluid Phase Equilibria, 448 (2017) 123-127.

[67] M.A. Kareem, F.S. Mjalli, M.A. Hashim, M.K.O. Hadj-Kali, F.S. Ghareh Bagh, I.M. Alnashef, Phase equilibria of toluene/heptane with deep eutectic solvents based on ethyltriphenylphosphonium iodide for the potential use in the separation of aromatics from naphtha, The Journal of Chemical Thermodynamics, 65 (2013) 138-149.

[68] S. Mulyono, H.F. Hizaddin, I.M. Alnashef, M.A. Hashim, A.H. Fakeeha, M.K. Hadj-Kali, Separation of BTEX aromatics from n-octane using a (tetrabutylammonium bromide + sulfolane) deep eutectic solvent - experiments and COSMO-RS prediction, RSC Advances, 4 (2014) 17597-17606.

[69] N.R. Rodriguez, B.S. Molina, M.C. Kroon, Aliphatic + ethanol separation via liquid–liquid extraction using low transition temperature mixtures as extracting agents, Fluid Phase Equilibria, 394 (2015) 71-82.

[70] N.R. Rodriguez, J. Ferre Guell, M.C. Kroon, Glycerol-Based Deep Eutectic Solvents as Extractants for the Separation of MEK and Ethanol via Liquid–Liquid Extraction, Journal of Chemical & Engineering Data, 61 (2016) 865-872.

[71] A.S.L. Gouveia, F.S. Oliveira, K.A. Kurnia, I.M. Marrucho, Deep Eutectic Solvents as Azeotrope Breakers: Liquid–Liquid Extraction and COSMO-RS Prediction, ACS Sustainable Chemistry & Engineering, 4 (2016) 5640-5650.

[72] A.P. Abbott, R.C. Harris, K.S. Ryder, C. D'Agostino, L.F. Gladden, M.D. Mantle, Glycerol eutectics as sustainable solvent systems, Green Chemistry, 13 (2011) 82-90.

[73] F. Bezold, M. Minceva, Liquid-liquid equilibria of n-heptane, methanol and deep eutectic solvents composed of carboxylic acid and monocyclic terpenes, Fluid Phase Equilibria, 477 (2018) 98-106.

[74] J.M. Prausnitz, R.N. Lichtenthaler, E.G. de Azevedo, Molecular Thermodynamics of Fluid-Phase Equilibria, Prentice Hall PTR, Upper Saddle River, NJ, 1999.

[75] J. Gmehling, B. Kolbe, M. Kleiber, J. Rarey, Chemical thermodynamics for process simulation, John Wiley & Sons, 2012.

[76] E. Hopmann, W. Arlt, M. Minceva, Solvent system selection in counter-current chromatography using conductor-like screening model for real solvents, Journal of Chromatography A, 1218 (2011) 242-250.

[77] A. Klamt, Conductor-like Screening Model for Real Solvents: A New Approach to the Quantitative Calculation of Solvation Phenomena, The Journal of Physical Chemistry, 99 (1995) 2224-2235.

[78] A. Klamt, Chapter 2 - Dielectric continuum solvation models and COSMO, in: A. Klamt (Ed.) COSMO-RS, Elsevier, Amsterdam, 2005, pp. 11-41.

[79] A. Klamt, The COSMO and COSMO-RS solvation models, Wiley Interdisciplinary Reviews: Computational Molecular Science, 1 (2011) 699-709.

[80] M. Diedenhofen, A. Klamt, COSMO-RS as a tool for property prediction of IL mixtures—A review, Fluid Phase Equilibria, 294 (2010) 31-38.

[81] F. Bezold, M.E. Weinberger, M. Minceva, Assessing solute partitioning in deep eutectic solvent-based biphasic systems using the predictive thermodynamic model COSMO-RS, Fluid Phase Equilibria, 437 (2017) 23-33.

[82] C. Florindo, L.C. Branco, I.M. Marrucho, Development of hydrophobic deep eutectic solvents for extraction of pesticides from aqueous environments, Fluid Phase Equilibria, 448 (2017) 135-142.

[83] M. Naushad, Z.A. Alothman, A.B. Khan, M. Ali, Effect of ionic liquid on activity, stability, and structure of enzymes: A review, International Journal of Biological Macromolecules, 51 (2012) 555-560.

[84] R. Buchfink, A. Tischer, G. Patil, R. Rudolph, C. Lange, Ionic liquids as refolding additives: Variation of the anion, Journal of biotechnology, 150 (2010) 64-72.

[85] H. Zhao, Effect of ions and other compatible solutes on enzyme activity, and its implication for biocatalysis using ionic liquids, Journal of Molecular Catalysis B: Enzymatic, 37 (2005) 16-25.

[86] M. Shinitzky, E. Katchalski, V. Grisaro, N. Sharon, Inhibition of lysozyme by imidazole and indole derivatives, Archives of Biochemistry and Biophysics, 116 (1966) 332-343.

[87] N.J. Greenfield, Using circular dichroism spectra to estimate protein secondary structure, Nature Protocols, 1 (2007) 2876.

[88] S.A. Oelmeier, C. Ladd Effio, J. Hubbuch, High throughput screening based selection of phases for aqueous two-phase system-centrifugal partitioning chromatography of monoclonal antibodies, Journal of Chromatography A, 1252 (2012) 104-114.

[89] S.A. Oelmeier, C. Ladd-Effio, J. Hubbuch, Alternative separation steps for monoclonal antibody purification: Combination of centrifugal partitioning chromatography and precipitation, Journal of Chromatography A, 1319 (2013) 118-126.

[90] A.M. Azevedo, A.G. Gomes, P.A.J. Rosa, I.F. Ferreira, A.M.M.O. Pisco, M.R. Aires-Barros, Partitioning of human antibodies in polyethylene glycol–sodium citrate aqueous two-phase systems, Separation and Purification Technology, 65 (2009) 14-21.

[91] J.A. Fagan, C.Y. Khripin, C.A. Silvera Batista, J.R. Simpson, E.H. Hároz, A.R. Hight Walker, M. Zheng, Isolation of Specific Small-Diameter Single-Wall Carbon Nanotube Species via Aqueous Two-Phase Extraction, Advanced Materials, 26 (2014) 2800-2804.

[92] M. Knight, R. Lazo-Portugal, S.N. Ahn, S. Stefansson, Purification of semiconducting single-walled carbon nanotubes by spiral counter-current chromatography, Journal of Chromatography A, 1483 (2017) 93-100.

[93] C. Ladd Effio, L. Wenger, O. Ötes, S.A. Oelmeier, R. Kneusel, J. Hubbuch, Downstream processing of virus-like particles: Single-stage and multi-stage aqueous two-phase extraction, Journal of Chromatography A, 1383 (2015) 35-46.

[94] K.L. Wade, Y. Ito, A. Ramarathnam, W.D. Holtzclaw, J.W. Fahey, Purification of Active Myrosinase from Plants by Aqueous Two-Phase Counter-Current Chromatography, Phytochemical Analysis, 26 (2015) 47-53.

[95] A.S. Schmidt, A.M. Ventom, J.A. Asenjo, Partitioning and purification of α-amylase in aqueous two-phase systems, Enzyme and Microbial Technology, 16 (1994) 131-142.

[96] C. Schwienheer, A. Prinz, T. Zeiner, J. Merz, Separation of active laccases from Pleurotus sapidus culture supernatant using aqueous two-phase systems in centrifugal partition chromatography, Journal of Chromatography B, 1002 (2015) 1-7.

[97] F.S. Oliveira, A.B. Pereiro, L.P.N. Rebelo, I.M. Marrucho, Deep eutectic solvents as extraction media for azeotropic mixtures, Green Chemistry, 15 (2013) 1326-1330.

[98] N.R. Rodriguez, T. Gerlach, D. Scheepers, M.C. Kroon, I. Smirnova, Experimental determination of the LLE data of systems consisting of {hexane + benzene + deep eutectic solvent} and prediction using the Conductor-like Screening Model for Real Solvents, The Journal of Chemical Thermodynamics, 104 (2017) 128-137.

[99] K.A. Kurnia, N.A. Athirah, F.J.M. Candieiro, B. Lal, Phase Behavior of Ternary Mixtures {Aliphatic Hydrocarbon + Aromatic Hydrocarbon + Deep Eutectic Solvent}: A Step Forward toward "Greener" Extraction Process, Procedia Engineering, 148 (2016) 1340-1345.

[100] M.A. Kareem, F.S. Mjalli, M.A. Hashim, M.K.O. Hadj-Kali, F.S.G. Bagh, I.M. Alnashef, Phase equilibria of toluene/heptane with tetrabutylphosphonium bromide based deep eutectic solvents for the potential use in the separation of aromatics from naphtha, Fluid Phase Equilibria, 333 (2012) 47-54.

[101] M.A. Kareem, F.S. Mjalli, M.A. Hashim, I.M. AlNashef, Liquid–liquid equilibria for the ternary system (phosphonium based deep eutectic solvent–benzene–hexane) at different temperatures: A new solvent introduced, Fluid Phase Equilibria, 314 (2012) 52-59.

[102] A. Das, S. Das, R. Biswas, Density relaxation and particle motion characteristics in a non-ionic deep eutectic solvent (acetamide + urea): Time-resolved fluorescence measurements and all-atom molecular dynamics simulations, Journal of Chemical Physics, 142 (2015) 034505.

[103] S.L. Perkins, P. Painter, C.M. Colina, Molecular Dynamic Simulations and Vibrational Analysis of an Ionic Liquid Analogue, The Journal of Physical Chemistry B, 117 (2013) 10250-10260.

[104] A. Das, S. Das, R. Biswas, Fast fluctuations in deep eutectic melts: Multi-probe fluorescence measurements and all-atom molecular dynamics simulation study, Chemical Physics Letters, 581 (2013) 47-51.

[105] S.L. Perkins, P. Painter, C.M. Colina, Experimental and computational studies of choline chloride-based deep eutectic solvents, Journal of Chemical and Engineering Data, 59 (2014) 3652-3662.

[106] G. García, M. Atilhan, S. Aparicio, The impact of charges in force field parameterization for molecular dynamics simulations of deep eutectic solvents, Journal of Molecular Liquids, 211 (2015) 506-514.

[107] S. Kaur, A. Gupta, H.K. Kashyap, Nanoscale Spatial Heterogeneity in Deep Eutectic Solvents, The Journal of Physical Chemistry B, 120 (2016) 6712-6720.

[108] S. Mainberger, M. Kindlein, F. Bezold, E. Elts, M. Minceva, H. Briesen, Deep eutectic solvent formation: a structural view using molecular dynamics simulations with classical force fields, Molecular Physics, 115 (2017) 1309-1321.

[109] R. Stefanovic, M. Ludwig, G.B. Webber, R. Atkin, A.J. Page, Nanostructure, hydrogen bonding and rheology in choline chloride deep eutectic solvents as a function of the hydrogen bond donor, Physical Chemistry Chemical Physics, 19 (2017) 3297-3306.

[110] Y. Cui, D.G. Kuroda, Evidence of Molecular Heterogeneities in Amide-Based Deep Eutectic Solvents, The Journal of Physical Chemistry A, 122 (2018) 1185-1193.

[111] I. Zahrina, M. Nasikin, K. Mulia, M. Prajanto, A. Yanuar, Molecular interactions between betaine monohydrate-glycerol deep eutectic solvents and palmitic acid: Computational and experimental studies, Journal of Molecular Liquids, 251 (2018) 28–34.

[112] S. Zahn, B. Kirchner, D. Mollenhauer, Charge Spreading in Deep Eutectic Solvents, ChemPhysChem, 17 (2016) 3354-3358.

[113] S. Zahn, Deep eutectic solvents: similia similibus solvuntur?, Physical Chemistry Chemical Physics, 19 (2017) 4041-4047.

[114] A. Korotkevich, D.S. Firaha, A.A.H. Padua, B. Kirchner, Ab initio molecular dynamics simulations of SO2 solvation in choline chloride/glycerol deep eutectic solvent, Fluid Phase Equilibria, 448 (2017) 59-68.

[115] D.V. Wagle, L. Adhikari, G.A. Baker, Computational perspectives on structure, dynamics, gas sorption, and bio-interactions in deep eutectic solvents, Fluid Phase Equilibria, 448 (2017) 50-58.

[116] R. Ullah, M. Atilhan, B. Anaya, M. Khraisheh, G. Garcia, A. ElKhattat, M. Tariq, S. Aparicio, A detailed study of cholinium chloride and levulinic acid deep eutectic solvent system for CO2 capture via experimental and molecular simulation approaches, Physical Chemistry Chemical Physics, 17 (2015) 20941-20960.

[117] D. Shah, F.S. Mjalli, Effect of water on the thermo-physical properties of Reline: An experimental and molecular simulation based approach, Physical Chemistry Chemical Physics, 16 (2014) 23900-23907.

[118] C. D'Agostino, L.F. Gladden, M.D. Mantle, A.P. Abbott, E.I. Ahmed, A.Y.M. Al-Murshedi, R.C. Harris, Molecular and ionic diffusion in aqueous - deep eutectic solvent mixtures: probing inter-molecular interactions using PFG NMR, Physical Chemistry Chemical Physics, 17 (2015) 15297-15304.

[119] T. Zhekenov, N. Toksanbayev, Z. Kazakbayeva, D. Shah, F.S. Mjalli, Formation of type III Deep Eutectic Solvents and effect of water on their intermolecular interactions, Fluid Phase Equilibria, 441 (2017) 43-48.

[120] H. Monhemi, M.R. Housaindokht, A.A. Moosavi-Movahedi, M.R. Bozorgmehr, How a protein can remain stable in a solvent with high content of urea: insights from molecular dynamics simulation of Candida antarctica lipase B in urea : choline chloride deep eutectic solvent, Physical Chemistry Chemical Physics, 16 (2014) 14882-14893.

[121] Y. Cui, K.D. Fulfer, J. Ma, T.K. Weldeghiorghis, D.G. Kuroda, Solvation dynamics of an ionic probe in choline chloride-based deep eutectic solvents, Physical Chemistry Chemical Physics, 18 (2016) 31471-31479.

[122] Y. Dai, R. Verpoorte, Y.H. Choi, Natural deep eutectic solvents providing enhanced stability of natural colorants from safflower (Carthamus tinctorius), Food chemistry, 159 (2014) 116-121.

[123] F. Kholiya, N. Bhatt, M.R. Rathod, R. Meena, K. Prasad, Fundamental studies on the feasibility of deep eutectic solvents for the selective partition of glaucarubinone present in the roots of Simarouba glauca, Journal of Separation Science, 38 (2015) 3170-3175.

[124] B. Tang, H. Zhang, K.H. Row, Application of deep eutectic solvents in the extraction and separation of target compounds from various samples, Journal of Separation Science, 38 (2015) 1053-1064.

[125] Z. Helalat–Nezhad, K. Ghanemi, M. Fallah–Mehrjardi, Dissolution of biological samples in deep eutectic solvents: An approach for extraction of polycyclic aromatic hydrocarbons followed by liquid chromatography-fluorescence detection, Journal of Chromatography A, 1394 (2015) 46-53.

[126] X.L. Qi, X. Peng, Y.Y. Huang, L. Li, Z.F. Wei, Y.G. Zu, Y.J. Fu, Green and efficient extraction of bioactive flavonoids from Equisetum palustre L. by deep eutectic solvents-based negative pressure cavitation method combined with macroporous resin enrichment, Industrial Crops and Products, 70 (2015) 142-148.

[127] N.m. Abdul Hadi, M.H. Ng, Y.M. Choo, M.A. Hashim, N.S. Jayakumar, Performance of Choline-Based Deep Eutectic Solvents in the Extraction of Tocols from Crude Palm Oil, Journal of the American Oil Chemists' Society, 92 (2015) 1709-1716.

[128] L. Duan, L.-L. Dou, L. Guo, P. Li, E.H. Liu, Comprehensive Evaluation of Deep Eutectic Solvents in Extraction of Bioactive Natural Products, ACS Sustainable Chemistry & Engineering, 4 (2016) 2405-2411.

[129] Y. Dai, E. Rozema, R. Verpoorte, Y.H. Choi, Application of natural deep eutectic solvents to the extraction of anthocyanins from Catharanthus roseus with high extractability and stability replacing conventional organic solvents, Journal of Chromatography A, 1434 (2016) 50-56.

[130] H. Lores, V. Romero, I. Costas, C. Bendicho, I. Lavilla, Natural deep eutectic solvents in combination with ultrasonic energy as a green approach for solubilisation of proteins: application to gluten determination by immunoassay, Talanta, 162 (2017) 453-459.

[131] C. Bai, Q. Wei, X. Ren, Selective Extraction of Collagen Peptides with High Purity from Cod Skins by Deep Eutectic Solvents, ACS Sustainable Chemistry & Engineering, 5 (2017) 7220-7227.

[132] A. Foucault, K. Nakanishi, Comparison of Several Aqueous two Phase Solvent Systems (ATPS) for the Fractionation of Biopolymers by Centrifugal Partition Chromatography (CPC), Journal of Liquid Chromatography, 13 (1990) 2421-2440.

[133] I.A. Sutherland, G. Audo, E. Bourton, F. Couillard, D. Fisher, I. Garrard, P. Hewitson, O. Intes, Rapid linear scale-up of a protein separation by centrifugal partition chromatography, Journal of Chromatography A, 1190 (2008) 57-62.

[134] I. Sutherland, P. Hewitson, R. Siebers, R. van den Heuvel, L. Arbenz, J. Kinkel, D. Fisher, Scale-up of protein purifications using aqueous two-phase systems: Comparing multilayer toroidal coil chromatography with centrifugal partition chromatography, Journal of Chromatography A, 1218 (2011) 5527-5530.

[135] D. Dasarathy, Y. Ito, An improved design of spiral tube assembly for separation of proteins by high-speed counter-current chromatography, Journal of Chromatography A, 1418 (2015) 77-82.

[136] R. Sadeghi, B. Jamehbozorg, Effect of temperature on the salting-out effect and phase separation in aqueous solutions of sodium di-hydrogen phosphate and poly(propylene glycol), Fluid Phase Equilibria, 271 (2008) 13-18.

[137] M.G. Freire, J.F.B. Pereira, M. Francisco, H. Rodríguez, L.P.N. Rebelo, R.D. Rogers, J.A.P. Coutinho, Insight into the Interactions That Control the Phase Behaviour of New Aqueous Biphasic Systems Composed of Polyethylene Glycol Polymers and Ionic Liquids, Chemistry – A European Journal, 18 (2012) 1831-1839.

[138] S.C. Silvério, A. Wegrzyn, E. Lladosa, O. Rodríguez, E.A. Macedo, Effect of Aqueous Two-Phase System Constituents in Different Poly(ethylene glycol)–Salt Phase Diagrams, Journal of Chemical & Engineering Data, 57 (2012) 1203-1208.

[139] T. Takekiyo, K. Yamazaki, E. Yamaguchi, H. Abe, Y. Yoshimura, High Ionic Liquid Concentration-Induced Structural Change of Protein in Aqueous Solution: A Case Study of Lysozyme, The Journal of Physical Chemistry B, 116 (2012) 11092-11097.

[140] R. Patel, M. Kumari, A.B. Khan, Recent Advances in the Applications of Ionic Liquids in Protein Stability and Activity: A Review, Applied Biochemistry and Biotechnology, 172 (2014) 3701-3720.

[141] M. Hübner, C. Lodziak, H.T.J. Do, C. Held, Measuring and modeling thermodynamic properties of aqueous lysozyme and BSA solutions, Fluid Phase Equilibria, 472 (2018) 62-74.

[142] T. Reschke, C. Brandenbusch, G. Sadowski, Modeling aqueous two-phase systems: I. Polyethylene glycol and inorganic salts as ATPS former, Fluid Phase Equilibria, 368 (2014) 91-103.

Appendix: Supplementary information for Paper I, II, and IV

Supporting Information

Ionic Liquids as Modifying Agents for Protein Separation in Centrifugal Partition Chromatography

Franziska Bezold, Simon Roehrer, Mirjana Minceva*

DOI: 10.1002/ceat.201800369

Correspondence: Dr. Mirjana Minceva (mirjana.minceva@tum.de), Technical University of Munich, Biothermodynamics, TUM School of Life and Food Sciences Weihenstephan, Maximus-von-Imhof-Forum 2, 85354 Freising, Germany.

Table S1. Summarized partition coefficients in the biphasic system PEG 1000/K_2HPO_4/KH_2PO_4/H_2O 15.00/9.68/5.32/70.00 wt/wt/wt/wt without and with [EMIM]Cl or [BMIM]Cl.

ATPS	$P_{myoglobin}$ /-		$P_{lysozyme}$ /-		P_{IL} /-
Analytical method	spectroscopy	CPC	spectroscopy	CPC	HPLC
No additive	0.02±0.01	0.04	2.86±0.15	3.02	-
+ 0.5 wt% [EMIM]Cl	0.05±0.01	-	2.51±0.09	-	0.85±0.03
+ 1.0 wt% [EMIM]Cl	0.04±0.00	-	2.44±0.18	-	0.89±0.04
+ 1.5 wt% [EMIM]Cl	0.04±0.01	0.11 ($V_{inj.}$=10 ml) 0.22 ($V_{inj.}$=50 ml)	1.91±0.11	2.17 ($V_{inj.}$=10 ml) 2.11 ($V_{inj.}$=50 ml)	0.90±0.01
+ 2.5 wt% [EMIM]Cl	0.02±0.00	0.07	1.98±0.11	1.84	0.90±0.01
+ 0.5 wt% [BMIM]Cl	0.03±0.01	-	2.74±0.12	-	1.35±0.00
+ 1.0 wt% [BMIM]Cl	0.04±0.03	-	2.23±0.19	-	1.38±0.02
+ 1.5 wt% [BMIM]Cl	0.02±0.00	-	2.55±0.33	-	1.52±0.01
+ 2.5 wt% [BMIM]Cl	0.03±0.01	-	1.68±0.40	-	1.27±0.01

Table S2. Summarized values of S_f for ascending and descending mode without feed injection in PEG 1000/K_2HPO_4/KH_2PO_4/H_2O 15.00/9.68/5.32/70.00 wt/wt/wt/wt without and with additional [EMIM]Cl.

ATPS	Mobile phase flow rate /ml min^{-1}	Ascending mode	Descending mode
No additive	5	0.79	0.79
	10	0.63	0.72
	15	0.49	0.70
	20	0.36	0.61
+ 1.5 wt% [EMIM]Cl	5	0.75	0.79
	10	0.62	0.73
	15	0.44	0.68
	20	-	0.62
+ 2.5 wt% [EMIM]Cl	10	-	0.67
	15	-	0.63
	20	-	0.55

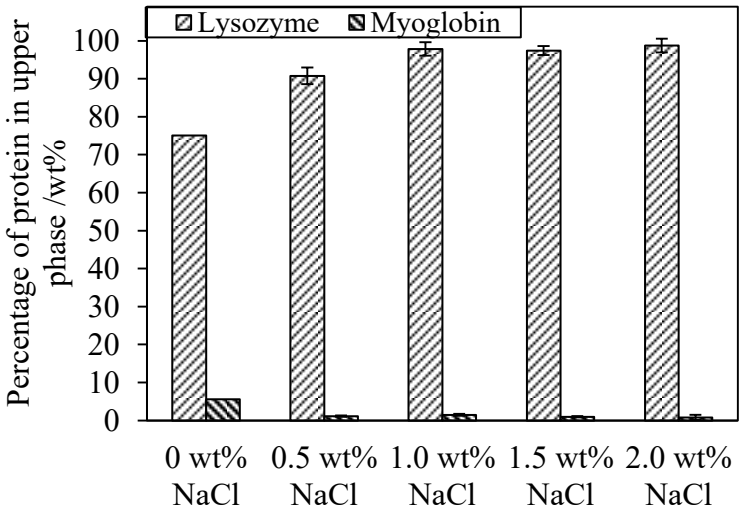

Figure S1. Percentage of protein in the upper phase of PEG 1000/K_2HPO_4/KH_2PO_4/H_2O 15.00/9.68/5.32/70.00 wt/wt/wt/wt with addition of sodium chloride.

Table S3. Percentage of lysozyme and myoglobin in the phases of PEG 1000/K_2HPO_4/KH_2PO_4/H_2O 15.00/9.68/5.32/70.00 wt/wt/wt/wt with addition of sodium chloride.

ATPS	Lysozyme		Myoglobin	
	wt% in upper phase	wt% in lower phase	wt% in upper phase	wt% in lower phase
No additive	75.12	24.88	5.66	94.34
+ 0.5 wt% NaCl	90.76	9.24	1.13	98.87
+ 1.0 wt% NaCl	97.87	2.13	1.48	98.52
+ 1.5 wt% NaCl	97.43	2.57	0.99	99.01
+ 2.0 wt% NaCl	98.74	1.26	0.84	99.16

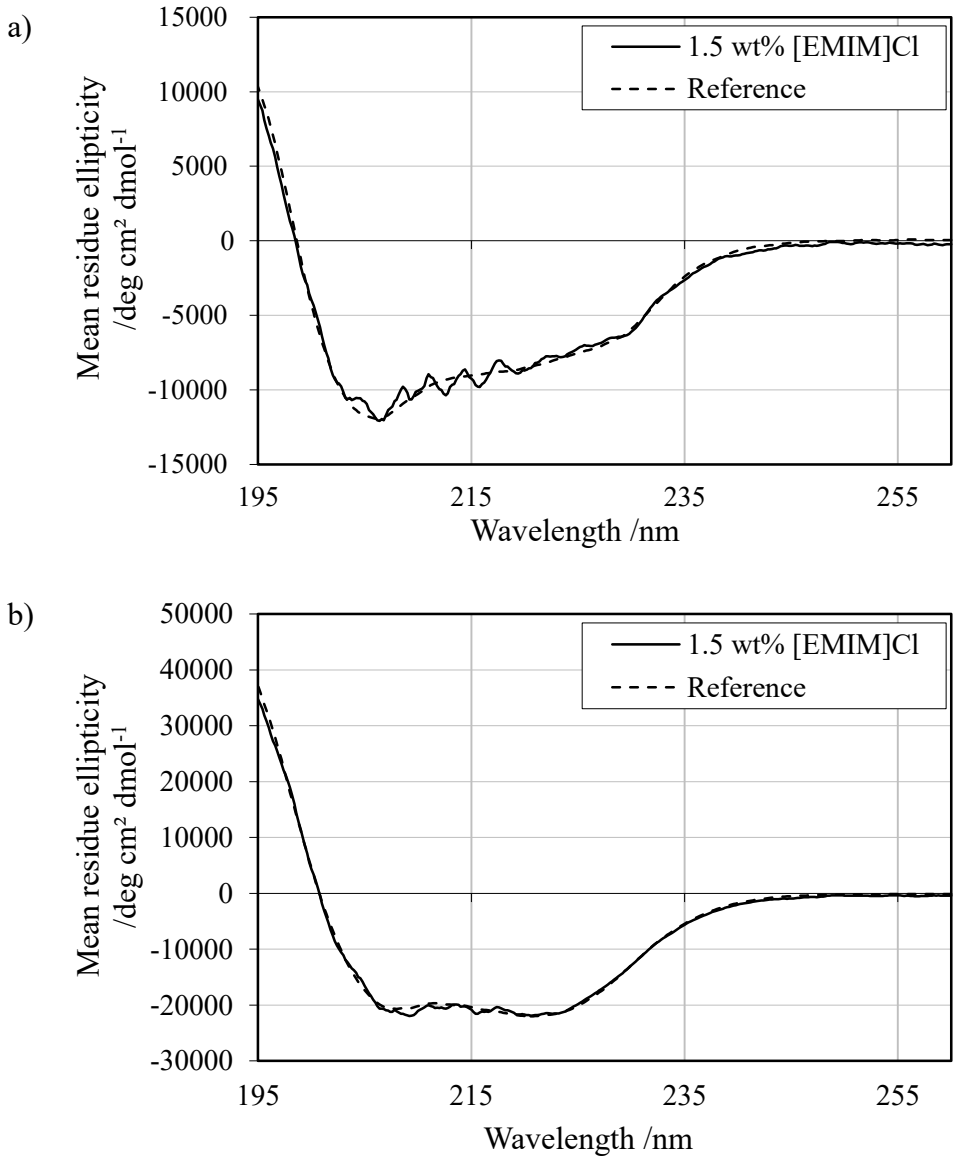

Figure S2. Circular dichroism spectra of (a) lysozyme in phosphate buffer (reference, dashed line) and lysozyme after exposure to [EMIM]Cl, and (b) myoglobin in phosphate buffer (reference, dashed line) and myoglobin after exposure to [EMIM]Cl, all at pH 7. The reference spectrum was recorded in 5 mM phosphate buffer with 50 µM of the respective protein. The samples with [EMIM]Cl were prepared with 1.5 wt% [EMIM]Cl in phosphate buffer with 0.14 mM lysozyme or 0.15 mM myoglobin and had to be diluted with 5mM phosphate buffer for CD-measurement.

Assessing solute partitioning in deep eutectic solvent-based biphasic systems using the predictive thermodynamic model COSMO-RS

Franziska Bezold, Maria E Weinberger, Mirjana Minceva

Supporting information

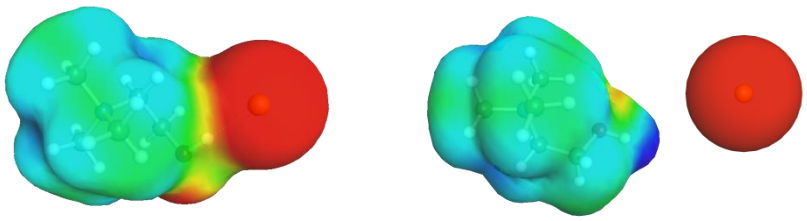

Figure S1: Associated (ion pair, left) and dissociated (electroneutral, right) representation of choline chloride in COSMOtherm.

Table S1: Logarithmic activity coefficients at infinite dilution of various organic solvents in the DES choline chloride-glycerol 1:1. COSMO-RS predictions were done with TZVP and TZVPD-FINE parameterization and different modeling approaches, experimental values taken from [1]

compound	experimental	parameterization	ion pair	electro-neutral
octane	6.43	TZVP	5.29	2.73
		TZVPD-FINE	9.19	7.48
n-decane	6.74	TZVP	6.44	3.39
		TZVPD-FINE	11.25	9.09
dodecane	7.20	TZVP	7.57	4.04
		TZVPD-FINE	13.27	10.62
tetradecane	8.52	TZVP	8.69	4.67
		TZVPD-FINE	15.29	12.10
benzene	3.30	TZVP	1.55	0.39
		TZVPD-FINE	2.99	2.44
toluene	4.10	TZVP	2.11	0.69
		TZVPD-FINE	4.08	3.40
cyclohexane	5.43	TZVP	3.30	1.49
		TZVPD-FINE	5.91	4.84
methanol	-0.51	TZVP	-0.83	-1.93
		TZVPD-FINE	-0.92	-1.16
ethanol	0.79	TZVP	-0.44	-1.72
		TZVPD-FINE	0.01	-0.41
propanol	1.63	TZVP	-0.08	-1.65
		TZVPD-FINE	0.85	0.37
1-butanol	2.24	TZVP	0.35	-1.46
		TZVPD-FINE	1.61	1.02
1-pentanol	3.52	TZVP	0.79	-1.28
		TZVPD-FINE	2.64	1.94
methyl isobutyl ketone	4.19	TZVP	1.79	0.46
		TZVPD-FINE	3.61	2.40
acetonitrile	1.06	TZVP	0.00	-0.18
		TZVPD-FINE	-0.28	-0.66
ethylacetate	3.33	TZVP	1.11	0.17
		TZVPD-FINE	2.31	1.58
tetrahydrofuran	2.42	TZVP	0.82	-0.17
		TZVPD-FINE	2.04	0.91
pyridine	1.53	TZVP	0.44	-0.33
		TZVPD-FINE	1.02	0.09
RMSD		TZVP	1.61	3.22
		TZVPD-FINE	2.63	1.78

Prediction of liquid-liquid equilibria

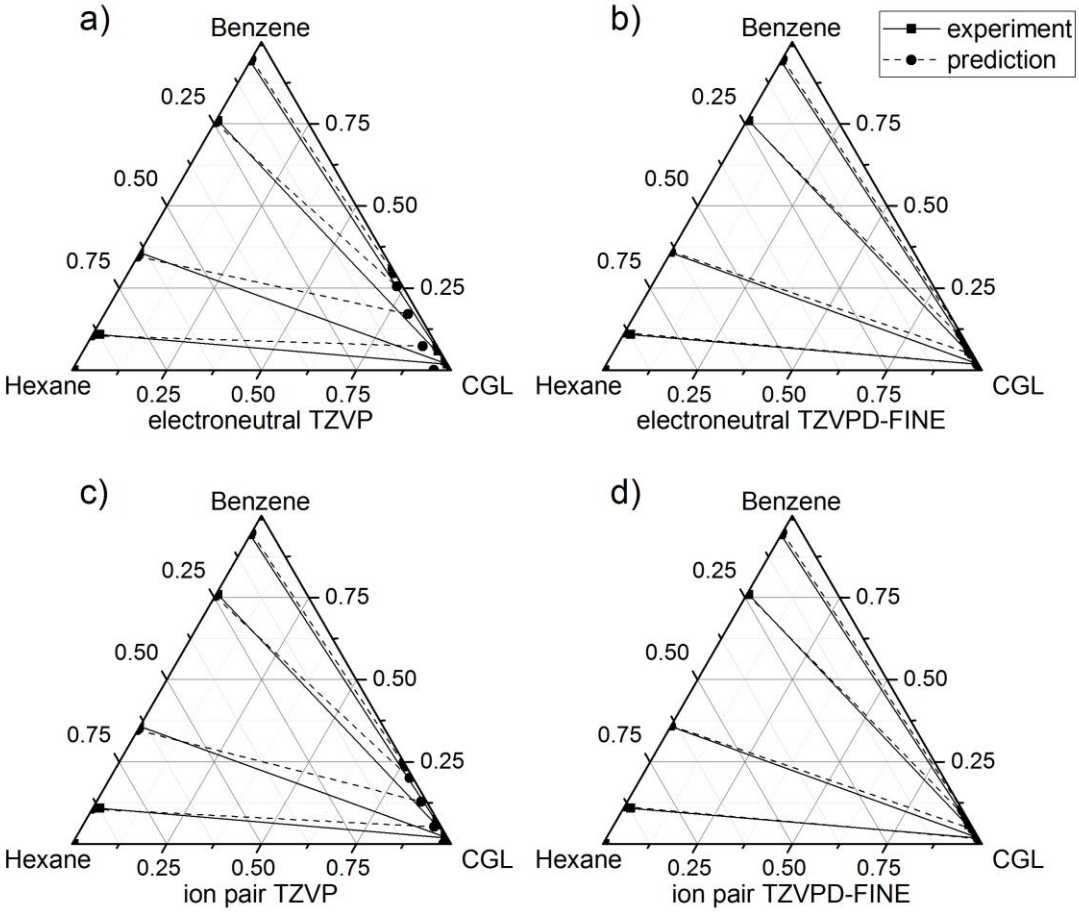

Figure S2: Experimental vs. COSMO-RS predicted tie lines for the ternary system hexane/benzene/CGL with (a) TZVP parameterization with electroneutral, (b) TZVPD-FINE parameterization with electroneutral, (c) TZVP parameterization and ion pair, and (d) TZVPD-FINE parameterization with ion pair representation of DES molecules; experimental data taken from [2]

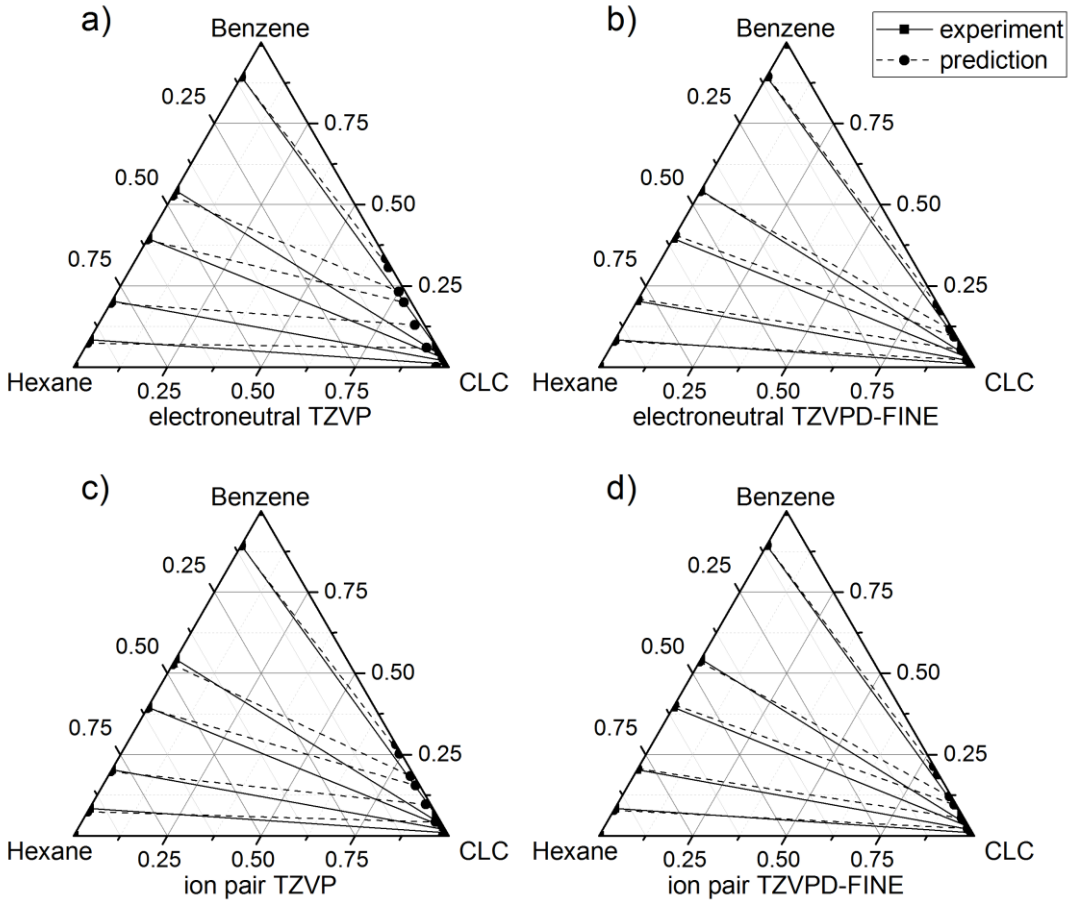

Figure S3: Experimental vs. COSMO-RS predicted tie lines for the ternary system hexane/benzene/CLC with (a) TZVP parameterization with electroneutral, (b) TZVPD-FINE parameterization with electroneutral, (c) TZVP parameterization and ion pair, and (d) TZVPD-FINE parameterization with ion pair representation of DES molecules; experimental data taken from [2]

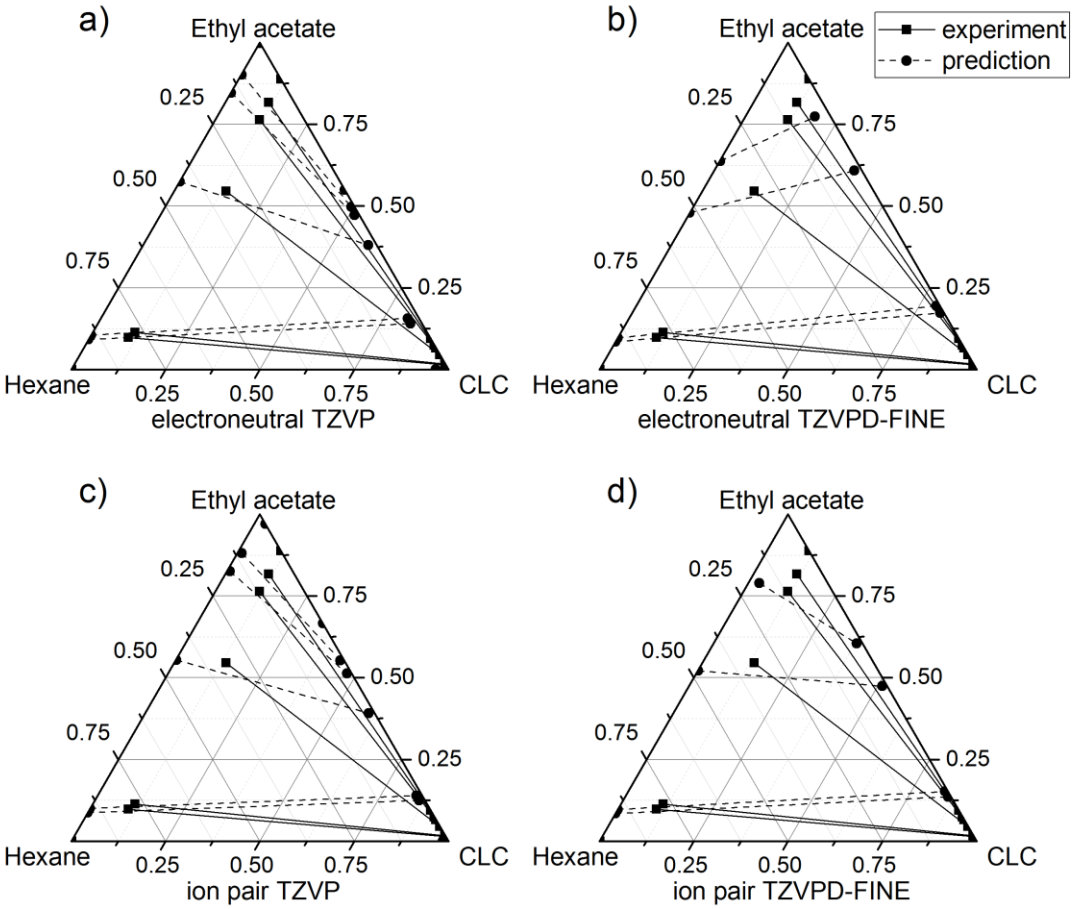

Figure S4: Experimental vs. COSMO-RS predicted tie lines for the ternary system hexane/ethyl acetate/CLC with (a) TZVP parameterization with electroneutral, (b) TZVPD-FINE parameterization with electroneutral, (c) TZVP parameterization and ion pair, and (d) TZVPD-FINE parameterization with ion pair representation of DES molecules; experimental data taken from [2]

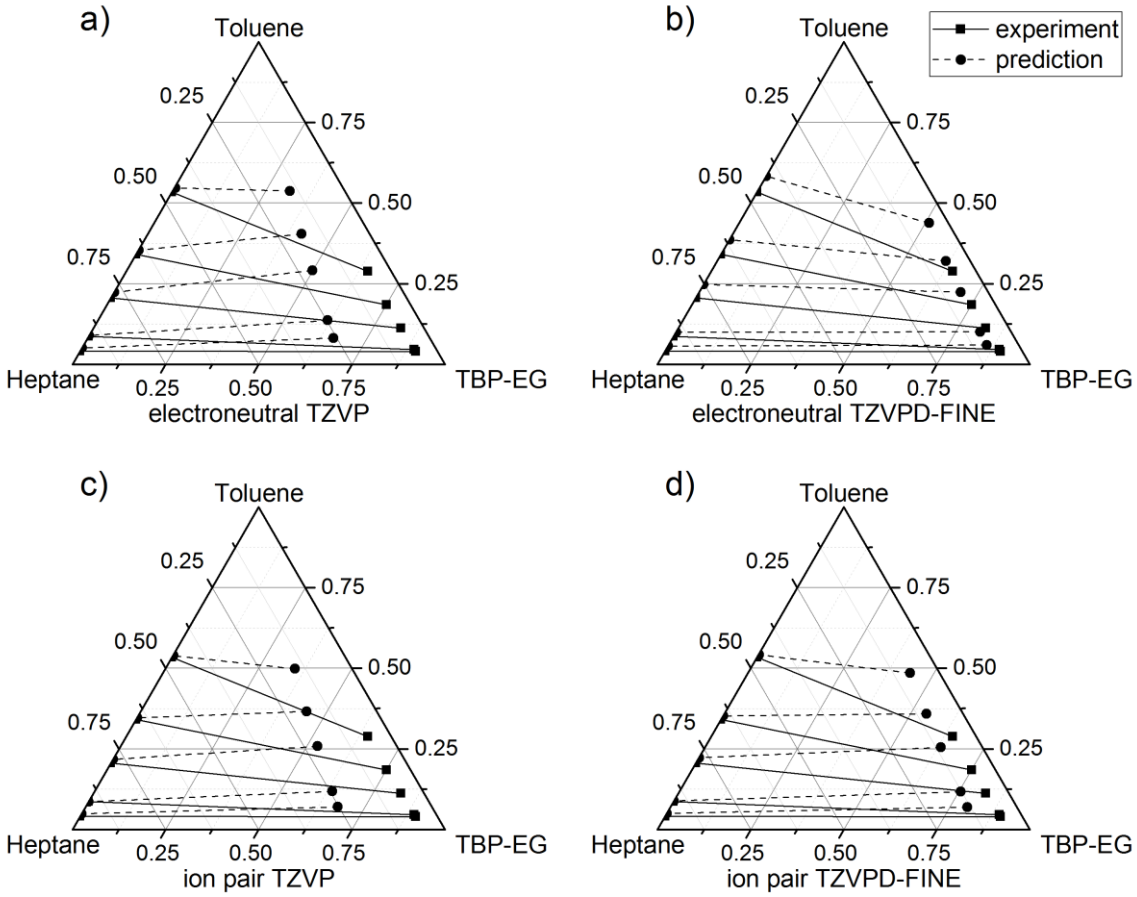

Figure S5: Experimental vs. COSMO-RS predicted tie lines for the ternary system heptane/toluene/TBP-EG with (a) TZVP parameterization with electroneutral, (b) TZVPD-FINE parameterization with electroneutral, (c) TZVP parameterization and ion pair, and (d) TZVPD-FINE parameterization with ion pair representation of DES molecules; experimental data taken from [3]

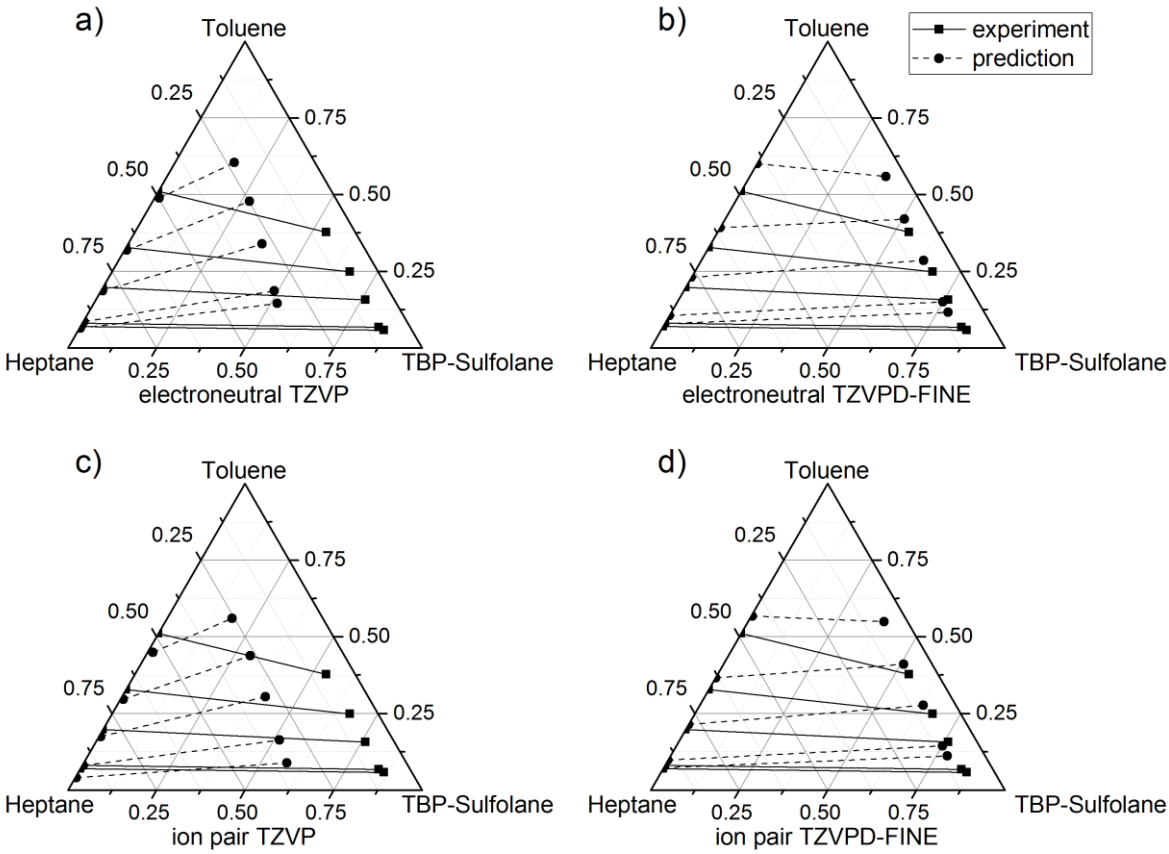

Figure S6: Experimental vs. COSMO-RS predicted tie lines for the ternary system heptane/toluene/TBP-Sulfolane with (a) TZVP parameterization with electroneutral, (b) TZVPD-FINE parameterization with electroneutral, (c) TZVP parameterization and ion pair, and (d) TZVPD-FINE parameterization with ion pair representation of DES molecules; experimental data taken from [3]

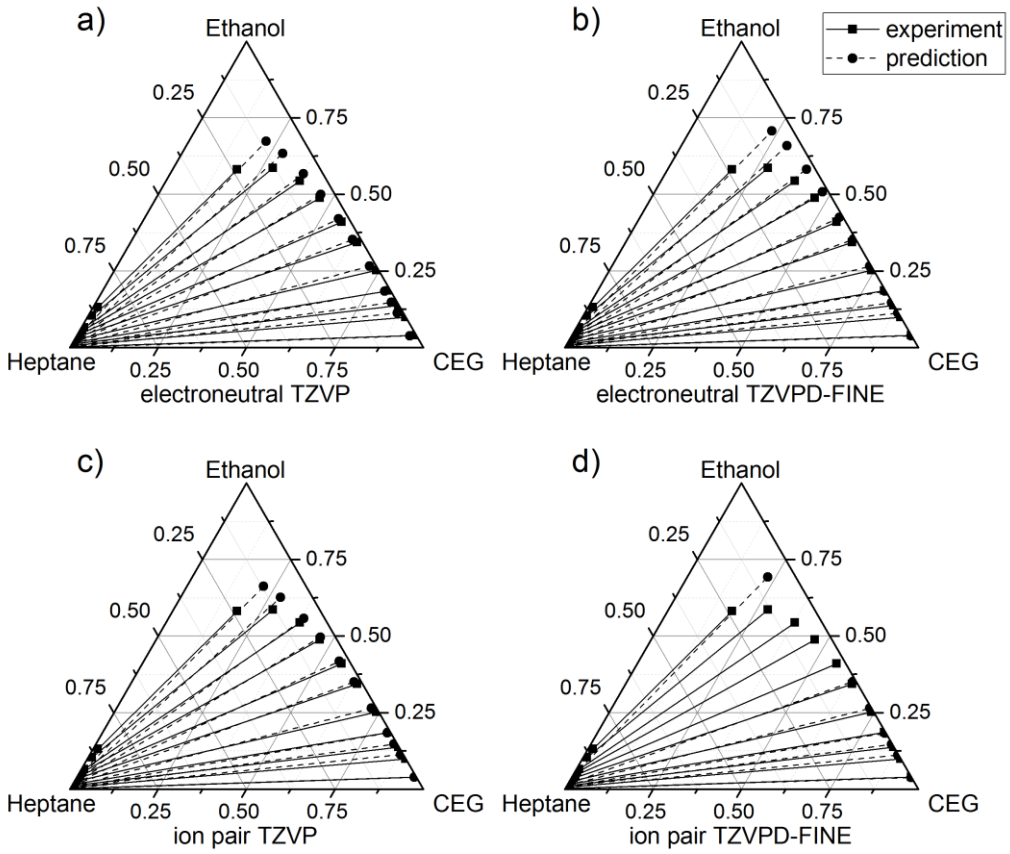

Figure S7: Experimental vs. COSMO-RS predicted tie lines for the ternary system heptane/ethanol/CEG with (a) TZVP parameterization with electroneutral, (b) TZVPD-FINE parameterization with electroneutral, (c) TZVP parameterization and ion pair, and (d) TZVPD-FINE parameterization with ion pair representation of DES molecules; experimental data taken from [4]

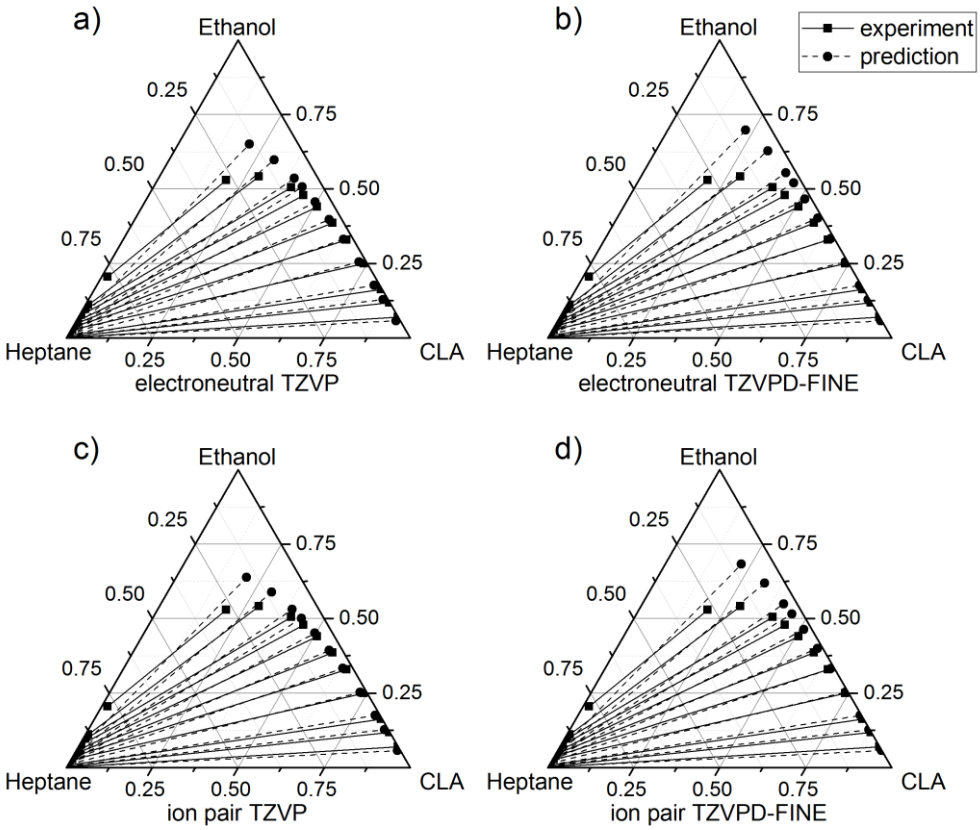

Figure S8: Experimental vs. COSMO-RS predicted tie lines for the ternary system heptane/ethanol/CLA with (a) TZVP parameterization with electroneutral, (b) TZVPD-FINE parameterization with electroneutral, (c) TZVP parameterization and ion pair, and (d) TZVPD-FINE parameterization with ion pair representation of DES molecules; experimental data taken from [4]

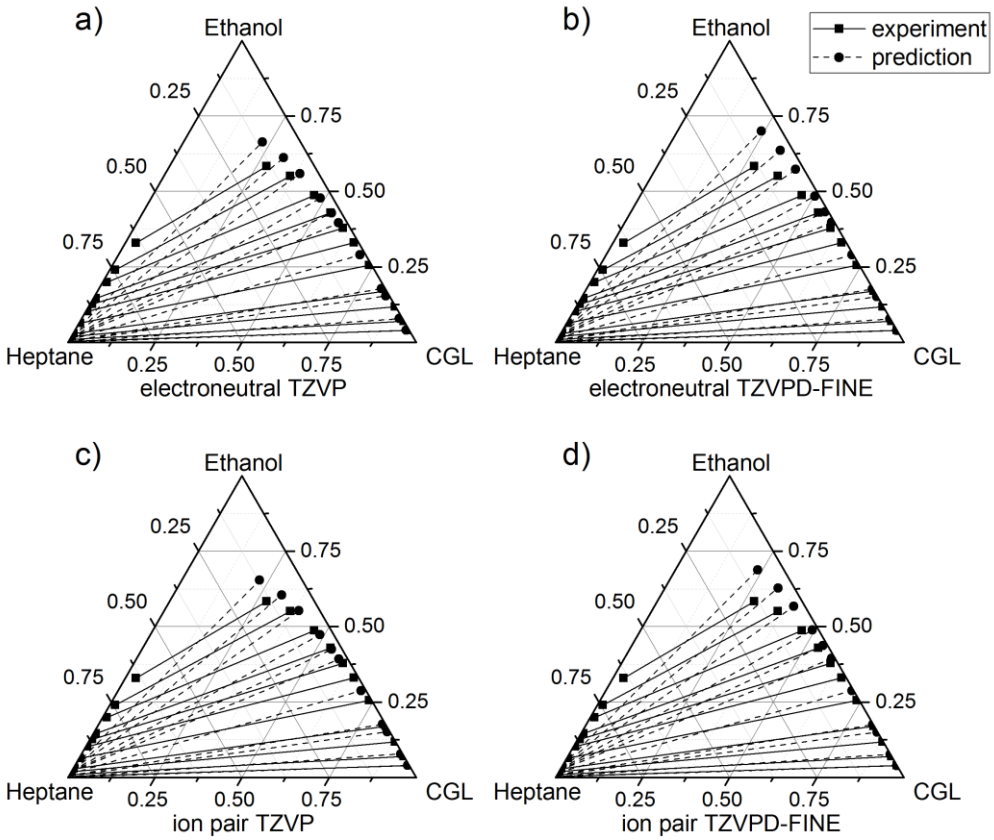

Figure S9: Experimental vs. COSMO-RS predicted tie lines for the ternary system heptane/ethanol/CGL with (a) TZVP parameterization with electroneutral, (b) TZVPD-FINE parameterization with electroneutral, (c) TZVP parameterization and ion pair, and (d) TZVPD-FINE parameterization with ion pair representation of DES molecules; experimental data taken from [4]

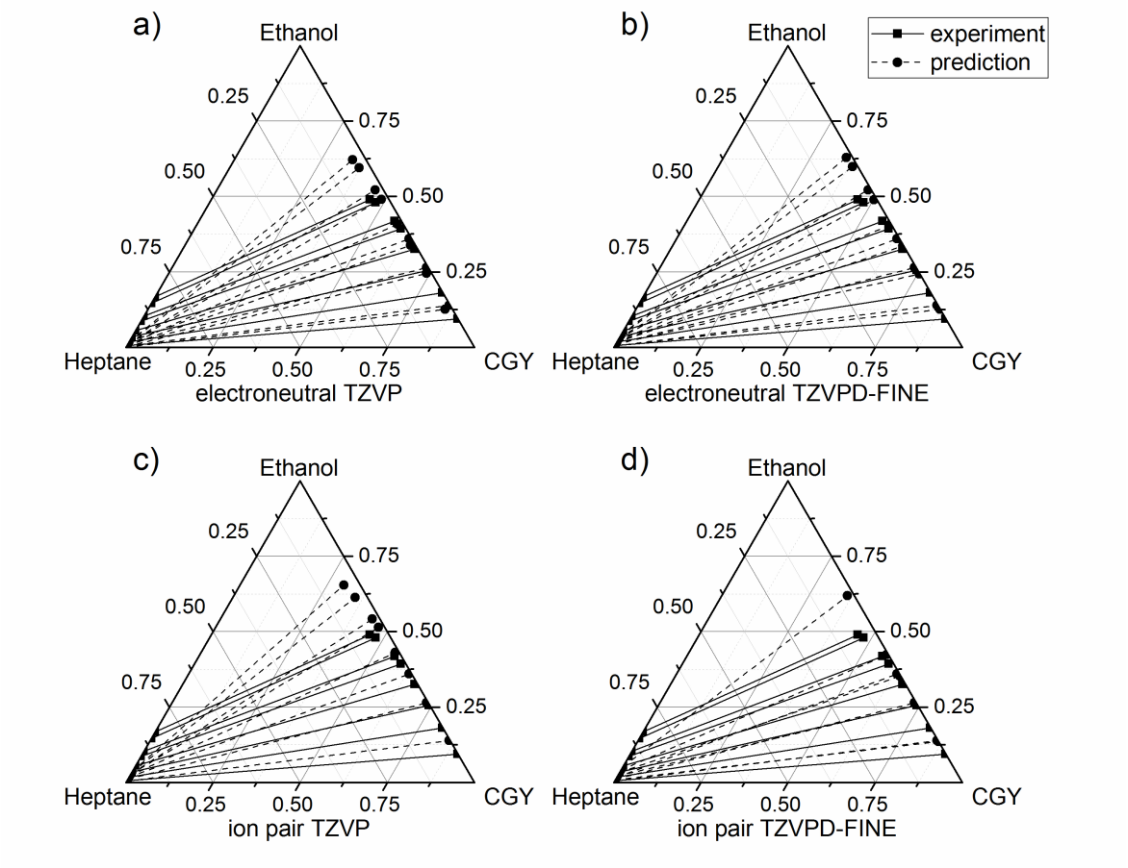

Figure S10: Experimental vs. COSMO-RS predicted tie lines for the ternary system heptane/ethanol/CGY with (a) TZVP parameterization with electroneutral, (b) TZVPD-FINE parameterization with electroneutral, (c) TZVP parameterization and ion pair, and (d) TZVPD-FINE parameterization with ion pair representation of DES molecules; experimental data taken from [5]

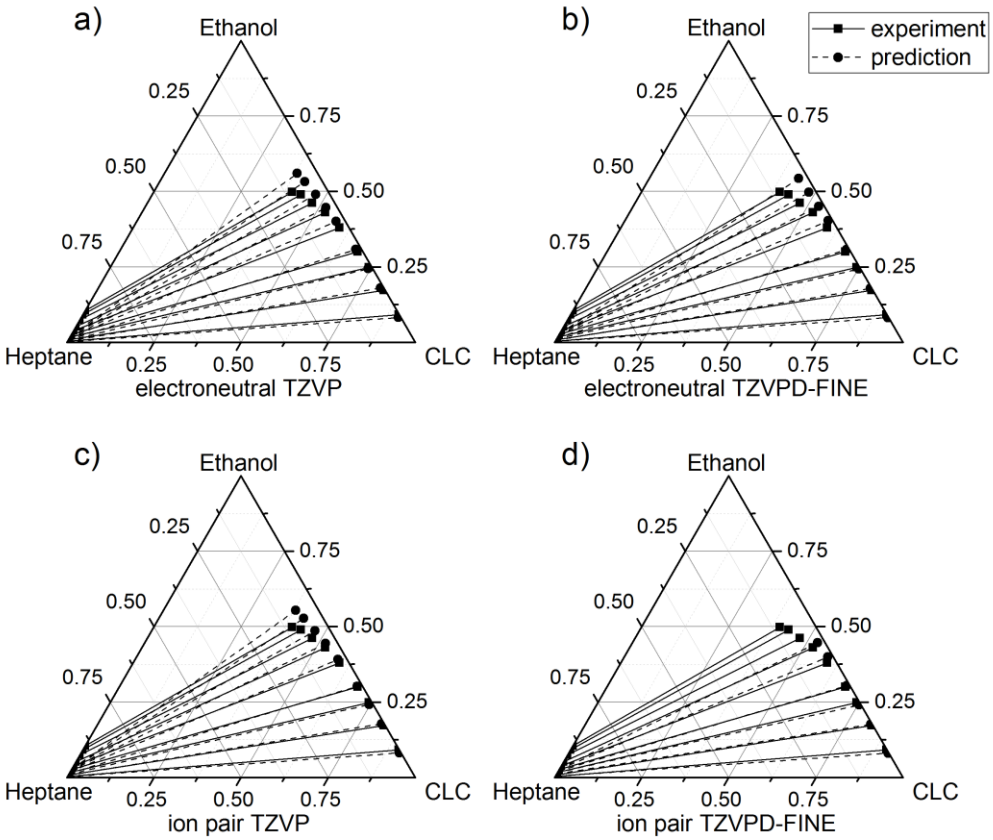

Figure S11: Experimental vs. COSMO-RS predicted tie lines for the ternary system heptane/ethanol/CLC with (a) TZVP parameterization with electroneutral, (b) TZVPD-FINE parameterization with electroneutral, (c) TZVP parameterization and ion pair, and (d) TZVPD-FINE parameterization with ion pair representation of DES molecules; experimental data taken from [5]

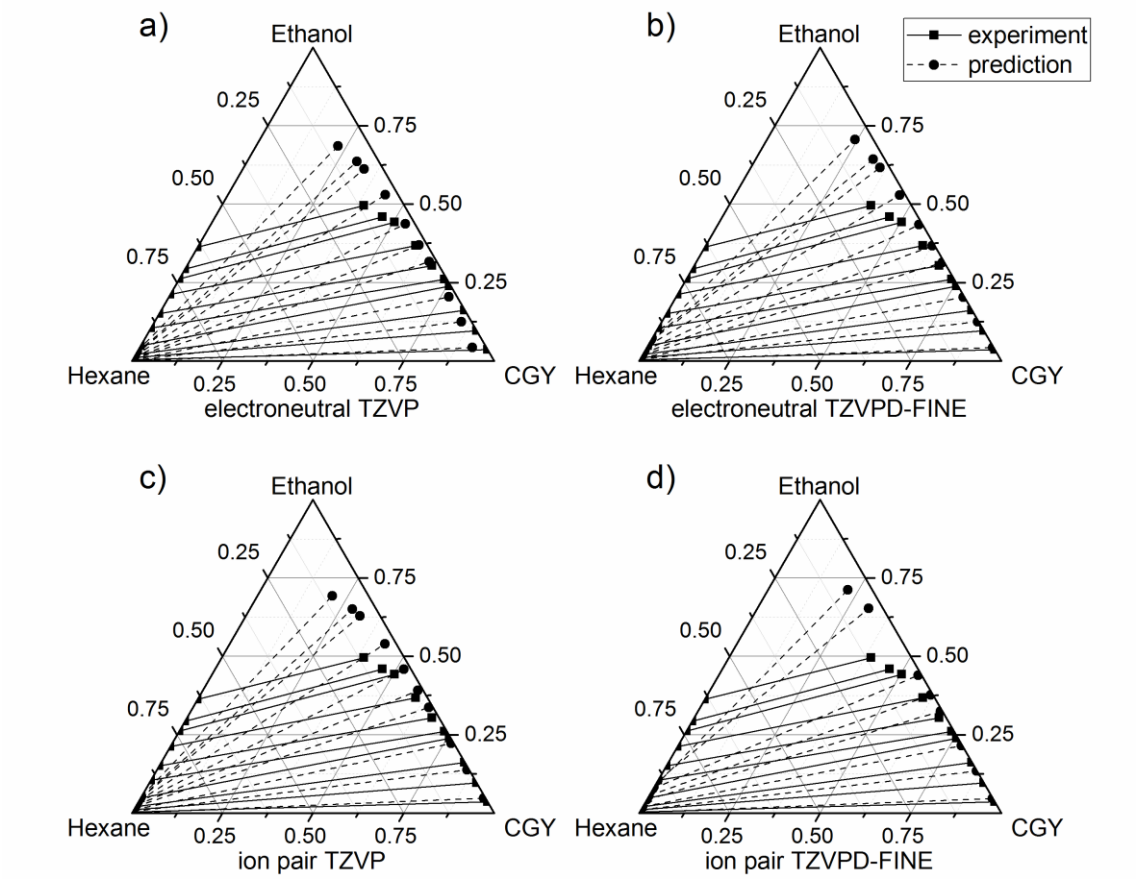

Figure S12: Experimental vs. COSMO-RS predicted tie lines for the ternary system hexane/ethanol/CGY with (a) TZVP parameterization with electroneutral, (b) TZVPD-FINE parameterization with electroneutral, (c) TZVP parameterization and ion pair, and (d) TZVPD-FINE parameterization with ion pair representation of DES molecules; experimental data taken from [5]

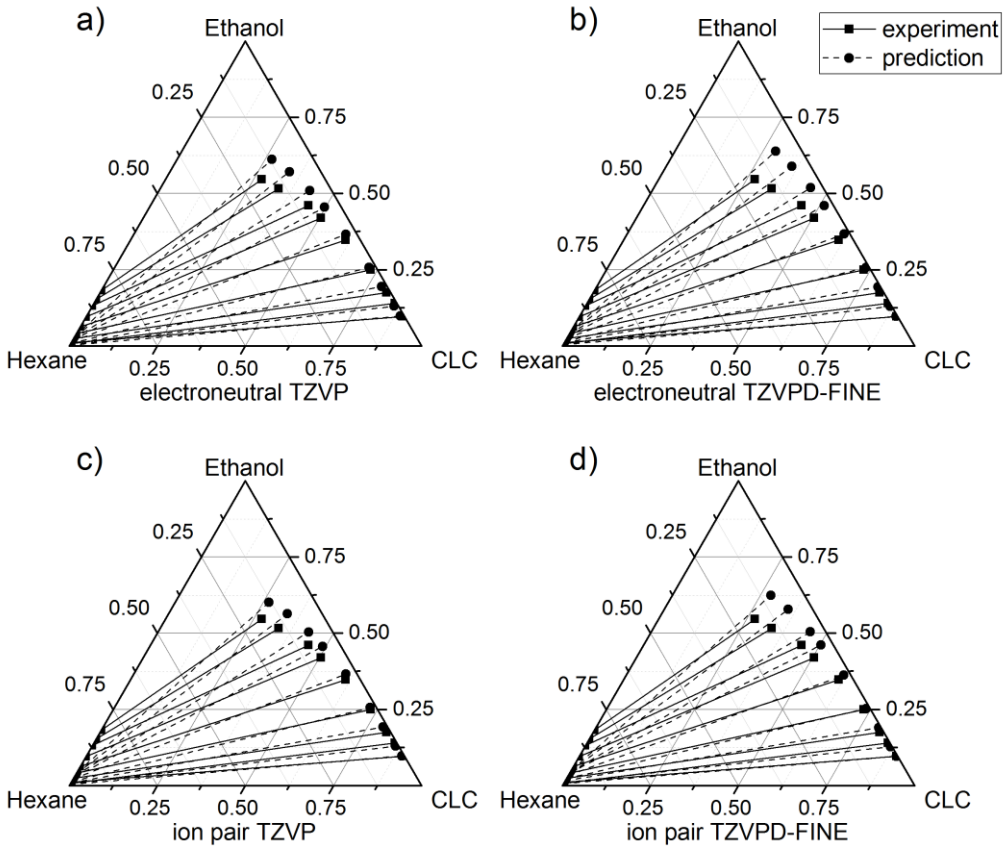

Figure S13: Experimental vs. COSMO-RS predicted tie lines for the ternary system hexane/ethanol/CLC with (a) TZVP parameterization with electroneutral, (b) TZVPD-FINE parameterization with electroneutral, (c) TZVP parameterization and ion pair, and (d) TZVPD-FINE parameterization with ion pair representation of DES molecules; experimental data taken from [5]

Table S2: Results of the quaternary LLE with the ion pair approach of (1) heptane, (2) ethanol, (3) choline chloride, and (4) levulinic acid

heptane/ ethanol/CLA		x`(1)	x`(2)	x`(3)	x`(4)	x``(1)	x``(2)	x``(3)	x``(4)	LA:ChCl`	LA:ChCl``
quaternary 30/40/30 ion pair	TZVP	0.9375	0.0614	0.0000	0.0010	0.0483	0.7414	0.0702	0.1401	3041.54	2.00
	TZVPD-FINE	0.9334	0.0658	0.0000	0.0007	0.0236	0.7583	0.07277	0.1453	39580.90	2.00
quaternary 40/40/20 ion pair	TZVP	0.9274	0.0717	0.0000	0.0010	0.0660	0.7842	0.0500	0.0998	2286.44	1.99
	TZVPD-FINE	0.9269	0.0724	0.0000	0.0007	0.0356	0.8093	0.0518	0.1034	29514.85	1.99
quaternary 45/10/45 ion pair	TZVP	0.9842	0.0151	0,0000	0.0007	0.0130	0.3622	0.2084	0.4163	12309.12	2.00
	TZVPD-FINE	0.9817	0.0179	0.0000	0.0004	0.0035	0.3641	0.2109	0.4215	106297.92	2.00

Table S3: Results of the quaternary LLE with the ion pair approach of (1) hexane, (2) ethyl acetate, (3) choline chloride, and (4) lactic acid

heptane/ ethanol/CLA		x`(1)	x`(2)	x`(3)	x`(4)	x``(1)	x``(2)	x``(3)	x``(4)	LAC:ChCl`	LAC:ChCl``
quaternary 08/52/40 ion pair	TZVP	0.1481	0.7897	0.0020	0.0602	0.0048	0.2134	0.2815	0.5003	29.37	1.78
	TZVPD-FINE	0.1301	0.7302	0.0054	0.1343	0.0017	0.1425	0.359	0.4967	24.77	1.38
quaternary 23/37/40 ion pair	TZVP	0.4346	0.5404	0.0001	0.0250	0.0066	0.1565	0.2885	0.5484	455.16	1.90
	TZVPD-FINE	0.3871	0.5221	0.0002	0.0907	0.0027	0.1179	0.3405	0.5390	523.83	1.58
quaternary 52/08/40 ion pair	TZVP	0.8978	0.1011	0.0000	0.0011	0.0057	0.0512	0.3148	0.6282	44545.83	2.00
	TZVPD-FINE	0.8892	0.1009	0.0000	0.0098	0.0028	0.0507	0.3201	0.6265	1425584.43	1.96

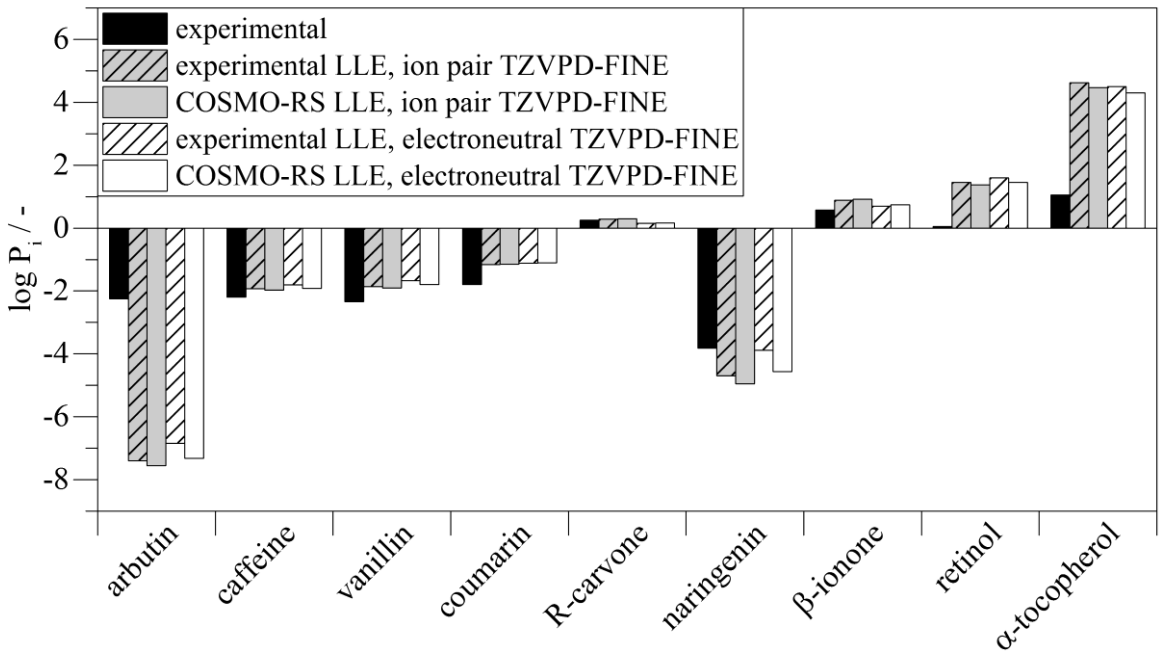

Figure S14: Experimental and predicted logarithmic partition coefficients of solutes with different polarity in the biphasic system composed of Heptane/Ethanol/CLA with a composition of 45/10/45 wt/wt/wt calculated using COSMO-RS with the TZVPD-FINE parameterization and experimental and predicted LLE data

Influence of variation in LLE-data on partition coefficient prediction

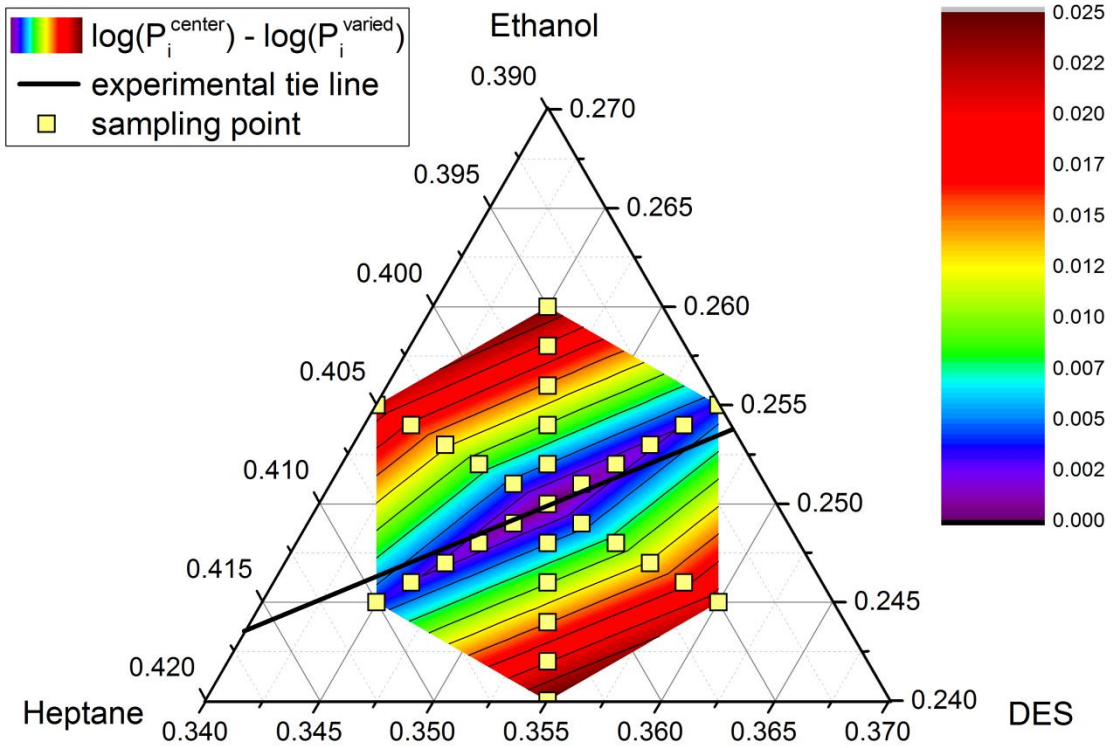

Figure S15: Deviation in the partition coefficient of β-ionone for a small variation in the global input composition for the LLE calculation. TZVPD-FINE parameterization and ion pair approach were used in the calculations.

The sensitivity of the partition coefficient calculations to a variation in phase composition due to small deviations in the global input composition was investigated. As mentioned in chapter 3.3, for some input compositions the algorithm to solve the equilibrium did not converge and the input composition was slightly modified to get a solution. The problem occurred mainly for TZVPD-FINE in combination with the ion pair approach for the representation of the HBA and TZVP with ion pair approach. With the electroneutral representation of the HBA the convergence problem also occurred a few times TZVPD-FINE (less than for ion pair) and never for TZVP. The procedure for varying the global input composition can be automated, but it has to be considered whether the additional error introduced by the variation is small enough to still achieve comparable results. LLE and partition coefficients of the nine model solutes in the biphasic system heptane/ethanol/CLA were calculated for 31 global input compositions, the results for one of them, namely β-ionone, are shown in Figure S15. The square symbols mark the chosen input compositions and the line represents the predicted tie line for the original input composition. The sampling points where set in 0.002 steps from the original composition. As expected, along the original tie line the resulting RMSD for the partition coefficient is very small and the RMSD increases compositions outside the original tie line. However, the results show that RMSD for the partition coefficients are small and the additional error introduced by varying the global input composition can be neglected for small changes.

Table S4: Logarithmic partition coefficient of vanillin in different biphasic systems

Biphasic system	Global system composition /wt%	Logarithmic partition coefficient $P_{vanillin}$ /-	Standard deviation of $P_{vanillin}$ /-
heptane/methanol/CLA	37.5/25.0/37.5	-2,22	0,01
heptane/ethanol/CLA	37.5/25.0/37.5	-1,91	0,02
heptane/acetonitrile/CLA	37.5/25.0/37.5	-2,28	0,01
heptane/methanol/BLA	37.5/25.0/37.5	-2,31	0,01
heptane/ethanol/BLA	37.5/25.0/37.5	-1,79	0,01
heptane/propanol/BLA	37.5/25.0/37.5	-1,43	0,02
heptane/acetonitrile/BLA	37.5/25.0/37.5	-2,41	0,03

Table S5: Logarithmic partition coefficient of β-ionone in different biphasic systems

Biphasic system	Global system composition /wt%	Logarithmic partition coefficient Pβ-ionone /-	Standard deviation of Pβ-ionone /-
heptane/methanol/CLA	37.5/25.0/37.5	0,25	0,02
heptane/ethanol/CLA	37.5/25.0/37.5	0,20	0,02
heptane/acetonitrile/CLA	37.5/25.0/37.5	0,30	0,02
heptane/methanol/BLA	37.5/25.0/37.5	0,22	0,01
heptane/ethanol/BLA	37.5/25.0/37.5	0,21	0,02
heptane/propanol/BLA	37.5/25.0/37.5	0,43	0,04
heptane/acetonitrile/BLA	37.5/25.0/37.5	0,31	0,03

Table S6: Logarithmic partition coefficient of α-tocopherol in different biphasic systems

Biphasic system	Global system composition /wt%	Logarithmic partition coefficient $P_{\alpha\text{-tocopherol}}$ /-	Standard deviation of $P_{\alpha\text{-tocopherol}}$ /-
heptane/methanol/CLA	30/40/30	1,08	0,15
heptane/ethanol/CLA	30/40/30	0,57	0,05
heptane/methanol/BLA	30/40/30	0,88	0,09
heptane/ethanol/BLA	30/40/30	0,56	0,03
heptane/propanol/BLA	30/40/30	0,49	0,05

References

1. Verevkin, S.P., et al., *Separation Performance of BioRenewable Deep Eutectic Solvents.* Industrial & Engineering Chemistry Research, 2015. **54**(13): p. 3498-3504.
2. Gonzalez, A.S.B., et al., *Liquid–liquid equilibrium data for the systems {LTTM + benzene + hexane} and {LTTM + ethyl acetate + hexane} at different temperatures and atmospheric pressure.* Fluid Phase Equilibria, 2013. **360**: p. 54-62.
3. Kareem, M.A., et al., *Phase equilibria of toluene/heptane with tetrabutylphosphonium bromide based deep eutectic solvents for the potential use in the separation of aromatics from naphtha.* Fluid Phase Equilibria, 2012. **333**: p. 47-54.
4. Oliveira, F.S., et al., *Deep eutectic solvents as extraction media for azeotropic mixtures.* Green Chemistry, 2013. **15**(5): p. 1326-1330.
5. Rodriguez, N.R., B.S. Molina, and M.C. Kroon, *Aliphatic + ethanol separation via liquid–liquid extraction using low transition temperature mixtures as extracting agents.* Fluid Phase Equilibria, 2015. **394**: p. 71-82.

Supplementary information

Liquid-liquid equilibria of heptane, methanol and deep eutectic solvents composed of carboxylic acid and monocyclic terpenes

F. Bezold, M. Minceva
Biothermodynamics, TUM School of Life Sciences Weihenstephan, Technical University of Munich

Table S1: Initial molar composition for the system n-heptane (1)/methanol (2)/L-menthol (3)/levulinic acid (4)

System	x_1	x_2	x_3	x_4
M1	0.5761	0.0000	0.2120	0.2120
M2	0.5063	0.1584	0.1677	0.1677
M3	0.4516	0.2825	0.1329	0.1329
M4	0.4076	0.3825	0.1050	0.1050
M5	0.3714	0.4646	0.0820	0.0820
M6	0.3411	0.5334	0.0627	0.0627
M7	0.3154	0.5918	0.0464	0.0464
M8	0.2932	0.6420	0.0324	0.0324
M9	0.2740	0.6856	0.0202	0.0202
M10	0.2572	0.7239	0.0095	0.0095
M11	0.2423	0.7577	0.0000	0.0000
M12	0.2743	0.6864	0.0235	0.0157
M13	0.3162	0.5934	0.0542	0.0362
M14	0.3731	0.4668	0.0960	0.0640
M15	0.4551	0.2847	0.1561	0.1041
M16	0.2739	0.6853	0.0185	0.0224
M17	0.3150	0.5910	0.0426	0.0514
M18	0.3705	0.4636	0.0751	0.0907
M19	0.4500	0.2815	0.1217	0.1469

Table S2: Initial molar composition for the system n-heptane (1)/methanol (2)/thymol (3)/levulinic acid (4)

System	x_1	x_2	x_3	x_4
T1	0.5706	0.0000	0.2147	0.2147
T2	0.5025	0.1572	0.1702	0.1702
T3	0.4489	0.2808	0.1351	0.1351
T4	0.4057	0.3806	0.1068	0.1068
T5	0.3700	0.4629	0.0835	0.0835
T6	0.3401	0.5319	0.0640	0.0640
T7	0.3147	0.5906	0.0474	0.0474
T8	0.2928	0.6411	0.0331	0.0331
T9	0.2738	0.6850	0.0206	0.0206
T10	0.2571	0.7236	0.0097	0.0097
T11	0.2423	0.7577	0.0000	0.0000
T12	0.2741	0.6857	0.0241	0.0161
T13	0.3154	0.5920	0.0555	0.0370
T14	0.3716	0.4649	0.0981	0.0654
T15	0.4520	0.2827	0.1592	0.1061
T16	0.2735	0.6843	0.0169	0.0253
T17	0.3139	0.5891	0.0388	0.0582
T18	0.3684	0.4609	0.0683	0.1024
T19	0.4458	0.2788	0.1102	0.1652

Table S3: Initial molar composition for the system n-heptane (1)/methanol (2)/carvacrol (3)/levulinic acid (4)

System	x_1	x_2	x_3	x_4
C1	0.5706	0.0000	0.2147	0.2147
C2	0.5025	0.1572	0.1702	0.1702
C3	0.4489	0.2808	0.1351	0.1351
C4	0.4057	0.3806	0.1068	0.1068
C5	0.3700	0.4629	0.0835	0.0835
C6	0.3401	0.5319	0.0640	0.0640
C7	0.3147	0.5906	0.0474	0.0474
C8	0.2928	0.6411	0.0331	0.0331
C9	0.2738	0.6850	0.0206	0.0206
C10	0.2571	0.7236	0.0097	0.0097
C11	0.2423	0.7577	0.0000	0.0000
C12	0.2741	0.6857	0.0241	0.0161
C13	0.3154	0.5920	0.0555	0.0370
C14	0.3716	0.4649	0.0981	0.0654
C15	0.4520	0.2827	0.1592	0.1061
C16	0.2735	0.6843	0.0169	0.0253
C17	0.3139	0.5891	0.0388	0.0582
C18	0.3684	0.4609	0.0683	0.1024
C19	0.4458	0.2788	0.1102	0.1652

Table S4: Molar ratio of HBD:HBA in the investigated biphasic systems.

System	L-Menthol:levulinic acid		Thymol:levulinic acid		Carvacrol:levulinic acid	
	Upper phase	Lower phase	Upper phase	Lower phase	Upper phase	Lower phase
1	1.91±0.00	0.18±0.00	3.24±0.20	0.97±0.01	3.39±0.05	0.95±0.00
2	1.96±0.03	0.26±0.00	2.80±0.01	0.94±0.01	3.15±0.01	0.93±0.00
3	1.95±0.01	0.36±0.00	2.72±0.01	0.91±0.00	3.01±0.02	0.92±0.00
4	1.93±0.00	0.49±0.00	2.89±0.02	0.95±0.01	3.04±0.02	0.93±0.00
5	2.11±0.04	0.63±0.01	2.85±0.01	0.92±0.00	3.01±0.11	0.93±0.00
6	2.35±0.04	0.76±0.01	3.22±0.09	0.99±0.02	3.22±0.06	0.89±0.00
7	2.99±0.02	0.86±0.00	3.40±0.03	0.96±0.01	3.42±0.03	0.91±0.00
8	4.00±0.02	0.90±0.02	4.05±0.09	1.00±0.00	3.81±0.02	0.92±0.01
9	5.61±0.06	0.97±0.02	5.20±0.37	0.95±0.01	4.48±0.07	0.95±0.00
10	35.86±1.26	0.93±0.02	6.90±0.41	0.99±0.02	5.80±0.36	0.91±0.00
12	NA	NA	1.99±0.01	1.47±0.00	2.56±0.00	1.44±0.01
13	NA	NA	2.57±0.01	1.49±0.01	2.92±0.01	1.37±0.00
14	NA	NA	3.59±0.04	1.53±0.02	3.86±0.01	1.43±0.01
15	6.21±0.46	1.51±0.04	6.56±0.24	1.81±0.05	6.44±0.35	1.58±0.02
16	2.51±0.03	0.25±0.00	2.87±0.04	0.63±0.01	2.97±0.04	0.62±0.00
17	NA	NA	2.83±0.08	0.63±0.01	2.92±0.12	0.61±0.00
18	3.28±0.15	0.51±0.01	3.08±0.12	0.65±0.01	3.15±0.06	0.63±0.00
19	4.71±0.07	0.62±0.01	3.40±0.06	0.68±0.01	3.73±0.05	0.68±0.01

Table S5: Mean ratio of upper phase to lower phase volume.

System	Ratio of phase volume /-		
	L-Menthol-levulinic acid	**Thymol-levulinic acid**	**Carvacrol-levulinic acid**
1	7.83±0.02	1.17±0.01	1.27±0.03
2	6.47±0.07	1.17±0.01	1.21±0.01
3	4.31±0.10	1.10±0.03	1.17±0.00
4	3.04±0.06	1.05±0.04	1.09±0.02
5	1.92±0.02	0.92±0.01	0.97±0.01
6	1.20±0.05	0.85±0.01	0.84±0.01
7	0.84±0.02	0.76±0.01	0.77±0.01
8	0.68±0.01	0.70±0.02	0.70±0.01
9	0.63±0.01	0.68±0.01	0.68±0.00
10	0.61±0.01	0.63±0.02	0.64±0.00
11		0.61±0.02	
12	NA	0.77±0.00	0.92±0.02
13	NA	0.61±0.01	0.73±0.01
14	NA	0.54±0.01	0.60±0.01
15	0.47±0.00	0.57±0.01	0.57±0.00
16	2.82±0.06	1.23±0.02	1.23±0.01
17	NA	1.07±0.03	1.06±0.02
18	0.94±0.01	0.87±0.01	0.86±0.01
19	0.69±0.00	0.71±0.02	0.71±0.00

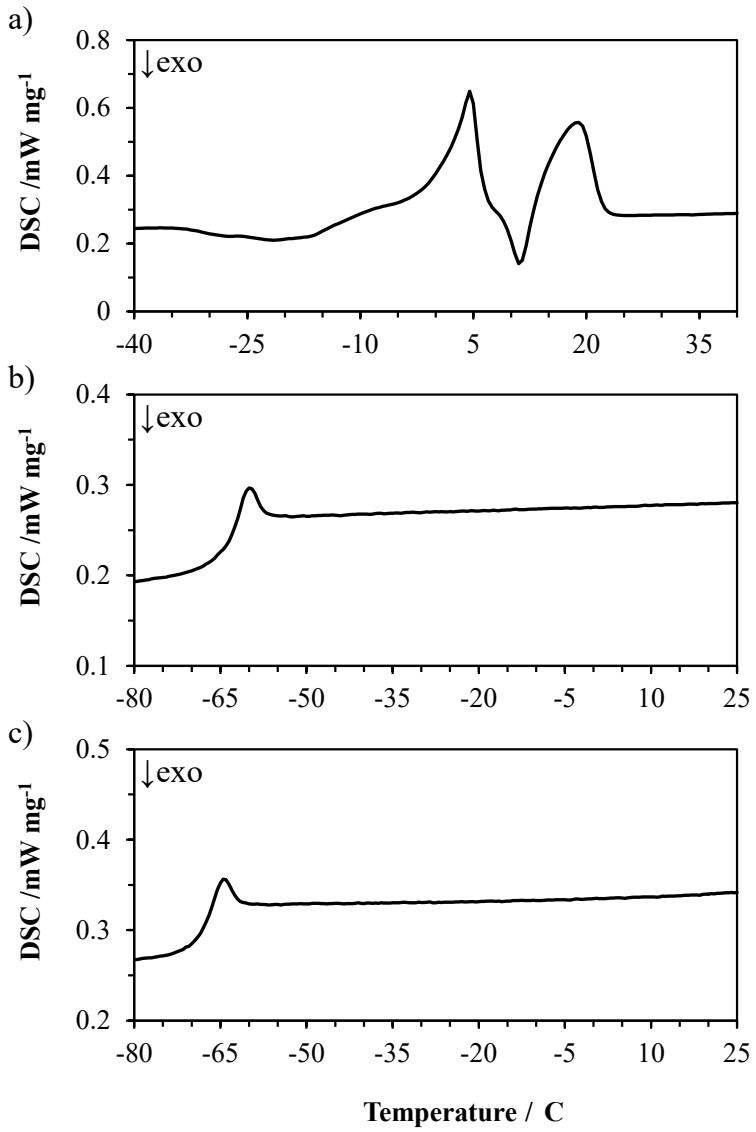

Figure S1: DSC curves of (a) L-menthol-levulinic acid in a ratio of 1:1 mol:mol with eutectic at 0.2 °C (onset), and liquidus temperature at 14.8 °C (peak maximum), (b) thymol-levulinic acid in a ratio of 1:1 mol:mol with glass transition at -64.1 °C (onset), and (c) carvacrol-levulinic acid in a ratio of 1:1 mol:mol with glass transition temperature at -68.8 (onset)